# HYPERON 99

## Proceedings of the Hyperon Physics Symposium

**FERMILAB, September 27-29 1999**

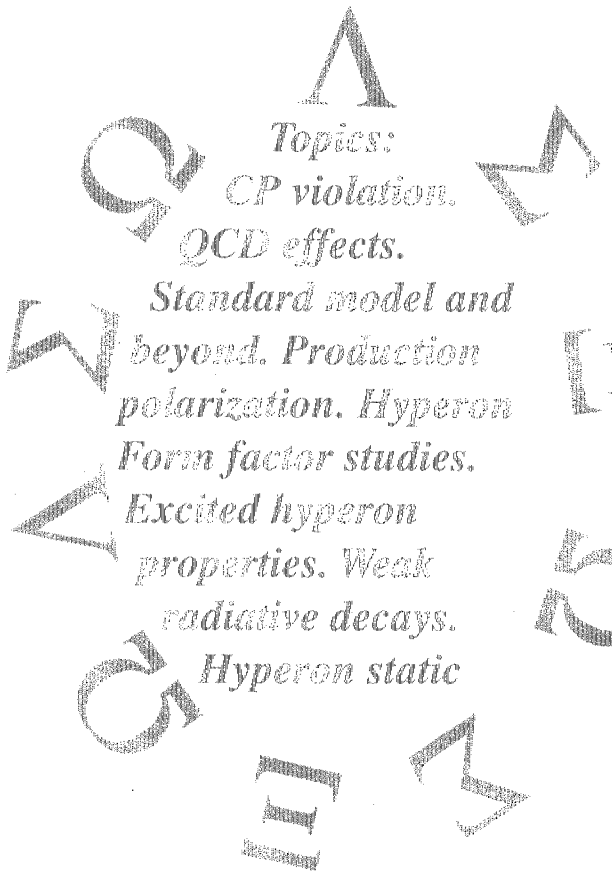


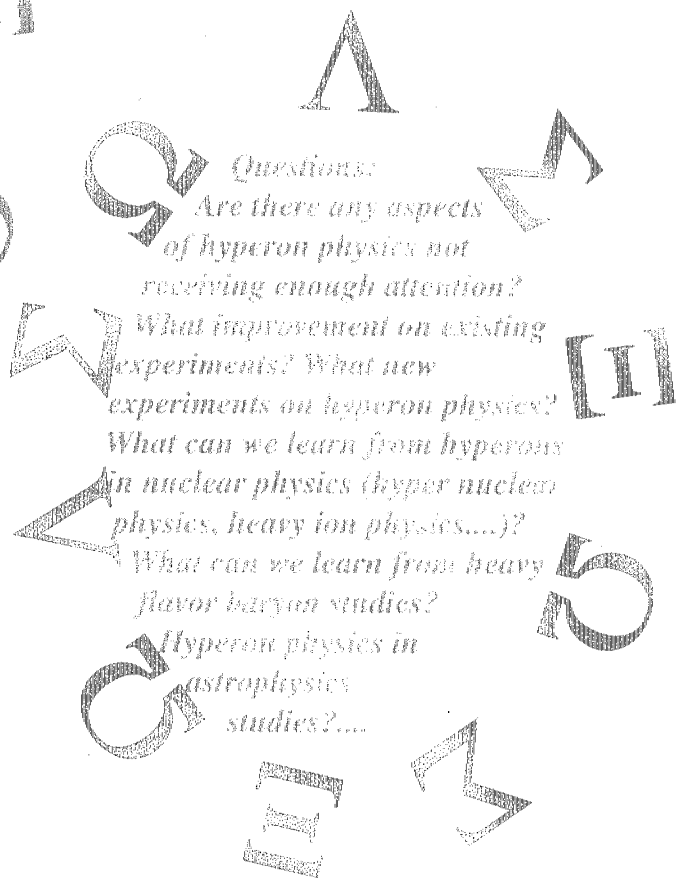


**Edited by: D.A. Jensen**
**E. Monnier**

## Disclaimer



## Distribution



## Copyright Notification

FERMILAB-Conf-00/059-E

# Hyperon Physics Symposium

# Hyperon 99

**September 27-29, 1999**

**Fermi National Accelerator Laboratory, Batavia, Illinois.**

**Editors**

**D. A. Jensen**
Fermilab

**E. Monnier**
Enrico Fermi Institute
University of Chicago
Chicago, Illinois, 60637
*(On leave from C.P.P. Marseille, France)*

**Sponsored by the Fermi National Accelerator Laboratory, The University of Chicago, Elmhurst College, University of Virginia, University of Wisconsin, and the French Government**

# Hyperon Physics Symposium

# Hyperon 99

September 27-29, 1999

Fermi National Accelerator Laboratory, Batavia, Illinois.

Organizing committee:

| | | |
|---|---|---|
| Th. Alexopoulos | | University of Wisconsin, Madison |
| J. F. Donoghue | | Massachusetts University, Amherst |
| C. E. Dukes | | University of Virginia |
| D. A. Jensen | Cochair/Coeditor | Fermilab |
| J. Lach | | Fermilab |
| E. Monnier | Cochair/Coeditor | University of Chicago |

Sponsored by the Fermi National Accelerator Laboratory, The University of Chicago, Elmhurst College, University of Virginia, University of Wisconsin, and the French Government

# Acknowledgments

As organizers of the Hyperon99 symposium we would like to thank all the speakers as well as the participants. There efforts made this conference a success.

But above all, the success of this conference has been achieved thanks to the critical assistance provided to the organizers by Mary Cullen and Marilyn Smith before, during and after the conference.

We are grateful for the help of Patricia Oleck and Susan Grommes throughout the conference.

We thank warmly Roland Winston for his assistance.

We were pleased to obtain wide support for this symposium and thank the Laboratory Directorate, under both John Peoples and Mike Witherell, for providing major support for this conference.

Finally, we thank again the University of Chicago, Elmhurst College, the University of Virginia, the University of Wisconsin and the French Government for their sponsorship of this symposium.

# Contents


**1 Opening Session** **1**

1.1 V. J. Smith, Historical Overview . . . . . 3

1.2 B. Holstein, Hyperon Physics: a Personal Overview . . . . . 4

**2 New Results** **11**

2.1 D. C. Christian, $\Lambda^0$ polarization in 800 GeV/$c$ $pp \to p_f(\Lambda^0 K^+)$ . . . . . 13

2.2 M. V. Purhoit, Resonances in $\Lambda_c^+ \to p K^- \pi^+$ and $\Lambda_c^+$ polarization . . . . . 17

2.3 H. Krueger, The $\Sigma^-$ hyperon radius . . . . . 21

2.4 E. McCliment, Two polarization studies: polarization of Inclusively produced $\Sigma^+$ by 800 GeV/$c$ protons and inclusively produced $\Lambda^0$ by 600 GeV/$c$ $\Sigma^-$ . . . . . 25

2.5 L. Landsberg, The search for pentaquark baryon with hidden strangeness . . . . . 29

2.6 J. Tandean, Recent theoretical results on $|DI| = 3/2$ decays of hyperons . . . . . 33

2.7 S. Bright, First measurement of the $\Xi^0 \to \Sigma^+ e^- \overline{\nu}_e$ form factors . . . . . 37

2.8 G. Karl, Isospin violation in hyperon semileptonic decays . . . . . 41

2.9 V. J. Smith, Test of isospin mixing in hyperon semileptonic decays . . . . . 43

2.10 J. C. Anjos, Particle - antiparticle asymmetries in the production of baryons in 500 GeV/$c$ $\pi^-$ nucleon interactions . . . . . 44

2.11 A. R. Erwin, Polarization of the $\Xi^0$ and $\overline{\Xi^0}$ at KTeV Experiment . . . . . 48

**3 Hyperon Beta Decays and Form Factors** **53**

3.1 A. Garcia, Baryon semileptonic decays . . . . . 55

3.2 A. Alavi-Harati, Hyperon semileptonic decays: an experimental overview . . . . . 60

**4 Radiative Hyperon Decays** **67**

4.1 P. Zenczykowski, Weak radiative hyperon decays: questioning the basics . . . . . 69

4.2 U. Koch, Weak radiative hyperon decays: experimental status . . . . . 77

**5 QCD and Hyperons** **85**

5.1 H. J. Lipkin, The new $\sigma_t ot(\Sigma p)$ data,the new PDG fit to hadron total cross sections and the TCP alternative . . . . . 87

**6 CP Violation in Hyperons** **93**

6.1 G. Valencia, Theoretical status of CP violation . . . . . 95

6.2 K. Nelson, A review of experimental searches for CP violation in hyperon decays . . . . . 99

**7 Hyperon static properties** **105**

7.1 H. J. Lipkin, Theoretical analysis of static hyperon data . . . . . 107

7.2 P. S. Cooper, Hyperon static properties . . . . . 115

**8 Hyperon Production and Polarization** **119**

8.1 J. Soffer, Is the ridle of the hyperon polarizations solved? . . . . . 121

8.2 L. G. Pondrom, Hyperon polarization news . . . . . 127

8.3 G. R. Goldstein, Polarization of inclusive $\Lambda_c$'s in a hybrid model . . . . . 132

8.4 U. Mueller, Strange particle production by $\Sigma^-$, $\pi^-$ and neutrons in WA89 . . . . . 137

**9 Excited Hyperon Properties and Extension to Heavy Flavors** **145**

9.1 J. S. Russ, Excited hyperons - charmed and strange . . . . . 147

**10 Beyond the Typical Hyperon Field** **151**

10.1 R. Bellwied, The role of hyperons in relativistic heavy ion collisions . . . . . 153

**11 Panel Discussion** **163**

11.1 D. Kaplan, contribution to the panel . . . . . 165

11.2 L. Landsberg, contribution to the panel . . . . . 167

11.3 P. Zenczykowski, contribution to the panel . . . . . 169

**12 Summary Talks** **171**

12.1 P. Ratcliffe, Theory summary . . . . . 173

12.2 E. Ramberg, Experiment summary . . . . . 183

**13 Finale !** **189**

13.1 N. Cabibbo, Hyperons and quark mixing . . . . . 191

# Chapter 1

# Opening Session

- Introduction: Organizers
- Welcome: K. Stanfield
- Historical Overview: V. J. Smith
- Conference Preview: B. Holstein

# Historical Overview of Hyperon Beam Experiments

Vincent J. Smith[a]

[a]H H Wills Physics Laboratory, University of Bristol, UK-BS8 1TL

The original conception of this talk was to review hyperon beam experiments at the CERN SPS, but it was extended to include some experiments at Fermilab. The author apologises that there was not time to cover all of the important results from more than two decades of experimentation.

## 1. SUMMARY

The talk made extensive use of some excellent reviews[1–4] of these experiments, already published and easily available. These are listed in the References section, and readers are encouraged to go there to learn more.

## REFERENCES

1. J. Lach and L. Pondrom: 'Hyperon Beam Physics', Ann Rev Nucl Part Sci 29, 203-242 (1979)
2. M. Bourquin and J.-P. Repellin: 'Experiments with the CERN SPS Hyperon Beam', Physics Reports 114, 99-180 (1984)
3. L. G. Pondrom: 'Hyperon Experiments at Fermilab', Physics Reports 122, 57-172 (1985)
4. J. Lach: 'Hyperons at Fermilab', FERMILAB-Conf-95/372

# Hyperon Physics—a Personal Overview

Barry R. Holstein
Department of Physics and Astronomy
University of Massachusetts
Amherst, MA 01003

A range of issues in the field of hyperon physics is presented, together with an assessment of where important challenges remain.

## 1. Introduction

The subject of hyperon physics is a vast one, as indicated by the fact that this workshop will run for three days, with presentations involving a range of different issues. Obviously it would be impossible for me to cover all of the interesting features in this introductory presentation. Instead, I will present a very personal picture of some of the issues in hyperon physics which *I* think need to be answered, and will trust the various speakers to fill in areas which I have omitted.

## 2. Hyperon Processes

I have divided my presentation into sections, which cover the various arenas which I think need attention:

### 2.1. Nonleptonic Hyperon Decay

The dominant decay mode of the $\frac{1}{2}^+$ hyperons is, of course, the pionic decay $B \to B'\pi$. On the theoretical side there remain two interesting and important issues which have been with us since the 1960's—the origin of the $\Delta I = 1/2$ rule and the S/P-wave problem[1]:

i) The former is the feature that $\Delta I = 3/2$ amplitudes are suppressed with respect to their $\Delta I = 1/2$ counterparts by factors of the order of twenty or so. This suppression exists in both hyperon as well as kaon nonleptonic decay and, despite a great deal of theoretical work, there is still no simple explanation for its existence. The lowest order weak nonleptonic $\Delta S = 1$ Hamiltonian possesses comparable $\Delta I = 1/2$ and $\Delta I = 3/2$ components and leading log gluonic effects can bring about a $\Delta I = 1/2$ enhancement of a factor of three to four or so[2]. The remaining factor of five seems to arise from the validity of what is called the Pati-Woo theorem in the baryon sector[3] while for kaons it appears to be associated with detailed dynamical structure[4]. Interestingly the one piece of possible evidence for its violation comes from a hyperon reaction—-hypernuclear decay[5]. A hypernucleus is produced when a neutron in an atomic nucleus is replaced by a $\Lambda$. In this case the usual pionic decay mode is Pauli suppressed, and the hypernucleus primarily decays via the non-mesonic processes $\Lambda p \to np$ and $\Lambda n \to nn$. There does exist a rather preliminary indication here of a possibly significant $\Delta I = 1/2$ rule violation, but this has no Fermilab relevance and will have to be settled at other laboratories[6].

ii) The latter problem is not as well known but has been a longstanding difficulty to those of us theorists who try to calculate these things. Writing the general decay amplitude as

$$\text{Amp} = \bar{u}(p')(A + B\gamma_5)u(p) \qquad (1)$$

The standard approach to such decays goes back to current algebra days and expresses the S-wave (parity-violating) amplitude—$A$—as a contact term—the baryon-baryon matrix element of the axial-charge-weak Hamiltonian commutator. The corresponding P-wave (parity-conserving) amplitude—$B$—uses a simple pole model (*cf.* Figure 1) with the the weak baryon to baryon matrix element given by a fit to the S-wave sector. Parity violating $BB'$ matrix elements are neglected in accord with the Lee-Swift theorem[7]. With this procedure one can obtain a good S-wave fit but finds P-wave amplitudes which are in very poor agreement with experiment. On the other hand, one can fit the P-waves, in which case the

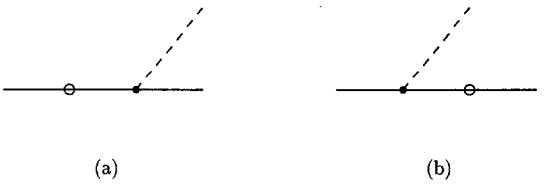

(a) (b)

Figure 1. Pole diagrams used to calculated parity-conserving nonleptonic hyperon decay.

S-wave predictions are very bad[8]. Clearly the solution requires the input of additional physics, such as inclusion of $(70, 1^-)$ intermediate states as done in an SU(6) calculation by Le Youaunc et al.[9] or of intermediate $\frac{1}{2}^-$ and $\frac{1}{2}^+$ resonant states by Borasoy and myself in a chiral picture[10].

In either case, we do *not* require more and better data. The issues are already clear. What we need is more and better theory!

Where we *do* need data involves the possibility of testing the standard model prediction of CP violation, which predicts the presence of various asymmetries in the comparision of hyperon and antihyperon nonleptonic decays[11]. The basic idea is that one can write the decay amplitudes in the form

$$A = |A| \exp i(\delta_S + \phi_S), \quad B = |B| \exp i(\delta_P + i\phi_P) \tag{2}$$

where $\delta_S, \delta_P$ are the strong S,P-wave phase shifts at the decay energy of the mode being considered and $\phi_S, \phi_P$ are CP-violating phases which are expected to be of order $10^{-4}$ or so in standard model CP-violation. One can detect such phases by comparing hyperon and antihyperon decay parameters. Unfortunately nature is somewhat perverse here in that the larger the size of the expected effect, the more difficult the experiment. For example, the asymmetry in the overall decay rate, which is the easiest to measure, has the form[1]

$$\begin{aligned} C &= \frac{\Gamma - \bar{\Gamma}}{\Gamma + \bar{\Gamma}} \\ &\sim \big(-2(A_1 A_3 \sin(\delta_S^1 - \delta_S^3) \sin(\phi_S^1 - \phi_S^3) \\ &+ B_1^r B_3^r \sin(\delta_P^1 - \delta_P^3) \sin(\phi_P^1 - \phi_P^3)\big) \\ &/ \ |A_1|^2 + |B_1^r|^2 \end{aligned} \tag{3}$$

[1]Here $B^r$ indicates a reduced amplitude—$B^r = B(E' - M_{B'})/(E' + M_{B'})$.

where the subscripts, superscripts 1,3 indicate the $\Delta I = \frac{1}{2}, \frac{3}{2}$ component of the amplitude. We see then that there is indeed sensitivity to the CP-violating phases but that it is multiplicatively suppressed by *both* the the strong interaction phases ($\delta \sim 0.1$) as well as by the $\Delta I = \frac{3}{2}$ suppression $A_3/A_1 \sim B_3/B_1 \sim 1/20$. Thus we find $C \sim \phi/100 \sim 10^{-6}$ which is much too small to expect to measure in present generation experiments.

More sanguine, but still not optimal, is a comparison of the asymmetry parameters $\alpha$, defined via

$$W(\theta) \sim 1 + \alpha \vec{P}_B \cdot \hat{p}_{B'} \tag{4}$$

In this case, one finds

$$\begin{aligned} A &= \frac{\alpha + \bar{\alpha}}{\alpha - \bar{\alpha}} = -\sin(\phi_S^1 - \phi_P^1) \sin(\delta_S^1 - \delta_P^1) \\ &\sim 0.1\phi \sim 4 \times 10^{-4} \end{aligned} \tag{5}$$

which is still extremely challenging.

Finally, the largest signal can be found in the combination

$$B = \frac{\beta + \bar{\beta}}{\beta - \bar{\beta}} = \cot(\delta_S^1 - \delta_P^1) \sin(\phi_S^1 - \phi_P^1) \sim \phi \tag{6}$$

Here, however, the parameter $\beta$ is defined via the general expression for the final state baryon polarization

$$\begin{aligned} < \vec{P}_{B'} > &= \frac{1}{W(\theta)} \Big( (\alpha + \vec{P}_B \cdot \hat{p}_{B'}) \hat{p}_{B'} \\ &+ \beta \vec{P}_B \times \hat{p}_{B'} + \gamma (\hat{p}_{B'} \times (\vec{P}_B \times \hat{p}_{B'})) \Big) \end{aligned} \tag{7}$$

and, although the size of the effect is largest—$B \sim 10^{-3}$—this measurement seems out of the question experimentally.

Despite the small size of these effects, the connection with standard model CP violation and the possibility of finding larger effects due to new physics demands a no-holds-barred effort to measure these parameters.

### 2.2. Nonleptonic Radiative Decay

Another longstanding thorn in the side of theorists attempting to understand weak decays of hyperons is the nonleptonic radiative mode $B \to B'\gamma$[12]. In this case one can write the most general decay amplitude as

$$\begin{aligned} \text{Amp} &= \frac{e}{M_B + M_{B'}} \epsilon^{*\mu} q^\nu \\ &\times \ \bar{u}(p') \left(-i\sigma_{\mu\nu} C - i\sigma_{\mu\nu}\gamma_5 D\right) u(p) \end{aligned} \tag{8}$$

(a) (b)

Figure 2. Pole diagrams used to calculate radiative hyperon decay.

where $C$ is the magnetic dipole (parity conserving) amplitude and $D$ is its (parity conserving) electric dipole counterpart. There are two quantities of interest in the analysis of such decays—the decay rate and photon asymmetry, which go as

$$\Gamma \sim |C|^2 + |D|^2, \quad A_\gamma = \frac{2\mathrm{Re}C^* D}{|C|^2 + |D|^2} \qquad (9)$$

The difficulty here is associated with "Hara's Theorem" which requires that in the SU(3) limit the parity violating decay amplitude must vanish for decay between states of a common U-spin multiplet—*i.e.* $\Sigma^+ \to p\gamma$ and $\Xi \to \Sigma^-\gamma$[13]. (The proof here is very much analogous to the one which requires the vanishing of the axial tensor form factor in nuclear beta decay between members of a common isotopic spin multiplet[14].) Since one does not expect significant SU(3) breaking effects, we anticipate a relatively small photon asymmety parameter for such decays. However, in the case of $\Sigma^+ \to p\gamma$ the asymmetry is known to be large and negative[15]

$$A_\gamma(\Sigma^+ \to p\gamma) = -0.76 \pm 0.08 \qquad (10)$$

and for thirty years theorists have been struggling to explain this result. In leading order the amplitude is given by the simple pole diagrams, with the weak baryon-baryon matrix elements being those determined in the nonradiative decay analysis. The Lee-Swift theorem asserts that such matrix elements must be purely parity conserving in the SU(3) limit and this is the origin of Hara's theorem in such a model[7]. Although SU(3) breaking corrections have been calculated, none is large enough to explain the experimental result—Eq. 10[16]. As in the case of the S/P-wave puzzle, what is clearly required is the inclusion of additional physics and here too the inclusion of $(70, 1^-)$ states by Le Youaunc et al.[9] or of $\frac{1}{2}^-$ and $\frac{1}{2}^+$ resonant states in a chiral framework by Borasoy and myself[17] appears to naturally predict a large negative asymmetry. However, in order to confirm the validity of these or any model what will be required is a set of measurements of *both* rates and asymmetries for such decays. In this regard, it should be noted that theoretically one expects all asymmetries to be negative in any realistic model[18]. It would be very difficult to accomodate a large positive asymmetry. Thus the present particle data group listing[15]

$$A_\gamma(\Xi^0 \to \Lambda\gamma) = +0.43 \pm 0.44 \qquad (11)$$

deserves to be carefully remeasured.

### 2.3. Hyperon Beta Decay

A mode that theory does well in predicting (in fact some would say *too* well) is that of hyperon beta decay—$B \to B'\ell\nu_\ell$, where $\ell$ is either an electron or a muon. Since this is a semileptonic weak interaction, the decays are described in general by matrix elements of the weak vector, axial-vector currents

$$\begin{aligned} < B'|V_\mu|B > &= \bar{u}(p')(f_1\gamma_\mu + \frac{-if_2}{M_B + M_{B'}}\sigma_{\mu\nu}q^\nu \\ &+ \frac{f_3}{M_B + M_{B'}}q_\mu)u(p) \\ < B'|A_\mu|B > &= \bar{u}(p')(g_1\gamma_\mu + \frac{-ig_2}{M_B + M_{B'}}\sigma_{\mu\nu}q^\nu \\ &+ \frac{g_3}{M_B + M_{B'}}q_\mu)\gamma_5 u(p) \end{aligned} \qquad (12)$$

Here the dominant terms are the vector, axial couplings $f_1, g_1$ and the standard approach is simple Cabibbo theory, wherein one fits the $g_1$ in terms of SU(3) F,D coefficients and $f_1$ using CVC and simple F coupling. When this is done, one finds in general a very satisfactory fit—$\chi^2/d.o.f \sim 2.0$—which can be made even better by inclusion of simple quark model SU(3) breaking effects—$\chi^2/d.o.f. \sim 0.85$[19]. An output of such a fit is the value of the KM mixing parameter $V_{us} = 0.220 \pm 0.003$, which is in good agreement with the value $V_{us} = 0.2196 \pm 0.0023$ measured in $K_{e3}$ decay. However, differing assumptions about SU(3) breaking will lead to slightly modified values.

The importance of such a measurement of $V_{us}$ has to do with its use as an input to a test of the standard model via the unitarity prediction

$$|V_{ud}|^2 + |V_{us}|^2 + |V_{ub}|^2 = 1 \qquad (13)$$

From an analysis of B-decay one obtains $|V_{ub}| \sim 0.003$, which when squared leads to a negligible contribution to the unitarity sum. So the dominant effect comes from $V_{ud}$, which is measured via $0^+ - 0^+$ superallowed nuclear beta decay—

$$V_{ud}^2 = \frac{2\pi^3 \ln 2 m_e^{-5}}{2G_F^2(1+\Delta_R^V)\bar{\mathcal{F}}t} \tag{14}$$

Here $\Delta_R^V = 2.40 \pm 0.08\%$ is the radiative correction and $\bar{\mathcal{F}}t = 3072.3 \pm 0.9$ sec. is the mean (modified) ft-value for such decays. Of course, there exist important issues in the analysis of such ft-values including the importance of isotopic spin breaking effects and of possible Z-dependence omitted from the radiative corrections, but if one takes the above-quoted number as being correct we obtain[20]

$$V_{ud} = 0.9740 \pm 0.0005$$
$$\text{and}$$
$$|V_{ud}|^2 + |V_{us}|^2 + |V_{ub}|^2 = 0.9968 \pm 0.0014 \tag{15}$$

which indicates a possible violation of unitarity. If correct, this would suggest the existence of non-standard-model physics, but clearly additional work, both theoretical and experimental, is needed before drawing this conclusion.

What is needed in the case of hyperon beta decay is good set of data including rates *and* asymmetries, both in order to produce a possibly improved value of $V_{us}$ but also to study the interesting issue of SU(3) breaking effects, which *must* be present, but whose effects seem somehow to be hidden. A related focus of such studies should be the examination of higher order—recoil—form factors such as weak magnetism ($f_2$) and the axial tensor ($g_2$). In the latter case, Weinberg showed that in the standard quark model $G = C\exp(i\pi I_2)$-invariance requires $g_2 = 0$ in neutron beta decay $n \to pe^-\bar{\nu}_e$[21]. (This result usually is called the stricture arising from "no second class currents.") In the SU(3) limit one can use V-spin invariance to show that $g_2 = 0$ also obtains for $\Delta S = 1$ hyperon beta decay, but in the real world this condition will be violated. A simple quark model calculation suggests that $g_2/g_1 \sim -0.2$[22] but other calculations, such as a recent QCD sum rule estimate give a larger number—$g_2/g_1 \sim -0.5$. In any case good hyperon beta decay data—with rates and asymmetries—will be needed in order to extract the size of such effects.

### 2.4. Hyperon Polarizabilities

Since this subject is not familiar to many physicists, let me spend just few moments giving a bit of motivation. The idea goes back to simple classical physics. Parity and time reversal invariance, of course, forbid the existence of a permanent electric dipole moment for an elementary system. However, consider the application of a uniform electric field to a such a system. Then the positive charges will move in one direction and negative charges in the other—*i.e.* there will be a charge separation and an electric dipole moment will be induced. The size of the edm will be proportional to the applied field and the constant of proportionality between the applied field and the induced dipole moment is the electric polarizability $\alpha_E$

$$\vec{p} = 4\pi\alpha_E \vec{E} \tag{16}$$

The interaction of this dipole moment with the field leads to an interaction energy

$$U = -\frac{1}{2}\vec{p}\cdot\vec{E} = -\frac{1}{2}4\pi\alpha_E\vec{E}^2, \tag{17}$$

where the "extra" factor of $\frac{1}{2}$ compared to elementary physics result is due to the feature that the dipole moment is *induced*. Similarly in the presence of an applied magnetizing field $\vec{H}$ there will be generated an induced magnetic dipole moment

$$\vec{\mu} = 4\pi\beta_M\vec{H} \tag{18}$$

with interaction energy

$$U = -\frac{1}{2}\vec{\mu}\cdot\vec{H} = -\frac{1}{2}4\pi\beta_M\vec{H}^2. \tag{19}$$

For wavelengths large compared to the size of the system, the effective Hamiltonian describing the interaction of a system of charge $e$ and mass $m$ with an electromagnetic field is, of course, given by

$$H^{(0)} = \frac{(\vec{p} - e\vec{A})^2}{2m} + e\phi, \tag{20}$$

and the Compton scattering cross section has the simple Thomson form

$$\frac{d\sigma}{d\Omega} = \left(\frac{\alpha_{em}}{m}\right)^2\left(\frac{\omega'}{\omega}\right)^2[\frac{1}{2}(1+\cos^2\theta)], \tag{21}$$

where $\alpha_{em}$ is the fine structure constant and $\omega, \omega'$ are the initial, final photon energies respectively. As the energy increases, however, so does the resolution and one must also take into account polarizability effects, whereby the effective Hamiltonian becomes

$$H_{\text{eff}} = H^{(0)} - \frac{1}{2}4\pi(\alpha_E\vec{E}^2 + \beta_M\vec{H}^2). \tag{22}$$

The Compton scattering cross section from such a system (taken, for simplicity, to be spinless) is then

$$\begin{aligned}\frac{d\sigma}{d\Omega} &= \left(\frac{\alpha_{em}}{m}\right)^2\left(\frac{\omega'}{\omega}\right)^2\left(\frac{1}{2}(1+\cos^2\theta)\right. \\ &- \frac{m\omega\omega'}{\alpha_{em}}[\frac{1}{2}(\alpha_E+\beta_M)(1+\cos\theta)^2 \\ &+ \left.\frac{1}{2}(\alpha_E-\beta_M)(1-\cos\theta)^2]\right) \qquad (23)\end{aligned}$$

It is clear from Eq. 23 that from careful measurement of the differential scattering cross section, extraction of these structure dependent polarizability terms is possible provided

i) that the energy is large enough that these terms are significant compared to the leading Thomson piece and

ii) that the energy is not so large that higher order corrections become important.

In this fashion the measurement of electric and magnetic polarizabilities for the proton has recently been accomplished at SAL and at MAMI using photons in the energy range 50 MeV $< \omega <$ 100 MeV, yielding[23] [2]

$$\begin{aligned}\alpha_E^p &= (12.1 \pm 0.8 \pm 0.5) \times 10^{-4}\ \mathrm{fm}^3 \\ \beta_M^p &= (2.1 \mp 0.8 \mp 0.5) \times 10^{-4}\ \mathrm{fm}^3. \qquad (24)\end{aligned}$$

Note that in practice one generally exploits the strictures of causality and unitarity as manifested in the validity of the forward scattering dispersion relation, which yields the Baldin sum rule[27]

$$\begin{aligned}\alpha_E^{p,n} &+ \beta_M^{p,n} = \frac{1}{2\pi^2}\int_0^\infty \frac{d\omega}{\omega^2}\sigma_{\mathrm{tot}}^{p,n} \\ &= \begin{cases}(13.69 \pm 0.14) \times 10^{-4}\mathrm{fm}^3 & \text{proton} \\ (14.40 \pm 0.66) \times 10^{-4}\mathrm{fm}^3 & \text{neutron}\end{cases} \qquad (25)\end{aligned}$$

as a rather precise constraint because of the small uncertainty associated with the photoabsorption cross section $\sigma_{\mathrm{tot}}^p$.

As to the meaning of such results we can compare with the corresponding calculation of the electric polarizability of the hydrogen atom, which yields[28]

$$\alpha_E^H = \frac{9}{2}a_0^2 \quad \text{vs.} \quad \alpha_E^p \sim 10^{-3} < r_p^2 >^{\frac{3}{2}} \qquad (26)$$

[2]Results for the neutron extracted from $n - Pb$ scattering cross section measurements have been reported[24], but have been questioned[25]. Extraction via studies using a deuterium target may be possible in the future[26].

where $a_0$ is the Bohr radius. Thus the polarizability of the hydrogen atom is of order the atomic volume while that of the proton is only a thousandth of its volume, indicating that the proton is much more strongly bound.

The relevance to our workshop is that the polarizability of a hyperon can also be measured using Compton scattering, via the reaction $B+Z \to B+Z+\gamma$ extrapolated to the photon pole—*i.e.* the Primakoff effect. Of course, this is only feasible for charged hyperons—$\Sigma^\pm, \Xi^-$, and the size of such polarizabilities predicted theoretically are somewhat smaller than that of the proton[29]

$$\alpha_E^{\Sigma^+} \sim 9.4 \times 10^{-4}\,\mathrm{fm}^3, \qquad \alpha_E^{\Xi^-} \sim 2.1 \times 10^{-4}\,\mathrm{fm}^3 \qquad (27)$$

but their measurement would be of great interest.

### 2.5. Polarization and Hyperon Production

My final topic will be that of polarization in strong interaction production of hyperons, a field that began here at FNAL in 1976 with the discovery of $\Lambda$ polarization in the reaction[30]

$$p(300\ \mathrm{GeV}) + Be \to \vec{\Lambda} + X \qquad (28)$$

This process has been well studied in the intervening years[31] and we now know that in the fragmentation region the polarization is large and negative—$\vec{P}\cdot\hat{p}_{inc}\times\hat{p}_\Lambda < 0$—and that it satisfies scaling, *i.e.* is a function only of $x_F = \frac{p_\Lambda^\parallel}{p_p}, p_\Lambda^\perp$ and not of the center of mass energy . Various theoretical approaches have been applied in order to try to understand this phenomenon—*e.g.*, Soffer and Törnqvist have developed a Reggized pion exchange picture[32], while DeGrand, Markkanen, and Miettinen have used a quark-parton approach wherein the origin of the polarization is related to the Thomas precession[33]—but none can be said to be definitive. One thing which seems to be clear is that there exists a close connection with the large negative polarizations seen in inclusive hyperon production and the large positive analyzing powers observed at FNAL in inclusive meson production with polarized protons[34]

$$\vec{p} + p \to \pi^+ + X \qquad (29)$$

Another input to the puzzle may be the availability in the lower energy region of new exclusive data from Saturne involving[35]

$$\vec{p} + p \to p + \vec{\Lambda} + K^+ \qquad (30)$$

which seems best described in terms of a kaon exchange mechanism. Clearly there is much more to do in this field.

## 3. Summary

I conclude by noting that, although the first hyperon was discovered more then half a century ago and much work has been done since, the study of hyperons remains an interesting and challenging field. As I have tried to indicate above, many questions exist as to their strong, weak, and electromagnetic interaction properties, and I suspect that these particles will remain choice targets for particle hunters well into the next century.

## REFERENCES


1. See, *e.g.*, **Dynamics of the Standard Model**, J.F. Donoghue, E. Golowich, and B.R. Holstein, Camabridge University Press, New York (1992).
2. F. Gilman and M. Wise, Phys. Rev. **D20** (1979) 2392.
3. J. Pati and C.Woo, Phys. Rev. **D3** (1971) 2920; K. Muira and T. Minamikawa, Prog. Theor. Phys. **38** (1967) 954; J. Körner, Nucl. Phys. **B25** (1970) 282.
4. See, *e.g.* G. Buchalla, A.J. Buras, and M.E. Lautenbacher, Rev. Mod. Phys. **68** (1996) 1125; J. Bijnens, hep-ph/9907514.
5. See, *e.g.* J.F. Dubach, G.B. Feldman, B.R. Holstein, and L. de la Torre, Ann. Phys. (NY) **249** (1996) 146.
6. See, *e.g.* J.F. Dubach, G.B. Feldman, B.R. Holstein, and L. de la Torre, Ann. Phys. (NY), **249** (1996) 146.
7. B.W. Lee and A. Swift, Phys. Rev. **136** (1964) B228.
8. J.F. Donoghue, E. Golowich, and B.R. Holstein, Phys. Rept. **131** (1986) 319.
9. A. Le Yaouanc et al., Nucl. Phys. **B149** (1979) 321.
10. B. Borasoy and B.R. Holstein, Phys. Rev. **D59** (1999) 054025.
11. J.F. Donoghue, X.G. He, and S. Pakvasa, Phys. Rev. **D34** (1986) 833; S. Pakvasa, hep-ph/9910232.
12. See, *e.g.* J. Lach and P. Zencykowski, Int. J. Mod. Phys. **A10** (1995) 3817.
13. Y. Hara, Phys. Rev. Lett. 12 (1964) 378; R.H. Graham and S. Pakvasa, Phys. Rev. **140** (1965) B1144.
14. B.R. Holstein and S.B. Treiman, Phys. Rev. **C3** (1971) 1921.
15. Particle Data Group, Phys. Rev. **D54** (1996) 1.
16. See, *e.g.*, E. Golowich and B.R. Holstein, Phys. Rev. **D26** (1982) 182.
17. B. Borasoy and B.R. Holstein, Phys. Rev. **D59** (1999) 054019.
18. I am very grateful to P. Zencykowski for a discussion of this point.
19. See, *e.g.*, J.F. Donoghue, B.R. Holstein, and S. Klimt, Phys. Rev. **D35** (1987) 934; R. Flores-Mendieta, A. Garcia, and G. Sanchez-Colon, Phys. Rev. **D54** (1996) 6855.
20. J. Hardy and I. Towner,nucl-th/9807049.
21. S. Weinberg, Phys. Rev. **112** (1958) 1375.
22. , J.F. Donoghue and B.R. Holstein, Phys. Rev. **D25** (1982) 206.
23. F.J. Federspiel et al., Phys. Rev. Lett. **67** (1991) 1511; A.L. Hallin et al., Phys. Rev. **C48** (1993) 1497; A. Zieger et al., Phys. Lett. **B278** (1992) 34; B.E. MacGibbon et al., Phys. Rev. **C52** (1995) 2097.
24. J. Schmiedmayer et al., Phys. Rev. Lett. **66** (1991) 1015.
25. L. Koester, Phys. Rev. **C51** (1995) 3363.
26. S. Beane, M. Malheiro, D.R. Phillips, and U. van Kolck, Nucl. Phys. **A656** (1999) 367.
27. D. Babusci, G. Giordano, and G. Matone, Phys. Rev. **C57** (1998) 291.
28. E. Merzbacher, **Quantum Mechanics**, Wiley, Nw York (1998), Ch. 18.
29. V. Bernard, N. Kaiser, J. Kambor, and U.-G. Meissner, Phys. Rev. **D46** (1992) 2756.
30. A. Lesnik et al., Phys. Rev. Lett **35** (1975) 770; G. Bunce et al., Phys. Rev. Lett. **36** (1976) 1113.
31. K. Heller, in **Proc. Intl. Symposium on Spin Physics, Amsterdam, 1996**, World Scientific, Singapore (1997).
32. J. Soffer and N.A. Tornqvist, Phys. Rev. Lett. **68** (1992) 907.
33. T.A. DeGrand, J. Markkanen, and H.I. Miettinen, Phys. Rev. **D32** (1985) 2445.
34. L. Zuo-tang and C. Boros, Phys. Rev. Lett. **79** (1997) 3608.
35. F. Balestra et al., Phys. Rev. Lett. **83** (1999) 1534.

# Chapter 2

# New Results

- D. Christian
- M. Purohit
- H. Krueger
- E. McCliment
- L. Landsberg
- J. Tandean
- S. Bright
- G. Karl
- V.J. Smith
- J.C. Anjos
- A. Erwin

# $\Lambda^0$ Polarization in 800 GeV/c $pp \to p_f(\Lambda^0 K^+)$

J. Félix [a], M.C. Berisso [b], D.C. Christian [c], A. Gara [d], E.E. Gottschalk[c], G. Gutierrez[c], E.P. Hartouni [e], B.C. Knapp[d], M.N. Kreisler[b], S. Lee[b], K. Markianos[b], G. Moreno[a], M.A. Reyes[a], M. Sosa[a], M.H.L.S. Wang[b,e], A. Wehmann[c], D. Wesson[b]

[a]Universidad de Guanajuato, León, Guanajuato, México

[b]University of Massachusetts, Amherst, Massachusetts, USA

[c]Fermilab, Batavia, Illinois, USA

[d]Columbia University, Nevis Laboratory, New York, USA

[e]Lawrence Livermore National Laboratory, Livermore, California, USA

We report preliminary results from a study of $\Lambda^0$ polarization in the exclusive reaction $pp \to p_f(\Lambda^0 K^+)$ at 800 GeV/c. These data are a part of the $5 \times 10^9$ diffractive event sample collected by Fermilab E690. We observe a large dependence of the polarization on the $\Lambda^0 K^+$ invariant mass. This observation confirms the result of the CERN ISR R608 experiment and extends the range over which the effect is observed.

## 1. INTRODUCTION

The polarization of $\Lambda^0$ hyperons at high energy is well established [1]. Most of the experimental observations at high energy have been of *inclusive* $\Lambda^0$ production. Despite this work, an understanding of the source of the polarization remains elusive. Several experiments have measured $\Lambda^0$ polarization in *exclusive* events [2–6]. The main motivation of these studies is the hope that important clues might be uncovered regarding the origin of the polarization by studies of specific final states.

We report here the preliminary results of a study of $\Lambda^0$ polarization in the diffractive reaction:

$$pp \to p_f(\Lambda^0 K^+), \tag{1}$$

at a beam momentum of 800 GeV/c. These data were collected by Fermilab E690 during the 1991 fixed target run using a multiparticle spectrometer located in Lab G of the Neutrino Lab in conjunction with a beam spectrometer system. A detailed description of this apparatus can be found in [4]. In what follows we will discuss the method used to isolate the particular final state, delineate the procedure for determining the $\Lambda^0$ polarization and present the polarization measured in this analysis.

## 2. EXCLUSIVE EVENTS

This analysis of E690 data is performed after the track and vertex reconstruction stage of the data analysis. The $2.4 \times 10^9$ events used in this analysis represent roughly 50% of the total data sample. A further selection requires: that the event has 3 reconstructed tracks, that both a primary and secondary vertex are reconstructed, that the secondary vertex is uniquely identified as a $\Lambda^0 \to p\pi^-$ decay, that the secondary vertex points back to the primary vertex and that the third charged particle is also assigned to the primary and has a positive charge. Another requirement of the event is that the outgoing "fast" proton ($p_f$) is reconstructed in the beam spectrometer system and has interacted in the target. The above selection reduces the sample size to 87,233 events.

An additional selection is performed on this reduced sample. Two event variables are used: $(\Delta p_T)^2$, the square of the difference of the initial beam $\mathbf{p_T}$ and the sum of the final state particle $\mathbf{p_T}$, and $\Delta(E - p_L)$, the difference of the initial $E - p_L$ and the sum of the final state $E - p_L$. These two variables should be zero if energy and momentum are conserved in the event, *i.e.* if all of the particles in the event have been observed. The exclusive isolation cuts are: $(\Delta p_T)^2 < 0.001$ $(\mathrm{GeV/c})^2$ and $-0.020$ GeV $< \Delta(E - p_L) < 0.015$ GeV. Figure 1 and figure 2 show the distributions of these variables before and after the cuts. These

plots also indicate that backgrounds from other event topologies are small. The final sample size is 17,683 events.

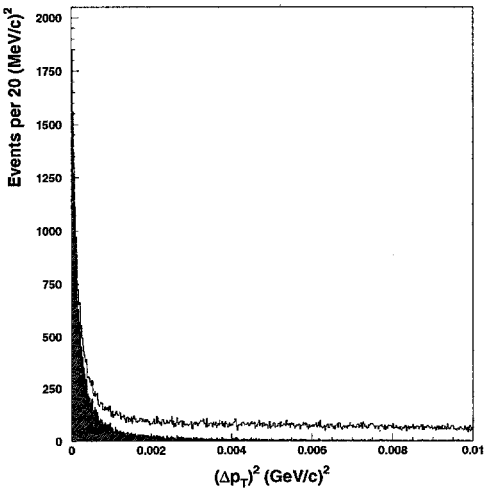


Figure 1. The $(\Delta \mathbf{p_T})^2$ distribution before (open) and after (shaded) the $\Delta(E - p_L)$ cut.

## 3. POLARIZATION MEASUREMENT

The polarization of the $\Lambda^0$ is determined by a linear fit to the $cos\theta$ distribution of the proton decay direction with respect to the normal vector to the $\Lambda^0$ production plane in the $\Lambda^0$ center-of-mass. This normal vector has the standard definition:

$$\hat{n} \equiv \frac{\vec{P}_{beam} \times \vec{P}_\Lambda}{|\vec{P}_{beam} \times \vec{P}_\Lambda|} \tag{2}$$

where $\vec{P}_{beam}$ and $\vec{P}_\Lambda$ are the momentum vector of the incident beam proton and of the $\Lambda^0$, respectively. The angular distribution of the proton has the following dependence on the $\Lambda^0$ polarization:

$$\mathrm{dN/d\Omega} = N_0(1 - \alpha \mathcal{P} cos\theta), \tag{3}$$

where $\alpha$ is the decay asymmetry parameter (equal to $0.642 \pm 0.013$ [7]) and $\mathcal{P}$ is the $\Lambda^0$ polarization (note the sign change which accounts for the fact that the $\Lambda^0$ is part of the target fragmentation). A Monte Carlo simulation has been run to correct the effect of the finite detector acceptance of the apparatus. The resulting fits of the $cos\theta$ distributions before and after the corrections agree.

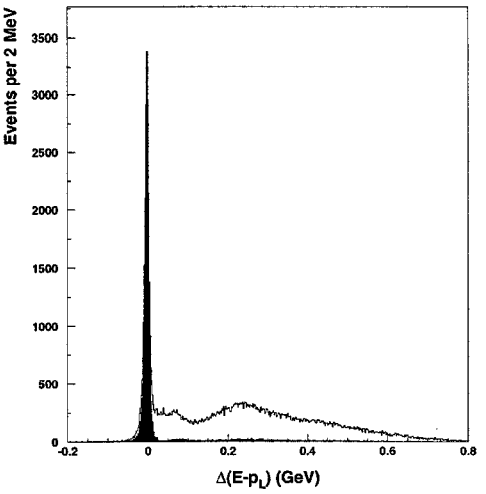


Figure 2. The $\Delta(E - p_L)$ distribution before (open) and after (shaded) the $(\Delta \mathbf{p_T})^2$ cut.

The $cos\theta$ distribution for a particular kinematic bin ($-0.85 < x_F < -0.75$ and $0.3 < p_T < 0.5$ GeV/c) is shown in figure 3 before and after correction.

## 4. RESULTS

The data are binned as a function of $\Lambda^0$ $x_F$ and $|\mathbf{p_T}|$ and the polarization is determined for the $\Lambda^0$'s in each bin. The data distribution in these variables is shown in figure 4. Table 1 shows bins with large *positive* polarization which is quite surprising in view of the measurements using inclusive $\Lambda^0$'s. The standard empirical functions used to describe $\Lambda^0$ polarization dependence on $x_F$ and $|\mathbf{p_T}|$ would not adequately describe these data. Interpreting the reactions to be of the form:

$$pp \rightarrow pX \tag{4}$$

with the $X$ system subsequently "decaying" to $\Lambda^0 K^+$ implies that there are two kinematic degrees of freedom to describe the dynamics of the reaction. We choose the perpendicular momentum, $|\mathbf{p_T}|$ and the mass, $M_X$ of the $X$ system. These distributions are shown in figure 5 and figure 6. Note that the distribution in $|\mathbf{p_T}|$ is indicative of the diffractive nature of these events, *i.e.* forward peaking of the scattered beam proton. We then bin the data in $M_X$ and perform the polarization analysis; the result is found in table 2. These results are plotted along with those

Table 1
$\Lambda^0$ polarization %

| | $x_F$ bins | | | |
|---|---|---|---|---|
| $p_T$ bins GeV/c | $-0.95 \rightarrow -0.85$ | $-0.85 \rightarrow -0.75$ | $-0.75 \rightarrow -0.65$ | $-0.65 \rightarrow -0.55$ |
| $0.0 \rightarrow 0.1$ | | $24 \pm 13$ | $-17 \pm 18$ | |
| $0.1 \rightarrow 0.3$ | $7 \pm 13$ | $35 \pm 4$ | $38 \pm 5$ | $23 \pm 14$ |
| $0.3 \rightarrow 0.5$ | $18 \pm 37$ | $58 \pm 6$ | $27 \pm 5$ | $2 \pm 12$ |
| $0.5 \rightarrow 0.8$ | | $67 \pm 14$ | $21 \pm 9$ | $-8 \pm 15$ |
| $0.8 \rightarrow 3.0$ | | $-35 \pm 25$ | $-49 \pm 13$ | $-53 \pm 17$ |

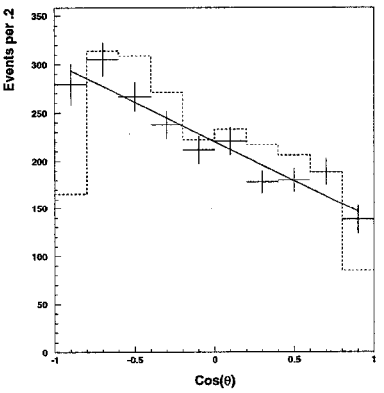


Figure 3. $cos\theta$ distribution for $-0.85 < x_F < -0.75$ and $0.3 < p_T < 0.5$ GeV/c before (dashed) and after (points with error bars) acceptance correction. Line is the result of a fit to (3).

from [2] in figure 7.

Table 2
$\Lambda^0$ polarization %

| | |
|---|---|
| $1.5 < M_X < 1.7$ GeV/c$^2$ | $63 \pm 5$ |
| $1.7 < M_X < 1.8$ GeV/c$^2$ | $30 \pm 4$ |
| $1.8 < M_X < 1.95$ GeV/c$^2$ | $24 \pm 5$ |
| $1.95 < M_X < 2.2$ GeV/c$^2$ | $20 \pm 6$ |
| $2.2 < M_X < 2.5$ GeV/c$^2$ | $2 \pm 8$ |
| $2.5 < M_X < 2.8$ GeV/c$^2$ | $-37 \pm 11$ |
| $2.8 < M_X < 5.0$ GeV/c$^2$ | $-67 \pm 13$ |

## 5. DISCUSSION

The dependence of the $\Lambda^0$ polarization on $M_X$ seen in our results and in those of R608 suggests that more can be learned about the origin of the polarization by studying the production dynamics of the $X$ system (in this case, the $\Lambda^0 K^+$ two particle system). The large variation of the polarization over the kinematic range of the E690 data set and the high statistics of the data set should allow more detailed studies of the polarization. In particular it may be possible to investigate the polarization dependence on the angular momentum states of the two particle final state. Work on other exclusive final states (e.g. $\Lambda^0 K^0_s \pi^+$) may also provide additional information regarding the nature of $\Lambda^0$ polarization in high energy hadronic reactions.

## 6. ACKNOWLEDGEMENTS

We acknowledge the superb efforts by the staffs at the University of Massachusetts, Columbia University, Fermilab and Lawrence Livermore National Laboratory. This work was supported in part by National Science Foundation Grants No. PHY90-14879 and No. PHY89-21320, by the Department of Energy Contracts No. DE-AC02-76 CHO3000, No. DE-AS05-87ER40356 and No. W-7405-ENG-48, and by CoNaCyT of México under Grants 1061-E9201, 458100-5-3793E, and 458100-5-4009PE.

## REFERENCES

1. L. G. Pondrom, Phys. Rep. **122**, 57 (1985).
2. T. Henkes *et al.*, Phys. Lett. **B 283**, (1992) 155.
3. J. Félix, Ph.D. thesis, Universidad de Guanajuato, México, 1994.
4. S. Lee, Ph.D. thesis, University of Massachusetts, Amherst, 1994.
5. J. Félix *et al.*, Phys. Rev. Lett. **76**, 22 (1996).
6. J. Félix *et al.*, Phys. Rev. Lett. **82**, 5213 (1999).
7. Particle Data Group, Phys. Rev. **D 50**, 1 (1994).

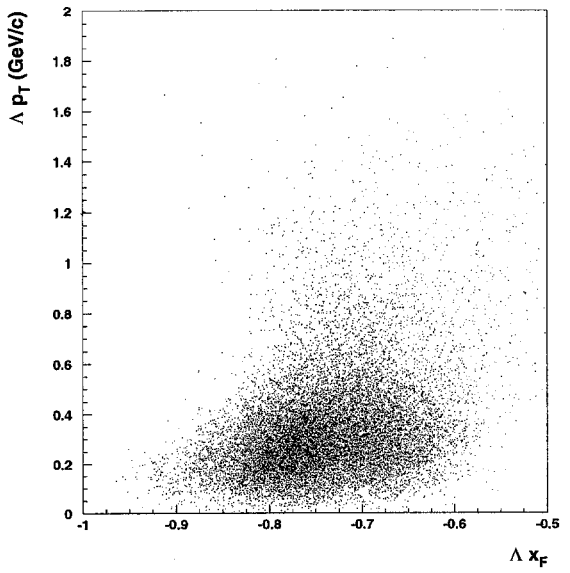


Figure 4. $x_F$ *vs.* $|\mathbf{p_T}|$ for $\Lambda^0$'s in the exclusive sample.

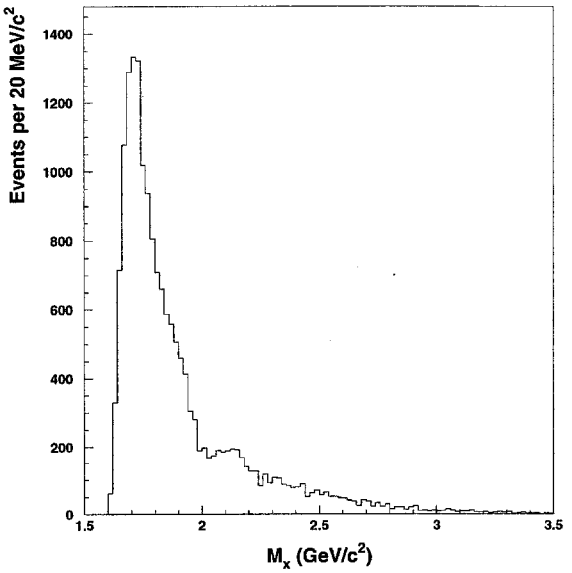


Figure 6. $M_X$ distribution.

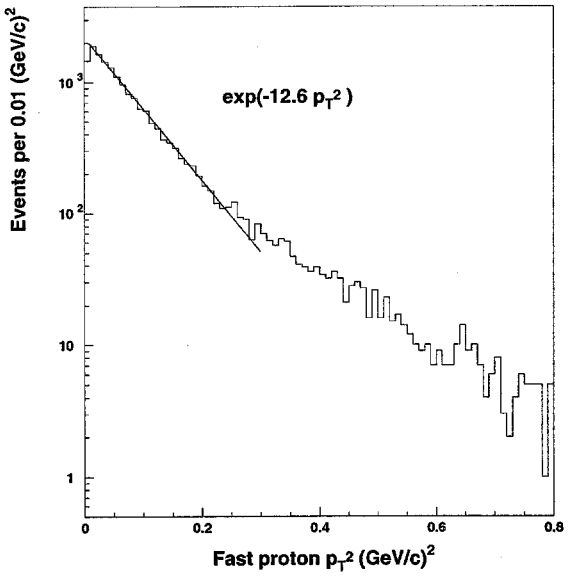


Figure 5. Fast proton $p_T^2$ distribution.

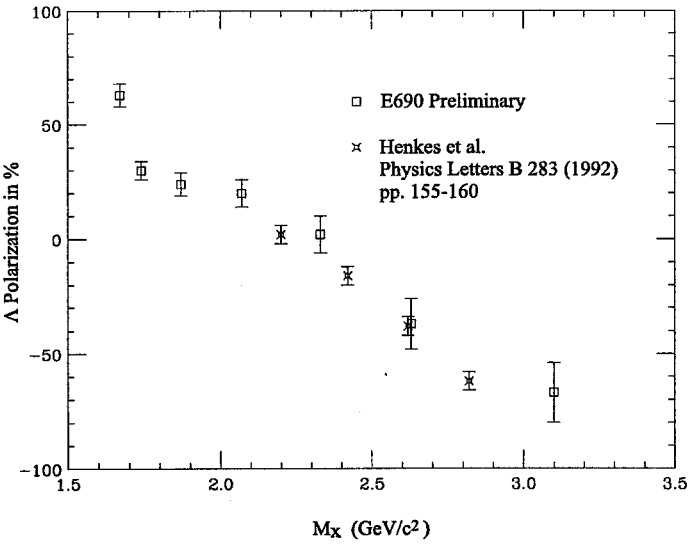


Figure 7. $\Lambda^0$ polarization as a function of $M_X$.

# Resonances in $\Lambda_c^+ \to pK^-\pi^+$ Decays and $\Lambda_c^+$ Polarization

M. V. Purohit [a]

[a]Dept. of Physics & Astronomy,
Univ. of South Carolina, SC 29208

We describe a recent analysis of $\Lambda_c^+ \to pK^-\pi^+$ decays using Fermilab experiment E791 data. Since this charm baryon carries spin it may be polarized when produced. A measurement of this polarization is reported and is in agreement with recent predictions[1]. We use the spin of the $\Lambda_c^+$ and that of the decay proton to do a fully coherent five-dimensional analysis of these decays. The analysis also yields the fit fractions for $\Lambda_c^+$ decays into the nonresonant mode and into the modes $\mathrm{p\overline{K}^{*0}}(890)$, $\Delta^{++}(1232)\mathrm{K}^-$ and and $\Lambda(1520)\pi^+$. Suggestions for further analysis are included.

## 1. Introduction

While charm baryon lifetimes and branching fractions have been measured in the past, these measurements are not as complete as for charm mesons[2]. For instance, there has been no amplitude analysis of any charm baryon decay. The most obvious components of the $\Lambda_c^+ \to \mathrm{pK}^-\pi^+$ decays (and charge conjugate decays, which are implied throughout this paper) include the nonresonant $\mathrm{pK}^-\pi^+$ decay, and the $\mathrm{p\overline{K}^{*0}}(890)$ and $\Lambda(1520)\pi^+$ two-body decays. These three decays can be described by spectator and W-exchange amplitudes. However, in lowest order, the $\Delta^{++}(1232)\mathrm{K}^-$ decay can occur only via the exchange amplitude. Thus, a significant presence of $\Delta^{++}(1232)\mathrm{K}^-$ decays would indicate that exchange amplitudes are important, unlike in charm meson decays where they are suppressed because helicity and form-factor effects. These effects are not expected to inhibit exchange amplitudes for charm baryons due to the three-body nature of the interaction.

The $\Lambda_c^+$ and its decay product the proton carry spin and the $\Lambda_c^+$ may be polarized upon production. Dalitz analyses of charm meson decays have studied structure in the two-dimensional space of the decay product effective masses. However, the spin effects just described require five kinematic variables for a complete description. Although this complicates the analysis, it affords greater sensitivity to the parameters of interest. As a by-product of the analysis, the production polarization of the $\Lambda_c^+$, $\mathbf{P}_{\Lambda_c}$, is also measured. This analysis is unique because it is the first five-dimensional amplitude analysis.

## 2. Experiment E791 at Fermilab

Fermilab E791 is a fixed-target pion-production charm collaboration representing over 17 institutions. Over 20 billion events were collected during 1991-92 and analyses of these data are now almost complete. The experiment used a segmented target with five thin foils (each about 1.2 mm thick) with about 1.5 cm center-to-center separation. With this target configuration and with 23 planes of silicon detectors we were able to suppress the large backgrounds due to combinatorics and secondary interactions. Complementing this vertex detector is a complete 2-magnet spectrometer with 35 planes of drift chambers and with Cherenkov detectors and calorimeters for particle identification and energy measurement. A more complete description of the detector may be found in Refs. [3,4]. Analyses of these data have led to over 20 publications and should be complete in a couple of years.

## 3. Formalism

We parameterize the observed decay rate as a function of the $\Lambda_c^+$ polarization, $\mathbf{P}_{\Lambda_c}$, and of the magnitudes and relative phases of each intermediate two-body resonance decay amplitude. We assume that the nonresonant decay is described by an amplitude that is constant across phase space.

The differential decay rate $d\Gamma$ (or signal density $S$) may be expressed as

$$d\Gamma \sim S(\vec{x}) = \frac{(1+\mathbf{P}_{\Lambda_c})}{2}(|\sum_r B_r(m_r)\alpha_{r,\frac{1}{2},\frac{1}{2}}|^2 + |\sum_r B_r(m_r)\alpha_{r,\frac{1}{2},-\frac{1}{2}}|^2) \quad (1)$$

$$+\frac{(1-\mathbf{P}_{\Lambda_c})}{2}(|\sum_{\mathrm{r}} B_{\mathrm{r}}(m_{\mathrm{r}})\alpha_{\mathrm{r},-\frac{1}{2},\frac{1}{2}}|^2 \quad (2)$$

$$+|\sum_{\mathrm{r}} B_{\mathrm{r}}(m_{\mathrm{r}})\alpha_{\mathrm{r},-\frac{1}{2},-\frac{1}{2}}|^2) \quad (3)$$

where $\alpha_{\mathrm{r,m},\lambda_{\mathrm{p}}}$ is the complex decay amplitude for resonance r given $m$, the spin projection of the $\Lambda_{\mathrm{c}}$ on the z-axis, and $\lambda_{\mathrm{p}}$, the proton helicity in the $\Lambda_{\mathrm{c}}$ rest frame.

$B_{\mathrm{r}}(m_{\mathrm{r}})$ in Equation 3 is the normalized relativistic Breit-Wigner amplitude corrected for the centrifugal barrier[5]. Given the decay mode $\Lambda_{\mathrm{c}} \to \mathrm{r}(\to \mathrm{ab})\mathrm{c}$,

$$B_{\mathrm{r}}(m_{\mathrm{r}}) = (-2|p_c||p_a|)^L \frac{F_{\Lambda_{\mathrm{c}}} F_{\mathrm{r}}}{m_0^2 - m_{\mathrm{r}}^2 - im_0\Gamma_{\mathrm{r}}} \quad (4)$$

where

$$\Gamma_{\mathrm{r}} = \Gamma_0(\frac{q}{q_0})^{2L+1}\frac{m_0}{m_{\mathrm{r}}}\frac{F_{\mathrm{r}}^2(q)}{F_{\mathrm{r}}^2(q_0)} \quad (5)$$

for resonance r of angular momentum $L$ at the reconstructed two body mass $m_{\mathrm{r}}$ with the momentum $q$ (and $q_0$ when $m_{\mathrm{r}} = m_0$) of a daughter particle in the resonance's rest frame, and with resonance mass and width $m_0$ and $\Gamma_0$ as found in Ref. [2]. Using this convention, we set $B_{\mathrm{r}}(m_{\mathrm{r}})$ for the nonresonant decay to be 1.0. $F_L$ is the strong coupling factor at the appropriate decay vertex, and takes the Blatt-Weisskopf form as described in Table 1 below. Table 2 lists the range of the strong interaction, $R_X$.

Table 1
We list here the expressions for $F$ used in the Breit-Wigner amplitude.

| $L$ | $F_L$ |
|---|---|
| 0 | 1 |
| 1 | $(1+R_X^2q^2)^{-1/2}$ |
| 2 | $(9+3R_X^2q^2+R_X^4q^4)^{-1/2}$ |

We derived the helicity amplitudes for $\Lambda_c^+$ decays to various possible resonances. Unlike the simple case of mesons, each resonance typically has 4 (or sometimes 2) complex amplitudes associated with it.

Table 2
We list here the values of $R$ used in the Breit-Wigner amplitude.

| $X$ | $R_X$ $(\mathrm{GeV}/c^2)^{-1}$ |
|---|---|
| $\overline{K}^{*0}(890)$ | 3.4 [6] |
| $\Delta^{++}(1232)$ | 5.22 [7] |
| $\Lambda(1520)$ | 6.29 [8] |
| $\Lambda_c^+$ | 5.07 [9] |

Each event in the final data sample is described by five kinematic variables of interest (two two-body masses and the decay angles $\theta_{\mathrm{p}}$, $\phi_{\mathrm{p}}$, and $\phi_{\mathrm{K}\pi}$) which are determined after the pK$\pi$ reconstructed mass is constrained to the $\Lambda_{\mathrm{c}}$ mass. We chose the quantization axis (the z-axis in the $\Lambda_{\mathrm{c}}$ rest frame) to be normal to the $\Lambda_{\mathrm{c}}$ production plane (as defined by $\hat{p}_{\mathrm{beam}} \times \hat{p}_{\Lambda_{\mathrm{c}}}$, where $\hat{p}_{\mathrm{beam}}$ is the beam direction and $\hat{p}_{\Lambda_{\mathrm{c}}}$ is the $\Lambda_{\mathrm{c}}$ production direction in the lab frame). The x-axis in the $\Lambda_{\mathrm{c}}$ rest frame is chosen to be the direction of the $\Lambda_{\mathrm{c}}$ in the lab frame.

## 4. Selection of Data

After the initial selection of data using "cuts" on many variables reflections were removed from the data. This was done by explicitly cutting out events whose $K^-\pi^+\pi^+$ and $K^-K^+\pi^+$ masses lay within $2\sigma$ of the $D^+$ and $D_s^+$ masses. At this point the data were reduced to approximately 20,000 events. These were then passed through a neural net trained to further improve the significance of the signal. The final result of all these efforts is shown in Figure 1.

## 5. Fit to the data

The data were fit to a density which was the sum of a signal component and a background component. The signal component was the differential decay distribution described earlier times an acceptance function. The acceptance was determined by passing Monte Carlo events through the same filtering procedure as the data and fitting the resulting events. The background density was determined from the wings of the $pK^-\pi^+$ mass plot. Both the acceptance and the background were fit using a variation of the standard "nearest neighbors" technique and thus was a truly five-dimensional fit. The quality of the ac-

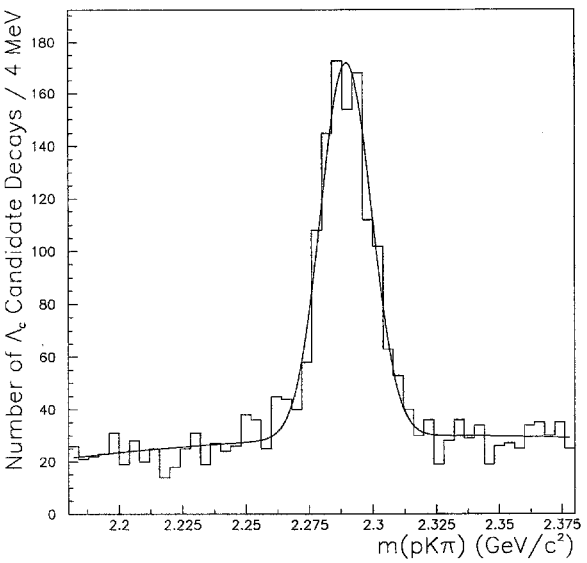


Figure 1. $\Lambda_c \to pK\pi$ signal being used in this analysis.

ceptance and background fits was demonstrated to be very good in the one- and two-dimensional projections as well as in five dimensions.

The results of the 34-parameter fit yielded the complex amplitudes and phases (the first nonresonant amplitude was held fixed) as well as the polarization and parameters of the shape of the mass distribution. Tables 3 and 4 below list the decay fractions and branching ratios of the important resonances that we fit to.

Table 3
The decay fractions for $\Lambda_c^+ \to pK^-\pi^+$ with statistical and systematic errors from the final fit.

| Mode | Fit Fraction (%) |
|---|---|
| $p\bar{K}^{*0}(890)$ | 19.5±2.6±1.8 |
| $\Delta^{++}(1232)K^-$ | 18.0±2.9±2.9 |
| $\Lambda(1520)\pi^+$ | 7.7±1.8±1.1 |
| Nonresonant | 54.8±5.5±3.5 |

Our results are compared to other published results in Table 4. Although we have better statistics than previous measurements, our uncertainties are comparable because of our more general fit.

The projections of the data and of the fit on the traditional $m^2$ variables as well as on the angular variables introduced by the spin-dependent 5-dimensional analysis show that we get had a good fit (the $\chi^2$/DF is 1.06). The only discrepancy between data and the fit is in the low $m^2_{pK}$ region. This may be due to the tail of a $\Lambda(1405)$ decaying to $pK^-$ (see Ref. [11]). We also searched for other resonances and found that the data weakly favor a $\frac{1}{2}^-$ resonance in $pK$ with mass 1556 ± 19 MeV/c$^2$ and width 279 ± 74 MeV/c$^2$. However, no such resonance is known to exist.

Table 4
$\Lambda_c$ branching ratios relative to the inclusive $\Lambda_c^+ \to pK^-\pi^+$ branching fraction. The NA32 values were calculated from one-dimensional projections only.

| Mode | E791 | NA32[10] |
|---|---|---|
| $p\bar{K}^{*0}(890)$ | $0.29\pm0.04\pm0.03$ | $0.35^{+0.06}_{-0.07}\pm0.03$ |
| $\Delta^{++}(1232)K^-$ | $0.18\pm0.03\pm0.03$ | $0.12^{+0.04}_{-0.05}\pm0.05$ |
| $\Lambda(1520)\pi$ | $0.15\pm0.04\pm0.02$ | $0.09^{+0.04}_{-0.03}\pm0.02$ |
| Nonresonant | $0.55\pm0.06\pm0.04$ | $0.56^{+0.07}_{-0.09}\pm0.05$ |

## 6. Polarization

In Figure 2 we show the result of measuring the polarization as a function of $p_T^2$. The average polarization $P$ for all our data is consistent with zero but there is a clear fall in $P$ as a function of $p_T^2$.

## 7. Conclusions

The size of our sample has allowed us to perform a fully coherent analysis of $\Lambda_c^+ \to pK^-\pi^+$ decays. The $\Delta(1232)^{++}K^-$ and $\Lambda(1520)\pi^+$ decay modes are observed in statistically significant amounts for the first time, even when uncertainties associated with phases and other variables are included. The observation of a substantial $\Delta^{++}K^-$ component provides strong evidence for the W-exchange amplitude in charm baryon decays. We find that the observed components of the $\Lambda_c^+ \to pK^-\pi^+$ decay do not interfere significantly. Finally, we find no evidence for either $\Lambda(1600)\pi^+$ or $\Sigma(1660)\pi^+$ in the data.

Despite the generally good fit there remains poor agreement of the fit model's pK-mass-squared projection with the data. Additional data from new experiments are needed in order to conclusively demonstrate additional resonances (or their tails).

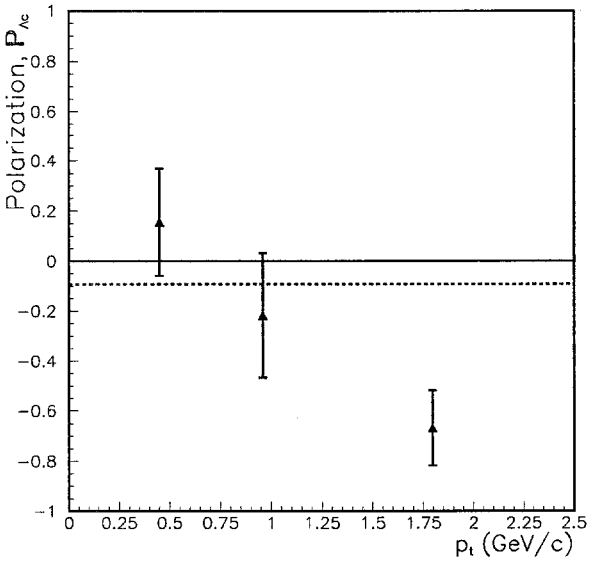


Figure 2. The polarization of the $\Lambda_c$ as a function of the $\Lambda_c$'s transverse momentum. The vertical bars represent the error as found by MINUIT. They are placed at the average $p_T^2$ value for that region. The bins are (in GeV/$c^2$): [0 – 0.71], [0.71 – 1.24] and [1.24 – 5.20]. The dotted line represents the value of the polarization when it was assumed constant for all data events.

Finally, we find evidence for an increasingly negative polarization of the $\Lambda_c$ baryons as a function of $p_T^2$, in agreement with a recent model[1]. As suggested by the authors of this model, the assumption of T-invariance leads to further constraints on resonant phases. Again, our data are consistent with these constraints but additional data from new experiments are needed for a stringent test of CP violation.

## 8. Acknowledgements

I would like to thank members of my collaboration (Fermilab E791) for sharing their results. This work was supported by a grant from the U.S. Department of Energy. Special thanks go to organizers of this conference and to Gary Goldstein for discussions of $\Lambda_c^+$ polarization.

## REFERENCES

1. W. G. D. Dharmaratna and G. R. Goldstein, Phys. Rev. D53 (1996) 1073. See also the LANL e-print hep-ph/9907573 by Gary R. Goldstein.
2. Particle Data Group, "Review of Particle Physics", Eur. Phys. J. C3 (1998) 1 and references therein.
3. E791 Collaboration, E. M. Aitala et al., Phys. Lett. B371 (1996) 157 and references therein.
4. E791 Collaboration, E. M. Aitala et al., Eur. Phys. J. C4 (1999) 1.
5. E687 Collaboration, P. L. Frabetti et al., Phys. Lett. B331 (1994) 217.
6. D. Aston et al., Nucl. Phys. B296 (1988) 493.
7. R. Koch and E. Pietarinen, Nucl. Phys. A336 (1980) 331.
8. M. B. Watson, M. Ferro-Luzzi, and R. D. Tripp, Phys. Rev. 131 (1963) 2248.
9. H. Pilkuhn, Relativistic Particle Physics (Springer-Verlag, New York, 1979).
10. ACCMOR Collaboration, A. Bozek et al., Phys. Lett. B312 (1993) 247.
11. R. Dalitz in [2], p. 676.

# The $\Sigma^-$ Hyperon Radius

H. Krüger [a] on behalf of the SELEX collaboration *

[a]Max-Planck-Institut für Kernphysik, Postfach 103980, 69029 Heidelberg, Germany

The electromagnetic charge radius of the $\Sigma^-$ hyperon and the total $\Sigma^-$-proton cross section at center of mass energy of $\sqrt{s} = 34\,\mathrm{GeV}$ have been determined. In parallel the total cross sections of $\Sigma^-$ and $\pi^-$ on Be- and C-targets were measured. The measurements were performed in the framework of the SELEX/E781 charm hadroproduction experiment at Fermilab which employs a 600 GeV/$c$ high-intensity $\Sigma^-/\pi^-$ beam and a three-stage magnetic spectrometer covering $0.1 \leq x_F \leq 1.0$. Scattering angles and momenta were measured with high precision using silicon microstrip detectors. Two TRDs provided full particle identification. Both measurements are compared and interpreted as the radius of the $\Sigma^-$ hyperon.

## 1. Introduction

The systematic measurement of the static properties of hadronic particles has already led in the past to a better understanding of their fundamental structure. Their finite size, one of the inevitable by-products of the confinement of quarks inside a spatial volume, is not thoroughly explored for all of the SU(3) hadrons.

Sizes of hadrons may be explored by their strong and electromagnetic interactions. Most commonly the electromagnetic charge radius

$$\langle r^2 \rangle = 4\pi \int r^2 \cdot \rho(r)\ r^2 dr \qquad (1)$$

is measured in elastic electron-hadron scattering. The electromagnetic charge radius of a baryon is defined as the slope of the Sachs form factor $G_E$ at zero momentum transfer $Q^2$:

$$\langle r^2 \rangle = -6 \left. \frac{\mathrm{d}G_E(Q^2)}{\mathrm{d}Q^2} \right|_{Q^2=0} \qquad (2)$$

It directly probes the charge distribution $\rho(r)$ of the quarks forming the hadron. The electromagnetic force is weak enough not to perturb the structure of hadrons.

Table 1
World data on electromagnetic radii of charged hadrons.

| hadron | $\langle r^2 \rangle$[fm$^2$] | | |
|---|---|---|---|
| p | 0.74± | 0.02 | [2] |
| | 0.79± | 0.03 | [3] |
| | 0.72± | 0.01 | [4] |
| $\Sigma^-$ | 0.9± | 0.5 | [5] |
| $\pi^-$ | 0.44± | 0.01 | [6] |
| $K^-$ | 0.34± | 0.05 | [7] |

In table 1, the existing measurements of electromagnetic charge radii are summarized. It is interesting to note that even for the proton there is disagreement between the radius measured in elastic scattering[4] and that determined from the hydrogen Lamb shift[3]. The charge radius of the $\pi^-$and the $K^-$ differ by approximately 0.1 fm$^2$. A simple explanation for this difference is that the $s$ quark in the kaon is more localized because of its higher mass compared to the $u$ and $d$ quarks. For the baryons, the existing measurement of the $\Sigma^-$-hyperon does not allow the comparison to the proton because of its large uncertainty.

Another way of determining the size of hadrons is by using another hadron to probe its strong structure. At high energies the slope parameter of the differential hadronic elastic scattering cross section, which is closely related to the square of the strong radius of the hadron, becomes proportional to its total cross section [1]. In this region absorption starts to dominate and the total cross section is proportional to the strong radius. Using the proton as a reference the size of other hadrons

*Ball State University, Bogazici University (Istanbul), Carnegie-Mellon University, Centro Brasiliero de Pesquisas Físicas (Rio de Janeiro), Fermilab, Institute for High Energy Physics (Protvino), Institute of High Energy Physics (Beijing), Institute of Theoretical and Experimental Physics (Moscow), Max-Planck-Institut für Kernphysik (Heidelberg), Moscow State University, Petersburg Nuclear Physics Institute, Tel Aviv University, Universidad Autónoma de San Luis Potosí (Mexico), Universidade Federal da Paraíba (Brazil) University of Bristol, University of Iowa, University of Michigan-Flint, University of Rome "La Sapienza" and INFN (Italy), University of São Paulo (Brazil), University of Trieste and INFN (Trieste)

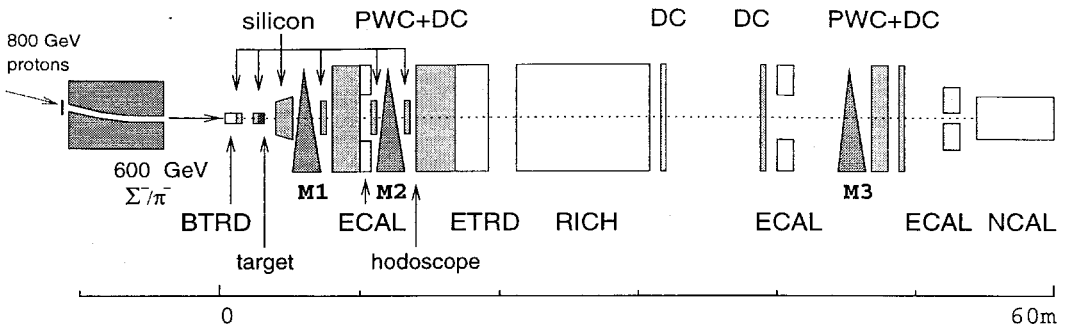


Figure 1. Schematic layout of the SELEX apparatus. The spectrometer stages are defined by the three magnets stylized as triangles. The transverse dimensions are not to scale.

can be determined:

$$\langle r^2_{\rm st}\rangle_h = \langle r^2_{\rm st}\rangle_p \, \frac{\sigma^{\rm tot}_{\rm hp}(s)}{\sigma^{\rm tot}_{\rm pp}(s)} \qquad (3)$$

In the E781/SELEX experiment both the total $\Sigma^-$-proton cross section and the $\Sigma^-$ charge radius are measured.

## 2. The E781/SELEX experiment

The E781/SELEX experiment is primarily designed to explore charm-baryon production and spectroscopy. It uses a 600 GeV $\Sigma^-$-hyperon beam produced by the 800 GeV Fermilab Tevatron proton beam impinging on one interaction length of beryllium and momentum selected by a magnet. In negative polarity the beam consists to equal parts of $\Sigma^-$ and $\pi^-$ with a small amount of $\Xi^-$at the exit of the hyperon magnet. Operating the magnet to select positive charged particles the beam contents are 94 % protons and admixtures of 3% $\pi^+$and 3 % $\Sigma^+$. The mean momenta of the beam are $625 \pm 40\,\mathrm{GeV}/c$ in negative and $540 \pm 35\,\mathrm{GeV}/c$ in positive polarity.

A transition radiation detector (BTRD) allows to separate the baryonic from the mesonic beam components. The charge radius measurement was done in parallel to the data taking for charm physics, using the same targets. These are two thin copper foils followed by three diamond targets. The total cross section measurement was performed in a dedicated running period.

The scattering particles after the targets are analyzed by twenty planes of silicon microstrip detectors with scattering angle resolution less than $30\,\mu$rad. The vertex region is followed by three magnet spectrometers. After each magnet the particles are detected using proportional wire chambers (PWC) and drift chambers (DC). Using the first two magnets a momentum resolution $\sigma_p/p^2 = 5 \cdot 10^{-5}\mathrm{GeV}^{-1}c$ corresponding to 0.5% for a 100 GeV particle is achieved. To improve the resolution for high momentum tracks up to $\sigma_p/p^2 = 1.4 \cdot 10^{-5}\mathrm{GeV}^{-1}c$ three stations of silicon microstrip detectors are mounted at the exits of the first two magnets and the entrance of the second magnet.

Downstream of the second magnet another transition radiation detector (ETRD) is used to identify electrons.

## 3. Elastic $\Sigma^-$-e$^-$ scattering

The $\Sigma^-$ charge radius is measured in elastic electron scattering. Its cross section

$$\frac{d\sigma}{dQ^2} = \frac{4\pi\alpha^2}{Q^4}\left(1 - \frac{Q^2}{Q^2_{max}}\right) \cdot F^2(G_E, G_M, Q^2) \qquad (4)$$

is given by the Mott cross section multiplied by the form factor $F$ which contains the Sachs electric and magnetic form factor $G_E$ and $G_M$. The maximum momentum transfer $Q^2_{max}$ is determined by the two-body kinematics and is typically around $0.25\,\mathrm{GeV}^2/c^2$ . Both Sachs form factors are parameterized by the dipole form with the charge radius as a free parameter:

$$G_E(Q^2) = \frac{1}{\kappa - 1} G_M = \left(1 + \frac{1}{12} Q^2 \langle r^2\rangle\right)^{-2} \qquad (5)$$

The $\Sigma^-$-hyperon is scattered off atomic electrons in the targets. For copper and carbon the binding energies are small compared to the electron mass so that they can be considered at rest.

The four-momentum transfer $Q^2$ from the incoming hadron to the electron can be measured by either the momentum loss of the hadron or the angle of the scattered electron with respect to the beam particle. The momentum of the electron is not used as the external bremsstrahlungsloss in the vertex silicon and target material is too large. In the analysis the elastic scattering events are selected by requiring that both the hadronic and the leptonic measurement of the momentum transfer $Q^2$ are consistent. Typically, the $Q^2$ resolution is better than 4%.

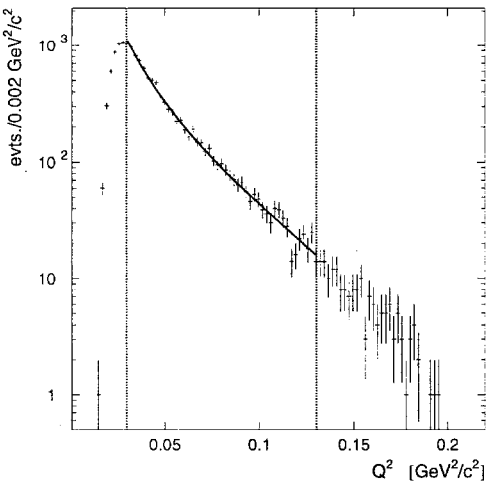


Figure 2. Four-momentum transfer $Q^2$ distribution for elastic $\Sigma^-$-e$^-$ scattering events with fitted radius.

The trigger uses the hodoscope after the second spectrometer magnet to select events with two particles of opposite charge. The minimal accepted electron momentum (25 GeV) defines the lower limit $Q^2_{min}(0.025\,\mathrm{GeV}^2/c^2)$ of the acceptance. Figure 2 shows the $Q^2$ distribution of the reconstructed elastic scattering events. As the spectrum covers a sufficiently large $Q^2$ region the radius can be fitted to the slope of the cross section and there is no need for an absolute normalization. The charge radius of the $\pi^-$and the proton is also measured in the experiment. The proton measurement allows a direct comparison to the $\Sigma^-$ in the same experiment. The results are given in table 2. Both the $\pi^-$ and proton measurement are consistent with the world data.

Table 2
Preliminary Charge Radii Results from E781/SELEX

| hadron | $\langle r^2\rangle \pm (stat.) \pm (syst.)[\mathrm{fm}^2]$ |
|---|---|
| $\Sigma^-$ | $0.60 \pm 0.08 \pm 0.08$ |
| p | $0.70 \pm 0.06 \pm 0.06$ |
| $\pi^-$ | $0.42 \pm 0.06 \pm 0.08$ |

## 4. Total cross section measurements

The total cross section measurement was done during a dedicated beam time with the first magnet switched off to enhance the fiducial volume for the reconstruction of the $\Sigma^-$ decay. A standard transmission technique was used to measure partial cross sections, which were extrapolated to $\Omega = 0$ to obtain the total cross section:

$$\sigma_{tot}(\Omega) := \frac{1}{\rho L} \lim_{\Omega\to 0} \log\left[\frac{F_0}{F_{tr}(\Omega)} \cdot \frac{E_{tr}(\Omega)}{E_0}\right] \qquad (6)$$

Here $\rho L$ denotes the area density of the target, $F_0$ the number of incoming and $F_{tr}$ the number of transmitted particles detected in a maximum opening angle $\Omega$. A measurement without the target ($E_0$,$E_{tr}$) cancels the influence of detector efficiencies and secondary interactions.

The setup of SELEX does not allow the usage of a liquid hydrogen target. To measure the total $\Sigma^-$-proton cross section two methods are used. Subtracting the cross section of carbon (C) and polyethylene ($CH_2$) yields the proton cross section. Another method is to measure cross sections for different nuclear targets and use the Glauber model to deduce the proton cross section. The A-dependence of nuclear cross sections of $\Sigma^-$ and $\pi^-$ are also determined. The results are shown in figure 3. The total cross sections are consistent with the parameterization

$$\sigma_{tot}(XA) = \sigma_0 A^\alpha \qquad (7)$$

with a mean slope parameter for all particles equal to $\alpha = 0.77 \pm 0.05$. Using the more detailed

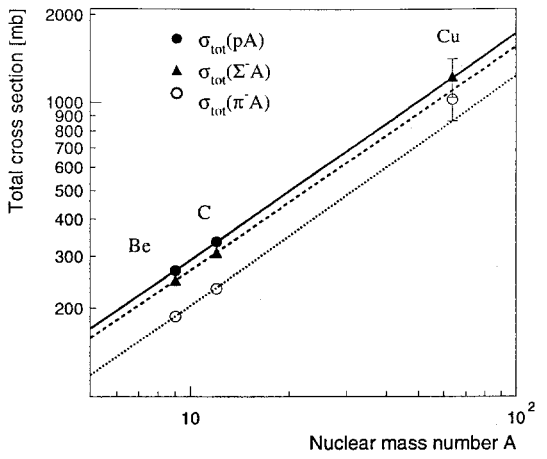


Figure 3. A-dependence of total cross sections measured at $\sqrt{s} \approx 34\,\mathrm{GeV}$ [9]

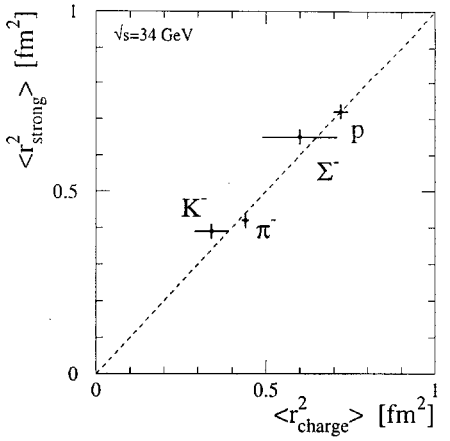


Figure 4. Comparison of strong and electromagnetic radius for different hadrons with the new measurement of the $\Sigma^-$from SELEX.

Glauber model the $\Sigma^-$-nucleon and $\pi^-$-nucleon total cross sections are obtained. Table 3 shows the results for both techniques and particles.

Table 3
total cross section measurements at $\sqrt{s}$ = 33.9 GeV ($p_{lab}$=610 GeV/$c$)

| method | $\sigma_{tot}^{\Sigma^- N}$ [mb] | $\sigma_{tot}^{\pi^- N}$ [mb] |
|---|---|---|
| CH2-C diff. | $33.7 \pm 3.1$ | $26.0 \pm 2.1$ |
| $\sigma_{tot}$(Be tgt) | $37.4 \pm 1.3$ | $27.1 \pm 1.5$ |
| $\sigma_{tot}$(C tgt) | $37.0 \pm 0.8$ | $26.4 \pm 1.3$ |
| total result | $37.0 \pm 0.7$ | $26.6 \pm 0.9$ |

## 5. Conclusion

The charge radius and the total cross section measurement [8] add a new data point in the comparison of the strong and electromagnetic radii of hadrons. For the direct comparison, which is shown in figure 4, the strong radii are calculated from the total cross sections. Both the $\Sigma^-$ and $\pi^-$ results are measured at $\sqrt{s} = 34\,\mathrm{GeV}$. The proton and kaon values are taken from a parameterization of existing data evaluated at this energy.

Although the interpretation of the total cross section measurement as the strong radius of a hadron is not model independent and the uncertainties in the electromagnetic $\Sigma^-$charge radii measurement are quite large, it is a clear indication that hadrons become smaller when a heavier $s$ quark is added.

## REFERENCES


1. B. Povh, J. Hüfner, Phys.Lett.B **245** (1990) 653
2. G. Simon, C. Schmitt, F. Borkowski, V. Walther, *Nucl. Phys.* A **333** (1980) 381.
3. T. Udem *et al.*, *Phys. Rev. Lett.* **79** (1997) 2646.
4. P. Mergell, U.G. Meissner, D. Drechsel, *Nucl. Phys.* A **596** (1996) 367.
5. M.I. Adamovich *el al.*, *Eur. Phys. J.* C **8** ( 1999) 59
6. S.R. Amendolia *et al.*, *Nucl. Phys.* B **277** (1986) 168.
7. S.R. Amendolia *et al.*, *Phys. Lett.* B **178** (1986) 435.
8. U. Dersch *et al.*, *submitted to Nucl. Phys. B* (hep-ex/9910052)
9. U. Dersch, Ph.D. thesis, Univ. Heidelberg

# TWO POLARIZATION STUDIES: POLARIZATION OF INCLUSIVELY PRODUCED $\Sigma^+$ BY 800 $GeV/c$ PROTONS AND INCLUSIVELY PRODUCED $\Lambda^0$ BY 600 $GeV/c$ $\Sigma^-$ .

E. McCliment [a] for E781 Collaboration

[a]University of Iowa, Department of Physics and Astronomy,
Iowa City, IA 52240

We present results of two polarization measurements based on data from the SELEX(E781) experiment at Fermilab, which ran in 1997. In the first measurement, the polarization of $\Sigma^+$ hyperons with momenta of 375, 500, and 572 $GeV/c$, which were produced by the 800 $GeV/c$ proton beam on copper and beryllium targets, is obtained. In the second measurement, the polarization of $\Lambda^0$'s, inclusively produced by a $\Sigma^-$ beam with a mean momentum of 610 $GeV/c$ on copper and carbon targets, is obtained. These results are compared with earlier experiments.

## 1. Inclusive Production of $\Sigma^+$ by 800 $GeV/c$ protons on Copper and Beryllium Targets

A large number of theoretical models have been constructed over the years since it was first observed that inclusively produced hyperons are polarized. These models have met with varying degrees of success, but it is clear that more data is needed to clarify the picture. A review of the current status is found in Ref [1]. The measurements of $\Sigma^+$ polarization described herein were carried out to extend the pool of polarization data to higher $x_F$ and also to study its A dependence. The $\Sigma^+$ has two principal two-body decay modes, $p\pi^0(51.6\%)$ and $n\pi^+(48.3\%)$. However, the latter mode has a small asymmetry parameter ($\alpha = 0.068$), too small to provide a meaningful measurement of the polarization with the limited statistics available in these measurements. In this study we concentrate on the $p\pi^0$ mode.

### 1.1. Apparatus

The Selex experiment (E781), which was run in the P-Center beamline at Fermilab in 1997, was designed primarily for the study of charm baryons produced by a hyperon beam on a segmented set of copper and diamond targets. For this purpose the apparatus contained a multistage spectrometer downstream of the targets. However, by modifying the E781 apparatus as shown in Figure 1 (the segmented targets and one of the spectrometers was removed) it became possible to study the polarization of $\Sigma^+$ hyperons in the hyperon beam itself. The $\Sigma^+$'s were produced by 800-GeV protons from the Tevatron in the primary target at the entrance to the hyperon magnet. This magnet was equipped with a curved channel to select particles within a given momentum bite. The secondary beam contained approximately 2% polarized $\Sigma^+$ hyperons, which were the object of this study. The removal of one spectrometer made room for a 6.4m fiducial decay region of the $\Sigma^+$ between the silicon detector system (SSD) and the Large Angle Silicon Detector system (LASD1) at the entrance to the analysing magnet.

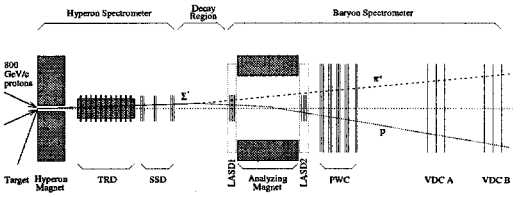


Figure 1. Modified SELEX apparatus.

### 1.2. Data Selection

Altogether 12 data sets were collected for these measurements. There were three different momentum settings of the hyperon magnet: 375, 500, and 572 $GeV/c$. At each momentum setting

the primary proton beam was steered onto the target at two different horizontal targeting angles, $\pm 4mrad$ to enable the well-known bias cancelling method to be used to measure the polarization Ref [2], [3].

And this set of 6 measurements was repeated with two different targets, copper and beryllium. A data sample suitable for polarization analysis was selected in each case from the raw data by first requiring each "good" event to have a $\Sigma^+$ candidate upstream of the decay region and a proton candidate downstream of this region, to wit:

- A single reconstructed track in the SSD system upstream of the decay region with less than 5 clusters in the TRD's (to eliminate pions) – to serve as the $\Sigma^+$ candidate.
- A single charged track in LASD2, the proportional wire chambers (PWC's), and the vector drift chambers (VDC's) downstream of the analysing magnet, which, when extended to the center of the analysing magnet, matched a track segment in LASD1 – to serve as the proton candidate.
- A reconstrutcted vertex ($3\sigma$ cut).

Additional cuts were made on the lab decay angle $\theta$ and the ratio R of the momentum of the charged daughter to the momentum of the $\Sigma^+$. These cuts greatly reduce the large backgound of noninteracting protons which comprise 94% of the beam. They also eliminate the $\Sigma^+ \to n\pi^+$ decay mode from the sample. Finally beam phase space cuts were made to match the phase-space distributions from the two targeting angles and reduce background from $\Sigma^+$'s which do not originate in the target. Figure 2 shows $\Sigma^+$ mass histograms before and after these cuts.

### 1.3. Results

In the rest frame of the decaying $\Sigma^+$ the theoretical angular distribution of the baryon daughter is given by

$$\frac{1}{N}\frac{dN}{dcos\Theta} = \frac{1}{2}(1 + \alpha P cos\Theta) \qquad (1)$$

where $\alpha$ is the asymmetry parameter (-0.98 for the $(p\pi^0)$ mode), P the polarization and $\Theta$ the angle between the proton's momentum and the (vertical) polarization vector. Asymmetry of the apparatus, which is folded into the corresponding experimental distribution is eliminated by the

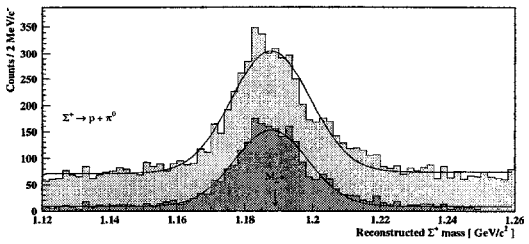


Figure 2. $\Sigma^+$ mass distribution. The upper and lower histograms were obtained before and after selection cuts, respectively.

bias cancelling technique. Figure 3 shows a plot of the results as a function of $x_F$ along with earlier measurements for comparison (see Ref [2]). Since these measurements were all done with the same targeting angles, $x_F$ and $p_t$ are proportional. Here we use $x_F$ to facilitate comparison with earlier data. The salient features of the data are the following:

- There is good agreement between our point at $x_F = 0.66$ and the corresponding E761 point.
- The polarization levels off and perhaps falls at high $x_F$.
- There is a significant A dependence of the polarization. The average value of the ratio of polarizations obtained in these measurements is given by

$$\frac{P_{Cu}}{P_{Be}} = 0.71 \pm 0.08 \qquad (2)$$

The error bars on the E781 points in Figure 3 are statisical only. Systematic error studies were done by varying the cuts used in the data selection and by varying the binning. The largest effect due to nonuniformity of the beam phase space showed an error of $\pm 0.009\%$, which is to be compared with statistical errors of approximately 3.0%. The systematic errors are thus a small fraction of the statistical errors.

### 1.4. Conclusion

This measurement extends previous measurement of the polarization to higher $x_F$ $(p_t)$ values. At the lowest $x_F$ our measurement is consistent with previous measurements. There is a significant A dependence of the polarization.

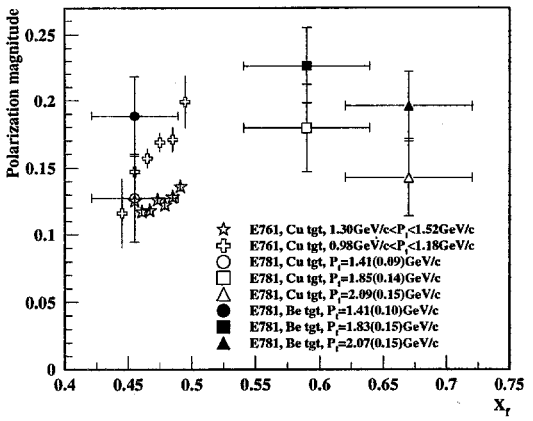


Figure 3. $x_F$ dependence of the $\Sigma^+$ polarization (statistical errors only shown.) E761 results are shown for comparison.

## 2. Polarization of Inclusively Produced $\Lambda^0$'s by 600 $GeV/c$ $\Sigma^-$ on Copper and Carbon Targets

In this study we exploit the full capability of the Selex apparatus to measure the polarization of $\Lambda^0$'s produced by a negative hyperon beam on copper and carbon (diamond) targets with the goal of extending the range in $x_F$ beyond that of earlier measurements. In this case there is insufficient data to study the A dependence. The data sample from both targets is combined. We determine the sign of the polarization and study its $x_F$ and $p_t$ dependence. The $\Lambda^0$'s are produced in the secondary "charm" targets and two downstream magnetic spectrometers are used to reconstruct them.

### 2.1. Data Selection

The negative hyperon beam does not suffer from the large flux of protons. Nevertheless, it is only roughly 50% $\Sigma^-$, the rest pions and a small fraction of kaons. Thus, to be able to select a data set suitable for polarization analysis it was necessary to identify the $\Sigma^-$'s in the beam and to identify the produced $\Lambda^0$'s. Accordingly, the requirements were:

- A single $\Sigma^-$ in the beam identified by the TRD's.
- A pion and proton identified by the RICH detector downstream of the targets.
- Reconstructed mass of the $\Lambda^0$ to lie within $\pm 0.005 GeV/c^2$ of the central value.

As the mass plot in Figure 4 shows a clean sample of $\Lambda^0$'s was obtained for measurement of the polarization. In this case there is no preferred azimuth for the polarization, which makes the bias cancelling technique more complicated. Nevertheless, by exploiting the vertical symmetry of the apparatus and azimuthal binning we were able to use bias cancelling to eliminate false asymmetries induced by the apparatus. This made necessary an additional cut on azimuths near the horizontal plane. Altogether, after all the cuts a sample of 360 K events was obtained, which was sufficient to do the azimuthal binning. The methods were checked with Monte Carlo and by applying the method to measure the polarization of a sample of $K_s$'s and obtaining a null result.

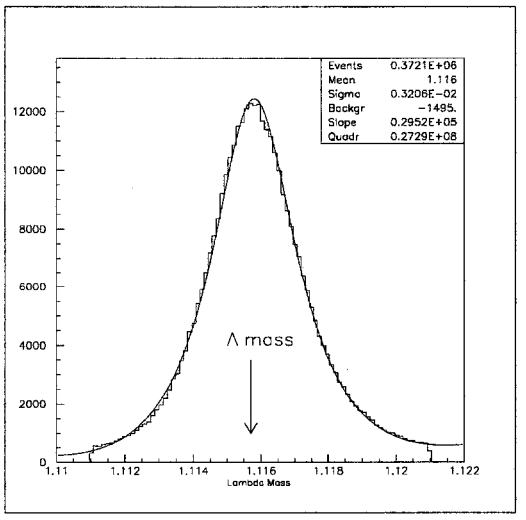


Figure 4. $\Lambda^0$ mass plot after cuts.

### 2.2. Results and Conclusion

The results are shown in Figure 5, which is a plot of our results as a function of $p_t$ for several $x_F$ values, along with earlier measurements for comparison. Ref [4],[5] The WA-89 measurement is similar to ours, i.e. the $\Lambda^0$'s were produced by $\Sigma^-$, whereas the E008 data corresponds to $\Lambda^0$'s produced by protons. As in the $\Sigma^+$ study the polarization appears to peak at a $p_t$ of about 1.0 $GeV/c$ then level off or decline. Here, however,

the most striking feature of our results is the positive sign compared to the earlier measurements which yielded a negative value. However, the data in the figure suggests a progression from negative to positive values with increasing $x_F$. It is hoped that the results of these two polarization studies will contribute to the understanding of production polarization.

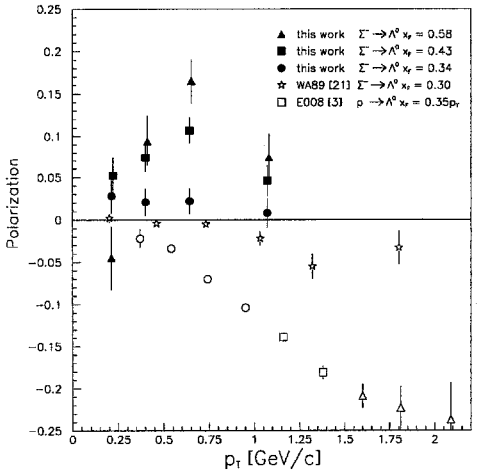


Figure 5. $p_t$ distribution of $\Lambda^0$ polarization. Included also are results from WA89 and E008 experiments.

## REFERENCES


1. J. Lach, Nuc. Phys. B (Proc. Suppl.) **50**, 216 (1996).
2. A. Morelos *et al.* Phys. Rev. Lett. **71**, 2172 (1993).
3. A. Morelos *et al.* Phys. Rev. D **52**, 3777 (1995).
4. M. I. Adamovich et al, Z. Phys. A **350**, 379 (1995).
5. K. Heller *et al.* Phys. Rev. Lett **41**, 607 (1978)

# The Search for Pentaquark Baryon with Hidden Strangeness

L.G.Landsberg
Institute for High Energy Physics, Protvino, Moscow region, 142284, Russia

Evidences for new baryon states with mass >1.8 GeV were obtained in the experiments of the SPHINX Collaboration in studying hyperon-kaon mass spectra in several proton diffractive reactions. The main result of these experiments is the observation of $X(2000) \to \Sigma K$ state with unusual dynamical features (narrow width, anomalously large branching ratios for the decay channels with strange particle emission). The possibility of the interpretation of this state as cryptoexotic pentaquark baryon with hidden strangeness is discussed. The additional data which are supported the real existence of $X(2000)$ baryon are also presented.

Extensive studies of the diffractive baryon production and search for cryptoexotic pentaquark baryons with hidden strangeness ($B_\phi = |qqqs\bar{s}>$; here $q = u,\ d$ quarks) are being carried out by the SPHINX Collaboration at IHEP accelerator with 70 GeV proton beam. This program was described in detail in reviews [1].

The cryptoexotic $B_\phi$ baryons do not have external exotic quantum numbers and their complicated internal valence quark structure can be established only indirectly, by examination of their unusual dynamic properties which are quite different from those for ordinary $|qqq>$ baryons. Examples of such anomalous features are as listed below (see [1] for more details):

1. The dominant OZI allowed decay modes of $B_\phi$ baryons are the ones with strange particles in the final state (for ordinary baryons such decays have branching ratios at the per cent level).

2. Cryptoexotic $B_\phi$ baryons can possess both large masses ($M > 1.8 - 2.0$ GeV) and narrow decay widths ($\Gamma \leq 50 - 100$ MeV). This is due to a complicated internal color structure of these baryons with significant quark rearrangement of color clusters in the decay processes and due to a limited phase space for the OZI allowed $B \to YK$ decays. At the same time, typical decay widths for the well established $|qqq>$ isobars with similar masses are $\geq 300$ MeV.

As was emphasized in a number of papers (see reviews [1,2]), diffractive production processes with Pomeron exchange offer new tools in searches for the exotic hadrons. Originally, the interest was concentrated on the model of Pomeron with small cryptoexotic ($qq\bar{q}\bar{q}$) component. In modern notions Pomeron is a multigluon system which allows for production of the exotic hadrons in gluon-rich diffractive processes.

The Pomeron exchange mechanism in diffractive production reactions can induce the coherent processes on the target nucleus. In such processes the nucleus acts as a whole. Owing to the difference in the absorptions of single-particle and multiparticle objects in nuclei, coherent processes could serve as an effective tool for separation of resonance against non-resonant multiparticle background.

In previous measurement on the SPHINX setup several unusual baryonic states were observed in the study of coherent diffractive production reactions

$$p + N(C) \to [\Sigma^0 K^+] + N(C) \qquad (1)$$

and

$$p + N(C) \to [\Sigma^*(1385)^0 K^+] + N(C) \qquad (2)$$

(see [1,2] and the references therein; here $C$ corresponds to coherent reaction on carbon nuclei):

a) the state $X(2000)^+ \to \Sigma^0 K^+$ with mass $M = 1997 \pm 7$ MeV and the width $\Gamma = 91 \pm 17$ MeV;

b) the state $X(1810)^+ \to \Sigma^0 K^+$ with $M = 1812 \pm 7$ MeV and $\Gamma = 56 \pm 16$ MeV;

c) the state $X(2050)^+ \to \Sigma^*(1385)^0 K^+$ with $M = 2052 \pm 6$ MeV and $\Gamma = 35^{+22}_{-35}$ MeV (preliminary data obtained in the old run; new data are now under analysis).

The states $X(1810)$ and $X(2050)$ are seen only in the region of very small $P_T^2 (\lesssim 0.01 - 0.02\ \mathrm{GeV}^2)$. The states $X(2000)$ and $X(2050)$ have anomalously large branching ratios for decay channels with strange particle emission

$$R = BR[X(2000);\ X(2050) \to YK]/BR(X(2000),$$
$$X(2050) \to p\pi^+\pi^-;\ \Delta^{++}\pi^-) \gtrsim 1 \div 10. \qquad (3)$$

This feature and their comparatively narrow decay widths make these states good candidates for exotic baryons with hidden strangeness.

In what follows we present the results of a new analysis [3] of the data obtained in the run with partially upgraded SPHINX spectrometer where conditions for $\Lambda$ and $\Sigma^0$ separation were greatly improved as compared to old version of this setup (see [4]). The key element of a new analysis consists in detailed study of the $\Sigma^0 \to \Lambda + \gamma$ decay separation. New analysis gave possibility to increase statistics more than in two times. Detailed GEANT Monte-Carlo simulation was used for efficiency calculations and cross section estimations.

The effective mass spectrum $M(\Sigma^0 K^+)$ in (1) for all $P_T^2$ is presented in Fig.1. The peak of $X(2000)$ baryon state with $M = 1986 \pm 6$ MeV and $\Gamma = 98 \pm 20$ MeV is seen very clearly in this spectrum with a good statistical significance. Thus, the reaction

$$p + N \to \quad X(2000) + N, \qquad (4)$$
$$\hookrightarrow \Sigma^0 K^+$$

is well separated in the SPHINX data. We estimated the cross section for $X(2000)$ production in (4):

$$\sigma[p + N \to X(2000) + N] \cdot BR[X(2000) \to \to \Sigma^0 K^+] = 95 \pm 20 \text{ nb/nucleon} \qquad (5)$$

(with respect to one nucleon under the assumption of $\sigma \propto A^{2/3}$, e.g. for the effective number of nucleons in carbon nucleus equal to 5.24). The parameters of $X(2000)$ peak are not sensitive to different photon cuts.

The $dN/dP_T^2$ distribution for reaction (4) is shown in Fig.2. From this distribution the coherent diffractive production reaction on carbon nuclei is identified as a diffraction peak with the slope $b \simeq 63 \pm 10$ GeV$^{-2}$. The cross section for coherent reaction is determined as

$$\sigma[p + C \to X(2000)^+ + C]_{\text{Coherent}} \cdot BR[X(2000)^+ \to \Sigma^0 K^+] = = 260 \pm 60 \text{ nb/C nuclei.} \qquad (6)$$

The errors in the values of (5) and (6) are statistical only. Additional systematic errors are about $\pm 20\%$ due to uncertainties in the cuts, in the Monte Carlo efficiency calculations and in the absolute normalization.

In the mass spectrum $M(\Sigma^0 K^+)$ in Fig.1 there is only a slight indication for X(1810) structure which was observed earlier in the study of coherent reaction (1). This difference is caused by a large background in this region for the events in Fig.1 (for all $P_T^2$ values).

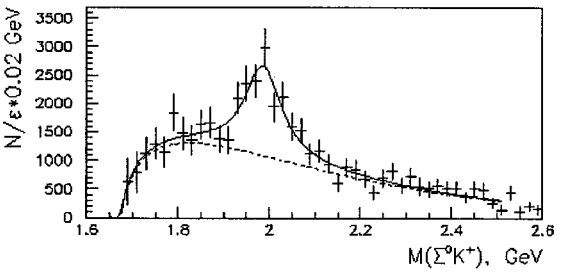


Figure 1. Invariant mass spectrum $M(\Sigma^0 K^+)$ in diffractive reaction $p + N \to [\Sigma^0 K^+] + N$ for all $P_T^2$ (weighted with the efficiency of the setup). The peak $X(2000)$ with parameters $M = 1986 \pm 6$ MeV and $\Gamma = 98 \pm 20$ MeV is clearly observed in this spectrum with a very high statistical significance.

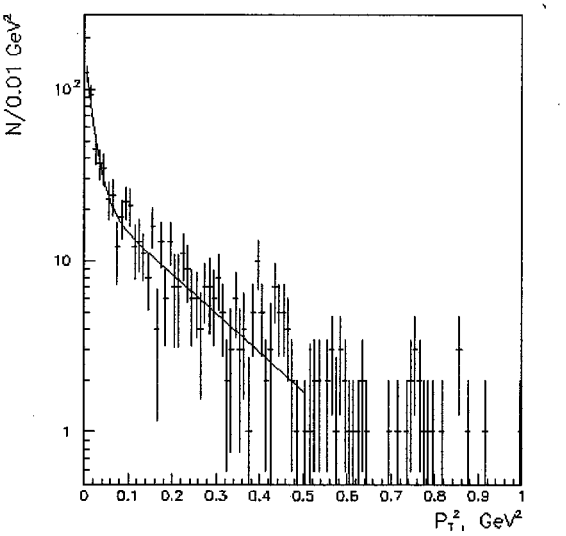


Figure 2. $dN/dP_T^2$ distribution for the diffractive production reaction $p + N \to X(2000) + N$. The distribution is fitted in the form $dN/dP_T^2 = a_1 exp(-b_1 P_T^2) + a_2 exp(-b_2 P_T^2)$ with parameters $b_1 = 63 \pm 10$ GeV$^{-2}$, $b_2 = 5.8 \pm 0.6$ GeV$^{-2}$.

But in the new data for coherent reaction (1) in the mass spectra $M(\Sigma^0 K^+)$ both states $X(2000)$ and $X(1810)$ are clearly seen. Study of the yield of $X(1810)$ as function of $P_T^2$ demonstrates that this state is produced only in the region of very small $P_T^2$ ($\lesssim 0.01$ GeV$^2$) where it is well defined (see Fig.3). From this data parameters of $X(1810)$ are determined

$$X(1810) \to \Sigma^0 K^+ \begin{cases} M = 1807 \pm 7 \text{ MeV} \\ \Gamma = 62 \pm 19 \text{ MeV}, \end{cases} \quad (7)$$

as well as the coherent cross section

$$\sigma[p + C \to X(1810) + C]_{p_T^2 < 0.01 \text{ GeV}^2} \cdot$$
$$\cdot BR[X(1810) \to \Sigma^0 K^+] =$$
$$= 215 \pm 44 \text{ nb } (\pm 30\% \text{ syst.}). \quad (8)$$

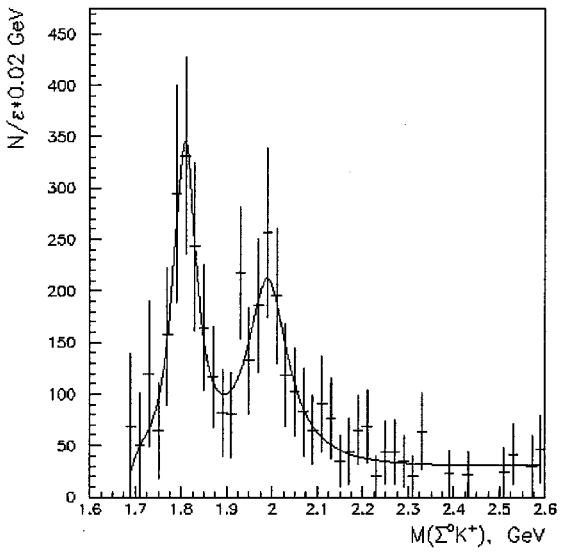


Figure 3. Invariant mass spectrum $M(\Sigma^0 K^+)$ in the coherent diffractive production reaction $p + C \to [\Sigma^0 K^+] + C$ in the region of very small $P_T^2 < 0.01\,\text{GeV}^2$ (weighted with the setup efficiency). In this region $X(1810)$ peak with parameters $M = 1807 \pm 7\,\text{MeV}$ and $\Gamma = 62 \pm 19\,\text{MeV}$ is clearly seen.

To explain the unusual properties of $X(1810)$ state in a very small $P_T^2$ region, the hypothesis of the electromagnetic production of this state in the Coulomb field of carbon nucleus was proposed [5] and it seems to be in no contradictions with the experimental data for the coherent cross section (8) — see [3]. This hypothesis is also supported by observation of $\Delta(1232)^+$ Coulomb production on carbon nuclei in the SPHINX experiment [5].

The data on $X(2000)$ baryon state with unusual dynamical properties (large decay branching with strange particle emission, limited decay width) were obtained with a good statistical significance in the different SPHINX runs with widely different experimental conditions and for several kinematical regions of reaction (1). The average values of the mass and width of $X(2000)$ state (for different kinematical regions and cuts) are

$$X(2000) \to \Sigma^0 K^+ \begin{cases} M = 1989 \pm 6 \text{ MeV} \\ \Gamma = 91 \pm 20 \text{ MeV} \end{cases} \quad (9)$$

Due to its anomalous properties the $X(2000)$ state can be considered as a serious candidate for pentaquark exotic baryon with hidden strangeness: $|X(2000)> = |uuds\bar{s}>$. Recently we have obtained some new additional data to support the reality of $X(2000)$ state.

1. In the experiments with the SPHINX setup we studied the reaction

$$p + N(C) \to [\Sigma^+ \quad K^0] + N(C). \quad (10)$$
$$\hookrightarrow p\pi^0 \ \hookrightarrow \pi^+\pi^-$$

In spite of a limited statistics, we observed the $X(2000)$ peak and the indication for $X(1810)$ structure in this reaction which are quite compatible with the data for reaction (1) [6].

2. In the experiment at the SELEX (E781) spectrometer [7] with the $\Sigma^-$ hyperon beam of the Fermilab Tevatron, the diffractive production reaction

$$\Sigma^- + N \to [\Sigma^- K^+ K^-] + N \quad (11)$$

was studied at the beam momentum $P_{\Sigma^-} \simeq 600$ GeV. In the invariant mass spectrum $M(\Sigma^- K^+)$ for this reaction a peak with parameters $M = 1962 \pm 12$ MeV and $\Gamma = 96 \pm 32$ MeV was observed (see Fig.4 and [8]). The parameters of this structure are very close to the parameters of $X(2000) \to \Sigma^0 K^+$ state which was observed in the experiments at the SPHINX spectrometer. Thus, the real existence of $X(2000)$ baryon seems to be supported by the data from another experiment and in another process.

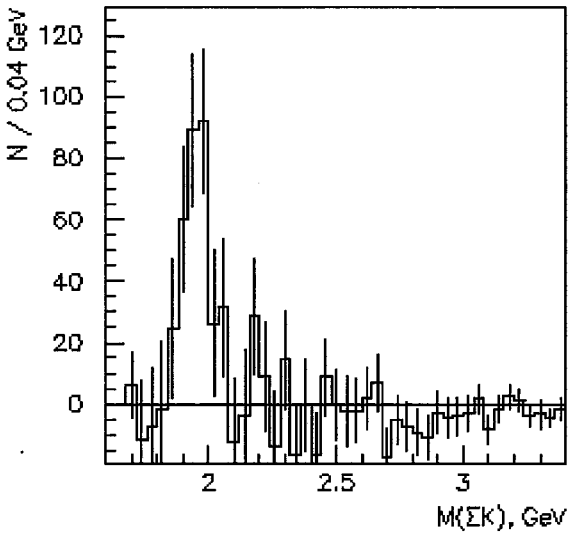


Figure 4. Invariant mass spectrum $M(\Sigma^- K^+)$ in diffractive production reaction $\Sigma^- + N \to [\Sigma^- K^+]K^- + N$ (after background subtraction – see [8]). In this spectrum the peak with parameters $M = 1962 \pm 12\,\mathrm{MeV}$ and $\Gamma = 96 \pm 32\,\mathrm{MeV}$ (which are very near to the parameters of $X(2000)$ peak in Fig.1) is observed.

## Conclusion

In the study of diffractive production proton reactions with the SPHINX setup we observed several interesting objects with anomalous properties. The most important data were obtained for a new baryon state $X(2000) \to \Sigma K$. Unusual features of this massive state (relatively narrow decay width, large branching ratio for decay channels with strange particle emission) make it a serious candidate for cryptoexotic pentaquark baryon with hidden strangeness. We hope to increase significantly our statistics in the near future and to obtain a new information about the supposed exotic baryons.

## REFERENCES


1. L.G.Landsberg, UFN **164** (1994) 1129 [Physics Uspekhi (Engl. Transl.) **37** (1994) 1043].
   L.G.Landsberg, Yad. Fiz. **60** 1997 1541 [Phys. At. Nucl. (Engl. Transl.) **60** (1997) 1397].
2. L.G.Landsberg, Phys. Rep. (1999) (in press).
   L.G.Landsberg, Yad. Fiz. **62** (1999) (in press).
3. S.V.Golovkin et al. (SPHINX Collab.), Eur. Phys. J., **A5** (1999) 408.
4. V.V.Bezzubov et al. (SPHINX Collab.), Yad. Fiz. **59** (1996) 2199 [Phys. At. Nucl. (Engl. Transl.) **59** (1996) 2117].
5. D.V.Vavilov et al. Yad. Fiz. **62** (1999) 501 [Phys. At. Nucl. (Engl. Transl.) **62** (1999) 459].
6. D.V.Vavilov et al. (SPHINX Collab.), Yad. Fiz. **63** (2000) (in press).
7. R.Edelstein et al., Fermilab Proposal P781, 1987 (revised in 1993);
   J.S.Russ, Nucl. Phys. **A585** (1995) 39.
8. L.G.Landsberg, Proc. 4th Workshop on Small-x and Diffractive Physics, Fermilab, Batavia, 17-20 Sept., 1998, p. 189.

# Recent theoretical results on $|\Delta I| = 3/2$ decays of hyperons

Jusak Tandean [a*]

[a]Department of Physics and Astronomy,
Iowa State University,
Ames, IA 50010

We present a discussion of the $|\Delta I| = 3/2$ amplitudes of the hyperon decays $B \to B'\pi$ in the context of chiral perturbation theory. We evaluate the theoretical uncertainty of the lowest-order predictions by calculating the leading non-analytic corrections. We find that the corrections to the lowest-order predictions are within the expectations of naive power-counting and, therefore, that this picture can be examined more quantitatively with improved measurements.

Hyperon nonleptonic decays have been much studied within the framework of chiral perturbation theory ($\chi$PT). The decay modes are $\Sigma^+ \to n\pi^+$, $\Sigma^+ \to p\pi^0$, $\Sigma^- \to n\pi^-$, $\Lambda \to p\pi^-$, $\Lambda \to n\pi^0$, $\Xi^- \to \Lambda\pi^-$, and $\Xi^0 \to \Lambda\pi^0$. Most of the calculations have dealt with the dominant $|\Delta I| = 1/2$ amplitudes of these decays, and the results have been mixed [1–7]. The theory can well reproduce either the S-waves or the P-waves, but not both simultaneously.

The $|\Delta I| = 3/2$ amplitudes of these decays have not been well studied in $\chi$PT. In view of the situation in the $|\Delta I| = 1/2$ sector, it is, therefore, instructive to carry out a similar analysis in the $|\Delta I| = 3/2$ sector. Such an analysis has recently been done [8], and some of its results will be presented here.

To apply $\chi$PT to interactions involving the lowest-lying mesons and baryons, we employ the heavy-baryon formalism [4,9]. In this approach, the theory has a consistent chiral expansion, and the baryons in the effective chiral Lagrangian are described by velocity-dependent fields. Here, we include both octet and decuplet baryons in the Lagrangian because the octet-decuplet mass difference is small enough to make the effects of the decuplet significant on the low-energy theory [4,10].

The leading-order chiral Lagrangian for the strong interactions is well known [4,9], and so we will discuss only the weak sector. In the standard model, the $|\Delta S| = 1$, $|\Delta I| = 3/2$ weak transitions are described by an effective Hamiltonian that transforms as $(27_{\rm L}, 1_{\rm R})$ under chiral rotations. At lowest order in $\chi$PT, the Lagrangian for such weak interactions of baryons that has the required transformation properties is [8,12]

$$\begin{aligned}\mathcal{L}^{\rm w} &= \beta_{27}\, T_{ij,kl}\, (\xi \bar{B}_v \xi^\dagger)_{ki}\, (\xi B_v \xi^\dagger)_{lj} \\ &\quad + \delta_{27}\, T_{ij,kl}\, \xi_{kd}\xi^\dagger_{bi}\, \xi_{le}\xi^\dagger_{cj}\, (\bar{T}^\mu_v)_{abc} (T_{v\mu})_{ade} \\ &\quad + \text{h.c.}\,,\end{aligned} \tag{1}$$

where $\beta_{27}$ ($\delta_{27}$) is the coupling constant for the octet (decuplet) sector, $T_{ij,kl}$ is the tensor that project out the $|\Delta S| = 1$, $|\Delta I| = 3/2$ transitions, and further details are given in Ref. [8].

One can now calculate the decay amplitudes. In the heavy-baryon approach, the amplitude for $B \to B'\pi$ can be written as [8]

$$\begin{aligned}\mathrm{i}\mathcal{M}_{B\to B'\pi} &= G_{\rm F} m_\pi^2 \times \\ &\quad \bar{u}_{B'} \left( \mathcal{A}^{(\rm S)}_{BB'\pi} + 2k\cdot S_v\, \mathcal{A}^{(\rm P)}_{BB'\pi} \right) u_B\,,\end{aligned} \tag{2}$$

where the superscripts refer to S- and P-wave contributions, the $u$'s are baryon spinors, $k$ is the outgoing four-momentum of the pion, and $S_v$ is the velocity-dependent spin operator [9].

At tree level, $\mathcal{O}(1)$ in $\chi$PT, contributions to the amplitudes come from diagrams each with a weak vertex from $\mathcal{L}^{\rm w}$ in (1) and, for the P-waves, a vertex from the lowest-order strong Lagrangian. At next order in $\chi$PT, there are amplitudes of order $m_s$, the strange-quark mass, arising both from one-loop diagrams with leading-order vertices and from counterterms. Currently, there is not enough experimental input to fix the counterterms. For this reason, we follow the approach that has been used for the $|\Delta I| = 1/2$ amplitudes [1,3] and calculate only nonanalytic terms up to $\mathcal{O}(m_s \ln m_s)$. These terms are uniquely determined from the one-loop amplitudes because

*This work was supported in part by DOE under contract number DE-FG02-92ER40730.

they cannot arise from local counterterm Lagrangians. It is possible to do a complete calculation at next-to-leading order and fit all the amplitudes (as was done in Ref. [13] for the $|\Delta I| = 1/2$ sector, without explicitly including the decuplet baryons in the effective theory), but then one loses predictive power, given the large number of free parameters available. Here, we want to limit ourselves to studying the question of whether the lowest-order predictions are subject to large higher-order corrections.

To compare our theoretical results with experiment, we introduce the amplitudes [3]

$$s = \mathcal{A}^{(\mathrm{S})}, \qquad p = -|\boldsymbol{k}|\mathcal{A}^{(\mathrm{P})} \tag{3}$$

in the rest frame of the decaying baryon. ¿From these amplitudes, we can extract for the S-waves the $|\Delta I| = 3/2$ components

$$\begin{aligned} S_3^{(\Lambda)} &= \tfrac{1}{\sqrt{3}}\left(\sqrt{2}\, s_{\Lambda\to n\pi^0} + s_{\Lambda\to p\pi^-}\right), \\ S_3^{(\Xi)} &= \tfrac{2}{3}\left(\sqrt{2}\, s_{\Xi^0\to\Lambda\pi^0} + s_{\Xi^-\to\Lambda\pi^-}\right), \\ S_3^{(\Sigma)} &= -\sqrt{\tfrac{5}{18}}\left(s_{\Sigma^+\to n\pi^+} - \sqrt{2}\, s_{\Sigma^+\to p\pi^0} \right. \\ &\qquad \left. - s_{\Sigma^-\to n\pi^-}\right), \end{aligned} \tag{4}$$

and the $|\Delta I| = 1/2$ components (for $\Lambda$ and $\Xi$ decays)

$$\begin{aligned} S_1^{(\Lambda)} &= \tfrac{1}{\sqrt{3}}\left(s_{\Lambda\to n\pi^0} - \sqrt{2}\, s_{\Lambda\to p\pi^-}\right), \\ S_1^{(\Xi)} &= \tfrac{\sqrt{2}}{3}\left(s_{\Xi^0\to\Lambda\pi^0} - \sqrt{2}\, s_{\Xi^-\to\Lambda\pi^-}\right), \end{aligned} \tag{5}$$

as well as analogous ones for the P-waves. We can then compute from data the ratios collected in Table 1, which show the $|\Delta I| = 1/2$ rule for hyperon decays. The experimental values for $S_3$ and $P_3$ are listed in the column labeled "Experiment" in Table 2.

To begin discussing our theoretical results,[2] we note that our calculation yields no contributions to the S-wave amplitudes $S_3^{(\Lambda)}$ and $S_3^{(\Xi)}$, as shown in Table 2. This only indicates that the two amplitudes are predicted to be smaller than $S_3^{(\Sigma)}$ by about a factor of three because there are nonvanishing contributions from operators that occur at the next order, $\mathcal{O}(m_s/\Lambda_{\chi\mathrm{SB}})$, with $\Lambda_{\chi\mathrm{SB}} \sim 1\,\mathrm{GeV}$ being the scale of chiral-symmetry breaking. (An example of such operators is considered in Refs. [8,12].) The experimental values of $S_3^{(\Lambda)}$ and $S_3^{(\Xi)}$ are seen to support this prediction.

The other four amplitudes are predicted to be nonzero. They depend on the two weak parameters $\beta_{27}$ and $\delta_{27}$ of $\mathcal{L}^{\mathrm{w}}$ (as well as on parameters from the strong Lagrangian, which are already determined), with $\delta_{27}$ appearing only in loop diagrams. Since we consider only the nonanalytic part of the loop diagrams, and since the errors in the measurements of the P-wave amplitudes are larger than those in the S-wave amplitudes, we can take the point of view that we will extract the value of $\beta_{27}$ by fitting the tree-level $S_3^{(\Sigma)}$ amplitude to experiment, and then treat the tree-level P-waves as predictions and the loop results as a measure of the uncertainties of the lowest-order predictions.

Thus we obtain $\beta_{27} = -0.068\sqrt{2}\, f_\pi G_{\mathrm{F}} m_\pi^2$, and the resulting P-wave amplitudes are placed in the column labeled "Tree" in Table 2. These lowest-order predictions are not impressive, but they have the right order of magnitude and differ from the central value of the measurements by at most three standard deviations. For comparison, in the $|\Delta I| = 1/2$ case the tree-level predictions for the P-wave amplitudes are completely wrong [1,3,7], differing from the measurements by factors of up to 20.

To address the reliability of the leading-order predictions, we look at our calculation of the one-loop corrections, presented in two columns in Table 2. The numbers in the column marked "Octet" come from all loop diagrams that do not have any decuplet-baryon lines, with $\beta_{27}$ being the only weak parameter in the diagrams. Contributions of loop diagrams with decuplet baryons depend on one additional constant, $\delta_{27}$, which cannot be fixed from experiment as it does not appear in any of the observed weak decays of a decuplet baryon. To illustrate the effect of these terms, we choose $\delta_{27} = \beta_{27}$, a choice consistent with dimensional analysis and the normalization of $\mathcal{L}^{\mathrm{w}}$, and collect the results in the column labeled "Decuplet".

We can see that some of the loop corrections in Table 2 are comparable to or even larger than the lowest-order results even though they are expected to be smaller by about a factor of

[2] In this work, we have assumed isospin invariance (massless $u$- and $d$-quarks [8]). With improved data in the future, a more quantitative analysis will have to take isospin breaking into account, as it may generate in the $|\Delta I| = 1/2$ amplitudes corrections comparable in size to the $|\Delta I| = 3/2$ amplitudes, especially for the P-waves [14].

Table 1
Experimental values of ratios of $|\Delta I| = 3/2$ to $|\Delta I| = 1/2$ amplitudes.

| $S_3^{(\Lambda)}/S_1^{(\Lambda)}$ | $S_3^{(\Xi)}/S_1^{(\Xi)}$ | $S_3^{(\Sigma)}/s_{\Sigma^-\to n\pi^-}$ | $P_3^{(\Lambda)}/P_1^{(\Lambda)}$ | $P_3^{(\Xi)}/P_1^{(\Xi)}$ | $P_3^{(\Sigma)}/p_{\Sigma^+\to n\pi^+}$ |
|---|---|---|---|---|---|
| $0.026 \pm 0.009$ | $0.042 \pm 0.009$ | $-0.055 \pm 0.020$ | $0.031 \pm 0.037$ | $-0.045 \pm 0.047$ | $-0.059 \pm 0.024$ |

Table 2
Summary of results for $|\Delta I| = 3/2$ components of the S- and P-wave amplitudes to $\mathcal{O}(m_s \ln m_s)$. We use the parameter values $\beta_{27} = \delta_{27} = -0.068\sqrt{2}\, f_\pi G_F m_\pi^2$ and a subtraction scale $\mu = 1\,\mathrm{GeV}$.

| Amplitude | Experiment | Theory | | |
|---|---|---|---|---|
| | | Tree | Octet | Decuplet |
| | | $\mathcal{O}(1)$ | $\mathcal{O}(m_s \ln m_s)$ | $\mathcal{O}(m_s \ln m_s)$ |
| $S_3^{(\Lambda)}$ | $-0.047 \pm 0.017$ | 0 | 0 | 0 |
| $S_3^{(\Xi)}$ | $0.088 \pm 0.020$ | 0 | 0 | 0 |
| $S_3^{(\Sigma)}$ | $-0.107 \pm 0.038$ | $-0.107$ | $-0.089$ | $-0.084$ |
| $P_3^{(\Lambda)}$ | $-0.021 \pm 0.025$ | 0.012 | 0.005 | $-0.060$ |
| $P_3^{(\Xi)}$ | $0.022 \pm 0.023$ | $-0.037$ | $-0.024$ | 0.065 |
| $P_3^{(\Sigma)}$ | $-0.110 \pm 0.045$ | 0.032 | 0.015 | $-0.171$ |

$M_K^2/(4\pi f_\pi)^2 \approx 0.2$. These large corrections occur when several different diagrams yield contributions that add up constructively, resulting in deviations of up to an order of magnitude from the power-counting expectation. This is an inherent flaw in a perturbative calculation where the expansion parameter is not sufficiently small and there are many loop-diagrams involved. We can, therefore, say that these numbers are consistent with naive expectations.

Although the one-loop corrections are large, they are all much smaller than their counterparts in the $|\Delta I| = 1/2$ sector, where they can be as large as 30 times the lowest-order amplitude [7] in the the P-wave in $\Lambda \to p\pi^-$. In that sector, the loop dominance in the P-waves was due to an anomalously small lowest-order prediction arising from the cancellation of two nearly identical terms [3]. Such a cancellation does not happen in the $|\Delta I| = 3/2$ case because each of the lowest-order P-waves has only one term [8].

In conclusion, we have discussed $|\Delta I| = 3/2$ amplitudes for hyperon nonleptonic decays in $\chi$PT. At leading order, these amplitudes are described in terms of only one weak parameter. We have fixed this parameter from the observed value of the S-wave amplitudes in $\Sigma$ decays. Then we have predicted the P-waves and used our one-loop calculation to discuss the uncertainties of the lowest-order predictions. Our predictions are not contradicted by current data, but current experimental errors are too large for a meaningful conclusion. We have shown that the one-loop nonanalytic corrections have the relative size expected from naive power-counting. The combined efforts of E871 and KTeV experiments at Fermilab could give us improved accuracy in the measurements of some of the decay modes that we have discussed and allow a more quantitative comparison of theory and experiment.

## REFERENCES


1. J. Bijnens, H. Sonoda and M. B. Wise, Nucl. Phys. B 261 (1985) 185.
2. H. Georgi, Weak Interactions and Modern Particle Theory, The Benjamin/Cummings Publishing Company, Menlo Park, 1984; J. F. Donoghue, E. Golowich and B. R. Holstein, Dynamics of the Standard Model, Cambridge University Press, Cambridge, 1992.
3. E. Jenkins, Nucl. Phys. B 375 (1992) 561.
4. E. Jenkins and A. Manohar, in Effective Field Theories of the Standard Model, edited by U.-G. Meissner, World Scientific, Singapore, 1992.
5. C. Carone and H. Georgi, Nucl. Phys. B 375 (1992) 243.
6. R. P. Springer, hep-ph/9508324; Phys. Lett. B 461 (1999) 167.
7. A. Abd El-Hady and J. Tandean, hep-

ph/9908498.
8. A. Abd El-Hady, J. Tandean and G. Valencia, Nucl. Phys. A 651 (1999) 71.
9. E. Jenkins and A. V. Manohar, Phys. Lett. B 255 (1991) 558.
10. E. Jenkins and A. Manohar, Phys. Lett. B 259 (1991) 353.
11. Review of Particle Physics. C. Caso et. al. Eur. Phys. J. C 3 (1998) 1.
12. X.-G. He and G. Valencia, Phys. Lett. B 409 (1997) 469; erratum Phys. Lett. B 418 (1998) 443.
13. B. Borasoy and B. R. Holstein, Eur. Phys. J. C 6 (1999) 85.
14. K. Maltman, Phys. Lett. B 345 (1995) 541; E. S. Na and B. R. Holstein, Phys. Rev. D 56 (1997) 4404;

# First Measuement of $\Xi^0 \to \Sigma^+ e^- \overline{\nu}$ Form Factors

S. Bright ( For the KTeV Collaboration ) [a]

[a]University of Chicago, Enrico Fermi Institute,
5640 S. Ellis Avenue, Chicago, Illinois, 60637
*bright@fnal.gov*

With the $\Xi^0 \to \Sigma^+ e^- \overline{\nu}$ data obtained by the KTeV experiment during the 1996-1997 Fermilab fixed target, we measure $g_1/f_1$ to be $1.24 \pm^{.20}_{.17} (stat) \pm .07(syst)$, assuming the absence of a second class current term $g_2/f_1$ and the $SU(3)_f$ value of $f_2(2.6)$. Our value is consistent with exact $SU(3)_f$ symmetry, relaxing the constraint $g_2/f_1 = 0$ we find no evidence for a second-class current term. From the energy spectrum of the electron in the $\Sigma^+$ frame, we measure the weak magnetism term $f_2/f_1$ to be $2.3 \pm 1.2(stat) \pm 0.7(syst)$, in agreement with the CVC hypothesis. We combine our value of $g_1/f_1$ to the measured rate for the process to obtain $f_1$ and $g_1$ which we compare with various theoretical predictions.

## 1. Introduction

The most general transition amplitude for the semileptonic decay of a spin 1/2 baryon ( $B \to b e^- \overline{\nu_e}$ ) is:

$$\begin{aligned} \mathcal{M} &= G_F V_{CKM} \frac{\sqrt{2}}{2} \overline{u}_b (O^V_\alpha + O^A_\alpha) u_B \\ &\times \overline{u_e} \gamma^\alpha (1+\gamma_5) v_\nu + H.c., \end{aligned} \quad (1)$$

where

$$\begin{aligned} O^V_\alpha &= f_1 \gamma_\alpha + \frac{f_2}{M_B} \sigma_{\alpha\beta} q^\beta + \frac{f_3}{M_B} q_\alpha, \\ O^A_\alpha &= (g_1 \gamma_\alpha + \frac{g_2}{M_B} \sigma_{\alpha\beta} q^\beta + \frac{g_3}{M_B} q_\alpha)\gamma_5, \\ q^\alpha &= (p_e + p_\nu)^\alpha = (p_B - p_b)^\alpha. \end{aligned} \quad (2)$$

For the fundamental baryon octet, in the limit of exact $SU(3)_f$ symmetry, any one of the form factors is given by:

$$\begin{aligned} f_i &= C(B,b)_F * F_{f_i} + C(B,b)_D * D_{f_i}, \\ g_i &= C(B,b)_F * F_{g_i} + C(B,b)_D * D_{g_i}, \end{aligned} \quad (3)$$

where $C(B,b)_F$ and $C(B,b)_D$ are $SU(3)$ Clebsch-Gordan coefficients [1].

For $\Xi^0 \to \Sigma^+ e^- \overline{\nu}$ and $n \to p e^- \overline{\nu}$ we have $C(B,b)_F = 1$ and $C(B,b)_D = 1$. Thus, in this limit, the decay $\Xi^0 \to \Sigma^+ e^- \overline{\nu}$ should have the same form factors as $n \to p e^- \overline{\nu}$ . Deviations from this exact symmetry should arise from the mass and charge difference between the quarks. Details of $SU(3)_f$ breaking can be studied through the experimental determination of the form factors.

The form factors $f_3$ and $g_3$ will always have contributions proportional to the electron mass and may therefore be neglected.

The predictions from exact $SU(3)_f$ symmetry are [2]:

$$\begin{aligned} f_1(q^2=0) &= 1.0\,(CVC) \\ g_1(q^2=0) &= 1.26\,(n \to p e^- \overline{\nu}\,) \\ f_2 &= 2.597\,(CVC : \frac{\mu_p - \mu_n}{2} \frac{M_\Xi}{M_p}) \\ g_2 &= 0.0\,(2nd\,class\,current) \end{aligned} \quad (4)$$

The ratios $g_1/f_1$, $g_2/f_1$ and $f_2/f_1$ can be found from the kinematic distributions of the decay products.

## 2. Detector

The KTeV neutral beam is produced by an 800 $GeV/c$ proton beam hitting a 30 $cm$ BeO target at an angle of 4.8 $\mu rad$. Collimators produce two square .35 $\mu sr$ secondary beams. Photons in the beams are converted by Pb absorber, and charged particles are swept out of the beam by a series of magnets. An evacuated decay volume extends from 94 $m$ to 159 $m$ downstream of the target.

The momentum of charged particles is measured by a spectrometer consisting of four drift chambers, the first of which is located immediately downstream of the vacuum window, and a dipole magnet imparting a transverse momentum kick of $\pm 205\,MeV/c$. Helium bags occupy the

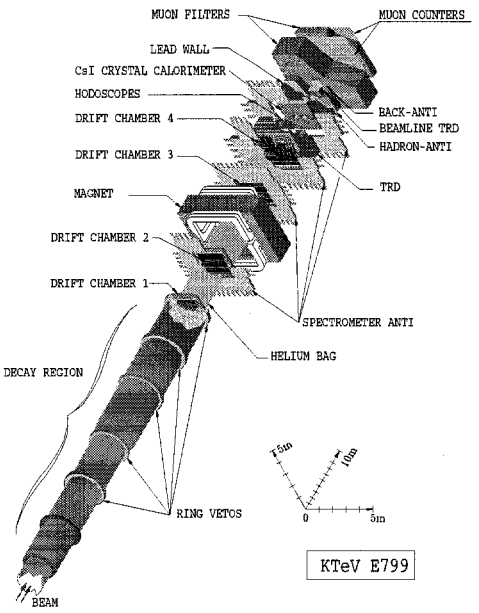


Figure 1. The KTeV detector

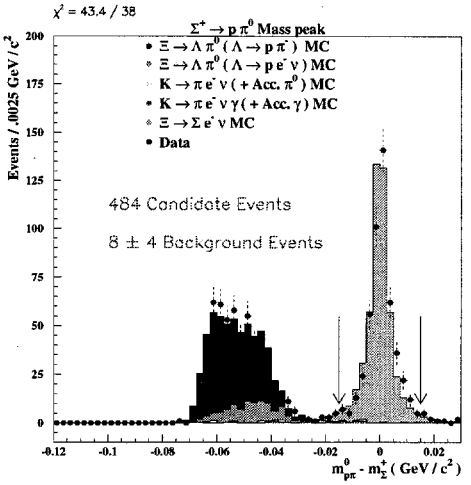


Figure 2. The $\Sigma^+ \to p\,\pi^0$mass peak, after all selection criteria have been applied.

space between the drift chambers to reduce multiple scattering and photon conversions.

Each drift chamber has two planes in both the horizontal and vertical views, each plane has a resolution of about 100 $\mu m$. The energy and position of photons are measured by a CsI calorimeter consisting of 3100 channels, covering an area of $.9\,m \times .9\,m$. The position resolution for electromagnetic clusters is about 1 $mm$ and the energy resolution is about 1 % for typical electron and photon energies in this decay. There are two $15\,cm \times 15\,cm$ beam holes, each one displaced 7.5 $cm$ horizontally from the center of the calorimeter.

A system of transition radiation detectors (TRD) further distinguishes pions from electrons in the beamline. There are additional systems not used in this analysis that are described elsewhere [3].

## 3. Event Selection and Reconstruction

The final state in $\Xi^0 \to \Sigma^+ e^- \overline{\nu}$ consists of a high momentum proton which travels down one of the beam holes, a neutrino which is unobserved, an electron and two photons which are required to hit the calorimeter.

The decay is reconstructed by finding the longitudinal position of the $\pi^0$ decay from the energies and positions of the photon clusters in the calorimeter ($z_{\pi^0}$). The momentum of the $\pi^0$ is then determined from the extrapolated position of the positive track at $z_{\pi^0}$, then the proton and $\pi^0$ momenta are added to give the momentum of the $\Sigma^+$. Finally, the $\Sigma^+$ momentum is traced back to its closest approach to the electron track, forming the $\Xi^0$ vertex.

Only events having a high momentum track traveling down the beam hole, a negative track in the CsI, and two CsI clusters not associated with charged tracks are considered. The positively charged track (proton) is required to have a momentum greater than 3.6 times the momentum of the negatively charged track (electron). We require that the proton have a momentum greater than 120 $GeV/c$ and less than 400 $GeV/c$. Additionally, we require the photon energies to be at least 3 $GeV$ and their position is required to be at least 1.5 $cm$ away from the edge of the beam hole. The ratio of the energy the cluster associated with the negative track (electron) is required to be within 10 % of the track's measured momentum. In order to obtain further $\pi^-/e^-$ rejection, we require the probability that the observed TRD signal associated with the negative track be less than 10 %.

In order to remove $K_L \to \pi^0\pi^+e^-\overline{\nu}$ decays,

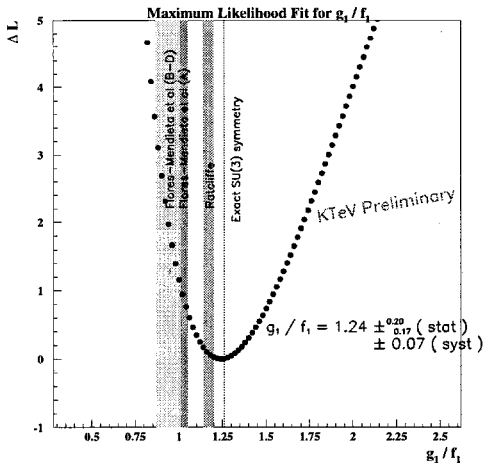


Figure 3. Maximum likelihood fit to $g_1/f_1$.

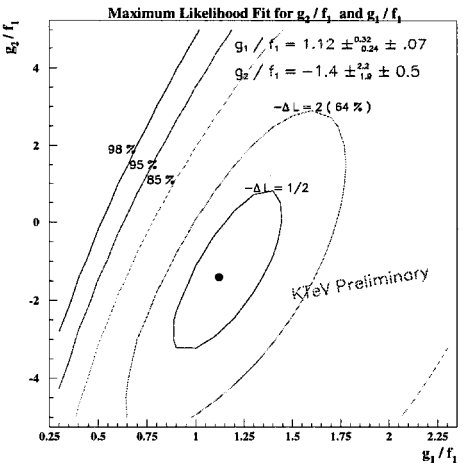


Figure 4. Maximum likelihood fit to $g_2/f_1$and $g_1/f_1$.

we require that the $\pi^0\pi^+e^-$ invariant mass be greater than 0.5 $GeV/c^2$, or that that $z_{\pi^0}$ is at least 3 $m$ greater than the z position of the $\Xi^0$ vertex. The $K_L \to \pi^+\pi^-\pi^0$ events are removed by the above particle identification requirements and requiring the $\pi^+\pi^-\pi^0$ invariant mass be greater than 0.57 $GeV/c^2$. In order to reject photon conversions in the drift chambers upstream of the analyzing magnet, we reject events having an extra in-time hit the horizontal views of these chambers. In order to reject background from $K_L \to \pi^+e^-\overline{\nu}\gamma$, we reject events where the upstream segment of the electron projected to the CsI is within 2 $cm$ of a neutral cluster. The z position of the $\Sigma^+$ is required to be not more than 6 $m$ upstream of the $\Xi^0$ vertex, and not more than 40 $m$ downstream of the $\Xi^0$ vertex. Finally, we remove events not having a physical longitudinal neutrino momentum.

The decay $\Xi^0 \to \Sigma^+\pi^-$ is forbidden by energy conservation, the signal mode is the only source of $\Sigma^+$ in the beam. Signal events are identified by having a proton-$\pi^0$ mass within 15 $MeV$ of the nominal $\Sigma^+$ mass. After the application of all election criteria, we have 484 events in the signal region. We estimate $8 \pm 4$ background events under the mass peak, these events are almost entirely due to $K_L \to \pi^+e^-\overline{\nu}\gamma$ decays with an accidental photon in the detector, and $K_L \to \pi^+e^-\overline{\nu}$ decays with two accidental photons in the detector.

Assuming the parent $\Xi^0$ are unpolarized, four kinematic variables are needed to completely describe the decay chain. The process $\Xi^0 \to \Sigma^+ e^- \overline{\nu}$ can be described by the energy of the electron in the $\Sigma^+$ frame and the angle between the electron and neutrino in the $\Xi^0$ frame. The polarization of the $\Sigma^+$ can be described by the angle between the proton and the electron, and the angle between the proton and the neutrino. The usefulness of the final state polarization is greatly enhanced by the large asymmetry of the decay $\Sigma^+ \to p\pi^0$ ($\alpha = -.98$).

The ambiguity that arises from having a missing particle is handled by keeping only the transverse component of the neutrino momentum, and calculating kinematic quantities involving the neutrino in the $\Sigma^+ - e^-$ frame, following Dworkin [4].

## 4. Results

### 4.1. Extraction of $g_1/f_1$

The fit to $g_1/f_1$uses the two final state polarization variables and the electron-neutrino correlation variable. The variables for the data are put in a three dimensional binned histogram ($10\times10\times10$). A corresponding histogram is made for different MC values of $g_1/f_1$, obtained by reweighting the differential decay rate in [5,6] using the *generated* Monte Carlo (MC) kinematic variables. We then calculate the log likelihood for

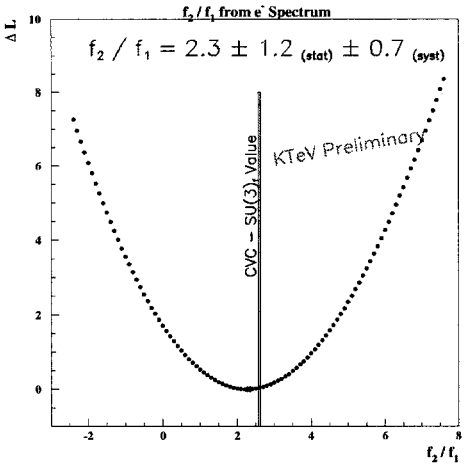


Figure 5. Maximum likelihood fit for $f_2$ using energy spectrum of electron.

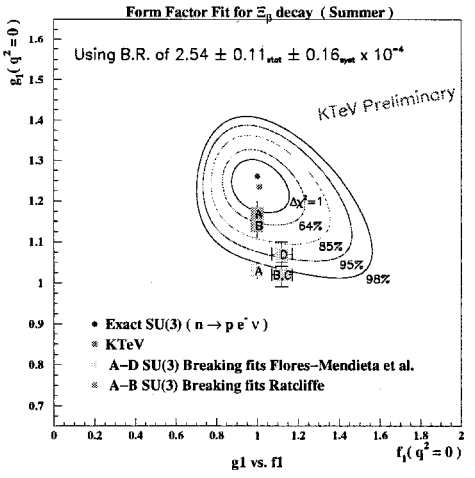


Figure 6. Fit to $f_1$ and $g_1$ using $g_1/f_1$value and measured rate.

each $g_1/f_1$by

$$\mathcal{L}(g_1/f_1) = \Sigma_{ijk} D_{ijk} \log MC(g_1/f_1)_{ijk}, \qquad (5)$$

where the MC histograms are all appropriately normalized. After correcting for background, our final value for $g_1/f_1$is $1.24 \pm^{.20}_{.17}$ $(stat) \pm .07(syst)$, the largest contribution to the systematic error is the background (.06).

### 4.2. Extraction of $g_2/f_1$

If we relax the requirement that $g_2 = 0$, and fit the distributions to $g_1/f_1$and $g_2/f_1$simultaneously, we see no evidence for a non-zero second class current term (figure 4).

### 4.3. Extraction of $f_2/f_1$from beta spectrum

Using our measured $g_1/f_1$, and assuming $g_2/f_1 = 0$, we then determine the value for $f_2/f_1$using the energy spectrum of the $\Sigma^+$ frame (the beta spectrum is the only kinematic quantity that depends on the $f_2/f_1$to lowest order ). Using a maximum likelihood method, we find the value for $f_2/f_1$is $2.3 \pm 1.2(stat) \pm 0.7(syst)$( see figure 5).

## 5. Conclusion

Combining our value for $g_1/f_1$with the total rate for $\Xi^0 \to \Sigma^+ e^- \overline{\nu}$ , we can determine $f_1$ and $g_1$ (figure 6). The rate is determined from our measured branching ratio, $2.54 \pm .11(stat) \pm .16(syst) \times 10^{-4}$[7]. The fit for $f_1$ and $g_1$ gives values consistent with exact $SU(3)_f$ symmetry ( i.e. $n \to p e^- \overline{\nu}$ ), and small deviations therein [8]. Fits to the octet and decuplet data which allow $f_1$ and $g_1$ to be renormalized[9] are disfavored. Furthermore, we find no evidence for a second-class term $g_2$, and our value for the weak magnetism term is consistent with the CVC hypothesis.

## REFERENCES


1. A. Garcia and P. Kielanowski, *The Beta Decay of Hyperons*, Lecture Notes in Physics Vol. 222 (Springer-Verlag, Berlin, 1985).
2. N. Cabibbo, Phys. Rev. Lett. **10**, 531 (1963).
3. A. Affolder *et al.*, Phys. Rev. Lett. **82**, 3751 (1999).
4. J. Dworkin et al., Phys. Rev. D **41** 780 (1990).
5. S. Bright et al., To appear in Phys. Rev. D, hep-ph/9907379, (1999).
6. J. M. Watson and R. Winston, Phys. Rev. **181**, 1907 (1969).
7. A. Alavi-Harati, Talk Given at DPF99 Conference,hep-ex/9903031, (1999).
8. P. G. Ratcliffe, Phys. Rev. D **59** 014038 (1999).
9. R. Flores-Mendieta et al., Phys. Rev. D **58** 094028 (1998).

# Isospin violation in hyperon semileptonic decays

Gabriel Karl
Department of Physics - University of Guelph
Guelph, ON, Canada N1G 2W1

This note emphasizes that because of isospin violation, the two central states in the octet ($\Sigma^\circ$, $\Lambda^\circ$) mix, and this mixing can be measured in semileptonic decays, in particular with an accurate determination of $\Sigma^+$ semileptonic branching ratio.

The work I am describing has been published [1] some five years ago, but due to circumstances has not been advertized at conferences. The issue is isospin violation in matrix elements for semileptonic decays. At first sight this proposal looks hopeless since one might argue that $SU_3$ violation should be much more important. However, one may envisage scenarios where the $SU_3$ wavefunctions remain pure octet while isospin mixing inside the octet takes place due to the mass difference between up and down quarks. In any case, a number of authors have argued that there is a small mixing between $\Sigma_8^\circ$ and $\Lambda_8$ due to this mass difference [2], so that the physical states $\Sigma^\circ$,$\Lambda$ are linear combinations of the pure isovector $\Sigma_8^\circ$ and the pure isoscalar $\Lambda_8$:

$$\Lambda = \Lambda_8 \cos\phi + \Sigma_8^\circ \sin\phi$$

$$\Sigma^\circ = -\Lambda_8 \sin\phi + \Sigma_8^\circ \cos\phi$$

with a mixing angle $\phi$:

$$\sin\phi = \phi = -\frac{\sqrt{3}}{4} \cdot \frac{m_d - m_u}{m_s - \hat{m}} \simeq -0.015$$

where $\hat{m}$ is the average mass of the up and down quarks, and $m_s$ is that of the strange one. These formulae are obtained both in the quark model and in the chiral quark model. The main point I wish to stress is that these are theoretical formulae which should be tested experimentally. The simplest direct tests are in semileptonic decays of hyperons which have a $\Lambda$ or $\Sigma^\circ$ in the initial or final state.

One such test involves the semileptonic decay of a charged $\Sigma$, say $\Sigma^-$ to a $\Lambda$. If isospin is conserved, the vector coupling vanishes [3], but with the mixing taken into consideration one finds [1,4]:

$$g_V/g_A\Big)_{\Sigma^- \to \Lambda} = \frac{\sqrt{3}}{D}\tan\phi = \frac{\sqrt{3}}{D}\phi \simeq -0.03$$

There is some data from CERN [5] which disagrees with the sign of this prediction, but the disagreement is not statistically significant. A precise measurement of $g_V$ in $\Sigma^-$ semileptonic decay would determine the magnitude of $\phi$.

An easier measurement [1,6] is the ratio of semileptonic decay rates for $\Sigma^+$ and $\Sigma^-$ where

$$R(\phi) = \frac{\Gamma(\Sigma^+ \to \Lambda \bar{e}\, \nu)}{\Gamma(\Sigma^- \to \Lambda e\, \bar{\nu})} =$$

$$R(0)\left(1 - \frac{4\sqrt{3}F}{D}\phi\right) \simeq 0.65$$

where R(0) is taken from the review [7]. Although the experimental ratio agrees with 0.65, the agreement is not statistically significant. One needs to measure the semileptonic branching ratio for $\Sigma^+$, which is based at present on 21 events.

There are other, smaller corrections which are given in reference [1]. In principle, when analyzing the semileptonic data one should keep as parameters the Cabibbo angle $\theta$, the matrix elements F,D and the mixing angle $\phi$ to obtain a better determination of all these quantities.

The author was encouraged by learning at the Symposium that Dr. V. Smith is actively promoting these experiments.

The author is grateful to the organizers of Hyperon 99 for the opportunity to advertize these ideas, and to NSERC Canada for financial support.

**REFERENCES**

[1] Gabriel Karl, Physics Letters B328, 149 (1994).
Erratum: Phys. Let. B341, 449 (1995).

[2] N. Isgur, Phys. Rev. D21, 779 (1980) and references therein.
J. Gasser and H. Leutwyler, Phys. Rep. 87, 77 (1982).
J.F. Donoghue, Ann. Rev. Nucl. Part. Sci. 39 (1989).

[3] N. Cabibbo and R. Gatto, Nuovo Cimento 15, 159 (1960).
V.P. Belov, B.S. Mingalev and V.M. Shekter, Sov. Phys. JET411, 392 (1960).
N. Cabibbo and P. Franzini, Phys. Lett. 3, 217 (1963).

[4] P. Bracken, A. Frenkel and G. Karl, Phys. Rev. D24, 2984 (1984).

[5] M. Bourquin et al., Z. Phys. C12, 307 (1982).

[6] E. Henley and J.E. Miller, Phys. Rev. D50, 7077 (1994).

[7] J.-M. Gaillard and G. Sauvage, Ann. Rev. Nucl. Part. Sci. 34, 351 (1984).

# Test of Isospin Mixing in Hyperon Semileptonic Decays

Vincent J. Smith[a] *

[a]H H Wills Physics Laboratory, University of Bristol, UK-BS8 1TL

Following the proposal of the previous speaker, preliminary calculations are presented for the design of an experiment to measure the isospin mixing of the $\Lambda$ through a comparison of the mirror decays $\Sigma^{\pm} \to \Lambda e^{\pm} \nu$ .

It is usually assumed that the breaking of isospin symmetry is due to the electromagnetic interaction acting on the different charges of the $u$ and $d$ quarks. However, a difference in the masses of the $u$ and $d$ quarks also leads to isospin symmetry breaking, even where electromagnetic effects are very small, and could give a measurable mixing between members of different isospin multiplets, for example the $\Lambda$ and $\Sigma^0$ hyperons. Such an effect would lift the $\Sigma^0$ and reduce the $\Lambda$ masses by a small amount: an order-of-magnitude estimate can be obtained by noting that the $\Sigma^0$ lies about 0.9 MeV above the mean of the $\Sigma^+$ and $\Sigma^-$ masses, while the $\Sigma - \Lambda$ splitting is about 77 MeV. The ratio of these is about 1.2%. Better theoretical calculations [1,2] suggest the mixing is approx 1.5% in the wavefunction.

Such a mixing would make small changes to the $\Lambda$ properties, so it is important to make an experimental determination of the size of the effect. One place where it might be seen is in a comparison of the mirror decays: $\Sigma^{\pm} \to \Lambda e^{\pm} \nu$ . Estimates have been made [3,4] which suggest that the ratio of the two partial rates could differ by as much as 6% from the value expected with no symmetry breaking.

Present data on these decays are not of sufficient precision to test this: the $\Sigma^- \to \Lambda e^- \overline{\nu}$ decay has been measured to $\pm 5\%$ with 1842 events [5] of which 1620 events were collected by the WA2 experiment at the CERN SPS [6]. The $\Sigma^+ \to \Lambda e^+ \nu$ decay has only been measured to $\pm 25\%$ accuracy with 21 events [5].

It would certainly be interesting to measure these branching ratios to an accuracy of $< \pm 1\%$ (*ie* to better than $10^{-8}$ in the total rates.) Assuming total beam rates of order $10^7 s^{-1}$ and making reasonable assumptions of duty cycle, $\Sigma^{\pm}$ fractions, fiducial volume in which decays can be accepted, trigger livetime and the $\Lambda \longrightarrow p\pi^-$ branching ratio, the measurement of branching ratios for both decays in the same apparatus could be achieved in a run of a few weeks. Detailed calculations, intended to lead to a proposal, are being undertaken at present. All the apparatus needed for such an experiment already exists in the SELEX experiment: only a minor reconfiguration is required.

Notice that a measurement of the ratio of partial decay rates from the branching ratios to better than 1% would also require improved measurements of the $\Sigma^+$ and $\Sigma^-$ lifetimes (presently known to $\pm 0.5\%$ and $\pm 0.7\%$ respectively [5].)

It might also be possible to measure the $g_V/g_A$ ratio in both decays, from the angular distributions between the electron momentum and the $\Lambda$ spin. This would be zero without mixing, but is predicted [3] to be $\pm 0.03$ for the two decays with the expected mixing.

With a good determination of the $\Lambda - \Sigma^0$ mixing, more accurate comparisons between experiment and theory can be made for the F and D parameters in hyperon semileptonic decays: however, the size of the correction is small [3].

In the case of the hyperon magnetic moments, it is interesting to note that a fit to all the measured octet magnetic moments *except* the $\Lambda$ gives the same value for the magnetic moment of the $s$ quark as the measured $\Lambda$ magnetic moment, to three significant figures.

## REFERENCES

1. R.H.Dalitz and F.von Hippel, Physics Letters **10**, 153 (1964)
2. N.Isgur, Physical Review **D21**, 779 (1980)
3. G.Karl, Physics Letters **B328**, 149 (1994)
4. E.M.Henley and G.A.Miller, Phys Rev **D50**, 7077 (1994)
5. Particle Data Group, Eur Phys J **C3**, 1 (1998)
6. M.Bourquin *et al.*, Z Phys **C12**, 307 (1982)

*I wish to express my thanks to KLM's 'Flying Dutchman' frequent traveler program for assistance with travel to this conference.

# Particle - antiparticle asymmetries in the production of baryons in 500 GeV/$c$ $\pi^-$-nucleon interactions

J.C. Anjos [a]
Representing the Fermilab E791 Collaboration

[a]Centro Brasileiro de Pesquisas Físicas,
Rua Dr. Xavier Sigaud 150 - Urca
22290-180 Rio de Janeiro, Brazil

We present the Fermilab E791 measurement of baryon - antibaryon asymmetries in the production of $\Lambda^\circ$, $\Xi$, $\Omega$ and $\Lambda_c$ in 500 GeV/$c$ $\pi^-$-nucleon. Asymmetries have been measured as a function of $x_F$ and $p_T^2$ over the range $-0.12 < x_F < 0.12$ and $p_T^2 < 4$ (GeV/$c$)$^2$ for hyperons and $-0.1 < x_F < 0.3$ and $p_T^2 < 8$ (GeV/$c$)$^2$ for the $\Lambda_c$ baryons. We observe clear evidence of leading particle effects and a basic asymmetry even at $x_F = 0$. These are the first high statistics measurements of the asymmetry in both the target and beam fragmentation regions in a fixed target experiment.

Particle - antiparticle asymmetry is an excess in the production rate of a particle over its antiparticle (or vice-versa). It can be quantified by means of the asymmetry parameter

$$A = \frac{N - \bar{N}}{N + \bar{N}}\,, \qquad (1)$$

where $N$ ($\bar{N}$) is the number of produced particles (antiparticles).

Measurements of this parameter show leading particle effects, which are manifest as an enhancement in the production rate of particles which have one or more valence quarks in common with the initial (colliding) hadrons, compared to that of their antiparticles which have fewer valence quarks in common.

Other effects, such as associated production of meson and baryons can also contribute to a non-zero value of the asymmetry parameter.

Leading particle effects in charm hadron production have been extensively studied in recent years from both the experimental [?] and theoretical point of view [?]. The same type of leading particle effects are expected to appear in strange hadron production. Although previous reports of global asymmetries in $\Lambda^\circ$, $\Xi$ and $\Omega$ hadroproduction already exist [?], there is a lack of a systematic study of light hadron production asymmetries.

From a theoretical point of view, models which can account for the presence of leading particle effects in charm hadron production use some kind of non-perturbative mechanism for hadronization, in addition to the perturbative production of charm quarks [?].

Given E791's $\pi^-$ beam incident on nucleon targets, strong differences are expected in the asymmetry in both the $x_F < 0$ and $x_F > 0$ regions. In particular, as $\Lambda$ (or $\Lambda_c$) baryons are double leading in the $x_F < 0$ region while both $\Lambda$ ($\Lambda_c$) and $\bar{\Lambda}$ ($\bar{\Lambda}_c$) are leading in the $x_F > 0$ region, a growing asymmetry with $|x_F|$ is expected in the negative $x_F$ region and no asymmetry is expected in the positive $x_F$ region. $\Xi^-$ baryons are leading in both the positive and negative $x_F$ regions, whereas $\Xi^+$ are not. Thus a growing asymmetry with $|x_F|$ is expected in this case. $\Omega^\pm$ are both non leading, so no asymmetry is expected at all.

Experiment E791 recorded data from 500 GeV/c $\pi^-$ interactions in five thin foils (one platinum and four diamond) separated by gaps of 1.34 to 1.39 cm. Each foil was approximately 0.4% of a pion interaction length thick (0.6 mm for the platinum foil and 1.5 mm for the carbon foils). A complete description of the E791 spectrometer can be found in Ref. [?].

An important element of the experiment was its extremely fast data acquisition system [?] which, combined with a very open trigger requiring a beam particle and a minimum transverse energy deposited in the calorimeters, was used to record a data sample of $2 \times 10^{10}$ interactions.

The E791 experiment reconstructed more than $2 \times 10^5$ charm events and many millions of strange baryons.

Hyperons produced in the carbon targets and with decay point downstream the SMD planes were kept for further analysis.

$\Lambda^\circ$ were selected in the $p\pi^-$ and c.c. decay mode. All combinations of two tracks with an *a priori* Cherenkov probability of being identified as a $p\pi^-$ combination were selected for further analysis if the tracks have a distance of closest approach less than 0.7 cm from the decay vertex. In addition, the invariant mass was required to be between 1.101 and 1.127 GeV/$c^2$, the ratio of the momentum of the proton to that of the pion was required to be larger than 2.5 and the reconstructed $\Lambda^\circ$ decay vertex must be downstream of the last target. The impact parameter must be less than 0.3 cm if the particle decays within the first 20 cm and 0.4 if decaying more than 20 cm downstream of the target region.

$\Xi$'s were selected in the $\Lambda^\circ\pi^-$ and c.c. decay mode and at the same time $\Omega$'s were selected in the $\Lambda^\circ K^-$ and c.c. channel. Starting with a $\Lambda^\circ$ candidate, a third distinct track was added as a possible pion or kaon daugther. All three tracks were required to be only in the drift chamber region. Cuts for the daughter $\Lambda^\circ$ were the same as above, except for that on the impact parameter. The invariant mass for the three track combination was required to be between 1.290 and 1.350 GeV/$c^2$ and 1.642 and 1.702 GeV/$c^2$ for $\Xi$ and $\Omega$ candidates respectively. In addition, the $\Xi$ and $\Omega$ decay vertices were required to be upstream the $\Lambda^\circ$ decay vertex and downstream the SMD region. For $\Omega$'s, the third track had to have a clear kaon signature in the Cherenkov counter.

From fits to a gaussian and a linear background we obtained $2,571,700 \pm 3,100$ $\Lambda^\circ$ and $1,669,000 \pm 2,600$ $\bar{\Lambda}^\circ$ from approximately 6.5% of the total E791 data sample, $996,200 \pm 1,900$ $\Xi^-$ and $706,600 \pm 1,700$ $\Xi^+$ and $8,750 \pm 130$ $\Omega^-$ and $7,469 \pm 120$ $\Omega^+$, these last four being from the total E791 data sample. The final data samples for hyperons are shown in Fig. ??.

For charm baryons, the five targets were used. In most cases, $\Lambda_c$'s decayed in air between the target foils, and before entering the silicon vertex detectors. All combinations of three tracks consistent with an *a priori* Cherenkov probability of being identified as a $pK\pi$ and c.c. combination were selected for further analysis if the distance between $\Lambda_c$ decay vertex to the primary vertex was at least 5 standard deviations, and the invariant mass was between 2.15 and 2.45 GeV/$c^2$. To further enrich the sample, we required the $\Lambda_c$ to decay at least five standard deviations downstream of the nearest target foil and between one and four lifetimes. The $\Lambda_c$ momentum vector,

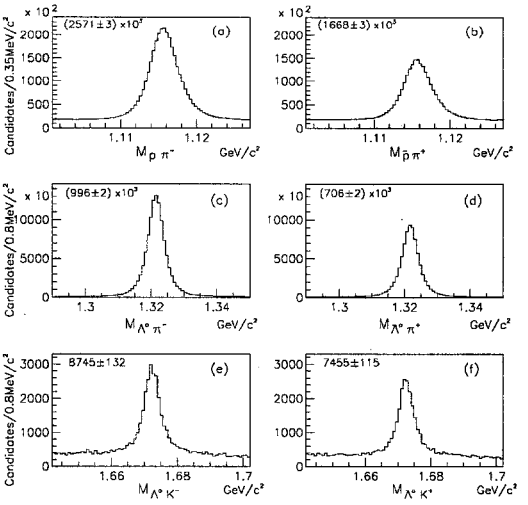


Figure 1. $\Lambda^\circ$ (upper), $\Xi$ (middle) and $\Omega$ (lower) invariant mass plots for the final data samples. Left side figures are particles, right side are antiparticles.

reconstructed from its decay products, was required to pass within $3\sigma$ of the primary vertex. It was required that primary and secondary vertex had acceptable $\chi^2$ per degree of freedom. We also required that at least two of the three $\Lambda_c$ decay tracks be inconsistent with coming from the primary vertex. The final data sample, fitted to a gaussian plus a quadratic background has $1,025 \pm 45$ $\Lambda_c^+$ and $794 \pm 42$ $\Lambda_c^-$. The invariant mass plot for the $pK\pi$ combination is shown in Fig. ??.

For each baryon - antibaryon pair, an asymmetry both as a function of $x_F$ and $p_T^2$ was calculated by means of eq. ??. Values for $N$ ($\overline{N}$) were obtained from fits to the corresponding effective mass plots for events selected within specific $x_F$ and $p_T^2$ ranges. In all cases, well defined particle signals were evident.

Efficiencies and geometrical acceptances were estimated using a sample of Monte Carlo (MC) events produced with the PYTHIA and JETSET event generators [?]. These events were projected through a detailed simulation of the E791 spectrometer and then reconstructed with the same algorithms used for data. In the simulation of the detector, special care was taken to represent the behaviour of tracks passing through the dead-

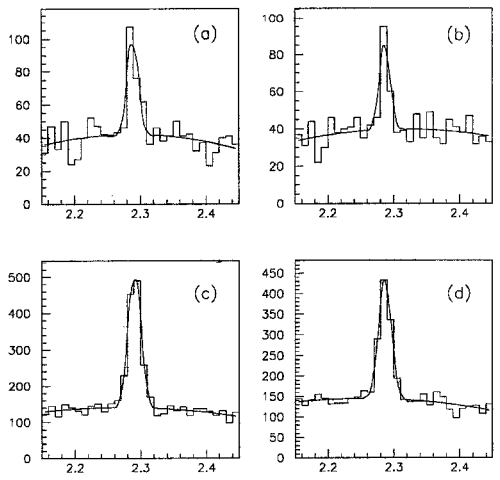


Figure 2. $pK^-\pi^+$ and $\bar{p}K^+\pi^-$ mass distributions showing clear $\Lambda_c^+$ and $\Lambda_c^-$ signals in each case in $x_F < 0$ and $x_F > 0$ regions. From fits with a Gaussian and a parabolic background we obtained 122 $\pm$ 17 $\Lambda_c^+$ (a) and 92 $\pm$ 15 $\Lambda_c^-$ (b) in the negative $x_F$ and 903 $\pm$42 $\Lambda_c^+$ (c) and 702 $\pm$40 (d) $\Lambda_c^-$ in the positive $x_F$ regions.

ened region of the drift chambers near the beam. The behavior of the apparatus and details of the reconstruction code changed during the data taking and long data processing periods, respectively. In order to account for these effects, we generated the final MC sample into subsets mirroring these behaviors and fractional contributions to the final data set. Good agreement between MC and data samples in a variety of kinematic variables and resolutions was achieved. We generated 5 million of $\Lambda^\circ$, 16.4 million of $\Xi$, 4.8 million of $\Omega$, and 7 million of $\Lambda_c$ MC events.

Sources of systematic uncertainties were checked in each case. For hyperons we looked for effects coming from changes in the main selection criteria, minimun transverse energy in the calorimeter required in the event trigger, uncertainties in the relative efficiencies for particle and antiparticle, effects of the 2.5%

$K^-$ contamination in the beam, effects of $K^\circ$ contamination in the $\Lambda^\circ$ sample, stability of the analysis for different regions of the fidutial volume and binning effects. For $\Lambda_c$'s we checked the effect of varying the main

selection criteria, the effect of the kaon contamination in the beam, the contamination of the data sample with $D$ and $D_s$ mesons decaying in the $K\pi\pi$ and $KK\pi$ modes and the parametrization of the background shape.

Systematic uncertainties are small and negligible in comparison with statistical errors for the $\Lambda_c$ asymmetry. However they are not for the hyperons, and are included in the error bars.

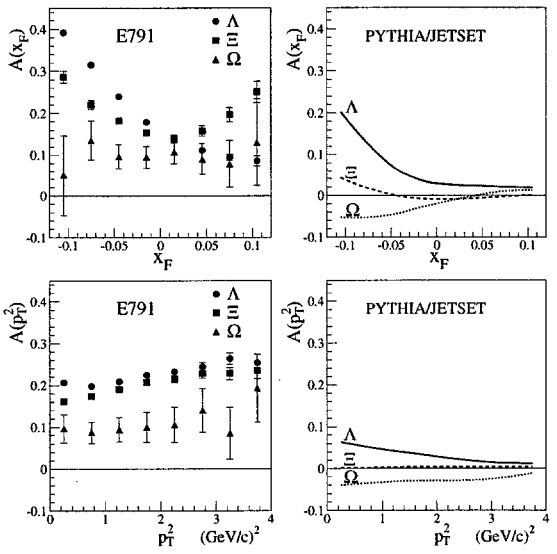


Figure 3. $\Lambda^\circ$, $\Xi$ and $\Omega$ asymmetries as a function of $x_F$ (upper right) and $p_T^2$ (lower right). The asymmetry for $x_F$ ($p_T^2$) is integrated over all the $p_T^2$ ($x_F$) range of the data set. The left column figures show the predictions of PYTHIA/JETSET.

Asymmetries in the corresponding $x_F$ ranges integrated over our $p_T^2$ and in the corresponding $p_T^2$ range integrated over our $x_F$ range are shown in Fig. ?? and ?? for hyperons and $\Lambda_c$ baryons respectively, in comparison with predictions from the default PYTHIA/JETSET.

We have presented data on hyperon and $\Lambda_c$ production asymmetries in the central region for both $x_F > 0$ and $x_F < 0$. The range of $x_F$ covered allowed the first simultaneous study of the hyperon and $\Lambda_c$ production asymmetry in both the negative and positive $x_F$ regions in a fixed target experiment. Our results show, in all cases, a positive asymmetry after acceptance corrections over all the kinematical range studied.

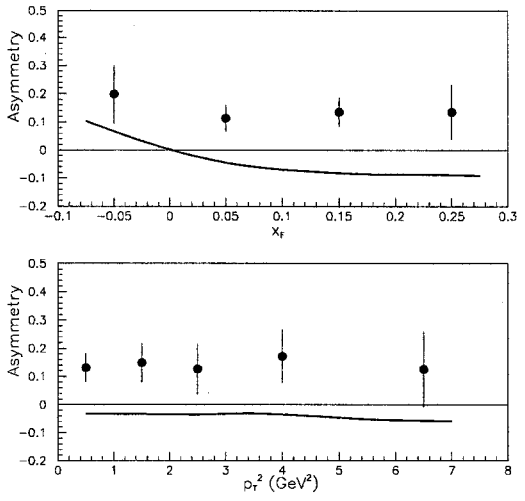


Figure 4. $\Lambda_c^+/\Lambda_c^-$ asymmetry as a function of $x_F$ (upper) and $p_T^2$ (lower). Full lines are the prediction of PYTHIA/JETSET. The asymmetry for $x_F$ ($p_T^2$) is integrated over all the $p_T^2$ ($x_F$) range of the data set. The thin horizontal lines are for reference only. Experimental points are in the center of the corresponding bin.

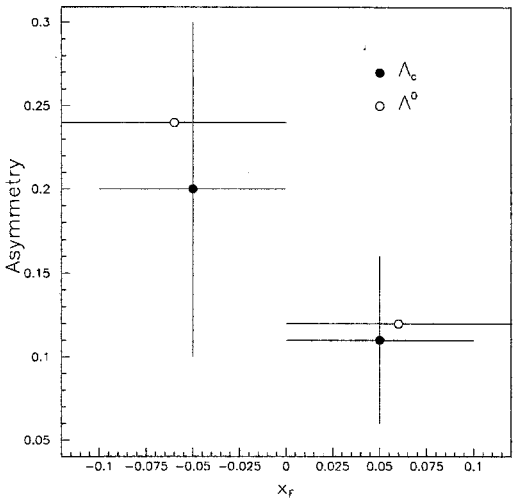


Figure 5. Comparison between the $\Lambda^\circ$ and $\Lambda_c$ asymmetries as a function of $x_F$. The horizontal error bars indicate the size of the bin in each case.

Our results are consistent with results obtained by previous experiments [?].

Our data shows that leading particle effects play an increasingly important role as $|x_F|$ increases. The non-zero asymmetries measured in regions close to $x_F = 0$ suggest that energy thresholds for the associated production of baryons and mesons play a role in particle antiparticle asymmetries.

On the other hand, the similarity in the $\Lambda^\circ$ and $\Lambda_c$ asymmetries as a function of $x_F$ (see Fig. ??) suggest that the *ud* diquark shared between the produced $\Lambda$ baryons and Nucleons in the target should play an important role in the measured asymmetry in the $x_F < 0$ region. However, one expects the $\Lambda_c$ asymmetry to grow more slowly than the $\Lambda^\circ$ asymmetry due to the mass difference between the two particles.

The PYTHIA/JETSET model describes only qualitatively our results, which in turn can be better described in terms of a model including recombination of valence and sea quarks already present in the initial (colliding) hadrons and effects due to the energy thresholds for the associated production of baryons and mesons [?].

## REFERENCES


1. G. A. Alves *et al.*, Phys. Rev. Lett. **77**(1996)2388, ibid, Phys. Rev. Lett. **72**(1994)812, M. Adamovich *et al.*, Phys. Lett. **B305**(1993)402, E.M. Aitala *et al.*, Phys. Lett. **B371**(1996)157, M. Adamovich *et al.*, Nucl. Phys. **B495** (1997)3, S. Barlag *et al.*, Phys. Lett. **B 247**, 113 (1990).
2. R. Vogt and S.J. Brodsky, Nucl. Phys. **B 478**, 311 (1996), G. Herrera and J. Magnin, Eur. Phys. J. **C 2**, 477 (1998).
3. S. Barlag *et al.*, Phys. Lett. **B325**, 531 (1994), D. Bogert *et al.*, Phys. Rev. **D16**, 2098 (1977), S. Mikocki *et al.*, Phys. Rev. **D34**, 42 (1986), R.T. Edwards *et al.*, Phys. Rev. **D18**, 76 (1978); N.N. Biswas *et al.*, Nucl. Phys. **B167**, 41 (1980).
4. E.M. Aitala, et al. (E791 Collaboration), Eur. Phys. J. **C 4** (1999) 1.
5. PYTHIA 5.7 and JETSET 7.4 Physics Manual, T. Sjostrand, CERN-TH-7112/93(1993). H. U. Bengtsson and T. Sjostrand, Computer Physics Commun. **46**, 43 (1987).
6. J.C. Anjos, J. Magnin, F.R.A. Simão and J. Solano, AIP Conf. Proc. No. 444, 540 (1998).

# Polarization of $\Xi^0$ and $\overline{\Xi}^0$ at KTeV Experiment

Theodoros Alexopoulos, Albert R. Erwin [a]

[a]University of Wisconsin
Madison, Wisconsin 53706

The KTeV experiment measured the polarization of the $\Xi^0$ and $\overline{\Xi}^0$ hyperons produced by 800 GeV protons on a BeO target at a fixed targeting angle of 4.8 mrad. Comparison with previous data at 400 GeV production energy and twice the targeting angle shows no significant energy dependence for the $\Xi^0$ polarization. No evidence for $\overline{\Xi}^0$ polarization at 800 GeV was found.

## 1. Introduction (History of Polarization)

The surprise discovery of polarization in the production of hyperons by G. Bunce *et al.* at Fermilab in 1976 [1] using unpolarized 400 GeV/c protons has led to many questions which could not be answered by PQCD (Perturbative Quantum Chromodynamics). In the simplest application of QCD to the question of polarization of massless quarks, predictions yield an overall $P$=0. If, however, both proton valence and sea quarks can be polarized in the collision, some correlation between SU(6) wavefunctions and the measured sign and magnitude of polarization is possible [2].

Both production and polarization of hyperons and anti-hyperons have historically been measured with their kinematic dependence, and this is the ultimate goal for the data studied in this analysis. The picture given by past experiments [3,4] shows that polarization is directly a function of momentum ($p$), production angle ($\theta$) and the target material. Polarization reverses sign with production angle, and $\theta = 0$ corresponds to zero polarization. Further studies of kinematics involve polarization dependence on transverse momentum, $p_t = p_\Xi \, sin\theta$, and $x_F$, the longitudinal momentum dependence[1]. Fig. 1 shows the details of the transverse momentum in the production plane.

Polarization is dependent on both of these kinematic variables. Specifically, past experiments report polarization increases with $p_t$ until either $p_t$ $\approx$ 1 GeV/c [5–7] or $p_t \approx$ 1.5 GeV [1,2], then decreases. Polarization has also been shown to increase with $x_F$ [4,2]. Other experiments report polarization increasing with $p_t$ [8] ($\Lambda$) or as an increasing function of both $p_t$ and $x_F$ [4] ($\Xi^0$). Some experiments on $\Xi^-$ [7] show monotonic increase with $p_t$ but no dependence on $x_F$.

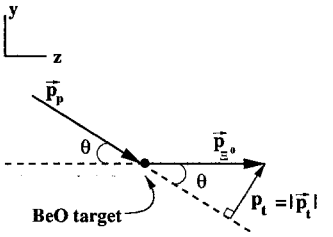


Figure 1. Direction of transverse momentum in the production plane.

These results differ from those for anti-hyperons, which have not been observed to be produced polarized, except for $\overline{\Xi}^+$ in E756 [9] and $\overline{\Sigma}^-$ in E761 [6], both with incident protons at 800 GeV/c. In these experiments, the anti-hyperons were produced with the same magnitude and sign of polarization as their hyperon counterparts.

Also of interest in the review of past experiments are differences in targeting angle, $\theta$, and in the incident energy of the proton. The work in reference [8] reports finding equal polarization of $\Lambda$ at 800 GeV/c, 4.8 mrad and at 400 GeV/c, 9.6 mrad. Hence the magnitude of the polarization remains constant at twice the targeting angle and half the energy. Further, [4] explicitly engages the question of target angle dependence by using 400 GeV protons at several different angles for $\Xi^0$. The results are that polarization increases as $\theta$ decreases. Pushing the envelope at the other end, Morelos *et al.* [6] study only the dependence of polarization magnitude on incident proton mo-

[1] $x_F$ = p/800 GeV/c is the fraction of the total incident momentum that the hyperon carries away after the collision in this experiment

mentum. They show that for $\Sigma^+$ ($\overline{\Sigma^-}$), the polarization magnitude is less at 800 GeV/c than at 400 GeV/c (proton momentum) indicating an inverse relationship between energy and polarization. Different results have been found by [7] for $\Xi^-$ where the magnitude of the polarization increases from 400 GeV/c to 800 GeV/c, indicating a direct relationship.

## 2. KTeV Experiment

The data discussed in this letter were obtained by Fermilab Experiment E799II which is part of the KTeV experiment.

An 800 GeV/c proton beam, with up to $5 \times 10^{12}$ protons per 19 s Tevatron spill every minute, was targeted at a vertical angle of 4.8 mrad on a 1.1 interaction length (30 cm) BeO target. A set of sweeping magnets was used to remove the charged particles and a set of collimators defined two nearly parallel neutral beams that entered the KTeV apparatus (Fig. 2) 94 m downstream from the target. The 65 m vacuum ($\sim 10^{-6}$ Torr) decay region extended to the first drift chamber. The targeting angle was fixed at 4.8 mrad in the vertical plane. Since we could not vary the production angle, the $\Xi^0$ spin direction was reversed by altering its precession angle in our beamline magnets.

Along the beam was defined to be the $Z$-axis while vertical was $Y$ and normal to the $YZ$-plane, or the plane of production, was the $X$ axis. This direction is defined as $\hat{n} = \hat{p}_p \times \hat{p}_\Xi / |\hat{p}_p \times \hat{p}_\Xi|$, which is along the $\Xi^0$ polarization (Fig. 1).

The sweeping magnets were located in the target area (Fig. 3) and had magnetic fields in the vertical ($Y$) direction producing a precession of the $\Xi^0$ spin in the $X - Z$ plane. By altering the field strength and polarity of just one sweeping magnet (NM2SR), the $\Xi^0$ spin precession was changed from 0° to 180°. The accepted value [10] of the $\Xi^0$ magnetic moment was used in calculating the required field strenth. The field of the NM2SR magnet was changed approximately every day.

The charged particle spectrometer consisted of a dipole magnet (NM4AN) surrounded by four drift chambers (DC1–4) with $\sim 100$ $\mu$m position resolution in both horizontal and vertical views. To reduce multiple scattering, helium filled bags occupied the spaces between the drift chambers. In E799-II, the magnetic field imparted a $\pm 205$ MeV/c horizontal momentum component

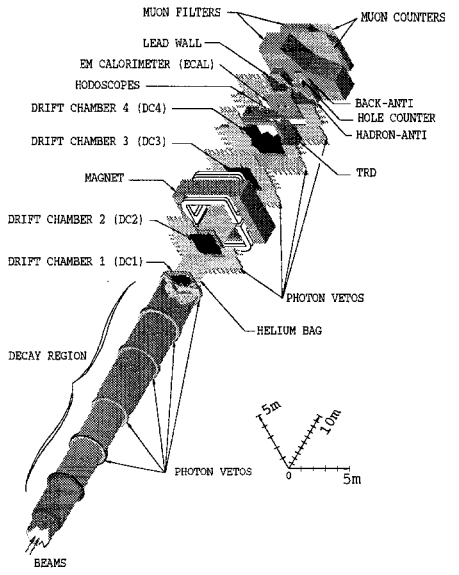


Figure 2. The KTeV apparatus in E799 configuration.

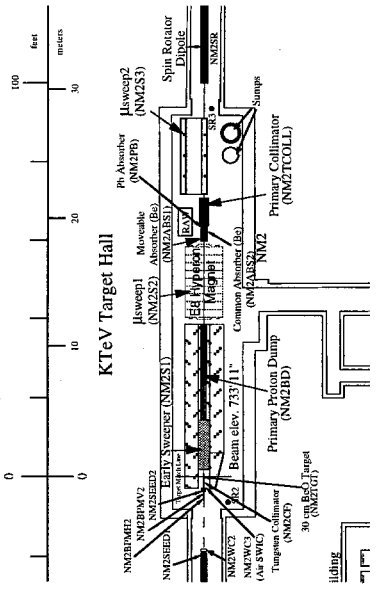


Figure 3. KTeV target area (detector not shown).

to charged particles, yielding a momentum resolution of $\sigma(P)/P = 0.38\% \oplus 0.016\% P\,(\mathrm{GeV/c})$.

The $(1.9 \times 1.9\ \mathrm{m}^2)$ electromagnetic calorimeter (ECAL) consisted of 3100 pure CsI crystals. Each crystal was 50 cm long (27 radiation lengths, 1.4 interaction lengths). Crystals in the central region $(1.2 \times 1.2\ \mathrm{m}^2)$ had a cross-sectional area of $2.5 \times 2.5\ \mathrm{cm}^2$; those in the outer region, $5 \times 5\ \mathrm{cm}^2$. After calibration, the ECAL energy resolution was better than 1% for the electron momentum between 2 and 60 GeV. The position resolution was ~1 mm. We also used the ECAL as the main particle identification detector. It had an $e/\pi$ rejection of better than 500:1.

Nine photon veto assemblies detected particles leaving the fiducial volume. Two scintillator hodoscopes in front of the ECAL were used to trigger on charged particles. Another scintillator plane (hadron-anti), located behind both the ECAL and a 10 cm lead wall, acted as a hadron shower veto. The hodoscopes and the ECAL detectors had two holes $(15 \times 15\ \mathrm{cm}^2$ at the ECAL) and the hadron-anti had a single $64 \times 34\ \mathrm{cm}^2$ hole to let the neutral beams pass through without interaction. Charged particles passing through these holes were detected by $16 \times 16\ \mathrm{cm}^2$ scintillators (hole counters) located along each beam line in the hole region just downstream of the hadron-anti.

## 3. Analysis

Both $\Xi^0 \to \Lambda\pi^0/\overline{\Xi}^0 \to \overline{\Lambda}\pi^0$ decays have a high momentum (>100 GeV/c) positive/negative track (proton/antiproton) which remained in or near the neutral beam region, a second lower momentum negative/positive track ($\pi^-/\pi^+$), and two neutral (*i.e.* not associated with any track) ECAL energy clusters (photons from a $\pi^0$). The $z$-plane of the cascade vertex is calculated using the energy and position of the photons entering the calorimeter. Using the known [10] value of the mass of the $\pi^0$, the $z$ plane is: $z = (\delta/m_{\pi^0})\sqrt{E_1 E_2}$, where $E_1$, $E_2$ are the energies of the photons and $\delta$ is the distance between the photons hitting the calorimeter. Using this calculated $z$-plane as one vertex, the sum of the proton and $\pi^-$ vectors (for the $\Xi^0$ case) is extrapolated backwards to the point where it intersects this plane. This yields the $x$ and $y$ coordinates of the $\Xi^0$ decay vertex.

Besides trigger requirements and reconstruction techniques, we applied some quality cuts which strongly suppressed accidental photons in the presence of $\Lambda$ events. Fig. 4 shows the effect on the reconstructed mass, $\Lambda\pi^0$, after all cuts for various NM4AN and NM2SR run conditions.

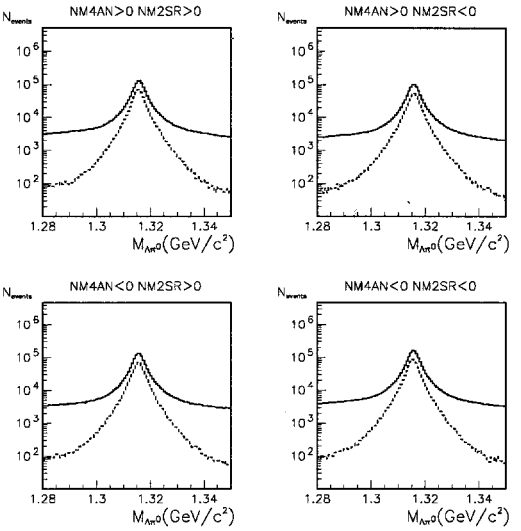


Figure 4. Reconstructed cascade mass from data

The $\Xi^0$ or $\overline{\Xi}^0$ polarization was determined by first splitting our data into two oppositely polarized samples and then calculating the direction cosines $[\cos\theta_x, \cos\theta_y, \cos\theta_z]$ of the $\Lambda$ momentum vector in the $\Xi^0$ rest frame. For a sample of decays where the $\Xi^0$ has an average polarization $P$, the normalized direction cosine distribution is:

$$f_\pm(\cos\theta_k) = \frac{dN}{d\cos\theta_k} = A(\cos\theta_k)(1 \pm \alpha_{\Xi^0} P_k cos\theta_k) \quad (1)$$

for k=x,y,z. $A(\cos\theta_k)$ is a function that describes the experimental acceptance for $\Xi^0$ decays as function of the $\Lambda$ direction cosine, $\alpha_{\Xi^0}$ is a constant, the $\Xi^0$ decay asymmetry parameter (PDG [10] reports $\alpha_{\Xi^0}$ = -0.411 ± 0.022). The quantity $f_+$ ($f_-$) is the fraction of the 0° (180°) precession sample with a given value of $\cos\theta_k$. Then the antisymmetric ratio:

$$R(\cos\theta_k) = \frac{(f_+ - f_-)}{(f_+ + f_-)} = \alpha_{\Xi^0} P_k \cos\theta_k \quad (2)$$

has a slope with respect to $\cos\theta_k$ which gives the asymmetry $\alpha_{\Xi^0} P_k$, from which the polarization

component $P_k$ is obtained. As long as the acceptance of the detector doesn't vary rapidly with time, it does not enter this calculation of the polarization because it cancels in the ratio. Fig. 5 shows a comparison between the $\Lambda$ direction cosine distributions for the two NM2SR magnet settings. As can been seen, the pairs of distributions are essentially identical in the $X$, and $Z$ directions. In the $Y$ direction, however, the two distributions are clearly different, showing the effect of the $\Xi^0$ polarization on the $\Lambda$ decay distribution.

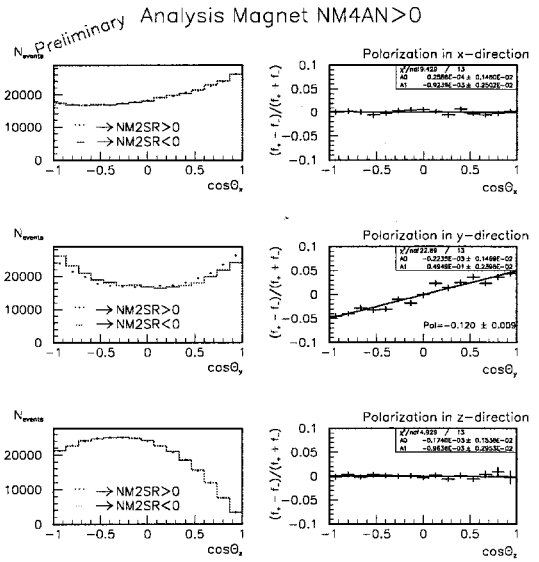


Figure 5. Normalized direction cosine distributions $f_\pm$ in $X, Y, Z$ for $\Xi^0 \to \Lambda\pi^0$ decays, on the left. Solid lines are $f_-$ and dashed are $f_+$. Graphs on the right, show the ratio $R(\cos\theta_k)$. Error bars are statistical only.

Also shown in Fig. 5 the plots of the ratio defined in Eq. (2). Linear fits to these graphs extract the polarization $P_Y$. After taking into account some small acceptance effect of the order of 1% (using Monte Carlo analysis), we derived the polarization to be $P_Y = -0.097 \pm 0.007_{(stat)} \pm 0.002_{(sys)}$, where 0.007 and 0.002 are the statistical and systematic errors, respectively.

Fig. (6) shows a comparison between the $\overline{\Lambda}$ direction cosine distributions for the two NM2SR magnet settings. As can been seen, the pairs of distributions are essentially identical in the $X$, $Y$ and $Z$ directions, resulting in no polarization effect.

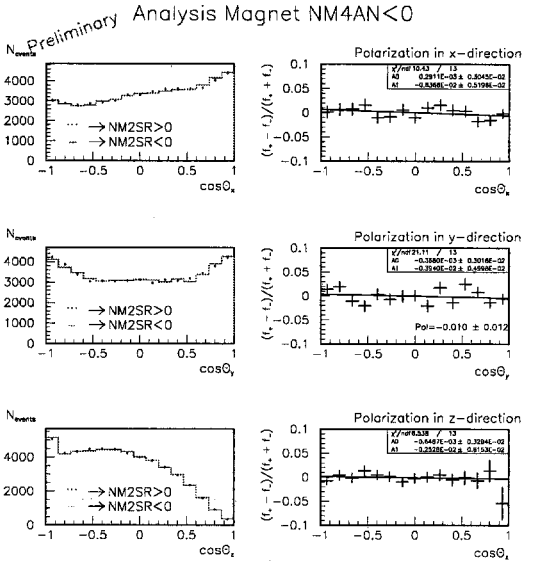


Figure 6. Normalized direction cosine distributions $f_\pm$ in $X, Y, Z$ for $\overline{\Xi}^0 \to \overline{\Lambda}\pi^0$ decays, on the left. Solid lines are $f_-$ and dashed are $f_+$. Graphs on the right, show the ratio $R(\cos\theta_k)$. Error bars are statistical only.

The $\Xi^0$ and $\overline{\Xi}^0$ data were divided into energy bins, and the polarization was calculated for each bin. Results are shown in Fig. (7).

Fig. (7) shows the variation of $\Xi^0$ and $\overline{\Xi}^0$ polarization with production transverse momentum. On this same graph, comparable data [4,8] from a past Fermilab experiment has been superimposed. The $\Xi^0$ [4] data had a targeting angle of 9.8 mrad, almost twice our targeting angle, and a proton beam energy of 400 GeV, half our energy. The target material for these data and for ours was Be. For a given value of $p_t$, these data samples [4] have the same $x_F$ value as the data presented here, and are therefore directly comparable. No significant change in $\Xi^0$ polarization is seen between the two production energies of 400 and 800 GeV. Also, the $\Lambda$ polarization from the Fermilab E799I [8] is shown, produced with the same targeting angle of 4.8 mrad and proton beam energy of 800 GeV.

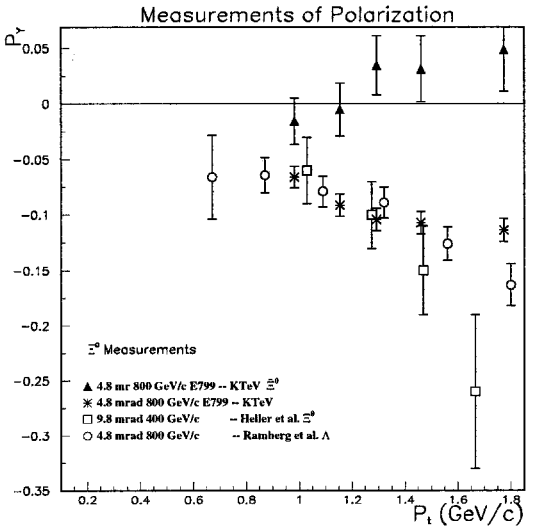


Figure 7. $\Xi^0$ and $\bar{\Xi}^0$ polarization versus production transverse momentum $p_t$. For comparison, $\Xi^0$ [4] and $\Lambda$ [8] data from 400 GeV are shown.

## 4. Conclusion

In conclusion, the polarization of the $\Xi^0$ hyperons produced by 800 GeV protons at a fixed targeting angle of 4.8 mrad was determined. Comparing our values with those determined previously for production at 400 GeV and a targeting angle of 9.8 mrad, we find no significant energy dependence in $\Xi^0$ polarization at these energies. We also find no significant $\bar{\Xi}^0$ polarization at 800 GeV. These results emphasize the still puzzling nature of the polarization pattern in hadroproduction of hyperons.

## REFERENCES


1. G. Bunce *et al.*, Phys. Rev. Lett. 36, 1133 (1976).
2. L. Pondrom, Phys. Rep. **122**, 57 (1985).
3. K. Heller, in *Spin and Polarization Dynamics in Nuclear and Particle Physics*, edited by A. Barut, Y Onel and A. Penzo (World Scientific, New Jersey, 1990), 36.
4. K. Heller *et al.*, Phys. Rev. Lett. **51**, 2025 (1983).
5. Peter S. Cooper, "Hyperon Beam Physics", Fermilab-Conf-96/063, Fermi National Laboratory, March 1996 (unpublished).
6. A. Morelos *et al.*, Phys. Rev. Lett. **71**, 2172 (1993).
7. J. Duryea *et al.*, Phy. Rev. Lett. **67**, 1193 (1991).
8. E.J. Ramberg *et al.*, Phys. Lett. B **338**, 403 (1994).
9. P. M. Ho *et al.*, Phys. Rev. D **44**, 3402 (1991).
10. C. Caso *et al.*, Eur. Phys. J. **C3**, 57 (1998).

# Chapter 3

# Hyperon Beta Decays and Form Factors


- A. Garcia
- A. Alavi-Harati

# Baryon Semileptonic Decays.

Augusto García [a]

[a]Departamento de Física, Centro de Investigación y de Estudios Avanzados del IPN, Apartado Postal 14-740, México, D. F. 07000

This review is organized in three parts. The first one covers the $\Delta S = 0$ and $\Delta S = 1$ hyperon semileptonic decays. The second one covers charm baryon semileptonic decays. The third part is devoted to free neutron beta decay.

## 1. Hyperon Semileptonic Decays (HSD).

The level of precision in HSD good, but it is not very good. The decay rates are comparable to the weak radiative decay rates, but the $g_1$, form factors are not close to the precision of magnetic moments. Only neutron beta decay has attained an already remarkable precision. There are two measured $\Delta S = 0$ hyperon beta decays. $\Sigma^+ \to \Lambda e\nu$ is so poorly measured that it is of no practical use. $\Sigma^- \to \Lambda e\nu$ is fairly well measured. Its decay rate and angular coefficients and the corresponding Cabibbo Theory [1] predictions collected in Tab.(1).

A $3.5\sigma$ discrepancy [2] with Cabibbo Theory is observed in the decay rate. This is the only discrepancy of this magnitude, but is due to the smallness of the error bars and not to a major discrepancy. this confirms that the Cabibbo Theory is only approximate (in Cabibbo's own words, the theory was never intended to be exact), but it is a very good approximation for hyperon demileptonic decays.

There are four $\Delta S = 1$ HSD but only three are of practical use. A fifth one $\Xi^0 \to \Sigma^+ e\nu$ is currently being measured, we shall only mention that predictions for it are already available and for detailed discussions we refer the reader to the talk of Alavi-Harati in this proceeding. To better understand the status of both theory and experiment in these three decays we shall discuss [3] the determination of the Cabibbo-Kobayashi-Maskawa matrix element $V_{us}$ from them and how it compares with its counterpart from $K_{l3}$ decays.

The rates and $g_1/f_1$ ratios do not use all of the experimental information available. It is better to use rates and angular coefficients. These are

Table 1
$\Sigma^- \to \Lambda e\nu$ data and predictions.

| | experiment | prediction | $\Delta\chi^2$ |
|---|---|---|---|
| $R$ | $0.388 \pm 0.018$ | 0.451 | 12.4 |
| $\alpha_{e\nu}$ | $-0.404 \pm 0.044$ | $-0.412$ | 0.03 |
| $A$ | $0.07 \pm 0.07$ | 0.06 | 0.02 |
| $B$ | $0.85 \pm 0.07$ | 0.90 | 0.51 |

the data we have ($R$ is in $10^6 sec^{-1}$) [4]

$$\Lambda \to pe\nu$$
$$R = 3.169 \pm 0.058$$
$$\alpha_{e\nu} = -0.19 \pm 0.013$$
$$\alpha_e = 0.125 \pm 0.066$$
$$\alpha_\nu = 0.821 \pm 0.060$$
$$\alpha_p = -0.508 \pm 0.065$$

$$\Sigma^- \to ne\nu$$
$$R = 6.876 \pm 0.235$$
$$\alpha_{e\nu} = 0.347 \pm 0.024$$
$$\alpha_e = -0.519 \pm 0.104$$
$$\alpha_\nu = -0.230 \pm 0.061$$
$$\alpha_n = 0.509 \pm 0.102$$

$$\Xi^- \to \Lambda e\nu$$
$$R = 3.36 \pm 0.19$$
$$\alpha_{e\nu} = 0.53 \pm 0.10$$
$$A = 0.62 \pm 0.10$$

To get $V_{us}$ we shall [5] use four models: I, relativistic quark model [6]; II, chiral perturbation theory with $O(m_s)$ corrections [7]; III, nonrelativistic bag model with wave function mismatch and center of mass corrections [8]; and IV,

Table 2
Predictions for $f_1/f_1$ ($SU_3$) and in parenthesis for $g_1/g_1$ ($SU_3$).

| | I | II | III | IV |
|---|---|---|---|---|
| $\Lambda \to pe\nu$ | 0.976 | 0.943 | 0.987 | 1.024 |
| | (1.072) | – | (1.050) | – |
| $\Sigma^- \to ne\nu$ | 0.975 | 0.987 | 0.987 | 1.100 |
| | (1.056) | – | (1.040) | – |
| $\Xi^- \to \Lambda e\nu$ | 0.976 | 0.957 | 0.987 | 1.059 |
| | (1.072) | – | (1.003) | – |

the same as II, but including $O(m_s^{3/2})$ corrections [9]. The choice of these models is because they all calculate second order $SU_3$ breaking to $f_1$. Models I and II also calculate the $g_1/f_1$. The predictions of these models are collected in Tab.(2)

None of these four models give predictions for the induced $f_2$ and $g_2$ form factors. In order to assess the success of these models we shall apply three criteria:

A) the value of $V_{us}$ must be common to the three decay,
B) the data must be well reproduced, and
C) comparison with $V_{us}$ from $K_{l3}$.

The $V_{us}$ obtained using I and III are given in Tab.(3)

These two models do not meet criteria A) and B). The values for $V_{us}$ are not common to the three decays and the data are not well reproduced. The source of the discrepancies can be traced to the predicted $g_1$. Therefore, one may drop these last predictions and keep only the predictions for $f_1$.

Instead, the values for $g_1$, can be obtained from the experimental data. This way the four models are treated on an equal footing. The $V_{us}$ obtained are displayed in Tab.(4).

Now, the four models satisfy criterion (A). The data is better reproduced, for $\Lambda \to pe\nu$ $\chi^2$ is lowered to around 11, for $\Sigma^- \to ne\nu$ it is slightly lowered to around 7.5, and for $\Xi^- \to \Lambda e\nu$ is becomes practically zero. So, criterion (B) it better satisfied. To improve the agreement with the data one must take into account the effect of the induced form factors $f_2$ and $g_2$.

This last we do by allowing changes of $\pm 0.10$ and $\pm 0.20$ in $f_2$ and $g_2$ with respect to their $SU_3$ predictions. $f_2$ has an imperceptible effect upon $V_{us}$. $g_2$ has a perceptible effect both on $\chi^2$ and $V_{us}$. Briefly, $g_2$ is required to be around (0.10,0.20) in $\Lambda \to pe\nu$ and around (-0.10,-0.20) in $\Sigma^- \to ne\nu$ and $\chi^2$ is reduced to 8 and 4, respectively. In $\Xi^- \to \Lambda e\nu$, $g_2$ gives no effect. Since (A) and (B) are rather well satisfied, one can quote average values of $V_{us}$. Taking into account the effect of $g_2$. These are displayed in the last column of Tab.(5). The average of models I, II and III are consistent with one another, but they are about 5 $\sigma$' $s$ away from model IV and from the $K_{l3}$ $V_{us} = 0.2188 \pm 0.0016$. In contrast, model IV and $K_{l3}$ agree remarkably well.

From the above analysis, one may conclude that experiment in HSD is in better shape than theory in determing $g_1$, The presence of $g_2$ is required in $\Lambda \to pe\nu$ and $\Sigma^- \to ne\nu$, but experiments do not yet determine precise values for it. The data are good enough as to be sensitive second order $SU_3$ breaking corrections.

Only the product is $|f_1 V_{us}|$ is experimentally accessible (to resolve $V_{us}$ experimentally one should be able to observe quarks individually). Therefore, both in $K_{l3}$ and HSD the separation of these factors is strictly a theoretical problem and in both types of decays only the vector current must be under theoretical control, since $g_1$ in HSD can be well determined experimentally. It is very important to confirm the theoretical calculations of model IV in order to see if, indeed, a unique reliable $V_{us}$, comparable to the one of $K_{l3}$, is obtained in HSD.

## 2. Charm Baryon Semileptonic Decays.

So far four semileptonic decays have been detected experimentally [4]. $\Xi_c^0 \to \Xi^0 e\nu$ (seen), $\Xi_c^+ \to \Xi^- e\nu$ (seen) and $\Lambda_c^+ \to \Lambda\mu\nu$ and $\Lambda_c^+ \to \Lambda e\nu$ measured. These latter two have a branching ratio of $(2.0 \pm 0.7)\%$ and $(2.0 \pm 0.6)\%$, respectively, and a combined $\alpha_e = -0.82 \pm^{0.11}_{0.07}$. We shall discuss the decay rate of $\Lambda_c^+ \to \Lambda e\nu$. Its current value is $R = (9.6 \pm 2.9) \times 10^{10} sec^{-1}$. The Cabibbo theory is no longer a good approximation, it predicts a branching ratio almost an order of magnituded higher than the observed one. at around 15%.

Theoretical predictions have been made for more than twenty years and they vary a lot. A quite thorough review can be found in Ref.[10].

Table 3
$V_{us}$ from I and III.

| | I:$V_{us}$ | $\chi^2$ | I:$V_{us}$ | $\chi^2$ |
|---|---|---|---|---|
| $\Lambda \to pe\nu$ | $0.2130 \pm 0.0020$ | 39 | $0.2153 \pm 0.0020$ | 25 |
| $\Sigma^- \to ne\nu$ | $0.2318 \pm 0.0040$ | 9 | $0.2307 \pm 0.0040$ | 8 |
| $\Xi^- \to \Lambda e\nu$ | $0.2434 \pm 0.0068$ | 1 | $0.2429 \pm 0.0068$ | 2 |

Table 4
Values of $V_{us}$ when $g_1$ is determined from the data. The last column quotes the average $V_{us}$ obtained in each model, when $g_2$ is included (see later in the text).

| | $\Lambda \to pe\nu$ | $\Sigma^- \to ne\nu$ | $\Xi^- \to \Lambda e\nu$ | Average |
|---|---|---|---|---|
| I | $0.2291 \pm 0.0036$ | $0.2349 \pm 0.0049$ | $0.2349 \pm 0.0106$ | $0.2348 \pm 0.0028$ |
| II | $0.2372 \pm 0.0037$ | $0.2320 \pm 0.0049$ | $0.2396 \pm 0.0108$ | $0.2392 \pm 0.0028$ |
| III | $0.2265 \pm 0.0035$ | $0.2320 \pm 0.0049$ | $0.2323 \pm 0.0105$ | $0.2321 \pm 0.0027$ |
| IV | $0.2183 \pm 0.0034$ | $0.2082 \pm 0.0044$ | $0.2165 \pm 0.0098$ | $0.2176 \pm 0.0026$ |

Here we reproduce a short table with a significant sample of predictions for $R$ (in units of $10^{10} sec^{-1}$). Line (a) of Table(5) reproduces the original predictions. Line (b) has a factor of 1/3 applied, corresponding to a spin-flavor suppresion leading to diquark states due to heavy quark symmetry.

There are more predictions. The nonrelativistic quark spectator model with QCD corrections gives [11] $R = 11.2 \times 10^{10} sec^{-1}$. A revision [12] of the NRQM with heavy quark symmetry yields $R = 7.1 \times 10^{10} sec^{-1}$. An improvement [13] of HQET infinite mass limit through full QCD sum rules predicts $R = (13.2 \pm 1.8) \times 10^{10} sec^{-1}$ (method 1) or $R = (20.7 \pm 3.5) \times 10^{10} sec^{-1}$ (method 2).

Even though the experimental value of $R$ is still rather loose, it already provides significant constraints of theoretical predictions. For example, the method 2 prediction of Ref.[13] is ruled out. Also, just applying the 1/3 suppresion factor as in Table(5) to the NRQM predictions is not favored.

Clearly, charm baryon semileptonic decays are merely in their infancy. Much experimental and theoretical work need be invested in what surely is a very interesting subject.

### 3. Free Neutron Beta Decay.

This decay, the very first of all semileptonic decays, has received much attention in last few years. The precision attained in two ($R$ and $\alpha_e$) of the four integrated observables ($R$, $\alpha_{e\nu}$, $\alpha_e$ and $\alpha_\nu$) has reached a level that makes this decay a very promising process to either detect physics beyond the standard model or put severe constraints on its existence.

Here, we shall discuss the current experimental situation and the, so to speak, resolving power of neutron beta decay to detect new physics. In this the last respect, what we shall do[14] is to determine the region in the three dimensional space defined by using $R$, $\alpha_e$, and $V_{ud}$ as cartesian coordinates within which the minimal standard model remains valid.

Ideally, this region is just a point. This would be the case if we could exactly compute $g_1$, $V_{ud}$, and all theoretical uncertanties that affect $R$ and $\alpha_e$ through the raditive corrections. This not being the case, our determination of $V_{ud}$ and $g_1$ comes from the CKM unitary and experimental value of $\alpha_e$ respectively. The uncertantiesin the radiative corrections can be handled as a theoretical error. It is a combination of all these error bars along with those of $R$ that defines a region in the ($R$, $\alpha_e$, $V_{ud}$) space. This region will become smaller the better $R$ and $\alpha_e$ are measured in the future.

The current state-of-the-art allows the error bars in $R$ and $\alpha_e$ to be reduced down to one-tenth of their present values. Also,a detailed analysis of the radiative corrections shows that the theoretical uncertainty in them is less that 5 in $10^{-4}$. What we still ignore is where the central values of $R$ and $\alpha_e$ will be found in the ($R$,$\alpha_e$) plane. Allowing for three of such future error bars and

Table 5
Sample of predictions for $R$ of $\Lambda_c^+ \to \Lambda e \nu$.

| | Buras | Gavela | NRQM | Simpleton | HQET |
|---|---|---|---|---|---|
| a) | 60 | 15 | 17 | 10 | 22 |
| b) | 20 | 5 | 5.6 | 10 | 7.3 |

for the theoretical uncertainty, we obtain a band in this plane, within which the standard model cannot be significantly invalidated. This band is depicted in Fig.(1).

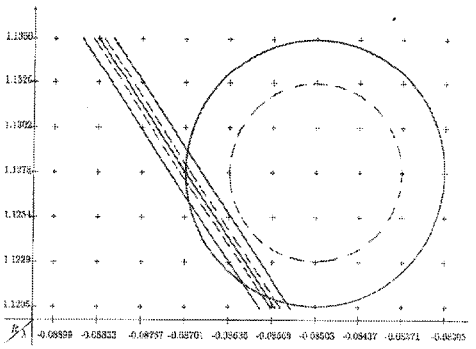

Figure 1.

In as-much-as, $V_{ub}$ is negligibly small and $V_{us}$ is reliably determined by $K_{l3}$ decays, we know $V_{ud}$, namely, $V_{ud} = 0.9756 \pm 0.0004$. The band becomes a tube in three dimensions, with an eliptical cross-section. This last is depicted in Fig.(2), allowing for the $3\sigma$ boundary. It is this tube that determines to what extent neutron beta decay will be able to resolve the existence of new physics in more than just the near future. If future values of $R$, $\alpha_e$ and $V_{ud}$ fall inside this tube then no new physics can be clearly observed in neutron beta decay, but stringent limits will be set up its existence. But if those future values lie outside, i.e., the very small region that can be determined in the future does not overlap significantly with the tube, then the need of physics beyond the standard model would be clearly established.

The region allowed by experiment up until September 1997 [15] is displayed in Figs.(1) and (2) (we chose the scales in the $R$, $\alpha_e$, $V_{ud}$ axes so that it appears like a sphere). Its boundary corresponds to $3\sigma's$ and it is centered at the central values of $R = 1.1278 \pm 0.0024$ (in $10^{-3} sec^{-1}$), $\alpha_e = -0.08503 \pm 0.00066$, and $V_{ud} = 0.9734 \pm 0.0007$ from nuclear physics. This illustrates the usefulness of knowing where the "no new physics" tube lies. It is interesting to remark that with these data one has an statistically significant signal for new physics.

However, real life is more difficult. In late 1997 a new measurement [16] of $\alpha_e$ was published, namely, $\alpha_e = -0.08829 \pm 0.00081$. This measurement excludes the previous central value by almost 4 of its $\sigma$, or viceversa, its central value is 4.8 of the previous $\sigma$ from the previous central value. There is an statistically significant discrepancy and one chould not average this new measurement with the earlier ones. This is not a new situation. History repeats itself. Something similar happened in measurering $R$, over a long period of time important dicrepancies kept appearing until the current already very precise value of $R$ was obtained. So, the present situation in $\alpha_e$ is really an important signal of progress. It is just that measuring at a high level of precision is very difficult and overcoming these discrepancies is an important challenge, and eventually a consistent very precise $\alpha_e$ will be obtained.

The values of $V_{ud}$ obtained from the above two $\alpha_e$ are $V_{ud} = 0.9783 \pm 0.0019$ and $V_{ud} = 0.9709 \pm 0.0022$, respectively. Both are in contradiction with the $V_{ud}$ from unitarity, but from opposite sides. We find that a detailed analysis with the $(R,\alpha_e)$ plane is more meaningful than just comparing $V_{ud}$ values.

Without entering into details, let us finally mention that it may not be necessary to reduce the errors bars of $R$ and $\alpha_e$ to 1/10. What is important is to reduce both error bars simultaneously and then it is quite possible that already at the 1/3 level one might see new physics.

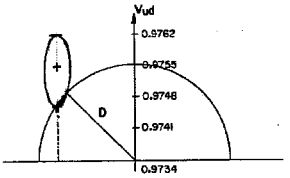


Figure 2.

## 4. Summary.

The experimental level of HSD is better than the theoretical one. It is sensitive the second order $SU_3$ breaking corrections. Neverthless, it is only necessary to better master theoretical calculations of the vector-current part. If the results of model IV are independently confirmed, one might quote the value of $V_{us} = 0.2176 \pm 0.0022$ from HSD, which is competive with the one of $K_{l3}$. Charm baryon semileptonic decays are at their infancy. However, the little so far measured provides already important guidance to model calculations. Neutron beta decay is the best measured of all baryon semileptonic decay and it is quite close to either put severe constraints on new physics or even detect it.

## ACKNOWLEDGMENTS.

The author wish to acknowledge Partial Support of CONACyT (México).The work of J.L. García-Luna is also acknowledged.

## REFERENCES

1. N. Cabibbo, Phys. Rev. Lett. **10**, 531 (1963).
2. J. Donoghue and B. Holstein, Phys. Rev. **D25**, 206 (1982).
   A. García and P. Kielanowski, Phys. Lett. **110B**, 498 (1982).
3. R. Flores, A. García and G. Sánchez-Colón, Phys. Rev. **D54**, 6855 (1996).
4. Particle Data Group, Eu. J. of Phys. **3** (1998).
5. For more details of the procedure see A. García and P. Kielanowski, Hyperon Beta Decay, Lecture Notes in Physics **222** (Springer–Verlag), Berlin, Heidelberg, New York, Tokyo, 1985.
6. F. Schlumpf, Phys. Rev. **D51**, 2262 (1995).
7. A. Krause, Helv. Phys. Acta, **63**, 3 (1990).
8. J. Donoghue, B. Holstein and W. Klimt, Phys. Rev. **D35**, 934 (1987).
9. J. Anderson and M. Luty, Phys. Rev. **D47**, 4975 (1993).
10. A.Körner, et al., Prog. Nucl. Part. Phys. **33**, 787 (1994).
11. R. Huerta, et al., Phys. Rev. **D47**, 4975 (1993).
12. H. Y. Cheng, Hep-ph/9608445.
13. Marques de Carvalho, et al., Phys. Rev. **D60**, 034001 (1999).
14. J.L. Garcia-Luna, unpublished.
15. Particle Data Group, Phys. Rev. **D54**, 1 (1996).
16. H. Abele, et al., Phys.Lett. **B407**, 212(1997).

# Hyperon Semi-Leptonic Decays: An Experimental Overview

Ashkan Alavi-Harati [a]

[a]University of Wisconsin
Madison, Wisconsin 53706

**We review the historical development of semi-leptonic decays of hyperons in the framework of the Cabibbo model which after 36 years still provides the best description of these decays. Emphasis is made on the experimental aspects of the field and the existing available data.**

## 1. Introduction

In 1963, Cabibbo first introduced [1] the mixing of d and s quarks to account for the weak decays of strange particles. The concept of quark mixing was generalized later to the other quark families [2], leading to the CKM matrix in the Standard Model. The Cabibbo mixing angle explained the unusually low rate of for example, $\Lambda \to p e^- \overline{\nu}_e$ and $\Sigma^- \to n e^- \overline{\nu}_e$ from the old bubble chamber experiments. The Cabibbo model provides a unique way to relate all the $\beta$-decays, or semi-leptonic decays, of hyperons together. Its simplicity and at the same time an excellent prediction power makes the model attractive.

In this talk, we review our knowledge of Hyperon Semi-Leptonic Decays (HSD) and the standing of the Cabibbo model from its proposal to date. Obviously, one can not cover every single experiment in the field. Only results from the most definitive experiments will be discussed. The theoretical status of this subject is discussed elsewhere [3].

## 2. Hyperon Semi-Leptonic Decays

Emission of an electron-neutrino pair in the weak interaction of HSD, provides us with a tool to probe the structure of hadronic matter by studying the strong interaction form factors. The fact that hyperons have spin, carry strange quarks and are massive, makes them richer in information compared to the semi-leptonic decays of the neutron and of mesons. Figure 1 shows the energetically allowed $\beta$-decays of type $A \to B e^- \overline{\nu}_e$ in the SU(3) baryon octet. The selection rule $\Delta S = \Delta Q$ for $\Delta S = 1$ is obeyed in these transitions. The observed decays are shown by the solid arrows which include the recently reported $\Xi^0 \to \Sigma^+ e^- \overline{\nu}_e$ decay [4]. The $\Sigma^0$ decays predominantly via electromagnetic interaction, and therefore the weak $\beta$-decay channels to p and $\Sigma^+$ are unlikely to be observed. The $\Xi^- \to \Xi^0 e^- \overline{\nu}_e$ decay has a very small available phase space.

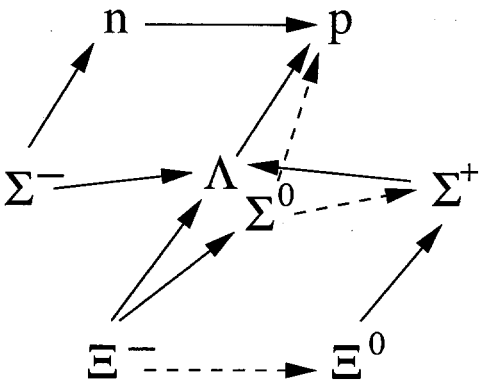


Figure 1. Allowed $\beta$-decays in the baryon octet. Solid arrows indicate the observed decays.

### 2.1. Characteristics of the Decays

As opposed to $\beta$-decay of the neutron which is the only decay mode of the neutron, $\beta$-decays of hyperons are rare and the experimental data is limited. Table 1 shows the Branching Ratio (BR) of the measured HSD listed in PDG [5], and the experimental sample of events based on which this value is extracted. They are in the order of $10^{-3}$ to $10^{-5}$ of the total decay rate. The dominant decay mode of hyperons is a two body decay of the type $A \to C\pi$. In cases where the final state baryon $C$ is the same as $B$ in $\beta$-decay, an excellent electron/pion identification is needed. The last column in table 1 shows this is

Table 1
HSD branching ratios

| | Branching Ratio | Number of Events | Two-body |
|---|---|---|---|
| $\Lambda \to p e^- \overline{\nu}_e$ | $8.32 \times 10^{-4}$ | $20k$ | $Y$ |
| $\Sigma^- \to n e^- \overline{\nu}_e$ | $1.02 \times 10^{-3}$ | $4.1k$ | $Y$ |
| $\Sigma^- \to \Lambda e^- \overline{\nu}_e$ | $5.73 \times 10^{-5}$ | $1.8k$ | $N$ |
| $\Sigma^+ \to \Lambda e^+ \overline{\nu}_e$ | $2.0 \times 10^{-5}$ | 21 | $N$ |
| $\Xi^- \to \Lambda e^- \overline{\nu}_e$ | $5.63 \times 10^{-4}$ | $2.9k$ | $Y$ |
| $\Xi^- \to \Sigma^0 e^- \overline{\nu}_e$ | $8.7 \times 10^{-5}$ | 154 | $N$ |
| $\Xi^0 \to \Sigma^+ e^- \overline{\nu}_e$ | $2.71 \times 10^{-4}$ | 176 | $N$ |
| $\Xi^- \to \Xi^0 e^- \overline{\nu}_e$ | $< 2.3 \times 10^{-3}$ | 0 | $N$ |

From [5], except $\Xi^0 \to \Sigma^+ e^- \overline{\nu}_e$ decay for which we used the recently measured BR from [4].

the case for the three highest statistics observed modes.

### 2.2. Effective V-A Theory and the Cabibbo Model

For the decay $A \to B\, l^- \overline{\nu}_l$, the most general transition amplitude in the V-A theory can be written:

$$\mathcal{M} = \frac{G_F}{\sqrt{2}} \begin{pmatrix} V_{us} \\ V_{ud} \end{pmatrix} \overline{u}(B)(V_\alpha + A_\alpha)u(A) \; \overline{u_e}\gamma^\alpha(1+\gamma_5)u_\nu \qquad (1)$$

Where $G_F$ is the universal weak coupling constant, and $V_{us}$ ($V_{ud}$) is the CKM matrix element for strangeness changing $\Delta$S=1 ($\Delta$S=0) decays. To a very good approximation $V_{us} = \sin\theta_C$ and $V_{ud} = \cos\theta_C$, where the Cabibbo mixing angle, $\theta_C$, is a free parameter to be determined from experimental data. $u(A)$ and $u(B)$ are the Dirac spinors of the initial and final baryons. The vector and axial vector currents can be written as:

$$\begin{aligned} V_\alpha &= f_1(q^2)\gamma_\alpha + \frac{f_2(q^2)}{M_A}\sigma_{\alpha\beta}q^\beta + \frac{f_3(q^2)}{M_A}q_\alpha \\ A_\alpha &= (g_1(q^2)\gamma_\alpha + \frac{g_2(q^2)}{M_A}\sigma_{\alpha\beta}q^\beta + \frac{g_3(q^2)}{M_A}q_\alpha)\gamma_5 \\ q^\alpha &= (p_e + p_\nu)^\alpha = (p_A - p_B)^\alpha \qquad (2) \end{aligned}$$

There are 3 vector from factors $f_1$ (vector), $f_2$ (weak magnetism) and $f_3$(induced scalar); plus 3 axial-vector from factors $g_1$ (axial-vector), $g_2$ (weak electricity) and $g_3$(induced pseudo-scalar) which are functions of the baryons' momentum transfer squared, $q^2$. Time invariance implies that all the form factors are real. $f_3$ and $g_3$ are suppressed by the mass of the lepton and can be ignored in the case of decays to an electron.

The Cabibbo theory relates the form factors of different HSD to one another by the SU(3) flavor symmetry assumption. In this limit $g_2$ vanishes (no second-class current) and the remaining form factors for e-mode processes at $q^2 = 0$ are written in terms of only two reduced form factors F and D which are the free parameters in this model. Furthermore, assuming the weak vector current and the electromagnetic current are members of the same SU(3) baryon octet, one can calculate $f_1$ and $f_2$ through conserved vector current (CVC) hypothesis. The axial-vector current belongs to a different octet and remain to be determined from the parameters $F$ and $D$. Table 2 shows a list of baryon $\beta$-decays with their dependence on the free parameters [6].

### 2.3. Integrated Observables

As mentioned before, HSD have small branching ratios. Besides, hyperons are not that abundant. Measurements of these decays became possible when we learned how to produce beams of hyperons and in particular polarized hyperons. Because of the low statistics of HSD, one has to lump the events together to produce certain integrated observables which can be calculated theoretically as functions of the form factors [7,8]. The commonly measured quantities are

- The total decay rate (or alternatively the branching ratio),
- $e - \nu$ angular correlation in the rest frame of the decaying hyperon,
- asymmetry coefficients of the decay products in the decay of a polarized initial hyperon,
- polarization of the decay baryon in its own frame for an unpolarized initial hyperon.

Table 2
Beta decay form factors in Cabibbo Model

| | scale | $f_1$ | $g_1$ |
|---|---|---|---|
| $n \to p e^- \overline{\nu}_e$ | $V_{ud}$ | 1 | $D+F$ |
| $\Lambda \to p e^- \overline{\nu}_e$ | $V_{us}$ | $-\sqrt{\frac{3}{2}}$ | $-\sqrt{\frac{1}{6}}(D+3F)$ |
| $\Sigma^- \to n e^- \overline{\nu}_e$ | $V_{us}$ | $-1$ | $D-F$ |
| $\Sigma^- \to \Lambda e^- \overline{\nu}_e$ | $V_{ud}$ | 0 | $-\sqrt{\frac{2}{3}}D$ |
| $\Sigma^+ \to \Lambda e^+ \overline{\nu}_e$ | $V_{ud}$ | 0 | $-\sqrt{\frac{2}{3}}D$ |
| $\Xi^- \to \Lambda e^- \overline{\nu}_e$ | $V_{us}$ | $\sqrt{\frac{3}{2}}$ | $-\sqrt{\frac{1}{6}}(D-3F)$ |
| $\Xi^- \to \Sigma^0 e^- \overline{\nu}_e$ | $V_{us}$ | $\sqrt{\frac{1}{2}}$ | $\sqrt{\frac{1}{2}}(D+F)$ |
| $\Xi^- \to \Xi^0 e^- \overline{\nu}_e$ | $V_{ud}$ | $-1$ | $D-F$ |
| $\Xi^0 \to \Sigma^+ e^- \overline{\nu}_e$ | $V_{us}$ | 1 | $D+F$ |

These experimentally measurable quantities have the advantage that their definitions do not assume any particular theoretical approach.

### 2.4. Muonic Channel of $\beta$-decays

There are six allowed decays of the form $A \to B\,\mu^-\,\overline{\nu}_\mu$ in the SU(3) baryon octet, four of which have been observed with poor statistics. Because of the greater mass of the muon compared to the electron and therefore the smaller available phase space of the decay, the BR of the energetically allowed decays are about an order of magnitude or two smaller than the corresponding electron channel. Also, the issue of background and particle identification becomes more challenging. High statistics measurements of muonic $\beta$-decays would provide the only ground to explore the smaller form factors of $f_3$ and $g_3$.

## 3. Precision Measurements of $\Lambda \to p e^- \overline{\nu}_e$ decay

Being the lightest hyperon, $\Lambda$ can be produced relatively easily and in large quantities. Measurements of $\Lambda \to p e^- \overline{\nu}_e$ decay provided the early tests of the Cabibbo model. This decay mode also provides information to investigate the possibility of physics beyond the Standard Model in the form of second class currents.

### 3.1. Early Measurements

A breakthrough in the field of HSD took place when the production of polarized hyperons became possible. This allowed for the form factor measurements in the post-bubble-chamber era.

An experiment performed at Argonne [9] investigated the $\Lambda \to p e^- \overline{\nu}_e$ decay of polarized $\Lambda$ hyperons. The polarized $\Lambda$'s were produced in a liquid hydrogen target by the reaction $\pi^- p \to K^0 \Lambda$ at 1025 MeV/$c$. They employed optical spark chambers and counters in a magnetic spectrometer. Their simultaneous measurements of $e-\nu$ angular correlation (which ignores the polarization) and the three spin correlations of p, e and $\nu$ with respect to the spin of $\Lambda$ yielded an axial-vector to vector form factor ratio of $g_1/f_1 = 0.53\pm^{0.11}_{0.09}$. Although they verified the general V-A nature of the decay, they suggested a smaller value than the Cabibbo prediction of $g_1/f_1 = 0.71$, and the world average from the bubble chamber data on unpolarized $\Lambda$'s, $g_1/f_1 = 0.74\pm^{0.08}_{0.06}$. In fact, this value was pulled down by the spin correlation results which were consistent with the rest of the spin correlation experiments. Otherwise, the $e-\nu$ angular correlation result by itself agreed well with the model. Hence, a slight disagreement between the analyses of polarized and unpolarized $\Lambda$'s was seen.

The Hildelberg group at CERN [10] also carried out a counter-spark chamber experiment to measure the BR of the decay as well as various coefficients of correlation ($\alpha_e$, $\alpha_n$ and $\alpha_\nu$) with respect to the $\Lambda$ spin. Polarized $\Lambda$'s were produced in a Be target through the reaction $\pi^+ n \to K^+ \Lambda$ by pions of momentum 1130 MeV/$c$. The results on the spin correlations were in agreement with the V-A theory with no second class currents. They too favored a smaller value of $g_1/f_1$ than its Cabibbo prediction.

### 3.2. High Statistics Experiments

A Brookhaven experiment [11] in late 70's took advantage of a neutral *hyperon beam* to perform the first high statistics measurement of $\Lambda \to p e^- \overline{\nu}_e$ decay. A proton beam of 28.5 GeV/$c$

interacted in an iridium target to produce the neutral beam . Collecting about 10,000 events, they measured $|g_1(0)/f_1(0)| = 0.734 \pm 0.031$ from angular correlation of $e-\nu$. Effects such as radiative corrections and $q^2$ dependence of the decay were also included.

Their result was verified later on by the CERN-WA2 group (see Sec. 5), and most precisely by a Fermilab very high statistics experiment [12]. Dworkin, *et al.* measured $g_1/f_1 = 0.731 \pm 0.013$ from the $e-\nu$ angular correlation.

All these experiments were in a remarkable agreement with the Cabibbo prediction. However, we have to point out that none of the above experiments took advantage of initially polarized $\Lambda$'s. A precise measurement of form factors on polarized $\Lambda$'s are desired to resolve the old disagreement of the spin correlation values mentioned in Sec. 3.1, or to look for surprises.

## 4. $\Sigma^- \to n e^- \overline{\nu}_e$ Decay

Perhaps the most critical test of the Cabibbo model was the issue of relative sign of axial-vector and vector currents in $\Sigma^- \to n e^- \overline{\nu}_e$ decay. From table 2, this sign for $\Sigma^- \to n e^- \overline{\nu}_e$ is negative, opposite to the positive sign in neutron beta decay and in other strangeness changing beta decays. Thus, the unambiguous determination of this sign which is a characteristic feature of the Cabibbo model, would provide a crucial qualitative test of the model. The experiments prior to the E715 at Fermilab [13] with polarized $\Sigma^-$ had failed to confirm the prediction of the negative sign [14] for $g_1/f_1$ in $\Sigma^- \to n e^- \overline{\nu}_e$. On the other hand, the experiments with unpolarized $\Sigma^-$ which were primarily sensitive to the absolute value $|g_1/f_1|$, were in agreement with each other and with the value from the Cabibbo model (Fig. 2). The WA2 group at CERN (Sec.5) favored a negative sign of $g_1/f_1$ from the electron spectrum [18].

Another breakthrough of the field was the discovery of the hyperon polarization at Fermilab in mid 70's. It is known that hyperons can be produced with significant polarization [15]. In 1983, the E715 experiment was carried out in the Fermilab Proton Center charged-hyperon beam. The $\Sigma^-$ beam was produced by 400 GeV/$c$ protons pinging on a Cu target. At a production angle of 2.5 mrad, the $\Sigma^-$'s were $(23.9 \pm 4.3\%)$ polarized. E715 was able to measure the electron, neutron, and anti-neutrino asymmetries ($\alpha_e$, $\alpha_n$ and $\alpha_\nu$) from a sample of about 50,000 beta decays of polarized $\Sigma^-$. In particular, a value of $\alpha_e = -0.519 \pm 0.102$ was measured, consistent with the prediction of $\alpha_e = -0.51 \pm 0.04$ from the global fits. They extracted the negative value of $g_1/f_1 = -0.328 \pm 0.019$. This result removed the existing disagreement with the Cabibbo model.

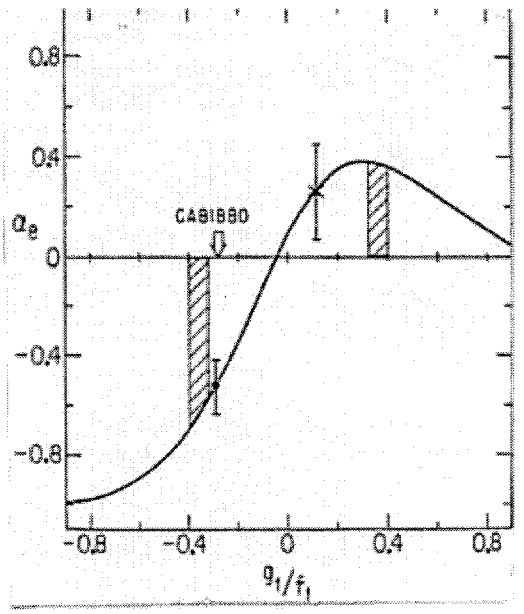


Figure 2. Plot of electron asymmetry of polarized $\Sigma^-$ vs $g_1/f_1$. The hatched areas, indicates results for unpolarized $\Sigma^-$ measurements of $|g_1/f_1|$. The data point on the positive side of curve represents the average of polarized $\Sigma^-$ experiments, and the data point on the negative side is the E715 result to be compared with the Cabibbo predicted value.

## 5. CERN-WA2 Experiment, Cabibbo Fits

A major problem encountered in tests of Cabibbo model is the the necessity to combine data from various experiments. These experiments have been analyzed under different assumptions which affect the values obtained for the form factors and branching ratios of HSD. For example the dependence of the form factors on $q^2$ has often been neglected, and this dependence in turn is sensitive to such factors as details of apparatus acceptance. In the case of branching ratio measurements there are uncertainties associated with radiative corrections.

The WA2 experiment performed in the charged hyperon beam at the CERN SPS [16–18], to collect data on the semileptonic decays of $\Sigma^-$, $\Xi^-$ and $\Lambda$ simultaneously. A magnetic channel selected 100 GeV/$c$ negatively charged particles produced in the forward direction by interaction of the 200 GeV/$c$ SPS proton beam on a BeO target. The $\Sigma^-$ and $\Xi^-$ were concurrently identified in a DISC Čerenkov counter, and their decay products were analyzed by a magnetic spectrometer. Table 3 summarizes the result of WA2 measurements [19].

With the exception of $\Lambda \to p e^- \overline{\nu}_e$ decay produced from the two body decay of $\Xi^- \to \Lambda \pi^-$ in which the produced $\Lambda$ were longitudinally polarized, the parent hyperons were unpolarized. Excellent agreement with the Cabibbo model was obtained using these data internally. They also added the accepted value of the neutron lifetime known at the time to their data which still produced an acceptable fit within the errors. They determined the free parameter of the Cabibbo Model, $F = 0.477 \pm 0.012$, $D = 0.756 \pm 0.011$ and $\sin\theta_C = 0.231 \pm 0.003$.

## 6. Status of $V_{us}$ Measurements From HSD Fits

One of the goals of HSD processes is to confirm the value of $V_{us}$ obtained in Kaon decays. There has been a long term controversy that the value of $V_{us}$ measured from HSD fits are inconsistent with that of the Kaon sector. Analysis of $K_{e3}$ decays yields [5]

$$|V_{us}| = 0.2196 \pm 0.0023, \tag{3}$$

significantly smaller than the WA2 value of

$$|V_{us}| = 0.231 \pm 0.003 \tag{4}$$

obtained in 1984. A problem encountered in these fits and other fits based on WA2 results was that the measurements of the neutron decay asymmetry and lifetime were inconsistent. As a result, the authors of reference [19] for instances, were forced to choose to include the lifetime but not the asymmetry in their fits. The discrepancy of their Cabibbo angle result were then ascribed to SU(3) corrections to the model. There has been several attempts [20] to incorporate SU(3) symmetry breaking corrections to bring this value down to the level of Eq. 3.

From a different point of view, we know that some of the measurements fit have been improved since the 84 fit, most importantly the neutron lifetime measurement. A refit of the measurements [21] based on PDG listing in 1992 with the '84 formalism', showed two of the rates, $\Sigma^- \to \Lambda e^- \overline{\nu}_e$ and $\Xi^- \to \Lambda e^- \overline{\nu}_e$, were off by more than $3\sigma$ from the new fit. Dropping these rates, the author gets a reasonable fit with the value of the Cabibbo angle

$$|V_{us}| = 0.2202 \pm 0.0017 \tag{5}$$

consistent with Eq. 3.

Therefore, it is not clear how the SU(3) breaking corrections have to be implemented in HSD measurements of the Cabibbo angle, or if they should be considered. In any case we are left with one open question that why the SU(3) symmetry in HSD is respected to a much less than the 10% level symmetry breaking expectations from the octet mass splitting.

PDG chooses not to trust the HSD values due to larger theoretical uncertainties because of first order SU(3) symmetry breaking effects in the axial-vector coupling. Obviously, there is a call for theoretical and experimental improvements in this sector.

## 7. $\Xi^0 \to \Sigma^+ e^- \overline{\nu}_e$ Decay

For $\Xi^0$ $\beta$-decay $f_1 = 1$ and $g_1 = F + D$, similar to the well studied neutron $\beta$-decay (Tab. 2). Thus, in the flavor symmetric quark model, differences between these two decays arise only from the differing particle masses and their CKM matrix elements. Although a redundant F and D dependence of the form factors for $\Xi^0 \to \Sigma^+ e^- \overline{\nu}_e$ does not add any extra constraints on the global picture of $\beta$-decays, the large mass difference between the n and the $\Xi^0$ in the baryon octet provides a direct powerful test of flavor symmetry violation effects. These effects [22,23] are expected to modify this branching ratio by as much as 20-30%.

KTeV-E799II experiment at Fermilab used the directly-measurable final state $\Sigma^+$ polarization in addition to the branching ratio to measure the form factors. The experiment [24] was mainly designed to study the Kaon system. The detector is far (about 94 m) from the production target to ensure mostly $K_L$ in the neutral beam would reach the detector. However, a copious amount of neutrons, and some very high momentum $\Lambda$ and the $\Xi^0$ hyperons entered the detector along with $K_L$'s.

Table 3
Results of WA2 experiments on HSD

| | Branching Ratio | $g_1/f_1(g_2=0)$ |
|---|---|---|
| $\Sigma^- \to \Lambda e^- \overline{\nu}_e$ | $(5.61 \pm 0.31) \times 10^{-5}$ | $+0.03 \pm 0.008$ |
| $\Sigma^- \to n e^- \overline{\nu}_e$ | $(0.96 \pm 0.05) \times 10^{-3}$ | $-0.34 \pm 0.05$ |
| $\Xi^- \to \Lambda e^- \overline{\nu}_e$ | $(5.64 \pm 0.31) \times 10^{-4}$ | $+0.25 \pm 0.05$ |
| $\Xi^- \to \Sigma^0 e^- \overline{\nu}_e$ | $(8.7 \pm 1.7) \times 10^{-5}$ | — |
| $\Lambda \to p e^- \overline{\nu}_e$ | $(8.57 \pm 0.36) \times 10^{-4}$ | $+0.70 \pm 0.03$ |

From [5], except $\Xi^0 \to \Sigma^+ e^- \overline{\nu}_e$ decay for which we used the recently measured BR from [4].

$\Xi^0$ formed less than 0.5% fraction of the neutral beam. The key to the success of delicate $\Xi^0 \to \Sigma^+ e^- \overline{\nu}_e$ measurements in such a kaon dominated environment was the excellent detector elements for event reconstruction and particle identification. KTeV was armed with a state-of-the-art CsI electromagnetic calorimeter. After calibration, the calorimeter energy resolution was better than 1% for the electron momentum between 2 and 60 GeV. The position resolution was ~1 mm. It was also used as the main particle identification detector with a $e/\pi$ rejection of better than 500:1. The charged particle spectrometer consisted of a dipole magnet surrounded by four drift chambers (DC1–4) with ~100 $\mu$m position resolution in both horizontal and vertical views.

Polarization of $\Sigma^+$ from the $\beta$-decay of unpolarized $\Xi^0$ as well as $e-\nu$ angular correlations were used to measure the form factors of the decay [25]. KTeV measured the ratio $g_1/f_1$ to be $1.24 \pm^{0.20}_{0.17}(stat) \pm 0.07(syst)$ in agreement with the flavor SU(3) symmetry prediction of 1.26. Combining the measured $g_1/f_1$ with the independent measurement of the branching ratio [26], Fig. 3 summarizes the measured values of $f_1$ and $g_1$. The Cabibbo prediction based on exact SU(3) symmetry is favored.

Furthermore, relaxing the constraint $g_2/f_1 = 0$, they found $g_2/f_1$ to be consistent with zero, which is an indication of no second-class currents. Also from the energy spectrum of the electron in the $\Sigma^+$ frame, they measured the weak magnetism $f_2/f_1$ to be $2.3 \pm 1.2 \pm 0.7$ in agreement with the CVC hypothesis.

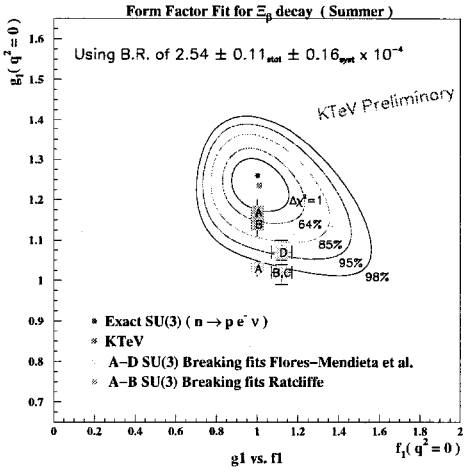


Figure 3. Plot of $g_1$ vs $f_1$ from branching ratio of $\Xi^0 \to \Sigma^+ e^- \overline{\nu}_e$ decay and measurement of $\Sigma^+$ polarization at KTeV. Excellent agreement with the Cabibbo model can be seen. The confidence level contours and some predictions based on SU(3) flavor breaking effects are also shown.

## 8. Conclusions

Experiments on HSD has evolved slowly in the past four decades. The Cabibbo model proposed in 1963 based on SU(3) flavor symmetry of the baryon octet provides the best description of these processes. The fact that no convincing SU(3) symmetry breaking effects have been seen in HSD is puzzling us. It challenges theorists to explain why these effects, if any, are not as large as expected. On the experimental front, only high statistics of two decays $\Lambda \to p e^- \overline{\nu}_e$ and $\Sigma^- \to n e^- \overline{\nu}_e$ exist. More experiments with high statistics of the other modes need to be performed. In particular, the branching ratio of $\Sigma^- \to \Lambda e^- \overline{\nu}_e$ and $\Xi^- \to \Lambda e^- \overline{\nu}_e$ should be reexamined.

The issue of inconsistency of $V_{us}$ measured from HSD with the value obtained from the Kaon sector remains to be resolved. Possible tests of HSD for anti-particles and also HSD outside the baryon octet would help to generalize the

Cabibbo model beyond its traditional frame.

## 9. Acknowledgments

The author would like to thank Prof. R. Winston, Prof. E. Swallow, Dr. P. Cooper, and S. Bright for valuable discussions and helpful information.

## REFERENCES

1. N. Cabibbo, Phys. Rev. Lett. **10**, 531 (1963)
2. M. Kobayashi and T. Maskawa Prog. Theor. Phys. **49**, 652 (1973)
3. A. Garcia, See A. Garcia's paper in this Proceedings.
4. A.Affolder, *et al.*, Phys. Rev. Lett. **82**, 3751 (1999)
5. Particle Data Group, C. Caso *et al.*, Eur. Phys. J. C **3**, 1 (1998)
6. E. Commins and P. Bucksbaum, *Weak interaction of leptons and quarks*, Cambridge University Press (1983)
7. V. Linke, Nucl. Phys. B **12** 669 (1969)
8. A. Garcia and P. Kielanowski, *The Beta Decay of Hyperons* (Lecture Notes in Physics, **222**, Springer–Verlag, (1985)
9. J. Lindquist *et al.*, Phys. Rev. D **16** 2104 (1977)
10. K. H. Althoff *et al.*, Phys. Lett. **37B** 531 (1971); **37B** 535 (1971); **43B** 237 (1973)
11. J. Wise *et al.*, Phys. Lett. **98B** 123 (1981)
12. J. Dworkin *et al.*, Phys. Rev. D **41** 780 (1990)
13. S. Y. Hsueh *et al.*, Phys. Rev. D **41** 780 (1990)
14. A. Garcia and E. Swallow, Phys. Rev. Lett. **35** 467 (1975)
15. L.G. Pondrom, Physics Report **122** 58 (1985)
16. M. Buorquin *et al.*, Z. Phys. C - Particles and Fields **12** 307 (1982)
17. M. Buorquin *et al.*, Z. Phys. C - Particles and Fields **21** 1 (1983)
18. M. Buorquin *et al.*, Z. Phys. C - Particles and Fields **21** 17 (1983)
19. M. Buorquin *et al.*, Z. Phys. C - Particles and Fields **21** 27 (1983)
20. M. Roos, Phys. Lett. B **246**, 179 (1990);
21. P. Cooper, Proceedings of *'Baryons 95', 7th International Conference on the Structure of Baryons*, Santa Fe, New Mexico, (1995)
22. R. Flores-Mendieta, E. Jenkins, and A. V. Manohar, Phys. Rev. D **58**, 094028 (1998)
23. P.G. Ratcliffe, Phys. Lett. B **365**, 383 (1996)
24. K. Arisaka *et al.*, *KTeV (Kaons at the Tevatron) Design Report*, Fermilab Report No. FN-580, (1992)
25. S. Bright, See S. Bright's paper in this Proceedings.
26. A. Alavi-Harati, Proceedings of *DPF99*, UCLA, (1999).

# Chapter 4

# Radiative Hyperon Decays


- P. Zenczykowski
- U. Koch

# Weak radiative hyperon decays: questioning the basics

P. Żenczykowski [a]

[a]Institute of Nuclear Physics,
Radzikowskiego 152, 31-342 Kraków, Poland

Main theoretical approaches to weak radiative hyperon decays are briefly reviewed. It is emphasized that only approaches with great predictive power should be seriously considered when seeking a resolution of the puzzle presented by observed large negative asymmetry $\alpha(\Sigma^+ \to p\gamma)$. In such cases, asymmetry in the $\Xi^0 \to \Lambda\gamma$ decay is always large while its sign is positive (negative) if Hara's theorem is violated (satisfied). Measuring this asymmetry is therefore crucial for determining whether the large value of $\alpha(\Sigma^+ \to p\gamma)$ is due to large SU(3) breaking or to some deeper reason. Some arguments suggesting that violation of Hara's theorem might be a feature of Nature, and hints as to its possible origin are also given.

## 1. INTRODUCTION

Weak radiative hyperon decays (WRHD's) present a yet unsolved problem in low-energy physics of hadronic weak interactions. The issue first appeared in 1969 when measurements of the $\Sigma^+ \to p\gamma$ decay asymmetry [1] gave $\alpha(\Sigma^+ \to p\gamma) = -1.0^{+0.5}_{-0.4}$. This value was not in agreement with expectations based on Hara's theorem [2], according to which the asymmetry in question should be small. Problems with Hara's theorem have plagued the issue of WRHD's ever since.

Hara's theorem states that the parity-violating amplitude $A$ for the $\Sigma^+ \to p\gamma$ (and $\Xi^- \to \Sigma^-\gamma$) decay should vanish in exact flavor SU(3). In reality, SU(3) is broken of course. However, if the parity-conserving amplitude $B$ is not small ($A \ll B$), one expects the asymmetry $\alpha = 2AB/(A^2 + B^2) \approx 2A/B$ to be small (i.e. not larger than ca $\pm 0.2$). The theorem follows if hadrons are described by an SU(3)-symmetric gauge- and $CP$- invariant local field theory. Although these assumptions (with the exception of SU(3), of course) are fundamental, one should note here that the very year the theorem was proved (1964), significant changes in our knowledge about these assumptions occurred. Thus, 1) it was proposed that SU(3) should follow from the underlying quark model, 2) violation of CP invariance was experimentally observed, and 3) the first paper pinning down the nonlocal nature of quantum physics appeared. These changes should be kept in mind when considering possible theoretical reasons for the experimentally found departure from expectations based on Hara's theorem.

At present, we know that asymmetry in the $\Sigma^+ \to p\gamma$ decay is large. The PDG average [3] is $\alpha(\Sigma^+ \to p\gamma) = -0.76 \pm 0.08$, with two main experimental results contributing equal to $-0.86 \pm 0.13 \pm 0.04$ [5], and $-0.72 \pm 0.086 \pm 0.045$ [6] respectively. Therefore, the situation is quite disturbing since with one baryon in the initial state and one baryon in the final state (and thus lacking strong interactions in the final state), the WRHD's are fairly clean transitions, similar to the semileptonic ones or to magnetic moments. With the only WRHD-specific complication being joint appearance of weak and electromagnetic interactions, a fairly precise theoretical description of WRHD's should be then possible.

## 2. SIZE OF DATA BASIS AND RELIABILITY OF CONCLUSIONS

Although we may sum up the experimental findings by saying that expectations based on Hara's theorem are strongly violated, we cannot draw any deeper conclusions as to the origin of the effect. In this respect the situation is similar to what might have happened if we had measured the magnetic moment of proton to be $\mu_p \approx 2.79$ but had not known anything about magnetic moments of other ground-state baryons. Although we might have stated then that large correction to the Dirac value of proton magnetic moment is present, no conclusions concerning the *symmetric* nature of flavor-spin wave functions (and hence color) would have been possible. Drawing such conclusions requires (at the very least) measuring the ratio $\mu_n/\mu_p$ which is $-2/3$ $(-2)$ for symmetric (antisymmetric) spin-flavor wave functions. The lesson is that large asymmetry observed in the $\Sigma^+ \to p\gamma$ decay must be analysed together with data and theory on the remaining

Table 1
Data

| Decay | Asymmetry | Br. ratio·$10^3$ |
|---|---|---|
| $\Sigma^+ \to p\gamma$ | $-0.76 \pm 0.08$ | $1.23 \pm 0.06$ |
| $\Lambda \to n\gamma$ | | $1.75 \pm 0.15$ |
| $\Xi^0 \to \Lambda\gamma$ | $+0.43 \pm 0.44$ | $1.06 \pm 0.16$ |
| $\Xi^0 \to \Sigma^0\gamma$ | $-0.65 \pm 0.13^{(*)}$ | $3.6 \pm 0.4$ |
| $\Xi^- \to \Sigma^-\gamma$ | $+1.0 \pm 1.3$ | $0.127 \pm 0.023$ |
| $\Omega^- \to \Xi^-\gamma$ | | $< 0.46$ |

$^{(*)}$ Ref. [4]

WRHD's, i.e. $\Lambda \to n\gamma$, $\Xi^0 \to \Lambda\gamma$, $\Xi^0 \to \Sigma^0\gamma$, as well as $\Xi^- \to \Sigma^-\gamma$ and $\Omega^- \to \Xi^-\gamma$. Of these, the first three turn out to be particularly important. Present experimental data [3] are gathered in Table 1.

Following the successes of the description of semileptonic decays and magnetic moments with the help of one (or two) parameters in each case, one may reasonably expect that the puzzle of an apparent violation of Hara's theorem in $\Sigma^+ \to p\gamma$ will be resolved successfully if all radiative decays are well described with the help of an approach using a very small number of parameters. In other words, we need an approach which accurately predicts experimental branching ratios and asymmetries, with errors below 20%. Description of asymmetries will provide here a particularly incisive test. When such an approach akin to the quark model description of baryon magnetic moments is available, its further and deeper analysis should be attempted.

## 3. THEORY - GENERAL

### 3.1. Hara's theorem

By using local field theory at hadron level, Hara's theorem may be obtained as follows. The most general parity-violating electromagnetic current may be written as:

$$j^{\mu}_{5,kl} = j^{(1)\mu}_{5,kl} + j^{(2)\mu}_{5,kl} \tag{1}$$

where $k, l$ are baryon indices,

$$j^{(1)\mu}_{5,kl} = g_{1,kl}(q^2)\overline{\psi}_k(\gamma^{\mu} - q^{\mu}\not{q}/q^2)\gamma_5\psi_l, \tag{2}$$

and

$$j^{(2)\mu}_{5,kl} = g_{2,kl}(q^2)\overline{\psi}_k(i\sigma^{\mu\nu}\gamma_5 q_{\nu})\psi_l. \tag{3}$$

Hermiticity and CP invariance of $A \cdot j_5$ require

$$g_{1,kl} = g_{1,lk} \tag{4}$$

and

$$g_{2,kl} = -g_{2,lk} \tag{5}$$

with $g_{i,kl}$ real.

Hara's theorem is obtained when hadron indices $k, l$ are replaced with $\Sigma^+$,$p$. Since no *exactly* massless hadron exists, there cannot be a pole at $q^2 = 0$. Consequently, $g_{1,kl}(q^2)$ must be proportional to $q^2$. Therefore, real transverse photons, for which $q^2 = q \cdot A = 0$, interact with the $j^{(2)}$ current only. Now, under $s \leftrightarrow d$ interchange, $\Sigma^+ = uus$ goes into $p = uud$ and vice versa. Thus, in exact SU(3) we must have $g_{2,\Sigma^+p} = g_{2,p\Sigma^+}$. Since $g_{2,\Sigma^+p}$ is simultaneously symmetric and antisymmetric (c.f. Eq.(5)), it must vanish. (We might have e.g. $g_{2,kl} \propto (m_k - m_l)$). If, for some reason, $g_{1,\Sigma^+p}$ were not equal to 0, Hara's theorem might be violated.

### 3.2. Quarks

Any acceptable approach to WRHD's must take into account the fact that baryons are composites made of quarks. ¿From the point of view of essentially any quark-inspired model, the WRHD's may be divided into two groups. The first group consists of decays arising solely from such transitions in which a single quark undergoes a weak transition and radiates a photon. This occurs e.g. for $\Xi^- \to \Sigma^-\gamma$ and $\Omega^- \to \Xi^-\gamma$. The other group involves more complicated two-quark processes $su \to ud\gamma$ as well. This group contains decays $\Sigma^+ \to p\gamma$, $\Lambda \to n\gamma$, $\Xi^0 \to \Lambda\gamma$, and $\Xi^0 \to \Sigma^0\gamma$.

Assuming that WRHD's are dominated by single-quark transitions, one can estimate the branching ratio of decay $\Sigma^+ \to p\gamma$ using that of $\Xi^- \to \Sigma^-\gamma$ [7]. Since the latter is experimentally very small (cf. Table 1), one calculates that single-quark transition may contribute only around 1% to the experimentally observed $\Sigma^+ \to p\gamma$ branching ratio. Thus, it is the two-quark transition $su \to ud\gamma$ which dominates the $\Sigma^+ \to p\gamma$ decay. Its properties should be accessible from detailed studies of the remaining decays of the second group, i.e. $\Lambda \to n\gamma$, $\Xi^0 \to \Lambda\gamma$, and $\Xi^0 \to \Sigma^0\gamma$.

### 3.3. Theoretical conflict

Although any reasonable theoretical approach must have a built-in dominance of two-quark transitions, such approaches may still differ in various ways. The issue of *how* we take quark degrees of freedom into account lies at the origin of conflict between these approaches. Namely,

various models proposed may be classified into two groups according to whether they satisfy or violate Hara's theorem. In my opinion, models violating Hara's theorem should not be rejected immediately in view of the fact that 1) we have already learned that the assumptions upon which Hara's theorem is based, although seemingly correct for WRHD's, are not valid in Nature in general, and 2) experimental data seem to be better described by models violating Hara's theorem (cf. Tables 1,4). Among the approaches that satisfy Hara's theorem we should mention the standard pole model of Gavela et al.[8], the chiral perturbation theory framework [9–11], and the QCD sum rules approach [12,13]. Hara's theorem violating approaches include simple quark-model calculations of Kamal and Riazuddin [14] and the combined $VMD \times SU(6)_W$ approach of ref.[15,16] and its pole-model implementation [17].

In order to analyze the issue of possible violation of Hara's theorem, we should be able to compare experimental asymmetries and branching ratios with their predictions in various models. In principle, models might differ not only on the issue of whether Hara's theorem is satisfied or violated (i.e. in the parity-violating amplitudes), but also in their description of the parity-conserving amplitudes.

### 3.4. Parity-conserving amplitudes

Clearly, if one wants to draw firm conclusions concerning parity-violating amplitudes on the basis of comparing theory with experiment, it is very important to use a reliable description of the parity-conserving amplitudes. Fortunately, there are no real "conflicts" among various approaches to the latter. Almost all papers agree here qualitatively, although they may differ somewhat in their numerical predictions. The most widely accepted approach is a hadron-level pole model, completely analogous to that successfully used in the description of nonleptonic hyperon decays (NLHD's). In this approach, quarks are used to find symmetry properties of two types of hadronic blocks: 1) the amplitudes of photon emission by baryons, and 2) the amplitudes of weak transitions in baryons. An alternative to that approach is to calculate the whole weak radiative parity-conserving amplitude at quark-level as one hadronic block, with no explicit intermediate hadronic poles (using for example a bag model). Predictions of such an alternative approach do not differ qualitatively from those of the pole model. Since the pole model describes the data on NLHD's very well, and one does not expect any physical complications (but rather simplification) if the pion is replaced by a photon, it is reasonable to accept the pole model as a reliable theoretical description of the parity-conserving WRHD amplitudes.

### 3.5. Parity-violating amplitudes

As in the case of parity-conserving amplitudes, the two-quark weak radiative transition $su \to ud\gamma$ may be described either in terms of several hadronic blocks, or as a single block. Among many papers using the first approach one should mention first and foremost the paper by Gavela, LeYaouanc, Oliver, Pene, and Raynal (GLOPR) [8] in which a standard pole-model description of WRHD's is developed, and which provides a basis for any subsequent discussion on WRHD's. This model satisfies Hara's theorem by construction. The first group comprises also the chiral perturbation theory approach [9–11], and the Hara's-theorem-violating VMD-based pole model of [17]. The single-block approach was used in simple quark-model calculations of Kamal and Riazuddin [14,18], in the bag model [19], in the QCD sum rules approach [12,13], and in the combined $SU(6)_W \times VMD$ approach of refs.[15,16].

## 4. SPECIFIC MODELS AND THEIR PREDICTIONS

### 4.1. QCD sum rules

QCD sum rules were applied to the description of WRHD's by Khatsimovsky [12] and by Balitsky et al. [13]. Results of their calculations are given in Table 2. One can see that $\alpha(\Sigma \to p\gamma)$ is predicted to be positive, in complete disagreement with the data (Table 1). The negative result of ref.[13] was obtained only in a second attempt: the original calculation produced a positive sign (disguised as a negative one, due to a different sign convention for asymmetry). Clearly, as agreed also by Khatsimovsky [12], QCD sum rules do not have much predictive power.

### 4.2. Chiral perturbation theory

Attempts to describe WRHD's within chiral perturbation theory (ChPT) have not led to a resolution of the problem. Ref.[10] contains several free parameters but the $\Sigma^+ \to p\gamma$ asymmetry is still predicted to be small. The analysis of Neufeld [9] contains only a small number of counterterms, and therefore has more predictive

Table 2
QCD sum rules: predictions

| Decay | Asymmetry | Br. ratio$\cdot 10^3$ |
|---|---|---|
| $\Sigma^+ \to p\gamma$ | $+1^{(1)}$ | $0.8^{(1)}$ |
| | $-0.85 \pm 0.15^{(2)}$ | 0.5 to $1.5^{(2)}$ |
| $\Lambda \to n\gamma$ | $+0.1^{(1)}$ | $2.1 - 3.1^{(1)}$ |
| $\Xi^0 \to \Lambda\gamma$ | $+0.9^{(1)}$ | $1.1^{(1)}$ |
| $\Xi^- \to \Sigma^-\gamma$ | $+0.4^{(1)}$ | |

(1) ref.[12]
(2) ref.[13], originally predicted positive

power. Using as input the data on $\Xi^0$ radiative decays available in 1992, ref.[9] predicts then $|\alpha(\Sigma^+ \to p\gamma)| < 0.2$, $\alpha(\Lambda \to n\gamma) \approx -0.7$ or $-0.3$, and $\alpha(\Xi^- \to \Sigma^-\gamma) \in (-0.4, +0.3)$. The conclusion of Neufeld is that "the predictive power of ChPT is limited by the occurrence of free parameters, which are not restricted by chiral (or other) symmetries alone". In a recent paper [11], a new attempt to attack the issue within a chiral approach has been made. This approach is very similar to the standard GLOPR paper because it is ultimately reduced to a pole model. Therefore, it would be more appropriate to discuss it alongside ref.[8]. However, since the paper of ref.[11] misses an important contribution of intermediate $\Lambda(1405)$ [20], its numerical predictions for neutral hyperon decays have to be changed. It turns out [20] that when this is done, one essentially recovers the predictions of ref.[8].

### 4.3. Standard pole model

The standard approach of Gavela et al. [8] was developed along the lines of their earlier paper on NLHD's [21]. Ref.[21] described parity-violating amplitudes of NLHD's as composed of two terms: the current algebra commutator and a (vanishing in SU(3)) correction ($\Delta P_{70}$) arising from $J^P = 1/2^-$ intermediate states belonging to $(70, 1^-)$ - the lowest-lying negative-parity multiplet of $SU(6) \times O(3)$, i.e. schematically:

$$A = [..., ...] + \Delta P_{70}(m_s - m_d) \qquad (6)$$

with $\Delta P_{70}(0) = 0$.

Alternatively, one might saturate the current algebra commutator with this part of contribution from $(70, 1^-)$ which does not vanish in $SU(3)$: $[..., ...] = P_{70}(0)$. In other words, instead of the decomposition made on the right-hand side of Eq.(6), one might use a pole model with $SU(3)$ breaking appropriately included:

$$A = P_{70}(m_s - m_d) = P_{70}(0) + \Delta P_{70}(m_s - m_d) \qquad (7)$$

Diagrams relevant for this model are shown in Fig.1, where $M$ stands for $\pi$ meson, and $B_{k*}$ - for all allowed $J^P = 1/2^-$ baryons from the $(70, 1^-)$ multiplet. If one wants to reproduce results of current algebra, one has to consider *all* allowed negative parity baryons from all SU(3) multiplets in $(70, 1^-)$, i.e. $\Lambda(1405)$ (a SU(3) singlet), $N(1535)$, $\Lambda(1670)$, $\Sigma(1750)$ (low-lying SU(3) octet), etc.

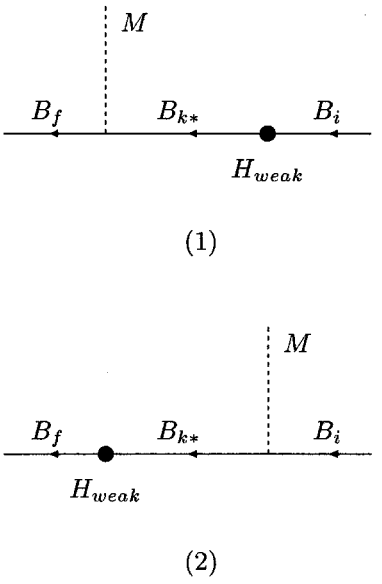


Fig.1. Baryon-pole diagrams

For WRHD's, ref.[8] switches to the pole model description. This should give both an analogue of the commutator term for NLHD's and the SU(3) breaking corrections.

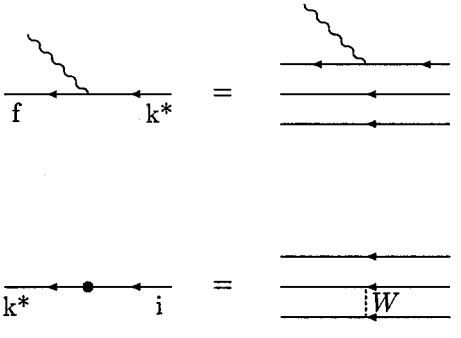


Fig.2 Hadron-level diagrams and their quark-level counterparts

Table 3
Weights of diagrams (1) and (2) of Fig.1

| Decay | Diagram (1) | Diagram (2) |
|---|---|---|
| $\Sigma^+ \to p\gamma$ | $-\frac{1}{3\sqrt{2}}$ | $-\frac{1}{3\sqrt{2}}$ |
| $\Lambda \to n\gamma$ | $+\frac{1}{6\sqrt{3}}$ | $+\frac{1}{2\sqrt{3}}$ |
| $\Xi^0 \to \Lambda\gamma$ | 0 | $-\frac{1}{3\sqrt{3}}$ |
| $\Xi^0 \to \Sigma^0\gamma$ | $\frac{1}{3}$ | 0 |

The procedure applied in ref.[8] is as follows:

1) Use quark model to evaluate symmetry properties of the two (weak and electromagnetic) hadronic blocks in diagram (1) of Fig.1 with $M$ now replaced by $\gamma$ (as shown in Fig.2).

2) Determine the amplitudes for diagram (2) in Fig.1 from hermiticity, CP- and gauge-invariance.

i) the weak amplitude is antisymmetric by $CP$ and hermiticity: $a_{jk^*} = -a_{k^*j}$ $(j = i, f)$.

ii) the obtained electromagnetic coupling is identified with gauge-invariant hadron-level parity-conserving coupling

$$f_{2,fk^*}\overline{u}_{1/2^+,f}\sigma^{\mu\nu}\gamma_5 q_\nu u_{1/2^-,k^*}A^\mu \qquad (8)$$

where $f_{2,jk^*} = f_{2,k^*j}$ by $CP$ and hermiticity.

By combining weak and electromagnetic transitions according to Fig.1, one gets

$$A \propto \sum_{k^*}\left\{\frac{f_{2,fk^*}a_{k^*i}}{m_i - m_{k^*}} + \frac{a_{fk^*}f_{2,k^*i}}{m_f - m_{k^*}}\right\} \times (9)$$

$$\times\overline{u}_f i\sigma^{\mu\nu}\gamma_5 q_\nu u_i A_\mu \qquad (10)$$

For $i = f$ (which is almost the Hara's case) we use symmetry properties of $a$ and $f_2$ to obtain:

$$f_{2,ik^*}a_{k^*i} = -a_{ik^*}f_{2,k^*i} \qquad (11)$$

which ensures cancellation of the first and second term in Eq.(9). The sums (over $k^*$) of the first and second terms can be evaluated (in SU(6)) and are given (in arbitrary normalization) in Table 3 (apart from the "$-$" sign requested by symmetries of $a$ and $f_2$). The prescription of the standard pole model is well defined and leads to definite predictions for the signs of asymmetries (Table 4). One obtains negative asymmetries for *all* four decays proceeding through two-quark transitions. This $(-,-,-,-)$ pattern of asymmetries for $\Sigma^+$, $\Lambda$, and two $\Xi^0$ decays is a characteristic feature of the standard Hara's-theorem-satisfying model.

### 4.4. "Naive" quark-level one-block calculation

In 1983 Kamal and Riazuddin (KR) calculated $W$-exchange accompanied by photon radiation in a simple quark framework [14]. The astonishing result of their calculation was an explicit violation of Hara's theorem (in the SU(3) limit). Although an agreement now exists that the calculation of ref.[14] is completely correct from the technical point of view ([22–24], the disagreement still lingers as to the origin of the offending result and, consequently, how to treat it.

Azimov [25] proposed a way of proceeding if one identifies the result of KR calculations with the $j_5^{(1)}$ ($\gamma_\mu\gamma_5$-like) term in the full electromagnetic current (if this term is present Hara's theorem may be violated - cf. section 3.1). He noticed that in principle the perturbative KR calculation may be supplemented with a $\gamma_5$-dependent renormalization. Using the latter he showed that the $\gamma_\mu\gamma_5$-like term may be rotated away. In other words, one can "hide" the $\gamma_\mu\gamma_5$ term of the axial current into the standard $\gamma_\mu$ piece of the vector current. This means that the concepts of left and right are redefined in such a way that ultimately all the offending KR contribution constitutes a weak-interaction correction to the usual electromagnetic vector current.

The above idea may be applied to charged baryons only. In reality however, KR-like calculations may be performed for neutral baryons as well. It turns out that the result is again non-zero. This time, however, this result (which conflicts with Hara-like considerations) cannot be rotated away since there is no $\gamma_\mu$ term in the vector current of neutral baryons [26]. One concludes [26] that the origin of KR result is completely unrelated to the mechanism considered in ref.[25].

In my opinion (shared by Holstein [23]), the result of KR is due to the use of free quarks in states of definite momenta. This violates Hara's theorem because one of the theorem's assumptions is that we deal with a single object - a baryon in a state of definite momentum, and not with a collection of free quarks. This seems to mean that the KR result should be considered to be an artefact of their model, and not a feature of reality [23].

I think that the KR result is an artefact of their model if interpreted literally: it arises from free Dirac quarks propagating over infinite distances. However, general features of the KR approach need not be incorrect. The problem is

that we still do not have a complete understanding of how unobservable quarks combine to form such composite states as hadrons. In the words of Donoghue et al. [27]: "The quark model was developed in the first place to explain flavor and spin properties of the observed hadrons and for this it does a good job. The spatial aspect is less well tested." It is precisely the question of position/momentum space description of hadrons as quark composites that leads to the result of KR.

### 4.5. Alternatives - bag model and VMD

The quark model used by KR may be viewed as deficient. Let us therefore accept for the time being that its result is an artefact. Consequently, one has to replace the KR model with another, more "reasonable" approach. This new approach should still exhibit spin-flavor symmetries that form the basis of all quark model successes, but quarks should not be treated as free Dirac particles. There are two possible ways of doing this: confining quarks to a bag or using the idea of VMD combined with spin-flavor symmetries of hadrons.

Bag model calculations of Lo [19] show that the parity-violating amplitude of the $\Sigma^+ \to p\gamma$ is much larger than the corresponding parity-conserving amplitude, again contradicting expectations based on Hara's theorem. Apparently, in bag model calculations Hara's theorem still seems to be violated [24], albeit the reasons are not clear and should be studied more closely. The bag model starts with the concept of free Dirac quarks, and then confines them. This proposes a resolution of the problem by brute force of an additional assumption and seems logically questionable to me: it assumes the answer. I much prefer using the combined $VMD \times SU(6)_W$ approach, where questions related to quark freedom or confinement are never asked, but which "always works", although, admittedly, it is not completely clear why. The approach does not use the concept of "free quarks" but yields quark model results. Among its many successes one may mention here the successful prediction of baryon magnetic moments by Schwinger [28] (unlike in the constituent quark model, even the scale was predicted). It is also known that a gauge-invariant formulation of the VMD approach is possible [29]. An additional asset of the $VMD \times SU(6)_W$ approach as applied to WRHD's is that essentially all parameters are set by NLHD's. Thus, we are dealing with an easily falsifiable approach of great predictive power.

The main idea of the VMD approach is as follows. One starts with the standard SU(3) symmetric model of parity-violating NLHD amplitudes (Eq.6) and uses spin-flavor $SU(6)_W$ symmetry to obtain weak strangeness-changing amplitudes for virtual transverse vector meson (V) emission from a baryon (B). This part is calculated following the ideas of ref.[30]. In this way, a transverse-vector-meson analogue of the commutator term in Eq.(6) is found [15]. In ref.[30] it is identified with the $\gamma_\mu\gamma_5$ term in the general expression for the BBV amplitude. The next step is to allow for standard VMD transition of vector meson into photon. Thus, VMD suggests that transverse photon coupling to the electromagnetic axial weak current should proceed through the $\gamma_\mu\gamma_5$ term. Clearly, the conditions under which Hara's theorem was proved are not satisfied now, and the approach chosen to avoid the use of free quarks (and the related problems with Hara's theorem) again exhibits its violation. The parity-violating amplitudes of the VMD approach may be saturated with the contribution from intermediate $J^P = 1/2^-$ baryons, in a way completely analogous to the case of NLHD's. The situation is similar to that occurring in the standard pole model of Gavela et al. [8]. There is an important difference visualised in Fig.3, though.

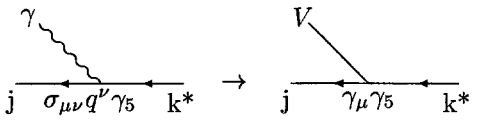


Fig.3 Photon emission in standard pole model and its vector meson counterpart

The difference is that $f_{2,jk^*}$, which accompanies the $\sigma_{\mu\nu}q^\nu\gamma_5$ term (Eq.8), is symmetric under $j \leftrightarrow k^*$ interchange, while the $f_{1,jk^*}$ accompanying the $\gamma_\mu\gamma_5$ vector-meson coupling is antisymmetric. When one combines weak and electromagnetic transitions according to Fig.1 with $M = V$ and subsequently uses VMD, one obtains

$$A \propto \sum_{k^*} \left\{ \frac{f_{1,fk^*} a_{k^*i}}{m_i - m_{k^*}} + \frac{a_{fk^*} f_{1,k^*i}}{m_f - m_{k^*}} \right\} \quad (12)$$

$$\times \overline{u}_f i\gamma^\mu\gamma_5 u_i A_\mu \quad (13)$$

Table 4
Model predictions

| Decay | VMD | KR | GLOPR |
|---|---|---|---|
| $\Sigma^+ \to p\gamma$ | $-0.95$ | $-0.56$ | $-0.80^{+0.32}_{-0.19}$ |
| $\Lambda \to n\gamma$ | $+0.8$ | $-0.54$ | $-0.49$ |
| $\Xi^0 \to \Lambda\gamma$ | $+0.8$ | $+0.68$ | $-0.78$ |
| $\Xi^0 \to \Sigma^0\gamma$ | $-0.45$ | $-0.94$ | $-0.96$ |

By using symmetry properties of $a$ and $f_1$ one finds that the term in brackets is now symmetric under $i \leftrightarrow f$ interchange. In other words, the two contributions in Table 3 add now rather than subtract. An immediate consequence is that 1) Hara's theorem is violated, and 2) asymmetries of the $\Lambda \to n\gamma$ and $\Xi^0 \to \Lambda\gamma$ are now positive. The $(-,+,+,-)$ pattern obtained here for the $\Sigma^+ \to p\gamma$, $\Lambda \to n\gamma$, $\Xi^0 \to \Lambda\gamma$, and $\Xi^0 \to \Sigma^0\gamma$ decays is a characteristic feature of Hara's-theorem-violating approaches. A comparison of asymmetry predictions of the VMD approach [31], the KR model [18], and the GLOPR standard pole model [8] is given in Table 4.

¿From the comparison of model predictions with data (Table 1) we see that at present the data favor approaches that violate Hara's theorem. Asymmetry of the $\Xi^0 \to \Lambda\gamma$ is crucial here. It is large in all approaches, with its sign being negative (positive) depending on whether Hara's theorem is satisfied (violated). The fact that it is almost equal in absolute value in all approaches with great predictive power is not an accident. It can be traced directly to the sign of contribution from diagram (2) and the vanishing of the contribution from diagram (1) (Fig.1 and Table 3). The data point is three standard deviations away from the standard pole model.

Information from the comparison of asymmetries is supplemented with that coming from branching ratios. So far all data are best described by the VMD model [16,31].

## 5. SUMMARY

The problem of WRHD's is already thirty years old. Data and some models hint that Hara's theorem may be violated. The KR result should certainly be treated as an artefact if it were the only model which violates Hara's theorem. However, other quark-inspired and elsewhere well-tested models also violate the theorem, unless it is imposed by brute force of an additional assumption, foreign to quark approaches themselves. Consequently, either our present models of how photons interact with quark composites are incorrect or, as I believe, one should treat model hints seriously and try to understand what they might mean.

The issue of Hara's theorem violation may be settled experimentally. The crucial information should come from the sign of the $\Xi^0 \to \Lambda\gamma$ asymmetry. If this asymmetry is large and negative, Hara's theorem is satisfied and one has to conclude that various hints were misleading. If, on the other hand, this asymmetry is positive, one has to conclude that violation of Hara's theorem is a feature of Nature. This would mean that at least one of the assumptions of Hara's theorem is violated.

The asumptions of CP-invariance and current conservation are satisfied explicitly in the KR paper. We have pointed out that in the KR paper violation of Hara's theorem results from the fact that in these calculations baryons consist of free quarks in plane-wave states of definite momenta. From the point of view of position space ,such states contain terms with far-away quarks. It is from such configurations that violation of Hara's theorem originates. This picture hints at the assumption of locality as the one that is violated. Hadron-level prescription (such as that of VMD) in which hadron is described by a local field may be also analysed from the point of view of position space. The net result is that CP-invariant interaction of photon with a conserved baryonic axial current does lead to the violation of Hara's theorem if the current exhibits a kind of nonlocality [32]. Thus, although the detailed origin for the violation of Hara's theorem is different in these two approaches, they both hint at nonlocality as the potential culprit. Since we know that nonlocality is a general feature of composite quantum states, the above conclusion is not in conflict with the general properties of the quantum world. However, it is certainly weird as it does challenge the generally accepted simple pictures of hadrons and photon-hadron interactions.

Since, apart from the arguments and hints presented in this talk, one can also invoke arguments of a much deeper, though usually disregarded kind, I find it quite believable that Hara's theorem may be violated in Nature.

## REFERENCES


1. L. K. Gershwin et al., Phys. Rev. 188, 2007 (1969).
2. Y. Hara, Phys. Rev. Lett. 12, 378 (1964).
3. Part. Data Group, Eur. Phys. J. C3 (1998) 1.
4. U. Koch, this conference.
5. M. Kobayashi et al. Phys. Rev. Lett. 59, 868 (1987).
6. M. Foucher et al., Phys. Rev. Lett. 68, 3004 (1992).
7. F. J. Gilman, M. B. Wise, Phys. Rev. D19, 976 (1979).
8. M. B. Gavela et al., Phys. Lett. B101, 417 (1981).
9. H. Neufeld, Nucl. Phys. B402, 166 (1992).
10. E. Jenkins et al., Nucl. Phys. B397, 84 (1993).
11. B. Borasoy, B. R. Holstein, Phys. Rev. D59, 054019 (1999).
12. V. M. Khatsimovsky, Sov J. Nucl. Phys. 46, 768 (1987).
13. I. I. Balitsky et al., Nucl. Phys. B312, 509 (1989).
14. A. N. Kamal, Riazuddin, Phys. Rev. D28, 2317 (1983).
15. P. Żenczykowski, Phys. Rev. D40, 2290 (1989).
16. P. Żenczykowski, Phys. Rev. D44, 1485 (1991).
17. P. Żenczykowski, Phys. Rev. D50, 402 (1994).
18. R. C. Verma, A. Sharma, Phys. Rev. D38, 1443 (1988).
19. C. H. Lo, Phys. Rev. D26, 199 (1982).
20. P. Żenczykowski, in preparation.
21. A. LeYaouanc et al., Nucl. Phys. B149, 321 (1979).
22. Ya. Azimov, private communication
23. B. R. Holstein, private communication.
24. P. Żenczykowski, unpublished calculations.
25. Ya. Azimov, Z. Phys. A359, 75 (1997).
26. P. Żenczykowski, Eur. Phys. J. C5, 701 (1998).
27. J. F. Donoghue et al., Phys. Rep.131, 319 (1986).
28. J. Schwinger, Phys. Rev. Lett. 18, 923 (1967).
29. N. M. Kroll et al., Phys. Rev. 157, 1376 (1967).
30. B. Desplanques et al., Ann. Phys. (N.Y.) 124, 449 (1980).
31. J. Lach, P. Żenczykowski, Int. J. Mod. Phys. A10, 3817 (1995).
32. P. Żenczykowski, Phys. Rev. D60, 018901 (1999).

# Weak Radiative Hyperon Decays - Experimental Status

U. Koch [a]

[a]University of Mainz, Institut für Physik, Staudinger Weg 7, D-55099 Mainz, Germany

The weak radiative hyperon decays offer a good possibility to study nonleptonic weak processes. The theoretical description of these processes is rather complicated as both electroweak and strong interactions contribute.

According to the Hara theorem (1964)[1], asymmetries should vanish in the decays $\Xi^- \to \Sigma^-\gamma$ and $\Sigma^- \to p\gamma$ in the SU(3) limit, assuming only CP invariance and left-handed currents in the weak interaction. In contradiction to this prediction, the first low statistics measurements of the asymmetry of the decay $\Sigma^+ \to p\gamma$ performed in bubble chambers found evidence for a large negative asymmetry.

Since then many measurements have been performed with better accuracy, however, many open questions remain. This article describes the experimental status as of today.

## 1. Weak Radiative Decays

In total there are 8 electroweak ($\Delta S = 1$) radiative decays for hyperons:

- $\Sigma^+ \to p\gamma$
- $\Lambda \to n\gamma$
- $\Xi^0 \to \Lambda\gamma$
- $\Xi^0 \to \Sigma^0\gamma$
- $\Sigma^0 \to n\gamma$
- $\Xi^- \to \Sigma^-\gamma$
- $\Omega^- \to \Xi^-\gamma$
- $\Omega^- \to \Xi^*(1530)\gamma$

The first 6 modes occur within the spin $(\frac{1}{2})^+$ octet, $\Omega^- \to \Xi^-\gamma$ is a transition from the spin $(\frac{3}{2})^+$ decuplet into the spin $(\frac{1}{2})^+$ octet, and $\Omega^- \to \Xi^*\gamma$ occurs within the spin $(\frac{3}{2})^+$ decuplet.

Up to now, most of the branching ratios and asymmetries have been measured. $\Sigma^0 \to n\gamma$ is inaccessible due to the overwhelming electromagnetic decay $\Sigma^0 \to \Lambda\gamma$. For the decay $\Omega^- \to \Xi^-\gamma$ only upper limits are known so far. Since for $\Omega^- \to \Xi^*(1530)\gamma$ the phase space is even smaller than for the latter decay, it will be hard to measure this mode in the near future.

The accuracy on the measurements still leaves room for improvements. Only the decay mode $\Sigma^+ \to p\gamma$ has been measured with an accuracy that allows one to check the various models.

## 2. Theory, a Brief Introduction

The transition matrix element T for a radiative hyperon decay $Y(p) \to B(p') + \gamma(q)$ (with Y: initial hyperon, B: Baryon, $\gamma$: photon and $p, p', q$: momenta of the particles) is given by

$$T = G_F \frac{e}{\sqrt{4\pi}} \epsilon_\nu \bar{u}(p')(A + B\gamma_5)\sigma_{\mu\nu} q_\mu u(p) \qquad (1)$$

where $\bar{u}(p'), u(p)$ are spinor wave functions of the baryon and the hyperon, $\epsilon_\nu$ is the polarization vector of the photon, A and B are the parity-conserving and parity-violating amplitudes, $\sigma_{\mu\nu}$ and $\gamma_5$ are the combinations of Dirac gamma matrices, $G_F$ is the Fermi constant, and $e$ is the electron charge.

Accessible to experiments are the branching ratios

$$BR \propto |A|^2 + |B|^2 \qquad (2)$$

and the asymmetry parameters

$$\alpha_\gamma = \frac{2Re(A * B)}{|A|^2 + |B|^2} \qquad (3)$$

For polarized hyperons, the differential center-of-mass angular distribution is given by

$$\frac{dN}{d\Omega} = \frac{N_0}{4\pi}(1 + \alpha P \hat{n}) \qquad (4)$$

with:
$N_0$: number of events
P: polarization vector of the hyperon
$\hat{n}$: unit vector in the direction of the outgoing baryon in the hyperon rest frame.

Different theoretical models try to describe radiative hyperon decays. The first phenomenological attempt to calculate a branching ratio and

asymmetry parameter for hyperon radiative decays was the pole model. It did not give a unified picture of radiative decays.

Later Zencykowski related hyperon nonleptonic and radiative decays in a combined symmetry and vector dominance model which describes the branching ratios and the asymmetries for all hyperon radiative decays [18–21].

## 3. Experimental Situation before 1999 - Published Results

An overview of the best measurements for each decay is given in Table 1, including the fit performed by the PDG.

In the following, recent experimental results on weak radiative hyperon decays are presented.

### 3.1. E761

Three of the recent measurements of hyperon decays were done by the E761 collaboration. The experiment was located in the Proton Center beam line at Fermilab. The apparatus consisted of a charged hyperons beam line and three spectrometers, one each for the incident hyperon (Y), the decay baryon (B) and the photons of the radiative decay $Y \to B\gamma$ or the hadronic decay $Y \to B\pi^0, \pi^0 \to \gamma\gamma$.

- $\Sigma^+ \to p\gamma$

  Before E761 published the results on the branching ratio (1995) and the asymmetry (1992) of this decay mode, experimental data were meager and came from bubble chamber experiments only ([14,12,2,3]). The signal from radiative decays could be isolated using the high resolution of the bubble chambers. Two of the groups ([2,3]) were able to observe a first indication for a large and negative asymmetry in this decay in contradiction to the Hara theorem.

  With the publication of E761 the indications were confirmed with high precission. They measured

  $BR(\Sigma^+ \to p\gamma) = (1.20 \pm 0.06 \pm 0.05) \times 10^{-3}$

  from 31901 events [4] and

  $\alpha_\gamma = -0.720 \pm 0.086 \pm 0.045$

  from 34754 events [5].

- $\Xi^- \to \Sigma^-\gamma$

  For this mode, the E761 collaboration published the first result, based on 211 events. The branching ratio was measured to be

  $BR(\Xi^- \to \Sigma^-\gamma) = (0.122 \pm 0.023 \pm 0.006) \times 10^{-3}$.

  They also found an indication for a positive asymmetry with

  $\alpha_\gamma = 1.0 \pm 1.3$ [10].

- $\Omega^- \to \Xi^-\gamma$

  E761 was able to improve a previous limit given by the CERN experiment WA42 by a factor of four. WA42 measured

  $BR(\Omega^- \to \Xi^-\gamma) < 2.2 \times 10^{-3}$ [13],

  the present result from E761 is

  $BR(\Omega^- \to \Xi^-\gamma) < 0.46 \times 10^{-3}$ [9].

### 3.2. BNL E811

The experiment E811 was performed at BNL in the low energy separated beam LESB II of the AGS. They managed to increase statistics by about a factor of 35 compared to the previous world total. The branching ratio of $\Lambda \to n\gamma$ was found to be

$BR(\Lambda \to n\gamma) = (1.75 \pm 0.15) \times 10^{-3}$

The asymmetry on this decay mode has not yet been measured.

E811 also obtained a result on $\Sigma^+ \to p\gamma$ based on 408 events published in 1989 by Hessey et al. [16]. Only the branching ratio was measured to be

$BR(\Sigma^+ \to p\gamma) = (1.45 \pm 0.20^{+0.11}_{-0.22}) \times 10^{-3}$.

Within the errors, the result is in good agreement with the more accurate later measurement by E761.

### 3.3. Minnesota, Michigan, Wisconsin and Rutgers Collaboration

James et al. published in 1990 the best measurement so far on the decay $\Xi^0 \to \Lambda\gamma$ [7]. With 116 events they determined the branching ratio and the asymmetry parameter $\alpha_\gamma$ to be

$BR(\Xi^0 \to \Lambda\gamma) = (1.06 \pm 0.12_{stat} \pm 0.11_{syst}) \times 10^{-3}$

and

$\alpha_\gamma = 0.43 \pm 0.44(stat)$

### 3.4. Rutgers, Michigan and Minnesota Collaboration

In 1993, Teige et al. published the first result on the decay $\Xi^0 \to \Sigma^0\gamma$ [8]. In total they found 85 events. They also measured both the branching ratio and the asymmetry resulting in

$\frac{BR(\Xi^0 \to \Sigma^0\gamma)}{BR(\Xi^0 \to \Lambda\pi^0)} = (3.56 \pm 0.42_{stat} \pm 0.10_{syst}) \times 10^{-3}$

and

Table 1
Results on Weak Radiative hyperon decays until 1998

| | BR ($\times 10^{-3}$) | Asymmetry ($\times 10^{-1}$) | Year | Ref. |
|---|---|---|---|---|
| $\Lambda \to n\gamma$ | $1.75 \pm 0.15$ | | 1993 | [6] |
| | $1.75 \pm 0.15$ | | | [11] |
| $\Sigma^+ \to p\gamma$ | $1.20 \pm 0.06 \pm 0.05$ | | 1992 | [4] |
| | | $-7.20 \pm 0.86 \pm 0.45$ | 1994 | [5] |
| | $1.23 \pm 0.05$ | $-7.6 \pm 0.8$ | | [11] |
| $\Xi^0 \to \Lambda\gamma$ | $1.06 \pm 0.12 \pm 0.11$ | $4.3 \pm 4.4$ | 1990 | [7] |
| | $1.06 \pm 0.16$ | $4.3 \pm 4.4$ | | [11] |
| $\Xi^0 \to \Sigma^0\gamma$ | $3.56 \pm 0.42 \pm 0.10$ | $2.0 \pm 3.2 \pm 0.5$ | 1989 | [8] |
| | $3.5 \pm 0.4$ | $2.0 \pm 3.2 \pm 0.5$ | | [11] |
| $\Xi^- \to \Sigma^-\gamma$ | $0.122 \pm 0.023 \pm 0.006$ | $10 \pm 13$ | 1994 | [10] |
| | $0.127 \pm 0.023$ | | | [11] |
| $\Omega^- \to \Xi^-\gamma$ | $< 0.46$ | | 1994 | [9] |
| $\Omega^- \to \Xi^*\gamma$ | | | | |

$\alpha_\gamma = 0.20 \pm 0.32_{stat} \pm 0.05_{syst}$

It turns out that the asymmetry measurement is incorrect, since a dilution factor of -1/3 from the subsequent decay $\Sigma^0 \to \Lambda\gamma$ had not been taken into account [15].

## 4. New Measurements and Results to Come

Since the fixed target programs of the high energy laboratories are coming to an end, most of the hyperon experiments have been stopped. At the moment, there are only two experiments left with the capability to measure radiative hyperon decays: KTeV at Fermi National Lab and NA48 at CERN. Both experiments were built to measure the parameter $\mathrm{Re}(\frac{\epsilon'}{\epsilon})$ of direct CP violation in the neutral Kaon system. However, thea are also very well suited to measure radiative decays of neutral hyperons due to their excellent energy and momentum resolution for photons and charged tracks.

### 4.1. KTeV

The hyperons are generated at the $K_L$ target station about 250 m upstream of detector. All charged particles are swept away by a magnet. Therefore, only decays of the neutral hyperons $\Lambda$ and $\Xi^0$ coming from the target can be detected. $\Sigma^0$s can also be seen from secondary decays like $\Xi^0 \to \Sigma^0\gamma$. Since the target station is rather far away from the detector, only high energetic hyperons can reach the fiducial decay region.

The main components of the detector are a spectrometer to measure the momenta of charged particles and a high resolution CsI crystal calorimeter to measure the energy of neutral particles. During rare decay running conditions, a TRD in front of the electromagnetic calorimeter provides a better separation between pions and electrons.

An overview over the detector is shown in Figure 1.

KTeV first took data in 1997 and is currently taking data(1999). This second running period should increase the total amount of data by about a factor of five.

KTeV has preliminary results on two radiative hyperon decays:

- $\Xi \to \Lambda\gamma$

  From the winter data of 1997 KTeV observed about 1100 events of the type $\Xi \to \Lambda\gamma$. Figure 2 shows the reconstructed $\Lambda\gamma$ invariant mass. From this sample it was possible to determine the branching ratio of this decay.

  $BR(\Xi^0 \to \Lambda\gamma) = (0.94 \pm 0.04_{stat}) \times 10^{-3}$

- $\Xi^0 \to \Sigma^0\gamma$

  KTeV has collected about 4048 events of the type $\Xi^0 \to \Sigma^0\gamma$ and the subsequent decay $\Sigma^0 \to \Lambda\gamma$ on top of a background of 804 events. They measure the branching ratio and the asymmetry of this decay with high accuracy. Figure 3 shows the best combination (closest to the $\Sigma^0$ mass) of the $\Lambda\gamma$ invariant mass.

  They measure the branching ratio to be

  $BR(\Xi \to \Sigma^0\gamma) = (3.34 \pm 0.05_{stat} \pm 0.11_{syst}) \times 10^{-3}$,

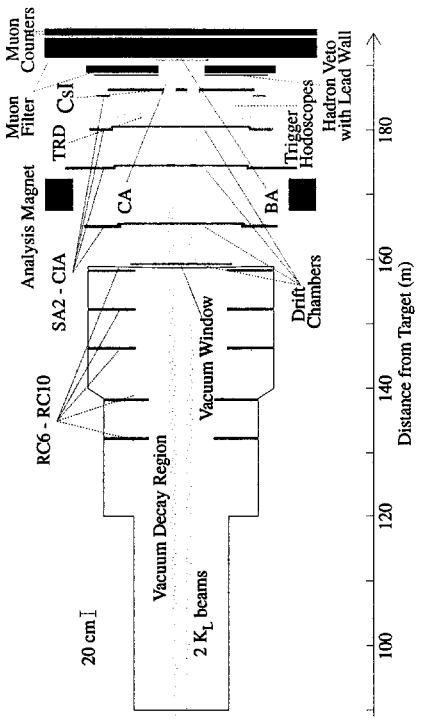


Figure 1. The KTeV Detector

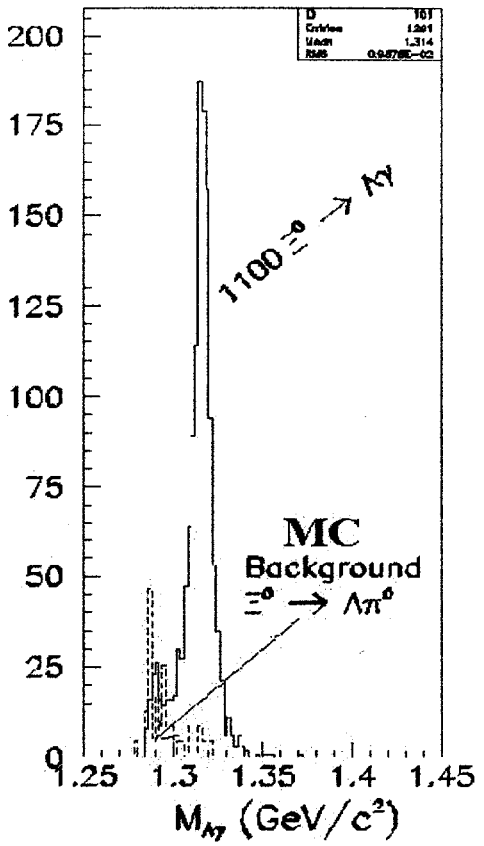


Figure 2. Reconstructed $\Xi^0$ mass from the decay $\Xi^0 \to \Lambda\gamma$

which is in good agreement with the previous measurement from Teige et al. [8].

In addition, the asymmetry has been measured.

For this analysis, three different intermediate states have to be taken into account. The $\Sigma^0$ from the $\Xi^0$ immediately decays to $\Lambda\gamma$. Being an electromagnetic transition, the $\Sigma^0$ decay is symmetric and carries information on the $\Sigma^0$ polarization. Therefore, to check the asymmetry, one has to look at a 2-dimensional distribution of decay angles in the $\Sigma^0$ and the $\Lambda$ center-of-mass frames.

If one ignores the decay $\Sigma^0 \to \Lambda\gamma$ and averages over all directions of the $\Lambda$ emission, the net observed asymmetry is diluted by a factor of -1/3, assuming that the experimental acceptance does not affect the decay asymmetrically.

To measure the asymmetry, 10 different Monte Carlo data sets have been generated with asymmetries between 0 and -1.

Figure 4 shows the $\chi^2/DOF$ comparison between the data and the 10 different Monte Carlo samples. A parabola fit was performed and a minimum at -0.65 was observed.

From this measurement the asymmetry has been extracted to be

$\alpha_\gamma = -0.65 \pm 0.13$ [15].

### 4.2. NA48

In contrast to KTeV, NA48 has two different beams to generate $K_S$ and $K_L$ mesons.

The so-called $K_L$ target is about 250 m upstream of the detector. For $K_S$ generation another target is located about 120 m in front of the detector. Since the hyperons have about the same

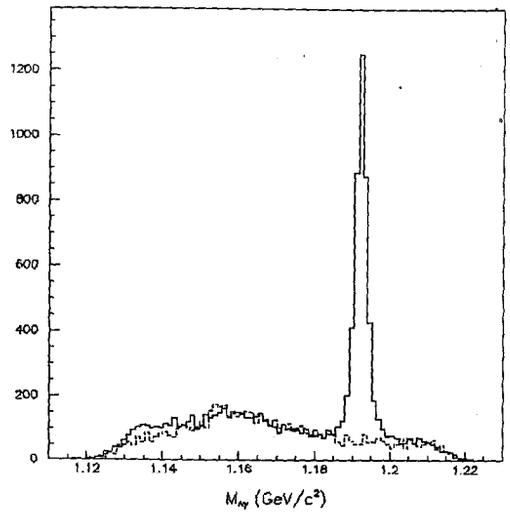


Figure 3. Reconstructed $\Sigma^0$ mass from the decay $\Xi^0 \to \Sigma^0\gamma$

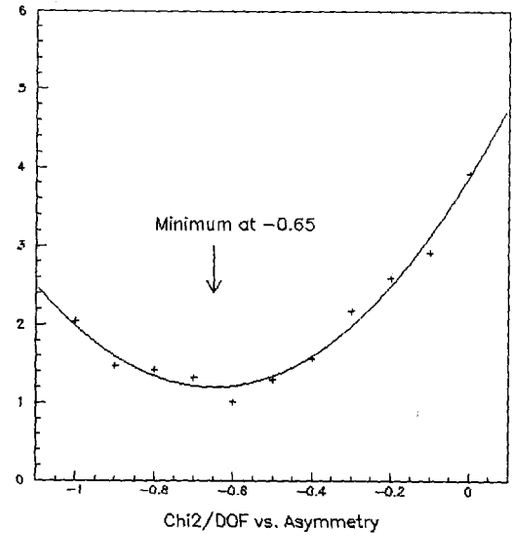


Figure 4. Asymmetry

lifetime ($O(10^{-10}s)$) as the $K_S$ mesons, NA48 yields a large sample of hyperons.

As for KTeV, all charged particles are bent out of the beam. Therefore from all hyperon decays produced at the target only $\Lambda$ and $\Xi^0$ can be detected. $\Sigma^0$'s can be observed from secondary decays ($\Xi^0 \to \Sigma^0\gamma$). Compared to KTeV, the decay region is closer to the detector. Therefore, the acceptance for low energy hyperons is much larger.

The main components of the detector are a spectrometer to measure the momenta of the charged particles and a Liquid Krypton electromagnetic calorimeter (LKR) to measure the energies of neutral particles. A Hadron Calorimeter (HAC) is located behind the LKR and followed by a muon veto counter. Spectrometer and the LKR calorimeter feature an excellent energy and momentum resolution.

An overview over the detector is shown in Figure 5.

Up to now, NA48 published two results concerning weak radiative hyperon decays using the data from 1997. The period of data taking was reduced to 44 days due to a fire in the SPS. Therefore the data sample is rather small compared to KTeV's . The complete data set available now (1997, 1998 and 1999) should contain 10 times more events.

- $\Xi^0 \to \Lambda\gamma$

  From the data in 1997, NA48 obtained 30 events of the type $\Xi \to \Lambda\gamma$. The reconstructed $\Lambda\gamma$ invariant mass spectrum of these events is shown in Figure 6.

  The $\Xi^0 \to \Lambda\gamma$ branching ratio was measured to be

  $BR(\Xi^0 \to \Lambda\gamma) = (1.90 \pm 0.34_{stat} \pm 0.19_{syst}) \times 10^{-3}$ [17].

  This result differs by $2\sigma$ from both the measurement by James et al. and the new result by KTeV. Due to the small data sample it was not possible to measure the asymmetry.

- $\Xi^0 \to \Sigma^0\gamma$

  Again using the 1997 data, NA48 found 17 events in the channel $\Xi^0 \to \Sigma^0\gamma$ with the subsequent decay $\Sigma^0 \to \Lambda\gamma$. The reconstructed $\Sigma^0$ invariant mass spectrum of these events is shown in Figure 7, where the $\Xi^0$ mass has been used as a constraint in the kinematic fit.

  The branching ratio has been measured to be

  $BR(\Xi \to \Sigma^0\gamma) = (3.14 \pm 0.76_{stat} \pm 0.32_{syst}) \times 10^{-3}$ [17].

  This result is in very good agreement with the previous measurement of Teige et al.. As for $\Xi^0 \to \Lambda\gamma$, it was not possible to mea-

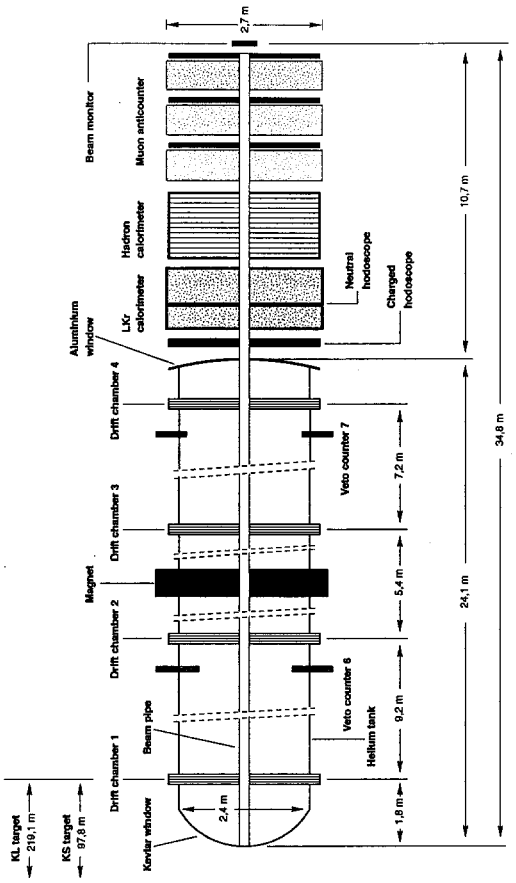


Figure 5. The NA48 Detector

sure the asymmetry due to the low statistics.

### 4.3. NA48 High Intensity $K_S$ Run

With the data taken under normal $\epsilon'$ conditions NA48 will not be competitive with KTeV. However, NA48 plans a high intensity $K_S$ run in 2001. An 8 hours test has already been performed this year. Even with a trigger downscaled by a factor of 10 it was possible to collect the equivalent statistics corresponding to one year of running (under normal conditions) within 8 hours.

One year of running in 2001 would allow to measure the branching ratios and asymmetries of the decay modes described above with a very good accuracy. In addition, it opens a possibility to observe many other decay channels, such as semi-leptonic decays of $\Xi^0$ hyperons.

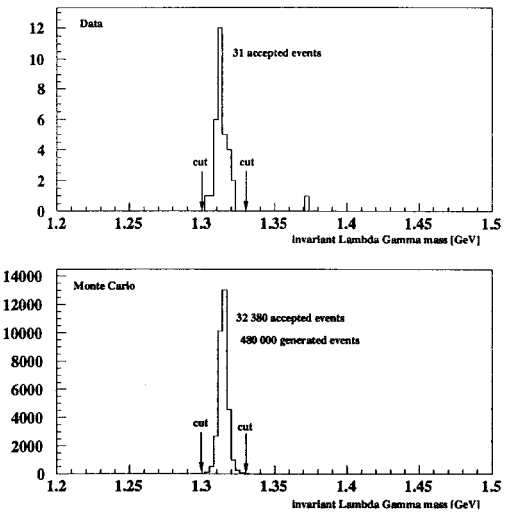


Figure 6. Reconstructed $\Sigma^0$ mass from the decay $\Xi^0 \to \Sigma^0\gamma$

## 5. Summary and Outlook

Between 1995 (last publication of E761) and today, there have been no publications in the field of weak radiative hyperon decays. However, the situation is changing at least for the neutral hyperons, in particular for the $\Xi^0$.

With the 1997 data, KTeV managed to improve the measurements for the branching ratios for the 2 radiative decay modes of the $\Xi^0$. In addition, they performed the first correct measurement of the asymmetry in $\Xi^0 \to \Sigma^0\gamma$. Their results are still preliminary.

KTeV and NA48 are the only experiments with the capability to measure the radiative decays of neutral hyperons in the near future. By including the 1999 data set, KTeV will increase statistics by a factor between three and ten. NA48 will have even more data as soon the high intensity $K_S$ data taking starts.

However, some interesting parameters like the asymmetry in the decay mode $\Lambda \to n\gamma$ can probably not be measured. Investigating charged hyperons would require a special experiment. Therefore, the modes $\Omega^- \to \Xi^-\gamma$ and $\Omega^- \to \Xi^*(1530)\gamma$ will remain unseen for the near future and the measurement of $\Xi^- \to \Sigma^-\gamma$ will not be improved.

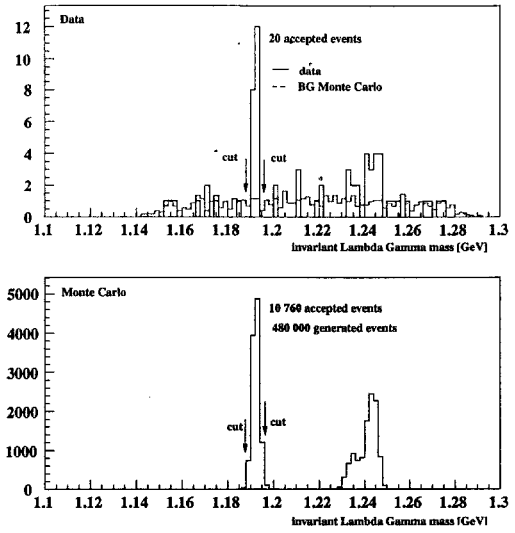


Figure 7. Reconstructed $\Sigma^0$ mass from the decay $\Xi^0 \to \Sigma^0\gamma$

## REFERENCES


1. Y.Hara, Phys Rev. Lett. 12, 378 (1964).
2. L.K. Gershwin et al., Phys. Rev. 188, 2077 (1969).
3. A.Manz et al., Phys. Lett. 96B, 217 (1980).
4. S.Timm et al., Phys. Rev. D 51, 4638 (1995).
5. M. Foucher et al., Phys. Rev. Lett. 68, 3004 (1992).
6. K.D. Larson et al., Phys. Rev. D 47, 799 (1993).
7. C. James et al., Phys. Rev. Lett. 64, 843 (1990).
8. S. Teige et al., Phys. Rev. Lett. 63, 2717 (1989).
9. I. Albuquerque et al., Phys. Rev. D 50, 18 (1994).
10. T. Dubbs et al., Phys. Rev. Lett. 72, 808 (1994).
11. The European Physical Journal C V3 Number 1-4 (1998).
12. G.Ang et al., Z. Phys. 228,151 (1969).
13. S.F. Biagi et al., Z. Phys. C 28, 495 (1985).
14. M. Bazin et al., Phys. Rev. Lett. 14, 154 (1965).
15. KTeV Hyperon Group, internal note (1999).
16. N.P. Hessey et al., Z. Phys. C 42, 175 (1989).
17. V.Fanti et al., coming in Eur. Phys. J. C 1999.
18. P. Zenczykowski, Phys. Rev. D 40, 2290 (1989).
19. P. Zenczykowski, Phys. Rev. D 44, 1485 (1991).
20. J. Lach and P. Zenczykowski, Int. J. Mod. Phys. A10, 3817 (1995).
21. Ya. I. Azimov, Proceedings LNPI22 Winter School of Physics (1987), p. 200

# Chapter 5

# QCD and Hyperons

• H. J. Lipkin

# The New $\sigma_{tot}(\Sigma p)$ Data, the new PDG fit to hadron total cross sections and the TCP alternative

Harry J. Lipkin [a]

[a] Department of Particle Physics
Weizmann Institute of Science, Rehovot 76100, Israel
School of Physics and Astronomy
Raymond and Beverly Sackler Faculty of Exact Sciences
Tel Aviv University, Tel Aviv, Israel
Department of Physics, U46
University of Connecticut, 2152 Hillside Rd., Storrs, CT 06269-3046
USA

The new SELEX measurement $\sigma_{tot}(\Sigma p) = 36.96 \pm 0.65$ at P = 609 GeV/c and the new 1998 Particle-Data-Group Regge (PDG) analysis of hadron total cross sections with an additional even-signature-exchange contribution recall the 1975 two-component-Pomeron model (TCP), which introduced such an additional term and predicted $\sigma_{tot}(\Sigma p) = 37.07$ mb. in 1975 as well as fitting all the same data now fit by PDG with fewer free parameters.and predicting $\sigma_{tot}(\Sigma p)$, (not predicted by PDG) at lower energies. The additional contribution confuses the extraction of the Pomeron intercept from data in the 600 GeV range and its dynamical origin is still unclear. But its surprising systematics suggests an interesting origin.

## 1. Implications of a Third Component

The new SELEX[1] result $\sigma_{tot}(\Sigma p) = 36.96 \pm 0.65$ at P = 609 GeV/c, is in surprising agreement with the 1975 prediction $\sigma_{tot}(\Sigma p) = 37.07$ mb. from the Two-Component-Pomeron model (TCP). This model arose from an analysis of the systematics of hadron-nucleon total cross section data[2] which showed the necessity of including a new third term in addition to the commonly used Pomeron and leading Reggeon contribuitions. The new accepted Particle-Data-Group (PDG) Regge analysis of hadron total cross sections[3] has now also shown that three terms are needed to fit the existing data. It is thus of interest to recall the TCP model which not only fits the same data with different and fewer parameters determined in 1975 and not changed since; it also successfully predicted hyperon-nucleon cross sections not predicted by PDG, now including the new SELEX result.

Both PDG and TCP use a Regge term which decreases with energy roughly like $s^{-0.5}$, and a universal Pomeron term which increases with energy roughly like $s^{0.1}$. They also use an additional even-signature term. with an intermediate energy variation ($s^{-0.34}$ in the PDG model and $s^{-0.2}$ in the TCP model). Both analyses express the total hadronic cross section for hadron A on a proton in the form

$$\sigma Ap = X_{Ap}s^{\epsilon} + Y_{1Ap}s^{-\eta_1} + Y_{2Ap}s^{-\eta_2} \quad (1)$$

PDG sets

$$\begin{aligned} X^{PDG}_{\bar{A}p} &= X_{Ap}; \\ Y^{PDG}_{1\bar{A}p} &= Y_{1Ap}; \\ Y^{PDG}_{2\bar{A}p} &= -Y_{2Ap} \end{aligned} \quad (2)$$

where $X_{AB}$, $Y_{1AB}$, $Y_{2AB}$, $\epsilon$, $\eta_1$, $\eta_2$ are determined by fitting data.

TCP sets

$$\begin{aligned} X^{TCP}_{Ap} &= X \cdot N_q(A); \\ Y^{TCP}_{1Ap} &= Y_1 \cdot N_q(A) \cdot N_n(A); \\ Y^{TCP}_{2Ap} &= Y_2 \cdot [2N_{\bar{u}}(A) + N_{\bar{d}}(A)]; \\ \eta_2 &= -0.5 \end{aligned} \quad (3)$$

where the coefficients $X$, $Y_1$ and $Y_2$ are universal for all hadrons, $N_q(A)$ is the total number of valence $q$ and $\bar{q}$ in $A$, $N_n(A)$ is the total number of nonstrange valence $q$ and $\bar{q}$ in $A$, $N_{\bar{u}}(A)$ and $N_{\bar{d}}(A)$ are respectively the numbers of valence $\bar{u}$ and $\bar{d}$ in $A$.

Both PDG and TCP fix parameters by fitting data, but there are many fewer free parameters in TCP than in PDG. In PDG the coefficients $X_{Ap}$, $Y_{1Ap}$ and $Y_{2Ap}$ are determined by fitting data and

are independent of one another, except for the equality of the isoscalar pomeron $X_{Ap}$ couplings between all states in the same isospin multiplet.

The particle-antiparticle relations in $Y_2$ are very different. In PDG $Y_2$ has only the odd signature $\rho$ and $\omega$ trajectories, and no contributions from the even signature $f$ and $A2$ trajectories. TCP uses the known exchange degeneracy of the $\rho$, $\omega$, $f$ and $A2$ trajectories and therefore follows the Harari-Rosner[6] duality description in which $Y_2 = 0$ in exotic channels which have no resonances.

In the original TCP notation

$$\sigma_{Ap}^{TCP} = \frac{N_q(A)}{2} \cdot \sigma_1 (P_{lab}/20)^{\epsilon} + \frac{N_q(A) \cdot N_n(A)}{2} \cdot \sigma_2 (P_{lab}/20)^{-\delta} + + [2N_{\bar{u}}(A) + N_{\bar{d}}(A)] \cdot \sigma_R (P_{lab}/20)^{-0.5} \quad (4)$$

where the values determined by fitting the data available in 1975 and not changed since were $\sigma_1$ = 13 mb, $\epsilon = 0.13$, $\sigma_2 = 4.4$ mb, $\delta = 0.2$ and $\sigma_R$ = 1.75 mb.

In both PDG and TCP the exponents $\epsilon$ and $\eta_1$ are determined by fitting data with no theoretical input beyond the relations between different hadrons already expressed in the formulas; i.e. the particle-antiparticle relations in PDG and the quark-counting relations in TCP. One sees immediately that there are many fewer free parameters in TCP and that the particle-antiparticle relations in the Regge term proportional to $Y_2$ are very different between the two formulas.

That two models with different parametrizations can fit the same data comes as no surprise. The data for $\sigma_{tot}(pp)$ vs. log(s) are very well fit by a parabola which is uniquely determined by three parameters[4]. Thus these data have been shown to be easily fit equally well by different two-Reggeon models which have four free parameters, two magnitudes and two exponents.

Because the TCP couplings are universal, the expression (4) predicts the hyperon-nucleon cross sections with the parameters above determined in 1975 by the other experimental cross sections and no further input.

## 2. Where is the physics? What can we learn?

In 1975 this question was investigated by making the most naive assumptions about the two leading terms, the Pomeron and the leading trajectories, subtracting these contributions from the total cross sections and looking at what remained. The surprising result, shown on fig. 4 of ref.[2], is still impressive. The additional contribution is universal above 20 GeV/c. The $pp$, $\bar{p}p$, $\pi^{\pm}p$ and $K^{\pm}p$ cross sections lie on a universal curve with scaling factors of 9:4:2 for protons, pions and kaons. This is just the product of the total number of quarks and the number of non-strange quarks, the scaling factor one would obtain for a Pomeron-f cut or for a triple-regge term in which the beam hadron couples to a Pomeron and an f.

What is this additional contribution? There is still no satisfactory explanation. But it continues to fit data and has predictive power. Note in particular the predictions for hyperon-nucleon cross sections then not available. The predicted scaling factors for $\Sigma p$ and $\Xi p$ are 6 and 3 and they work, including the new SELEX[1] measurement of $\sigma_{tot}(\Sigma p)$.

The initial motivation leading to TCP was to search beyond the simple pole approximation in Regge phenomenology. This first order approximation in strong interactions could not be the whole story. The total cross section data were already sufficiently precise to suggest a search for new higher-order physics. The ansatz of a double-exchange contribution to hadron-nucleon scattering with the flavor dependence of a pomeron-f cut or a triple-Regge diagram with a pomeron and an f coupled to the incident hadron led to a series of relations in remarkable agreement with experiment[8]. The present situation only reinforces the initial reaction to these results[9] "I don't believe a word of this crazy model, but the numbers are impressive. You must find a better explanation". Since then more and more impressive numbers have been found,[2,10–12] but no better explanation. A contribution with the flavor dependence of a Pomeron-f cut and an $s$ dependence fit by a unique decreasing power fits more and more data, but there is yet no credible explanation for this $s$ dependence.

The most naive assumptions used for the leading terms were that the Pomeron simply counts quarks and is fitted by a rising power of $s$ and that the leading Regge contribution counts Harari-Rosner Duality Diagrams[6] and decrases like $s^{-(1/2)}$. Plugging these assumptions and fixing the five universal parameters by fitting the 1975 data up to 200 GeV/c gave the TCP model with the same parameters that still fit data accumulated since 1975.

We now examine these assumptions from the point of view of QCD.

This model can be described in modern QCD language[4] in terms of a hierarchy of contributions inspired by large $N_c$ QCD: (1) multigluon exchange, (2) planar quark diagrams, (3) nonplanar quark-exchange diagrams.

The Pomeron is described by multigluon exchanges which do not know about flavor and are the same for pion and kaons and for protons and hyperons. The additive quark counting giving the 3/2 factor between baryons and mesons is obtained from color algebra for two-gluon and three-gluon exchanges[14]. There is no firm justification for neglecting higher exchanges but it fits the data.

The leading Regge exchanges are described Harari-Rosner duality diagrams are just the planar quark-exchange diagrams which are the leading contributions in large-$N_c$ QCD[4]. This immediately incorporates $s-t$ duality[15], since exotic channels which have no resonances have no contribution from planar quark diagrams.

The third term then comes from more complicated non-planar quark diagrams. Why these should scale in the way that they do is still open. But this term should be absent in processes like $\phi - n$ which cannot have such quark-exchange diagrams because there are no valence quarks in the beam and target with the same flavor. There are no extensive data for $\phi - n$. But we can consider as "gedanken" $\sigma_{tot}(\phi^- p)$ the linear combination

$$\sigma_{ged}(\phi^- p) \equiv$$
$$\sigma_{tot}(K^+ p) + \sigma_{tot}(K^- p) - \sigma_{tot}(\pi^- p) \qquad (5)$$

which is equal to $\sigma_{tot}(\phi^- p)$ in the quark model. The data for "gedanken" $\sigma_{tot}(\phi^- p)$ are shown on fig. 4 of ref.[2] and seen to rise monotonically and can be fit by a single power of s as expected for a cross section which has neither planar nor nonplanar quark exchange diagrams and has only a Pomeron contribution. The contribution of the third term to "gedanken" $\sigma_{tot}(\phi^- p)$ is shown on fig. 4 of ref.[2] to be consistent with zero above 10 GeV/c. But the ansatz still has no convincing basis and no firm connection with QCD beyond hand waving.

TCP pinpoints open questions and puzzles not fully understood about the relation between meson and baryon structure, the link between Regge phenomenology and QCD, and how the remarkable successes of the constituent quark model can be eventually described by QCD.

TCP assumes $s-t$ duality[15] in which $\sigma_{tot}(pp)$ is exotic and has no leading Regge contribution. The decrease in $\sigma_{tot}(pp)$ with energy observed at low energies thus indicates the existence of another decreasing contribution in addition to leading Regge. Assuming that this contribution is described by the double exchange ansatz and determining its parameters by fitting $\sigma_{tot}(pp)$ then gives unique nontrivial predictions for all other exotic cross sections; e.g. $\sigma_{tot}(K^+ p)$, $\sigma_{tot}(\Sigma p)$, $\sigma_{tot}(\Xi p)$ and the linear combination $\sigma_{tot}(K^- p) - \sigma_{tot}(\pi^- p)$. The linear combination "gedanken" $\sigma_{tot}(\phi^- p)$ has no double exchange contribution and is predicted to rise monotonically with the same single power of $s$ used to fit the rising term in $\sigma_{tot}(pp)$. All predictions continue to agree with new experimental data with no further adjustment of the five TCP parameters. Particularly impressive was the factor 2/3 predicted before the hyperon-nucleon cross sections were measured which contradicted all the conventional wisdom.

$$\sigma_{tot}(\pi^- p) - \sigma_{tot}(K^- p) =$$
$$(2/3)\{\sigma_{tot}(pp) - \sigma_{tot}(\Sigma p)\} =$$
$$= (2/3)\{\sigma_{tot}(\Sigma p) - \sigma_{tot}(\Xi p)\} \qquad (6)$$

The remarkable success of naive TCP for all hadron-nucleon cross sections was summarized in the 1981 Moriond report of the CERN hyperon experiment [13].

The simple systematics like the factor 3/2 between hyperon-nucleon and meson-nucleon strangeness differences and the monotonic rise with $s$ of the linear combinations which have no simple quark exchange diagrams suggest the the existence of some simple explanation based on QCD, even if the TCP ansatz is wrong. Further investigations may provide new insight into how QCD makes hadrons from quarks and gluons and should be encouraged.

## 3. Experimental evidence that mesons and baryons are made of the same quarks

The large number of relations between meson-nucleon and baryon-nucleon total cross sections which agree with experiment suggest that mesons and baryons are made of the same contituent quarks in the $q\bar{q}$ and $3q$ configurations. We summarize these here and examine them from different points of view to hopefully provide clues for theoretical explanations.

There is first the simple additive quark prediction,

$$\delta_{AQM} \equiv (2/3)\cdot\sigma_{tot}(pp) - \sigma_{tot}(\pi^- p) \leq 7\% \quad (7)$$

There is then the TCP prediction

$$\sigma_{tot}(\pi^- p) - \sigma_{tot}(K^- p) = \\ = (1/3)\sigma_{tot}(pp) - (1/2)\sigma_{tot}(K^+ p) \quad (8)$$

Both of these are confirmed by data up to $P_{lab} = 310$ GeV/c. There are as yet no data available for a complete set of all these reactions at the same single energy above $P_{lab} = 310$ GeV/c.

There are the TCP predictions for baryon-nucleon cross sections from meson-baryon cross sections at 100 GeV/c where data are available.

$$38.5 \pm 0.04\text{mb.} = \sigma_{tot}(pp) = \\ 3\sigma_{tot}(\pi^+ p) - (3/2)\sigma_{tot}(K^- p) \\ = 39.3 \pm 0.2\text{mb.} \quad (9)$$

$$33.3 \pm 0.31\text{mb.} = \sigma_{tot}(\Sigma p) = \\ (3/2)\{\sigma_{tot}(K^+ p) + \\ \sigma_{tot}(\pi^- p) - \sigma_{tot}(K^- p)\} = \\ 33.6 \pm 0.16\text{mb.} \quad (10)$$

$$29.2 \pm 0.29\text{mb.} = \sigma_{tot}(\Xi p) = \\ (3/2)\sigma_{tot}(K^+ p) = 28.4 \pm 0.1\text{mb.} \quad (11)$$

$$\sigma_{tot}(\Omega^- p) = \\ = (3/2)\{\sigma_{tot}(K^+ p) - \\ \sigma_{tot}(\pi^- p) + \sigma_{tot}(K^- p)\} \quad (12)$$

Another interesting way to view the data is to compare the strange and nonstrange quark contributions to the to baryon-nucleon and meson-nucleon total cross sections extracted using the additive quark model

Let $\sigma(fN)_H$ denote the total cross section on a nucleon target, for a single quark of flavor $f$ in a hadron $H$ on a nucleon target, where $f$ may be strange $s$ or nonstrange $n$ and $H$ may be a baryon $B$ or a meson $M$. The additive quark model gives

$$\sigma(nN)_B = \frac{1}{3}\cdot\sigma(pN) = 12.9 \pm 0.01mb. \quad (13)$$

$$\sigma(sN)_B = \\ \frac{1}{3}\{\sigma(\Sigma N) + \sigma(\Xi N) - \sigma(pN)\} = \\ = 7.7 \pm 0.1mb. \quad (14)$$

$$\sigma(nN)_M = \\ \frac{1}{2}\{\sigma(\pi N) - \sigma(\bar{K}N) + \sigma(KN)\}m = \\ = 11.2 \pm 0.05mb. \quad (15)$$

$$\sigma(sN)_M = \\ \frac{1}{2}\{\sigma(\bar{K}N) - \sigma(\pi N) + \sigma(KN)\} = \\ = 7.75 \pm 0.05mb. \quad (16)$$

where we have assumed $\sigma(sN)_M = \sigma(\bar{s}N)_M$.

We find the surprising result that the contribution of the strange quarks is the same to both meson-nucleon and baryon-nucleon total ross sections, but that the contribution of the nonstrange quarks is the less for meson-nucleon than for baryon-nucleon total cross sections. This immediately gives rise to speculations that nonstange quarks are more complicated than strange quarks because they can have a pion cloud. However. there has been no success in carrying this argument further quantitatively. Instead we obtain the following surprising relations, which go to the heart of the TCP ansatz; namely that one single mechanism is responsible for the breakings of both SU(3) flavor symmetry and the additive quark model.

$$\sigma(nN)_B - \sigma(nN)_M = 1.69 \pm 0.05mb. \quad (17)$$

$$\frac{1}{2}\{\sigma(nN)_M - \sigma(sN)_M\} = 1.73 \pm 0.04mb. \quad (18)$$

The difference between the contributions of nonstrange quarks to baryon-nucleon and meson-nucleon cross sections is equal to the difference between the contributions of nonstrange and strange quarks quarks to meson-nucleon cross sections.

This as yet unexplained connection between the deviation from SU(3) symmetry and the deviation from the Levin-Frankfurt AQM 3/2 ratio for baryons and mesons has been expressed by the experimentally satisfied relation[2]

$$\sigma_{tot}(\pi^- p) - \sigma_{tot}(K^- p) = \\ (1/3)\sigma_{tot}(pp) - (1/2)\sigma_{tot}(K^+ p) \quad (19)$$

This has been rearranged to give

$$\sigma_{ged}(\phi^- p) \equiv \\ \sigma_{tot}(K^+ p) + \sigma_{tot}(K^- p) - \sigma_{tot}(\pi^- p) = \\ = (3/2)\sigma_{tot}(K^+ p) - (1/3)\sigma_{tot}(pp) \quad (20)$$

The expressions on both sides of this relations are found experimentally not only to be equal but to

increase monotonically with energy and fit by a single power. This fits in with the picture that $\sigma_{ged}(\phi^- p)$ contains only a pure Pomoeron contribution. But that the right hand side which is a linear combination of meson and baryon cross sections behaves in the same way suggests some sort of universality for the Pomeron.

We also find that the difference between the contributions of nonstrange and strange quarks to baryon-nucleon cross sections is greater by a factor of (3/2) than the corresponding difference for meson-nucleon cross sections.

$$\sigma(nN)_B - \sigma(sN)_B = 5.15 \pm 0.07mb \quad (21)$$

$$\frac{3}{2}\{\sigma(nN)_M - \sigma(sN)_M\} = 5.2 \pm 0.1mb \quad (22)$$

As soon as one begins to think about some dynamical origin for these relations one encounters a very perplexing question. Why is there seemingly such a simple relation between hadron-nucleon total cross sections, when any credible scattering model suggests that they should be very different and depend upon radii and geometrical considerations, not simply quark counting? Perhaps a relevant interesting analogy is in the relation between hadronic elecromagnetic form factors and eloectric charges. The form factors of pions, nucleons and other hadrons are complicated and very different from one another. But their total electric charge is simple and given by adding up the charges of their constituent quarks. Rutherford scattering measures total charge. Does universality of contributions to $\sigma_{tot}(Hp)$ suggest measurements of some kinds of total charge in which the microscopic details are smehow not important?

## 4. Conclusions

We conclude by listing a hierarchy of the experimental systematics found in this phenomenological analysis and the questions to be resolved by further experiments at higher energies:

### 4.1. Summary of experimental systematic regularities

1. Odd signature universality

   $\rho$ universality (Sakurai) - conserved isospin current

   $\omega$ universality - related to $\rho$ by U(2)

   Energy dependence - like $s^{-1/2}$
2. Exchange degeneracy - No exotic contributions

   Only planar quark diagrams contribute
3. Universal Pomeron - Counts quarks

   Given by amplitude with no quark exchanges

   $\sigma_{ged}(\phi^- p) = \sigma_{tot}(K^+ p) + \sigma_{tot}(K^- p) - \sigma_{tot}(\pi^- p)$
4. What's left?

   Universal contribution scaling like Pomeron-f cut

   Scaling factors of 9:4:2 like for protons, pions and kaons.

   Extrapolated to 6 and 3 for $\Sigma p$ and $\Xi p$ - predict data!

   But what is it?

### 4.2. Interesting questions to be decided by future experiments

1. Does the ad-hoc third component continue to explain both the deviation from SU(3) symmetry and the deviation from the Levin-Frankfurt AQM 3/2 ratio for baryons and mesons; i.e. do $\sigma_{tot}(\pi^- p) - \sigma_{tot}(K^- p)$ and $(1/3)\sigma_{tot}(pp) - (1/2)\sigma_{tot}(K^+ p)$ continue to remain equal at higher energies?
2. Do both the SU(3) breaking and the deviation from 3/2 go to zero at high energies or does one or both level off. Data at around 200 GeV/c indicate that $\sigma_{tot}(\pi^- p) - \sigma_{tot}(K^- p)$ might be leveling off while $(1/3)\sigma_{tot}(pp) - (1/2)\sigma_{tot}(K^+ p)$ continues to decrease with increasing energy. But the differences are not convincing and better data at higher energies should easily resolve this question.
3. Is there a universal Pomeron that holds for all hadrons with a 3/2 ratio between baryon and meson couplings? Do $\sigma_{ged}(\phi^- p)$ and $(3/2)\sigma_{tot}(K^+ p) - (1/3)\sigma_{tot}(pp)$ continue to be equal and rise monotonically like a pure Pomeron conmtribution? To answer this question reliably one must go to high enough energies so that the contribution of the third component becomes negligible.

### 4.3. Bottom Line

There is much yet to learn from future experiments about how QCD makes hadrons out of quarks and gluons.

## REFERENCES


1. The SELEX Collaboration, U. Dersch, et al, hep-ex/9910052, FERMILAB-Pub-99/325-E, submitted to Nucl.Phys.B, U. Dersch, U. Heidelberg, Ph.D. thesis, 1998, Messung totaler Wirkungsquerschnitt mit Sigma-, Proton, Pi- und Pi+ bei 600 GeV/c Laborimpuls, http://axnhd0.mpi-hd.mpg.de/ selex/; I. Eschrich et al. (SELEX), Hyperon Physics

Results from SELEX, Workshop on Heavy Quarks at Fixed Target (HQ98), Fermilab, Oct. 1998, hep-ex/9812019; U. Dersch et al. (SELEX), Measurements of Total Cross Sections with Pions, Sigmas, and Protons on Nuclei and Nucleons around 600 GeV/c, PANIC99, http://pubtsl.tsl.uu.se/, Uppsala, Sweden, June 10-16, 1999, Abstract (& Poster) se02.

2. Harry J. Lipkin, Phys. Rev. D11 (1975) 1827
3. Particle Data Group, European Physics Journal, C3 (1998) 1, p. 205
4. Harry J. Lipkin, Physics Letters B335 (1994) 500
5. H. J. Lipkin, Z. Physik 202 (1967) 414 and Nucl. Phys. B9 (1969) 349
6. H. Harari, Phys. Rev. Lett. 22 (1969) 562; J. L. Rosner, Phys. Rev. Lett. 22 (1969) 689
7. H. J. Lipkin, Phys. Rev. Letters 16 (1966) 1015
8. Harry J. Lipkin, Nucl. Phys. B78 (1974) 381
9. H. Harari, Private Communication
10. Harry J. Lipkin, Phys. Lett B56 (1975) 76
11. Harry J. Lipkin, Phys. Rev. D17 (1978) 366
12. Harry J. Lipkin, Nucl. Phys. B214 (1983) 136
13. Pierre Extermann, in *New Flavors and Hadron Spectroscopy*, Proceedings of the Sixteenth Rencontre de Moriond, Les Arcs - Savoie - France, 1981 edited by J. Tran Thanh Van (Rencontre de Moriond, Laboratoire de Physique Theorique et Particules Elementaires, Universite de Paris-Sud, Orsay, France, (1981) Vol. II. p. 393
14. Harry J.Lipkin, Phys. Lett B116 (1982) 175.
15. G. Veneziano, Phys. Reports 9C (1974) 199

# Chapter 6

# CP Violation in Hyperons


- G. Valencia
- K. Nelson

# Theoretical Status of CP Violation in Hyperon Decays

G. Valencia [a]

[a]Department of Physics,
Iowa State University,
Ames, IA 50011

I review the status of theoretical estimates for the CP violating asymmetry $A(\Lambda^0_-)$.

## 1. Introduction

In non-leptonic hyperon decays such as $\Lambda \to p\pi^-$ it is possible to search for CP violation by comparing the decay with the corresponding anti-hyperon decay [1]. The usual notation and framework for this discussion have been reviewed by Kenneth Nelson in the previous talk [2]. We heard in that talk that the HyperCP experiment at Fermilab is measuring the combination $A(\Lambda^0_-) + A(\Xi^-_-)$, and that $A(\Lambda^0_-)$ can be written as [3],

$$A(\Lambda^0_-) \approx -\tan(\delta_p - \delta_s)\sin(\phi_p - \phi_s). \qquad (1)$$

In this talk I will first review the calculation of strong phases, the $\delta$'s, to show why we now believe that $A(\Lambda^0_-)$ is likely to be dominant. I will then review the calculation of the weak phases, the $\phi$'s, within the standard model and estimate the error guided by chiral perturbation theory. Finally I will discuss specific scenarios of physics beyond the standard model in which the asymmetry can be large.

## 2. Strong Phases

Watson's theorem tells us that the strong final state phases in the decay $\Lambda \to N\pi$, for each isospin and angular momentum $N\pi$ final state, are the same as the corresponding $N\pi$ scattering phases in the channel with the same quantum numbers at a center of mass energy equal to the $\Lambda$ mass. Since the latter have been measured, we know the strong phases needed in Eq. 1. They are $\delta_s = 6^o$, $\delta_p = -1.1^o$ with errors of the order of one degree [4].

For the asymmetry $A(\Xi^-_-)$ one needs instead the scattering phases of $\Lambda\pi$ at the $\Xi$ mass, which have not been measured. An early calculation indicated that the s-wave phase was large, $\delta_s = -20^o$ [5], making $A(\Xi^-_-)$ comparable in size to $A(\Lambda^0_-)$. Modern calculations suggest, however, that this phase is quite small and, therefore, $A(\Lambda^0_-)$ is likely to dominate the E871 measurement.

The calculation of $\Lambda\pi$ scattering is carried out using heavy baryon chiral perturbation theory. At leading order, Lu, Savage and Wise found that $\delta_p \sim -1.8^o$ and $\delta_s = 0$ [6]. At next to leading order $\delta_s$ no longer vanishes, but it is expected to be smaller than $\delta_p$. A recent calculation of $\Xi\pi$ scattering phases [7] (relevant for CP violation in $\Omega$ decay) has confirmed the result of Ref. [6]. From this calculation one can see that the uncertainty in the value of the input parameters may change the calculated value of $\delta_p$ by factors of two, and that $\delta_s$ remains zero at leading order. Furthermore, the calculation of $\Xi\pi$ scattering illustrates the conditions under which the strong phase could be large ($\sim 10^o - 20^o$): if the pion momentum is large (as it is in the $\Xi\pi$ state from $\Omega$ decay), or very near a resonance with the right quantum numbers. In $\Lambda\pi$ scattering from $\Xi$ decay, the pion momentum is very small, so the only way to have a large $\delta_s$ is if there is an $I = 1$, $J^P = 1/2^-$ resonance near the $\Xi$ mass. Datta and Pakvasa investigated this issue and found that the closest resonance with the correct quantum numbers, the $\Sigma(1750)$, could not contribute more than about half a degree to $\delta_s$ [8].

The ultimate resolution of this issue, nevertheless, lies in experiment. The phase can be measured both in $\Xi \to \Lambda\pi e\nu$ and in $\Xi \to \Lambda\pi$ decays. With our current knowledge, however, it would be very surprising to find a large phase.

## 3. Weak Phases

### 3.1. Standard Model

Within the standard model one writes the $|\Delta S| = 1$ effective weak Hamiltonian as a sum of four-quark operators multiplied by Wilson co-

efficients in the usual way,

$$H = \frac{G_F}{\sqrt{2}} V_{ud}^* V_{us} \sum_{i=1}^{12} c_i(\mu) Q_i(\mu) \qquad (2)$$

This is, of course, the same effective Hamiltonian responsible for Kaon non-leptonic decays and is very well known. In particular the Wilson coefficients, $c_i(\mu)$ have been calculated in detail by Buras and his collaborators [9]. The remaining problem is to calculate the matrix elements of the four-quark operators between hadronic states. This problem has not been resolved yet, and there is large theoretical uncertainty in these matrix elements. The usual way to proceed (which is the same as in kaon physics) is to take the real part of the matrix element from experiment (assuming CP conservation) and to use the calculated imaginary parts.

Unlike the case of $\epsilon'$, where both $\Delta I = 1/2, 3/2$ amplitudes are important, $A(\Lambda^0_-)$ is dominated by CP violation in $\Delta I = 1/2$ amplitudes. One expects that the asymmetry will be dominated by the penguin operator with small corrections from other operators. A detailed study using vacuum saturation to estimate the matrix elements has confirmed that $Q_6$ is mostly responsible for $A(\Lambda^0_-)$ [10].

Once we have determined that only $Q_6$ is important, the strategy is to calculate the matrix elements of the form $< B'|Q_6|B >$ using a model, and then use these results to treat the non-leptonic hyperon decay at leading order in chiral perturbation theory. Equivalently, the s-waves are obtained with a soft-pion theorem and the p-waves with baryon poles. At present, the baryon to baryon matrix elements are taken from the MIT bag model calculation of Ref. [11]. Combining this with $y_6 = -0.08$ [9], and using $A^2\lambda^4\eta \sim 10^{-3}$ one obtains,

$$A(\Lambda^0_-) = -0.018 A^2\lambda^4\eta \sim -2 \times 10^{-5}. \qquad (3)$$

It is difficult to quantify the theoretical error in this expression. There are the obvious uncertainties in the value of the CKM parameters used, a small uncertainty in the value of $y_6$, a small uncertainty due to the neglect of other operators, and an uncertainty of about 30% from the error in the strong phases that can easily be quantified. However, of greater concern is the issue of assigning an error to the hadronic matrix elements. Even if we assume that the baryon to baryon matrix elements calculated in the MIT bag model are accurate, we know from the study of CP conserving amplitudes that non-leading order terms in chiral perturbation theory can be as large as the leading order amplitudes. For example, the s-wave imaginary part calculated in vacuum saturation, is a higher order correction to the bag-model plus soft pion theorem amplitude outlined above, but it is larger [10]. To get an idea for the impact of this error we assign an overall error of a factor of two to the calculated matrix elements plus an overall 30% uncorrelated error between s and p-waves. This results in,

$$A(\Lambda^0_-) = (-3.0 \pm 2.6) \times 10^{-5}. \qquad (4)$$

### 3.2. Beyond the Standard Model

There have been several estimates of $A(\Lambda^0_-)$ in non-standard models of CP violation. For the most part these studies discuss specific models, concentrating on one or a few operators and normalizing the strength of CP violation by fitting $\epsilon$. Some of these results (which have not been updated to incorporate current constraints on model parameters) are:

$$A(\Lambda^0_-) = \begin{cases} -2 \times 10^{-5} & \text{SM [3]} \\ -2 \times 10^{-5} & \text{2 Higgs [3]} \\ 0 & \text{Superweak} \\ 6 \times 10^{-4} & \text{LR [12]} \end{cases} \qquad (5)$$

Perhaps a more interesting question is whether it is possible to have large CP violation in hyperon decays in view of what is known about $\epsilon$ and $\epsilon'$. This question has been addressed in a model independent way by considering all the CP violating operators that can be constructed at dimension 6 that are compatible with the symmetries of the standard model [13]. With this very general effective Lagrangian one can compute the contributions of each new CP violating phase to $\epsilon, \epsilon'$, and $A(\Lambda^0_-)$. Of course, there is the caveat that the hadronic matrix elements cannot be computed reliably. Nevertheless, one finds in general that parity even operators generate a weak phase $\phi_p$ and do not contribute to $\epsilon'$. Their strength can be bound from the long distance contributions to $\epsilon$ that they induce. Similarly, the parity-odd operators generate a weak phase $\phi_s$ and contribute to $\epsilon'$ (but not $\epsilon$).

The constraints from $\epsilon'$ turn out to be much more stringent than those from $\epsilon$, and, therefore, the only natural way (without invoking fine cancelations between different operators) to obtain a large $A(\Lambda^0_-)$ given what we know about $\epsilon'$ is with new CP-odd, P-even interactions. Within the model independent analysis, one can identify

a few new operators with the required properties, that can lead to [13],

$$A(\Lambda^0_-) \sim 5 \times 10^{-4} \quad \mathrm{P-even, CP-odd} \qquad (6)$$

This possibility has been revisited recently, motivated in part by the observation of $\epsilon'$. The average value $\epsilon'/\epsilon = (21.2 \pm 4.6) \times 10^{-4}$ [14] appears to be larger than the standard model central prediction with simplistic models for the hadronic matrix elements. This has motivated searches for new sources of CP violation that can give large contributions to $\epsilon'$, in particular, within supersymmetric theories. One such scenario generates a large $\epsilon'$ through an enhanced gluonic dipole operator. The effective Hamiltonian is of the form

$$\begin{aligned} H_{eff} &= (\delta^d_{12})_{LR} C_g \bar{d}\sigma_{\mu\nu} t^a (1+\gamma_5) s G^{a\mu\nu} \\ &+ (\delta^d_{12})_{RL} C_g \bar{d}\sigma_{\mu\nu} t^a (1-\gamma_5) s G^{a\mu\nu} \qquad (7) \end{aligned}$$

The quantity $C_g$ is a known loop factor, and the $(\delta^d_{12})_{LR,RL}$ originate in the supersymmetric theory [15]. Depending on the correlation between the value of $(\delta^d_{12})_{LR}$ and $(\delta^d_{12})_{RL}$ one gets different scenarios for $\epsilon'$ and $A(\Lambda^0_-)$ as shown in the figure [16]. For example, if only $(\delta^d_{12})_{LR}$ is non-zero, there can be a large $\epsilon'$ [17], but $A(\Lambda^0_-)$ is small as in the 2-Higgs model of [3]. However, in models in which $\mathrm{Im}(\delta^d_{12})_{LR} = \mathrm{Im}(\delta^d_{12})_{RL}$ the CP violating operator is parity-even. In this case there is no contribution to $\epsilon'$ and $A(\Lambda^0_-)$ can be as large as $10^{-3}$ [16]. It is interesting that this type of model is not an ad-hoc model to give a large $A(\Lambda^0_-)$, but is a type of model originally designed to naturally reproduce the relation $\lambda = \sqrt{m_d/m_s}$, as in Ref. [18], for example.

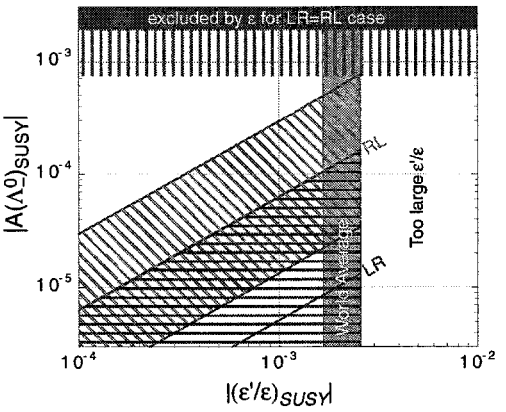


Figure 1. The allowed regions on $(|(\epsilon'/\epsilon)_{SUSY}|, |A(\Lambda^0_-)_{SUSY}|)$ parameter space for three cases: a) only $\mathrm{Im}(\delta^d_{12})_{LR}$ contribution, which is the conservative case (hatched horizontally), b) only $\mathrm{Im}(\delta^d_{12})_{RL}$ contribution (hatched diagonally), and c) $\mathrm{Im}(\delta^d_{12})_{LR} = \mathrm{Im}(\delta^d_{12})_{RL}$ case which does not contribute to $\epsilon'$ and can give a large $|A(\Lambda^0_-)|$ below the shaded region (or vertically hatched region for the central values of the matrix elements). The last case is motivated by the relation $\lambda = \sqrt{m_d/m_s}$. The vertical shaded band is the world average [14] of $\epsilon'/\epsilon$. The region to the right of the band is therefore not allowed.

## 4. Conclusion and Comments

The main points of this talk are that:

- $A(\Lambda^0_-)$ is likely to be significantly larger than $A(\Xi^-_-)$ dominating the measurement of E871.
- $A(\Lambda^0_-) = (-3 \pm 2.6) \times 10^{-5}$ is our current best guess for the standard model and the theoretical uncertainty is dominated by our inability to calculate hadronic matrix elements reliably. For this reason, the error assigned to this quantity is just an educated guess.
- $A(\Lambda^0_-)$ can be much larger if CP violation originates in P-even new physics. A specific realization of this scenario is possible in supersymmetric theories in which case $A(\Lambda^0_-)$ can be as large as $10^{-3}$.

I conclude that a non-zero measurement by E871 is not only possible but that it would provide valuable complementary information to what we already know from $\epsilon'$.

Finally I would like to mention two unrelated issues. A search for $\Delta S = 2$ hyperon non-leptonic decays is also a useful enterprise as it also provides information that is complementary to what we know from $K - \bar{K}$ mixing [19]. A CP violating rate asymmetry in $\Omega \to \Xi\pi$ decay can be as large as $2 \times 10^{-5}$ within the standard model (and up to ten times larger beyond), much larger than the corresponding rate asymmetries in octet-hyperon decay [7].

This work was supported by DOE under contract number DE-FG02-92ER40730. This talk describes work done in collaboration with John Donoghue, Xiao-Gang He, Barry Holstein, Hitoshi Murayama, Sandip Pakvasa, Herbert Steger

and Jusak Tandean.

## REFERENCES


1. S. Okubo, Phys. Rev. **109**, 984 (1958); A. Pais, Phys. Rev. Lett. **3**, 242 (1959).
2. K. Nelson, these proceedings.
3. J. Donoghue and S. Pakvasa, Phys. Rev. Lett. **55**, 162 (1985); J. Donoghue, X.-G. He and S. Pakvasa, Phys. Rev. **D34**, 833 (1986).
4. L. D. Roper, R. M. Wright and B. Feld, Phys. Rev. **138**, 190 (1965); A. Datta and S. Pakvasa, Phys. Rev. **D56**, 4322 (1997).
5. R. Nath and A. Kumar, Il Nuov. Cim. **XXXVI**, 1949 (1965).
6. M. Lu, M. Savage and M. Wise, Phys. Lett. **B337**, 133 (1994).
7. J. Tandean and G. Valencia, Phys. Lett. **B451**, 382 (1999).
8. A. Datta and S. Pakvasa, Phys. Lett. **B344**, 430 (1995); A. Kamal, Phys. Rev. **D58**, 077501 (1998).
9. G. Buchalla, A. Buras and M. Harlander, Nucl. Phys. **B337**, 313 (1990).
10. X.-G. He, H. Steger, and G. Valencia, Phys. Lett. **B272**, 411 (1991).
11. J. Donoghue *et. al.*, Phys. Rev. **D23**, 1213 (1981).
12. D. Chang, X.-G. He and S. Pakvasa, Phys. Rev. Lett. **74**, 3927 (1995).
13. X.-G. He and G. Valencia, Phys. Rev. **D52**, 5257 (1995).
14. This is the average of E731, NA31, KTeV and NA48 with the error bar inflated to obtain $\chi^2$/d.o.f. = 1 according to the Particle Data Group prescription.
15. F. Gabbiani, *et. al.*, Nucl. Phys. **B447**, 321 (1996).
16. X.-G. He, *et. al.*, hep-ph/9909562.
17. A. Masiero and H. Murayama, Phys. Rev. Lett. **83**, 907 (1999).
18. R. Barbieri, G. Dvali and L.J. Hall, Phys. Lett. **B377**, 76 (1996).
19. X.-G. He and G. Valencia, Phys. Lett. **B409**, 469 (1997) Erratum-ibid. **B418**, 443 (1998).

# A Review of Experimental Searches for $\mathcal{CP}$ Violation in Hyperon Decays

K.S. Nelson [a]

[a]Department of Physics,
205 McCormick Rd., Charlottesville, VA 22903

Although direct $\mathcal{CP}$ violation has only been measured conclusively in neutral kaon decays this effect is expected to occur elsewhere. The phenomenlogy of how $\mathcal{CP}$ violation can occur in hyperon decays is briefly reviewed. Previous experimental searches for $\mathcal{CP}$ violation in hyperon decays and the technique of a current search are presented.

## 1. Introduction

The large value of the direct $\mathcal{CP}$ violating parameter $\epsilon'/\epsilon$ has prompted a recent evaluation[1] of possible contributions in kaon decays beyond the standard model. Measurements of $\mathcal{CP}$-odd effects in other systems may help distinguish among the various scenarios.

Suggestions of searches for $\mathcal{CP}$ or $\mathcal{T}$ violations in hyperon decays developed shortly after the violation of parity in weak decays was established. Okubo [2] pointed out that $\mathcal{CP}$ violation would lead to a difference between the partial rates of $\Sigma^+$ and $\overline{\Sigma}^-$ decays, followed by Pais [3] who noted that any difference in the angular distributions of $\Lambda^\circ$ and $\overline{\Lambda}^\circ$ would break $\mathcal{CP}$ symmetry. Due to the low energy available in the 1960's and early 70's it was difficult to produce sufficient quantities of antihyperons to test these ideas. Nevertheless in the course of measuring hyperon decay parameters attempts to test $\mathcal{T}$ invariance were made by comparing[12] $\beta$ in $\Lambda$ decays to the $p\pi$ phase shifts and through comparison[13] of the ratio $\beta/\alpha$ for $\Xi^-$ and $\Xi^\circ$ decays. Advances in accelerator and detector technology in the early 80's finally allowed Pais' suggestion to be realized. The accuracies achieved to date have only been at the level of a percent and are not sufficient to confront theoretical predictions.

## 2. Phenomenlogy of Non-Leptonic Hyperon decays

The decays considered here are of a spin-1/2 hyperon to a spin-1/2 baryon and a pion in which strangeness changes by one. Since parity is not conserved in these weak decays the final state particles can be in either an $S$ or $P$ orbital state. Thus the decay can be described by three real quantities which are conventionally chosen to be; the partial decay rate

$$\Gamma = G_F^2 m_\pi^4 \frac{p_d(E_d + m_d)}{4\pi\, m_p}(|S|^2 + |P|^2) \qquad (1)$$

where the susbscripts $d$ and $p$ refer to the daughter baryon and parent hyperon respectively, and two independent decay parameters

$$\alpha = \frac{2\mathrm{Re}(S^*P)}{|S|^2 + |P|^2} \quad \beta = \frac{2\mathrm{Im}(S^*P)}{|S|^2 + |P|^2}\ . \qquad (2)$$

These decay parameters can be related to experimental measurements.

In the rest frame of a polarized hyperon the angular distribution of the daughter baryon, summed over its possible spins, is given by

$$\frac{dN}{d\Omega} = \frac{1}{4\pi}(1 + \alpha_p \vec{\mathbf{P}}_p \cdot \hat{\mathbf{q}}) \qquad (3)$$

where $\vec{\mathbf{P}}_p$ is the polarization of the parent hyperon and $\hat{\mathbf{q}}$ is the momentum unit vector of the daughter baryon. Moreoever the decay parameters govern the polarization imparted to the daughter baryon[4]

$$\begin{aligned}\vec{\mathbf{P}}_d \;=\; & \frac{1}{(1 + \alpha_p \vec{\mathbf{P}}_p \cdot \hat{\mathbf{q}})}[(\alpha_p + \vec{\mathbf{P}}_p \cdot \hat{\mathbf{q}})\hat{\mathbf{q}} + \\ & \beta_p(\vec{\mathbf{P}}_p \times \hat{\mathbf{q}}) + \gamma_p(\hat{\mathbf{q}} \times (\vec{\mathbf{P}}_p \times \hat{\mathbf{q}}))]\end{aligned} \qquad (4)$$

where the additional decay parameter $\gamma_p$

$$\gamma_p = \frac{|S|^2 - |P|^2}{|S|^2 + |P|^2}$$

is not independent but is contrained by $\alpha_p^2 + \beta_p^2 + \gamma_p^2 = 1$.

The decay of an antihyperon can be related to that of the hyperon by a $\mathcal{CP}$ transformation. This is illustrated for the case of $\Lambda$ decay in fig. 1. The polar angle $\theta_d$ of the daughter baryon relative to the parent polarization direction is mapped to

$\pi - \theta_d$. In the limit of $\mathcal{CP}$ invariance these two configurations have equal rates. In general if $\mathcal{CP}$ is conserved

$$\overline{\alpha}_p = -\alpha_p \quad \overline{\beta}_p = -\beta_p \quad \overline{\Gamma} = \Gamma \tag{5}$$

where overline quantities refer to the antihyperon decay.

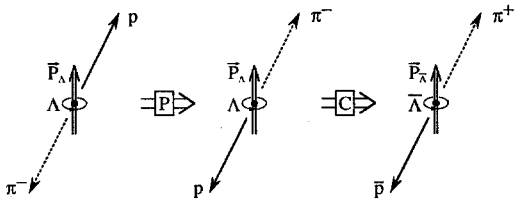


Figure 1. $\mathcal{P}$ and $\mathcal{C}$ operations on $\Lambda \to p\pi$.

Thus one arrives at Pais' original suggestion to search for $\mathcal{CP}$ violation by comparing the decay parameters of the hyperon and antihyperon. Including also the proposal of Okubo, several observables which are sensitive to $\mathcal{CP}$ odd effects are defined by

$$A = \frac{\alpha + \overline{\alpha}}{\alpha - \overline{\alpha}} \quad B = \frac{\beta + \overline{\beta}}{\beta - \overline{\beta}} \quad \Delta = \frac{\Gamma - \overline{\Gamma}}{\Gamma + \overline{\Gamma}} \tag{6}$$

Donoghue et al.[5] have given a model independent form for these and other $\mathcal{CP}$-odd observables for a variety of hyperon decays. Generally, the problem involves three small quantities, the strong scattering phases $\delta_{2I}^{\ell}$ of the final state particles having orbital angular momentum $\ell$ and isospin $I$, the $\mathcal{CP}$ violating phases $\phi_{2I,2\Delta I}^{\ell}$ and the ratio of the magnitudes of the $\Delta I = 3/2$ and $\Delta I = 1/2$ partial wave amplitudes. Their procedure yields the following approximate expressions for $\Lambda \to p\pi$ asymmtetries;

$$\Delta_\Lambda \approx \sqrt{2}\frac{S_3}{S_1}\sin(\delta_3^S - \delta_1^S)\sin(\phi_3^S - \phi_1^S) \tag{7}$$

$$A_\Lambda \approx \tan(\delta_1^P - \delta_1^S)\sin(\phi_1^S - \phi_1^P) \tag{8}$$

$$B_\Lambda \approx \cot(\delta_1^P - \delta_1^S)\sin(\phi_1^P - \phi_1^S) \tag{9}$$

and for charged $\Xi \to \Lambda\pi$ asymmetries;

$$\Delta_\Xi \equiv 0 \tag{10}$$

$$A_\Xi \approx \tan(\delta_2^P - \delta_2^S)\sin(\phi_1^S - \phi_1^P) \tag{11}$$

$$B_\Xi \approx \cot(\delta_2^P - \delta_2^S)\sin(\phi_1^P - \phi_1^S) \tag{12}$$

Note that to observe $\mathcal{CP}$ violation in these decays requires both a $\mathcal{CP}$ violating weak interaction phase as well as phases due to final state interactions. Consequently the partial rate asymmetry for $\Xi$ decays vanishes since there is only one final isospin state.

In the case of $\Lambda \to p\pi$ the pion–nucleon phase shifts have been measured[6], while in the charged $\Xi \to \Lambda\pi$ one must rely on theoretical calculations. Estimates of the $\Lambda\pi$ phase shifts have varied by by about an order of magnitude although recent calculations[7] have argued that both are very small if not zero. The weak interaction phases must similarly be evaluated in the context of a specific model[8] with further uncertainties arising in the evaluation of the hadronic matrix elements. However, within a given model there is a hierarchy in the magnitude of the asymmetries

$$B \gg A \gg \Delta \tag{13}$$

For technical reasons explained in the following section, the most practical observable through which to search for $\mathcal{CP}$ violation in hyperon decays is $A$. Some predictions for $A_\Lambda$ and $A_\Xi$ are given in table 1.

Table 1
Some predictions for $A_\Xi$ and $A_\Lambda$

| Model | $A_\Xi[10^{-4}]$ | $A_\Lambda[10^{-4}]$ |
|---|---|---|
| CKM[9] | $\approx -0.04$ | $\approx 0.4 - 0.5$ |
| Weinberg[5] | $\approx -3.2$ | $\approx -0.25$ |
| LR(isoconjugate)[10] | $\approx 0.25$ | $\approx -0.11$ |
| LR(with mixing)[11] | $\leq 1$ | $\leq 6$ |

## 3. Experimental Searches

The measurement of the partial rate asymmetry $\Delta$ requires precisely known normalizations of the hyperon and antihyperon samples and in general is too small to achieve a meaningful measurement in the forseeable future. The asymmetries $A$ and $B$ are expected to be larger than $\Delta$ although their measurement requires precisely known polarizations of the inital decaying hyperon and antihyperon samples. In addition a measurement of $\beta$ needed for $B$ requires comparable knowlege of the daughter polarization, *e.g.* through rescattering[12] or the self-analyzing decay of the daugh-

ter[13]. For these reasons all measurements to date have concentrated on $A$.

### 3.1. Past Searches

There have been three published attempts to measure $A$ in $\Lambda$ decay and none in $\Xi$ decay. Furthermore all were limited by statistical errors, not systematics. They are reviewed briefly below.

**R608 at the CERN ISR [14]**

This experiment studied inclusive production in the beam fragmentation region of $\Lambda^\circ$ in $pp$ collisions and $\overline{\Lambda}$ in $\bar{p}p$ collisions. The excellent agreement of the charged particle momentum distributions and $\Lambda^\circ$ and $\overline{\Lambda}^\circ$ between the two data sets led them to assume equality of the $\Lambda^\circ$ and $\overline{\Lambda}^\circ$ polarizations. The $p(\bar{p})$ distribution in the $\Lambda(\overline{\Lambda})$ rest frame was fit to equation 3 where the assumed polarization is in the direction normal to the production plane $\hat{\mathbf{n}} = \hat{\mathbf{p}} \times \hat{\mathbf{\Lambda}}$. Based on $17,028$ $\Lambda^\circ \to p\pi^-$ and $9,553$ $\overline{\Lambda}^\circ \to \bar{p}\pi^+$ events and assuming $P_\Lambda = P_{\overline{\Lambda}}$ the ratio $\alpha_\Lambda/\alpha_{\overline{\Lambda}}$ was found to be $-1.04 \pm 0.29$ which is equivalent to $A_\Lambda = -0.02 \pm 0.14$. Although this limit is dominated by statistical errors it is unlikely that the critical assumption of equality of polarizations could ever be verified to hold at the level needed to confront theory.

**DM2 at Orsay [15]**

Correlated pairs were obtained in the reaction $e^+e^- \to J/\psi \to \Lambda^\circ\overline{\Lambda}^\circ$ with the subsequent decay $\Lambda^\circ\overline{\Lambda}^\circ \to p\bar{p}\pi^-\pi^+$ at the DCI collider. The $\mathcal{CP}$ sensitive term in the triple differential cross section is the scalar product of the $p$ and $\bar{p}$ directions $\hat{\mathbf{a}} \cdot \hat{\mathbf{b}}$ in the $\Lambda^\circ$ and $\overline{\Lambda}^\circ$ rest frames. The product $\alpha_\Lambda\alpha_{\overline{\Lambda}}$ modulates this term. The theoretical distribution of $\hat{\mathbf{a}} \cdot \hat{\mathbf{b}}$, having $\alpha_\Lambda$ fixed to its canonical value and allowing $\alpha_{\overline{\Lambda}}$ to vary, was fit to the observed distribution. With a sample of $8.6 \times 10^6$ $J/\psi$ decaying to 1847 $\Lambda\overline{\Lambda} \to p\bar{p}\pi^-\pi^+$ events they obtained $A_\Lambda = 0.01 \pm 0.10$. Again this limit is dominated by statistical errors. Furthermore the technique, being sensitive only to the product $\alpha_\Lambda\alpha_{\overline{\Lambda}}$ requires external information. It has been argued[16] that a Tau Charm Factory having polarized beams could overcome this defect although it would likely be statistically inferior to hadronically produced hyperon samples.

**PS185 at LEAR [17]**

The best published limit on $A_\Lambda$ to date is that from the PS185 experiment at LEAR. In this experiment exclusive pairs of $\Lambda\overline{\Lambda}$ were produced in an energy range bounded above by the $\Lambda\Sigma^\circ$ threshold. Again $\mathcal{C}$ conservation in the strong interaction production process guarantees $P_\Lambda = P_{\overline{\Lambda}}$. The products $\alpha_\Lambda P_\Lambda$ and $\alpha_{\overline{\Lambda}}P_{\overline{\Lambda}}$ were extracted by a method that avoided detailed MC simulation but relied on the detector efficiency being symmetric about $\theta = 90^\circ$ in the hyperon rest frame. With a sample of $95,832$ events $A_\Lambda = 0.013 \pm 0.022$ was obtained , a result that is still more than an order of magnitude away from confronting theories. Verification of the above symmetry condition, although possible at the level of this result, would pose a serious challenge for future efforts to improve the limit significantly . Proposals[18] to extrapolate the $p\bar{p} \to \Lambda\overline{\Lambda}$ technique have so far been unsuccessful.

### 3.2. Current Search: HyperCP (E871) at Fermilab

The HyperCP experiment obtains samples of $\Lambda^\circ$ and $\overline{\Lambda}^\circ$ hyperons having precisely known polarizations from the decay of *unpolarized*[1] $\Xi^-$ and $\overline{\Xi}^+$ hyperons. According to equation 5 the $\Lambda^\circ$ in the decay of an unpolarized $\Xi^-$ is in a helicity state having polarization absolutely determined by the $\alpha$ parameter of the $\Xi^-$ decay.

$$\vec{\mathbf{P}}_\Lambda = \alpha_\Xi \hat{\mathbf{q}} \tag{14}$$

In the subsequent $\Lambda \to p\pi^-$ decay the distribution of the proton direction in the $\Lambda$ restframe oriented with the polar axis along the $\Lambda$ flight direction (the so-called helicity frame) is

$$\frac{dN_p}{d\cos\theta_{p\Lambda}} = 1 + \alpha_\Xi\alpha_\Lambda \cos\theta_{p\Lambda} \tag{15}$$

A similar expression is obtained for the $\bar{p}$ distribution in $\overline{\Xi}^+$ decay.

In the limit of $\mathcal{CP}$ conservation $\alpha_{\overline{\Xi}} = -\alpha_\Xi$ and $\alpha_{\overline{\Lambda}} = -\alpha_\Lambda$ and the slopes of the $p$ and $\bar{p}$ distributions are identical. The slope asymmetry, $A_{\Lambda\Xi}$, sought by this experiment is sensitive to $\mathcal{CP}$ violation in both[2] the $\Lambda$ and charged $\Xi$ decay;

$$A_{\Lambda\Xi} \equiv \frac{\alpha_\Lambda\alpha_\Xi - \alpha_{\overline{\Lambda}}\alpha_{\overline{\Xi}}}{\alpha_\Lambda\alpha_\Xi + \alpha_{\overline{\Lambda}}\alpha_{\overline{\Xi}}} \approx A_\Xi + A_\Lambda. \tag{16}$$

[1] Due to $\mathcal{P}$ conservation in the strong interaction, the hyperons emerging along the collision axis of unpolarized beam and target particles are themselves unpolarized.

[2] Recent theoretical calculations lean toward vanishing $\Lambda\pi$ phase shifts which would mean $A_{\Lambda\Xi}$ is dominated by $A_\Lambda$

A particularly advantageous property of the helicity frame is that its orientation varies from event to event. Thus the effects of biases that are fixed in space, *e.g.* detector inefficiencies or small residual $\Xi$ polarization due to imperfect targetting, are diluted.

The goal of the HyperCP experiment is a $10^{-4}$ sensitivity on $A_{\Lambda\Xi}$ which requires a sample on the order of $10^9$ reconstructed $\Xi^-$ and $\overline{\Xi}^+$ decays. Therefore, the primary considerations in the the design of the HyperCP spectrometer are that it be capable of operating at high rate and that it be simple in order to facilitate understanding potential biases at the level of the measurement. A plan view of the apparatus is shown in figure 2

An 800 Gev/$c$ proton beam strikes targets of Cu, either 2cm or 6cm in length, and the forward produced particles are intercepted by a curved magnetized collimator whose entrance is coaxial with the incoming beam. The two target lengths are chosen to equalize the rates ($\approx$ 15 MHz) through the spectrometer in $\Xi^-$ and $\overline{\Xi}^+$ running. Secondary charged particles within a few $\mu$sr of 0° and having momenta in the range of 120 GeV/$c$ to 240 GeV/$c$ are accepted by the collimator and emerge into a 13m long vacuum decay pipe where most $\Xi$ and $\Lambda$ hyperons will decay. Following the decay pipe is a magnetic spectrometer consisting of MWPC's optimized for high rate operation, an analyzing magnet, hodoscopes for triggering and a hadronic calorimeter.

A simple and selective trigger is formed by a requiring a coincidence of one or more hits in each hodoscope on either side of the beam line. The calorimeter is used to suppress muon and secondary interaction backgrounds to this main trigger. The polarities of both the magnetic collimator and the analysis magnets are reversed between $\Xi^-$ and $\overline{\Xi}^+$ running achieving a $\mathcal{CP}$ invariant trigger geometry. The final baryon ($p$ or $\bar{p}$) is always deflected into the calorimeter while the two pions are deflected to the hodoscope on the other side. A cycle of + and − runs is completed at least once per day.

The data aquisition system[19], based on parallel data paths and multiple VME processors, is designed to accomodate a maximum trigger rate of 100 kHz of $\approx$ 0.5 kB events.

The experiment took data in the 1996-97 fixed target run in which the projected yield is $9 \times 10^8$ reconstructed $\Xi^-$ and $2.5 \times 10^8$ $\overline{\Xi}^+$. The anticipated statistical uncertainty in $A_{\Lambda\Xi}$ from this data is about $2 \times 10^{-4}$. An indication of the stability of the two data sets is indicated by the similarity of the mass peaks in Fig. 3, obtained from a few percent of the data.

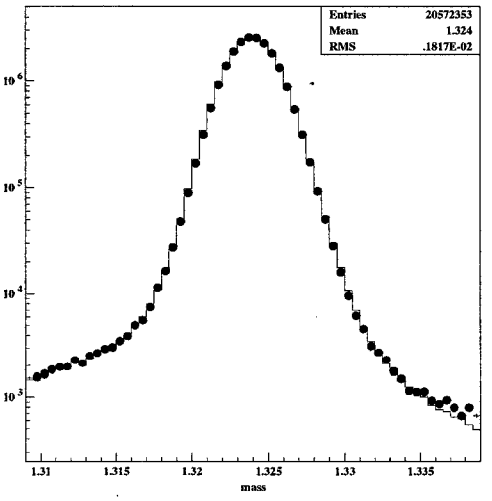


Figure 3. The $\Lambda\pi$ invariant mass for $\Xi^-$ (solid line) and $\overline{\Xi}^+$ (dots) events.

A demonstration of the reduction in biases that the use of the helicity frame affords can be seen by analyzing two sets of polarized $\Xi^-$ data in which the polarizations are in opposite directions. The decay products inhabit different regions of the spectrometer as illustrated by the $\cos\theta$ distributions along a fixed axis shown in fig. 4. Nevertheless, when the same data is analyzed in the $\Lambda$ helicity frame the two data sets agree nearly perfectly, Fig. 5.

A first pass of the 1997 data set through a computing farm at Fermilab, in which the particle trajectories are reconstructed, is now complete. The experiment is running again in the 1999 fixed target run with substantial improvements to the data aquisition system and various minor improvements to the spectrometer. An increase of at least three-fold in statistics is anticipated.

## 4. Conclusions

Although success in the search for $\mathcal{CP}$-odd effects in hyperon decays has lagged behind that of the neutral kaon system its observation may

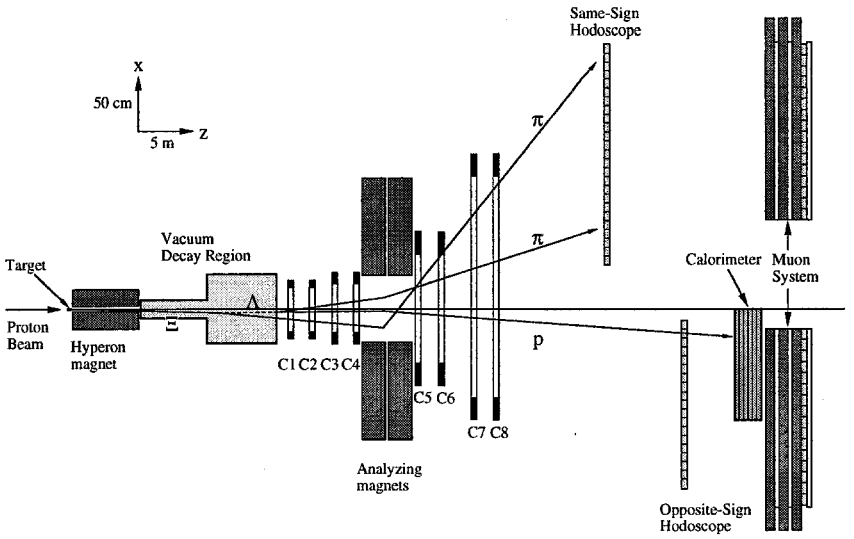


Figure 2. Plan view of the HyperCP spectrometer.

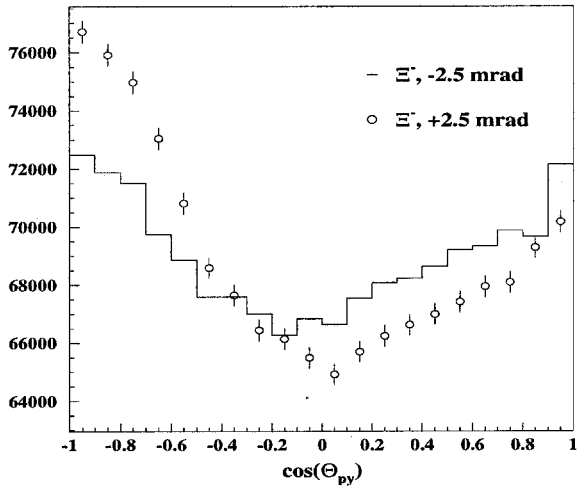


Figure 4. The $p \cos\theta$ distributions along the $y$ axis in the $\Lambda$ rest frame.

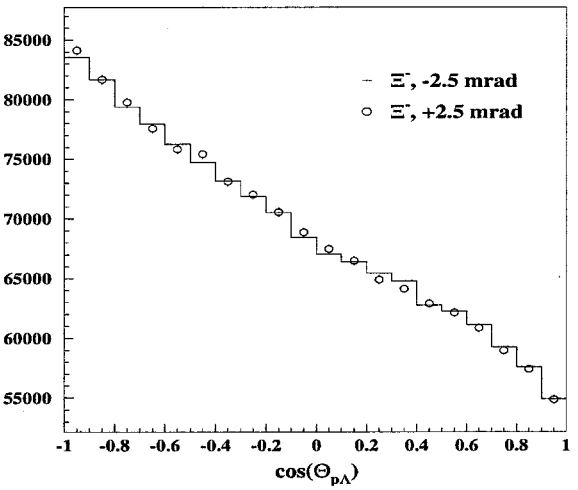


Figure 5. The $p \cos\theta$ distributions along the polar axis in the $\Lambda$ helicity frame.

influence the viability of proposed sources of $\mathcal{CP}$ violation beyond the standard model. The experiments which have been completed up to now fall short of standard model expectations by at least two orders of magnitude. The HyperCP experiment expects to improve the current experimental limit by about two orders of magnitude. The results of HyperCP will likely play a role in determining the direction of future efforts to un-

derstand the $\mathcal{CP}$ violating phenomenon in the hyperon sector.

## REFERENCES


1. X.G. He, *et al.*, hep-ph9909562
2. S. Okubo, Phys. Rev. **109**, 984 (1958).
3. A. Pais, Phys. Rev. Lett. **3**, 242 (1959).
4. see, for example, H. Muirhead, *The Physics of Elementary Particles*, Chap 12, Pergamon Press (1965)
5. J. Donoghue, X.G. He and S. Pakvasa, Phys. Rev. **D34**, 833 (1986).
6. L.D. Roper, R.M. Wright and B.T. Feld, Phys. Rev. **138**, B190 (1965).
7. M. Lu, M.B. Wise and M.J. Savage, Phys. Lett. B **337**, 133 (1994); A. Datta and S. Pakvasa, Phys. Lett. B **344**, 133 (1995).
8. G. Valencia, these proceedings.
9. S. Pakvasa, proceedings of KAON99, Univ. of Chicago Press.
10. S. Pakvasa, hep-ph/9808472, 1998, presented at Workshop on CP Violation, Adelaide, July 3-8, 1998.
11. D. Chang, X.-G. He, and S. Pakvasa, Phys. Rev. Lett. **74** (1995) 3927.
12. J.W. Cronin and O.E. Overseth, Phys. Rev. **129**, 1795 (1963).
13. C. Baltay *et al.*, Phys. Rev. **D9**, 49 (1974).
14. P. Chauvat *et al.*, Phys. Lett. 163B, 273 (1985).
15. M.H. Tixier et al., Phys. Lett. B212, 523 (1988).
16. E.M. Gonzalez and J.I. Illana, CERN-PPE/94-33 (1994).
17. P.D. Barnes *et al.*, Phys. Rev. C **54** 1877 (1996).
18. D.M. Kaplan, these proceedings and references therein.
19. D.M. Kaplan *et al.*, Proc. of Int. Conf. on Electronics for Particle Physics, LeCroy Corp., Chestnut Ridge NY, May 28-29 1997.

# Chapter 7

# Hyperon static properties


- H. J. Lipkin
- P. S. Cooper

# Theoretical Analysis of Static Hyperon Data

Harry J. Lipkin [a]

[a] Department of Particle Physics
Weizmann Institute of Science, Rehovot 76100, Israel
School of Physics and Astronomy

and

Raymond and Beverly Sackler Faculty of Exact Sciences
Tel Aviv University, Tel Aviv, Israel

and

Department of Physics, U46
University of Connecticut, 2152 Hillside Rd., Storrs, CT 06269-3046
USA

We consider all hyperon data relevant to spin and flavor structure of hyperons. In addition to masses and magnetic moments considered as static properties in Hyperon99 we include also relevant data from hyperon decays and spin structure determined from deep inelastic scattering. Any theoretical model for the hyperons with parameters to be determined from experiment should use input from all these data. Of particular interest are new data from $\Xi^o$ decay and the polarixation of $\Lambda's$ produced in $Z^o$ decays and deep inelastic scattering.

## 1. Introduction - What is Meant by Static Properties

In the context of this meeting, hyperon masses and magnetic moments are considered static properties to be discussed in this talk, while hyperon decays and spin structure determined from deep inelastic scattering are not considered static properties. But all of them depend upon the spin and flavor structure of the hyperons. Any theoretical model for the hyperons with parameters to be determined from experiment should use input from all these data.

The masses and magnetic moments are very well measured, and they are well described by the simple constituent quark model. Going beyond this model is difficult without input from other data, some of which are not so well measured. Thus progress in understanding hyperon structure will come from combining input from all relevant experimental data and improvements in the precision of data other than masses and magnetic moments.

### 1.1. New Data on $\Xi^o \to \Sigma^+$ decays

The new data for the semileptonic decay $\Xi^o \to \Sigma^+$ agrees with the SU(3) prediction

$$g_A(\Xi^o \to \Sigma^+) = g_A(n \to p) \tag{1}$$

where we use the shortened form $g_A$ to denote $G_A/G_V$.

The essential physics of this prediction is that the spin physics in the nucleon system which is probed in the neutron decay is unchanged when the $d$ quarks in the nucleon are changed to strange quarks. This very striking result is completely independent of any fitting of weak decays using the conventional D/F parametrization. We can immediately carry this physics further by inserting the $d \leftrightarrow s$ transformation into the well-known prediction for the ratio of the proton $(uud)$ to neutron $(udd)$ magnetic moments and obtain a prediction for the ratio of the $\Sigma^+(uus)$ to $\Xi^o(uss)$ magnetic moments. It is conventient to write the prediction in the form:

$$\frac{\mu_p}{\mu_n} = -1.46 = \frac{4\xi_{ud}+1}{4+\xi_{ud}} = -1.5 \tag{2}$$

where $\xi_{ud}$ is the ratio of the quark magnetic moments

$$\xi_{ud} = \mu_u/\mu_d = -2 \tag{3}$$

This is easily generalized to give

$$\frac{\mu^+_\Sigma}{\mu^o_\Xi} = -1.96 = \frac{4\xi_{us}+1}{4+\xi_{us}} = -1.89 \tag{4}$$

where $\xi_{us}$ is the ratio of the quark magnetic moments,

$$\xi_{us} = \mu_u/\mu_s = (\mu_u/\mu_d)\cdot(\mu_d/\mu_s) = -3.11(5)$$

and we have determined $(\mu_d/\mu_s)$ by the ratio between the experimental value of $\mu_\Lambda$ and the

SU(3) prediction $\mu_\Lambda = \mu_n/2$ which assumes that $\mu_d = \mu_s$

$$\mu_d/\mu_s = \mu_n/2\mu_\Lambda = -3.11 \quad (6)$$

The fact that the prediction for this ratio (4) agrees with experiment much better than either moment agrees with the SU(6) quark model[1] is very interesting.

### 1.2. New $\Lambda$ polarization measurements from Z decays and DIS

When a $\Lambda$ is produced either from $Z^o$ decay or in deep inelastic scattering, the accepted mechanism is the production of a polarized quark produced in a pointlike vertex from a $W$ boson or a photon, and the eventual fragmentation of this quark into the $\Lambda$ directly or into a $\Sigma^o$ or $\Sigma^*$ which eventually decays into a $\Lambda$. Now that experimental data on $\Lambda$ polarization are becoming available in both processes[2–4] a central theoretical question is which model to use for the spin structure of the $\Lambda$. In the simple quark model, the strange quark carries the spin of the $\Lambda$ and the $u$ and $d$ are coupled to spin zero. This model has been used in the first analysis of experimental data from $Z$ decay[3] and found to be consistent with the data. But the deep inelastic experiments have shown that the spin structure of the proton is different from that given by the simple quark model. An alternative approach is presented in [5] where SU(3) symmetry is assumed and the spin structure of SU(3) octet hyperons is deduced from that of the proton. But SU(3) symmetry is known to be broken. Several approaches to this symmetry breaking have been proposed by theorists[6,2], and other mechanisms are discussed in [8–11]. The question of how to do it right remains open.

## 2. Masses and Magnetic Moments

### 2.1. The Sakharov-Zeldovich 1966 Quark model (SZ66)

Andrei Sakharov was a pioneer in hadron physics who took quarks seriously already in 1966. He asked "Why are the $\Lambda$ and $\Sigma$ masses different? They are made of the same quarks!"[12]. His answer that the difference arose from a flavor-dependent hyperfine interaction led to relations between meson and baryon masses in surprising agreement with experiment[13]. Sakharov and Zeldovich *anticipated* QCD by assuming a quark model for hadrons with a flavor dependent linear mass term and hyperfine interaction,

$$M = \sum_i m_i + \sum_{i>j} \frac{\vec{\sigma}_i \cdot \vec{\sigma}_j}{m_i \cdot m_j} \cdot v_{ij}^{hyp} \quad (7)$$

where $m_i$ is the effective mass of quark $i$, $\vec{\sigma}_i$ is a quark spin operator and $v_{ij}^{hyp}$ is a hyperfine interaction with different strengths but the same flavor dependence for $qq$ and $\bar{q}q$ interactions.

Hadron magnetic moments are are described simply by adding the contributions of the moments of these constituent quarks with Dirac magnetic moments having a scale determined by the same effective masses. The model describes low-lying excitations of a complex system with remarkable success.

Sakarov and Zeldovich already in 1966 obtained two relations between meson and baryon masses in remarkable agreement with experiment. Both the mass difference $m_s - m_u$ between strange and nonstrange quarks and their mass ratio $m_s/m_u$ have the same values when calculated from baryon masses and meson masses[13,14]

The mass difference between $s$ and $u$ quarks calculated in two ways from the linear term in meson and baryon masses showed that it costs exactly the same energy to replace a nonstrange quark by a strange quark in mesons and baryons, when the contribution from the hyperfine interaction is removed.

$$\langle m_s - m_u \rangle_{Bar} = M_\Lambda - M_N = 177\,\mathrm{MeV} \quad (8)$$

$$\langle m_s - m_u \rangle_{mes} = \frac{3(M_{K^*} - M_\rho) + M_K - M_\pi}{4} = 180\,\mathrm{MeV} \quad (9)$$

$$\left(\frac{m_s}{m_u}\right)_{Bar} = \frac{M_\Delta - M_N}{M_{\Sigma^*} - M_\Sigma} = 1.53 \quad (10)$$

$$\left(\frac{m_s}{m_u}\right)_{Mes} = \frac{M_\rho - M_\pi}{M_{K^*} - M_K} = 1.61 \quad (11)$$

Further extension of this approach led to two more relations for $m_s - m_u$ when calculated from baryon masses and meson masses[15,16]. and to three magnetic moment predictions with no free parameters[17,18]

$$\langle m_s - m_u \rangle_{mes} = \frac{3M_\rho + M_\pi}{8} \cdot \left(\frac{M_\rho - M_\pi}{M_{K^*} - M_K} - 1\right) = 178 \quad (12)$$

$$\langle m_s - m_u \rangle_{Bar} = \frac{M_N + M_\Delta}{6} \cdot \left( \frac{M_\Delta - M_N}{M_{\Sigma^*} - M_\Sigma} - 1 \right) = 190. \quad (13)$$

$$\mu_\Lambda = -\frac{\mu_p}{3} \cdot \frac{m_u}{m_s} = -\frac{\mu_p}{3} \frac{M_{\Sigma^*} - M_\Sigma}{M_\Delta - M_N} = -0.61 \quad (14)$$

$$\frac{\mu_p}{\mu_n} = -1.46 = -\frac{3}{2} \quad (15)$$

$$\mu_p + \mu_n = 0.88 = \frac{M_p}{3m_u} = \frac{2M_p}{M_N + M_\Delta} = 0.865 \quad (16)$$

where masses are given in MeV and magnetic moments in nuclear magnetons.

### 2.2. Problems in going beyond Sakharov-Zeldovich

These successes and the success of the new relation (4) make it difficult to improve on the results of the simple constituent quark model by introducing new physics effects like higher order corrections. Any new effect also introduces new parameters. In order to keep any analysis significant, it is necessary to include large amounts of data in order to keep the total amount of data much larger than the number of parameters.

In contrast to the successes of the simple quark model in magnetic moments and hyperon decay, there are also failures. Pinpointing these failures and comparing them with the successes may offer clues to how to improve the simple picture.

Combining the experimental data for hyperon magnetic moments and semileptonic decays have provided some contradictions for models of hyperon structure. The essential difficulty is expressed in the experimental value of the quantity

$$\frac{(g_a)_{\Lambda \to p}}{(g_a)_{\Sigma^- \to n}} \cdot \frac{\mu_{\Sigma^+} + 2\mu_{\Sigma^-}}{\mu_\Lambda} = 0.12 \pm 0.04 \quad (17)$$

The theoretical prediction for this quantity from the standard SU(6) quark model is unity, and it is very difficult to see how this enormous discrepancy by a factor of $8 \pm 2$ can be fixed in any simple way.

The expression (17) is chosen to compare two ways of determining the ratio of the contributions of strange quarks to the spins of the $\Sigma$ and $\Lambda$. In the commonly used notation where $\Delta u(p)$, $\Delta d(p)$ and $\Delta s(p)$ denotes the contributions to the proton spin of the $u$, $d$ and $s$ - flavored current quarks and antiquarks respectively to the spin of the proton the SU(6) model gives

$$\Delta s(\Lambda)_{SU(6)} = 1 \quad (18)$$

$$\Delta s(\Sigma)_{SU(6)} = -1/3 \quad (19)$$

and

$$\frac{\Delta s(\Sigma)_{SU(6)}}{\Delta s(\Lambda)_{SU(6)}} = \frac{(g_a)_{\Sigma^- \to n}}{(g_a)_{\Lambda \to p}} = \frac{\mu_{\Sigma^+} + 2\mu_{\Sigma^-}}{3\mu_\Lambda} = -\frac{1}{3} \quad (20)$$

whereas experimentally

$$\frac{(g_a)_{\Sigma^- \to n}}{(g_a)_{\Lambda \to p}} = -0.473 \pm 0.026 \quad (21)$$

$$\frac{\mu_{\Sigma^+} + 2\mu_{\Sigma^-}}{3\mu_\Lambda} = -0.06 \pm 0.02 \quad (22)$$

The semileptonic decays give a value which which is too large for the $\Sigma/\Lambda$ ratio; the magnetic moments give a value which is too low. Thus the most obvious corrections to the naive SU(6) quark model do not help. If they fix one ratio, they make the other worse. Furthermore, the excellent agreement obtained by De Rujula, Georgi and Glashow[17] for $\mu_\Lambda$ assuming that the strange quark carries the full spin of the $\Lambda$ suggests that eq. (18) is valid, while the excellent agreement of the experimental value $-0.340 \pm 0.017$ for $(g_a)_{\Sigma^- \to n}$ with the prediction -(1/3) suggests that eq.(19) is valid.

The disagreement sharpens the paradox of other disagreements previously discussed because it involves only the properties of the $\Lambda$ and $\Sigma$ and does not assume flavor SU(3) symmetry or any relation between states containing different numbers of valence strange quarks. There is also the paradox that the magnetic moment of the $\Lambda$ fits the value predicted by the naive SU(6) quark model, while the magnetic moments of the $\Sigma$ are in trouble. In the semileptonic decays it is the opposite. It is the $\Sigma$ which fits naive SU(6) and both the $\Lambda$ and the nucleon are in trouble. If one assumes the obvious fix for the semileptonic decays by assuming a difference between constituent quarks and current quarks, one can fit the nucleon and $\Lambda$ decays but then the $\Sigma$ is in trouble.

The magnetic moments thus seem to indicate that the contribution of the strange quark to the spin of the $\Sigma$ is smaller than any reasonable model can explain, when the scale is determined by the $\Lambda$ moment. This result is far more general than the simple naive SU(6) quark model. But the new relation (4) between the $\Sigma^+$ and$\Xi^o$ moments seems to indicate that the strange quark contributions to these moments are the same.

## 3. Semileptonic Decays

We now consider the semileptonic weak decays and begin by comparing the available data[19] for four semileptonic decays with several theoretical predictions. The $\Xi^o \to \Sigma^+$ decay considered above and equal to the neutron decay is omitted here.

The nucleon and $\Lambda$ data are seen to be in strong disagreement with simple SU(6) but are smaller by about the same factor of about 5/4. Thus they are both fit reasonably well by the SU(6) constituent quark model which fixes $G_A/G_V$ for the constituent quark to fit the nucleon decay data and reduces the other simple SU(6) predictions by the same factor. But the $\Sigma$ data agree with simple SU(6) and therefore disagree with constituent SU(6). The SU(3) analysis fixes its two free parameters by using the nucleon and $\Sigma$ decays as input; its predictions for the $\Lambda$ and $\Xi$ fit the experimental data within two standard deviations. However the error on the $\Xi$ data is considerably larger than the other errors, and all three predictions fit the $\Xi$ data within two standard deviations. Thus the significance of this fit can be questioned.

Our SU(3) fit deals directly with observable quantities rather than introducing D and F parameters not directly related to physical observables. This makes both the underlying physics and the role of experimental errors much more transparent. The neutron decay which has the smallest experimental error fixes one of the two free parameters. The $\Sigma^-$ decay provides the smallest error in fixing the remaining parameter, the spacing between successive entries in Table I, required to be equal by the SU(3) "equal spacing rule" [20]. The success of this procedure is evident since the errors on the predictions introduced by using these two decays as input are much smaller than the experimental errors on the remaining decays.

The contrast between the good SU(6) fit of the $\Sigma$ and the bad SU(6) fit of the others may give some clues to the structure of these baryons. The $\Sigma$ data rule out the constituent SU(6) model which otherwise seems attractive as it preserves all the good SU(6) results for strong and electromagnetic properties at the price of simply renormalizing the axial vector couplings to constituent quarks. Any success of SU(3) remains a puzzle since no reasonable quark model has been proposed which breaks SU(6) without breaking SU(3).

## 4. The spin structure of baryons

### 4.1. Results from DIS experiments

Surprising conclusions about proton spin structure have arisen from an analysis [39] combining data from polarized deep inelastic electron scattering and weak baryon decays.

Polarized deep inelastic scattering (DIS) experiments provided high quality data for the spin structure functions of the proton, deuteron and neutron [21]-[27]. The first moments of the spin dependent structure functions can be interpreted in terms of the contributions of the quark spins ($\Delta\Sigma = \Delta u + \Delta d + \Delta s$) to the total spin of the nucleon. The early EMC results [21] were very surprising, implying that $\Delta\Sigma$ is rather small (about 10%) and that the strange *sea* is strongly polarized. More recent analyses [22,23], incorporating higher-order QCD corrections, together with most recent data, suggest that $\Delta\Sigma$ is significantly larger, but still less than 1/3 of nucleon's helicity, $\Delta\Sigma \approx 0.24 \pm 0.04$ and $\Delta s = -0.12 \pm 0.03$.

Conventional analyses to determine the quark contributions to the proton spin, commonly denoted by $\Delta u$, $\Delta d$ and $\Delta s$, use use three experimental quantities. The connection between two to proton spin structure is reasonably clear and well established. The third is obtained from hyperon weak decay data rather than nucleon data via SU(3) flavor symmetry relations and its use has been challenged.

### 4.2. How should SU(3) be used in analyzing hyperon decays and relating data to baryon spin structure?

We first note that the Bjorken sum rule together with isospin tell us that the neutron weak decay constant

$$g_A(n \to p) = \Delta u(p) - \Delta d(p) = 1.261 \pm 0.004 \qquad (23)$$

Table 1
Theoretical Predictions and Experimental Values of $G_A/G_V$

| | Values from theoretical models | | | Experiment |
|---|---|---|---|---|
| | Simple SU(6) | Constituent SU(6) | SU(3) | Experiment |
| $n \to p$ | 5/3 | input | input | $1.261 \pm 0.004$ |
| $\Lambda \to p$ | 1 | $0.756 \pm 0.003$ | $0.727 \pm 0.007$ | $0.718 \pm 0.015$ |
| $\Xi^- \to \Lambda$ | 1/3 | $0.252 \pm 0.001$ | $0.193 \pm 0.012$ | $0.25 \pm 0.05$ |
| $\Sigma^- \to n$ | -1/3 | $0.252 \pm 0.001$ | input | $-0.340 \pm 0.017$ |
| $\frac{\Sigma^- \to n}{\Lambda \to p}$ | -1/3 | -1/3 | no prediction | $-0.473 \pm 0.026$ |

and that

$$\Delta u(p) - \Delta d(p) = \Delta d(n) - \Delta u(n) = 1.261 \pm 0.004 \quad (24)$$

Its SU(3) rotations give

$$g_A(\Sigma^- \to n) = \Delta u(n) - \Delta s(n) = -0.340 \pm 0.017 \quad (25)$$

and

$$\Delta u(n) - \Delta s(n) = \Delta d(p) - \Delta s(p) = = \Delta s(\Sigma^-) - \Delta u(\Sigma^-) = -0.340 \pm 0.017 \quad (26)$$

as well as the prediction now satisfied by experiment

$$g_A(\Xi^o \to \Sigma^+) = \Delta s(\Xi^o) - \Delta u(\Xi^o) = = g_A(n \to p) = 1.261 \pm 0.004 \quad (27)$$

The two independent linear combinations of $\Delta u(p)$, $\Delta d(p)$ and $\Delta s(p)$ obtained directly from the data without any assumptions about the $D$ and $F$ couplings commonly used can be combined to project out isoscalar component of eq.(24) and eq.(26),

$$\Delta u + \Delta d - 2\Delta s = g_A(n \to p) + 2g_A(\Sigma^- \to n) = = 0.58 \pm 0.03 \quad (28)$$

The commonly used procedure to determine these two linear conbinations includes the data for the $\Lambda \to p$ and $\Xi^- \to \Lambda$ decays, which do not directly determine any linear combination of but require an additional parameter, the $D/F$ ratio to give these quantities. Thus the standard procedure uses includes two more pieces of data at the price of an additional free parameter. Since the $\Xi^- \to \Lambda$ decay has a much larger error than all the other decays, there seems to be little point in introducing the D/F ratio.

### 4.3. How does SU(3) symmetry relate the valence and sea quarks in the octet baryons

We first note the following relations between the baryon spin structures following from SU(3) Symmetry

$$\Delta u(p) = \Delta d(n) = \Delta u(\Sigma^+) = \Delta d(\Sigma^-) = \Delta s(\Xi^o) = \Delta s(\Xi^-) \quad (29)$$

$$\Delta d(p) = \Delta u(n) = \Delta s(\Sigma^+) = \Delta s(\Sigma^-) = \Delta s(\Sigma^o) = \Delta u(\Xi^o) = \Delta d(\Xi^-) \quad (30)$$

$$\Delta s(p) = \Delta s(n) = \Delta d(\Sigma^+) = \Delta u(\Sigma^-) = \Delta d(\Xi^o) = \Delta u(\Xi^-) \quad (31)$$

$$\Delta u(\Sigma^o) = \Delta d(\Sigma^o) = (1/2) \cdot [\Delta u(\Sigma^+) + \Delta d(\Sigma^+)] \quad (32)$$

$$\Delta q(\Sigma^o) + \Delta q(\Lambda) = (2/3) \cdot [\Delta u(n) + \Delta d(n) + \Delta s(n)] \quad (33)$$

These relations allow all the baryon spin structures to be obtained from the values of $\Delta u(n)$, $\Delta d(n)$ and $\Delta s(n)$

However, we know that SU(3) symmetry is badly broken. This can be seen easily by noting that all these SU(3) relations apply separately to the valence quark and sea quark spin contributions. Thus SU(3) requries that the sea contributions satisfy eq.(26).

Since the strange contribution of the sea in the proton is known experimentally to be suppressed[28], this suggests that the strange sea in the $\Sigma$ must be enhanced. This simply does not

make sense in any picture where SU(3) is broken by the large mass of the strange quark. We are therefore led naturally to a model in which SU(3) symmetry holds for the valence quarks and is badly broken in the sea while the sea is the same for all octet baryons, is a spectator in weak decays and does not contribute to the magnetic moments. The sea thus does not contribute to the coupling of the photon or the charged weak currents to the nucleon. The one place where the sea contribution is crucial is in the DIS experiments, which measure the coupling of the neutral axial current to the nucleon.

The Bjorken sum rule and its SU(3) rotations relate the weak decays to the spin contributions of the active quarks to the baryon, without separating them into valence and sea contributions. The effects of the flavor symmetry breaking in the sea can be avoided by assuming that the flavor symmetry is exact for the algebra of currents, but the the hadron wave functions are not good SU(3) states but are broken in the sea. In this way one can obtain relations for the differences between spin contributions in which the sea contribution cancels out if the sea is the same for all octet baryons, even if SU(3) is broken in the sea.

## 5. Where is the physics? What can we learn?

### 5.1. How is SU(3) broken?

We now examine the underlying physics of some of these decays in more detail. The weak decays measure charged current matrix elements, in contrast to the EMC experiment which measures neutral current matrix elements related directly via the Bjorken sum rule to $\Delta u(p)$, $\Delta d(p)$ and $\Delta s(p)$. The charged and neutral current matrix elements have been related by the use of symmetry assumptions whose validity has been questioned [30,31].

We now examine the $\Sigma^- \to n$ decay and see how SU(3) breaking affects the relations

$$g_A(\Sigma^- \to n) = \Delta u(n) - \Delta s(n) = \Delta d(p) - \Delta s(p) \quad (34)$$

$$\Delta s(\Sigma^-) - \Delta u(\Sigma^-) = \Delta d(p) - \Delta s(p) \quad (35)$$

$$|G_V(\Sigma^- \to n)| = |G_V(n \to p)| \quad (36)$$

The quantity denoted by $g_A$ is a ratio of axial-vector and vector matrix elements. Although only the axial matrix element is relevant to the spin structure, breaking SU(3) in the baryon wave functions breaks both the relations between axial and vector couplings, as well as those from CVC for strangeness changing currents. Serious constraints on possible SU(3) breaking in the baryon wave functions are placed by the known agreement with Cabibbo theory of experimental vector matrix elements, uniquely determined in the SU(3) symmetry limit. On the other hand, the strange quark contribution to the proton sea is already known from experiment to be reduced roughly by a factor of two from that of a flavor-symmetric sea [28], due to the effect the strange quark mass. This suppression is expected to violate the $\Sigma^- \leftrightarrow n$ mirror symmetry, since it is hardly likely that the strange sea should be enhanced by a factor of two in the $\Sigma^-$. Yet Cabibbo theory requires retaining the relation between the vector matrix elements eq.(36).

### 5.2. A model which breaks SU(3) only in the sea

We now move to the discussion of the model described above mechanism for breaking SU(3) [29] which keeps all the good results of Cabibbo theory like eq.(36) by introducing a baryon wave function

$$|B_{phys}\rangle = |B_{bare} \cdot \phi_{sea}(Q=0)\rangle \quad (37)$$

where $|B_{bare}\rangle$ denotes a valence quark wave function which is an SU(3) octet satisfying the condition eq.(36) and $\phi_{sea}(Q=0)$ denotes a sea with zero electric charge which may be flavor asymmetric but is *the same* for all baryons. The wave function eq.(37) is shown[6] to satisfy eq.(36) and to *to give all charged current matrix elements by the valence quark component.* This provides an explicit justification for the hand-waving argument [29] that the sea behaves as a spectator in hyperon decays.

Unlike the charged current, the matrix elements of the neutral components of the weak currents *do* have sea contributions, and these contributions are observed in the DIS experiments. The SU(3) symmetry relations eqs.(29-33) are no longer valid. However, the weaker relation obtained from current algebra [40] still holds.

$$g_A(\Sigma^- \to n) = \frac{\langle n|\,\Delta u - \Delta s\,|n\rangle - \langle \Sigma^-|\,\Delta u - \Delta s\,|\Sigma^-\rangle}{2} \quad (38)$$

SU(3) says

$$\langle \Xi^o|\,\Delta s - \Delta u\,|\Xi^o\rangle = \langle p|\,\Delta u - \Delta d\,|p\rangle \quad (39)$$

If the strange sea is suppressed, this is clearly wrong. However, Current Algebra relations require only that

$$\langle \Xi^o | \Delta s - \Delta u | \Xi^o \rangle + \langle \Sigma^+ | \Delta u - \Delta s | \Sigma^+ \rangle = \langle p | \Delta u - \Delta d | p \rangle + \langle n | \Delta d - \Delta u | n \rangle \quad (40)$$

This is immune to strange sea suppression in all baryons.

### 5.3. Getting $\Delta u$, $\Delta d$ and $\Delta s$ From Data

Breaking up the quark contributions into valence and sea contributions becomes necessary to treat SU(3) breaking and the suppression of the strange sea. Two ways of doing this have been considered[6], one using hyperon decay data and the other using the ratio of the proton and neutron magnetic moments.

What is particularly interesting is that each of the two approaches makes assumptions that can be questioned, but that although these assumptions are qualitatively very different, both give very similar results. The use of hyperon data requires a symmetry assumption between nucleon and hyperon wave functions, which is not needed for the magnetic moment method. But the use of magnetic moments requires that the sea contribution to the magnetic moments be negligible, which is not needed for the hyperon decay method.

## 6. Conclusions

The question how flavor symmetry is broken remains open. Model builders must keep track of how proposed SU(3) symmetry breaking effects affect the good Cabibbo results for hyperon decays confirmed by experiment. The observed violation of the Gottfried sum rule remains to be clarified, along with the experimental question of whether this violation of $\bar{u} - \bar{d}$ flavor symmetry in the nucleon exists for polarized as well as for unpolarized structure functions. The question of how SU(3) symmetry is broken in the baryon octet can be clarified by experimental measurements of $\Lambda$ polarization in various ongoing experiments.

## REFERENCES


1. Peter S. Cooper, These Proceedings
2. D. Ashery and H. J. Lipkin hep-ph/9908335. Weizmann Preprint WIS99/30/Aug.-DPP Physics Letters B (in press)
3. The ALEPH Collaboration, D. Buskulic *et al. Phys. Lett.* **B374**, 319 (1996), The OPAL collaboration, K. Ackerstaff *et al., European Physical Journal* **C2**, 49 (1998).
4. D. de Florian, M. Stratmann and W. Vogelsang, hep-ph/9710410;
5. R.L. Jaffe, *Phys. Rev.* **D54**, R6581 (1996).
6. Marek Karliner and Harry J. Lipkin, Tel Aviv University preprint TAUP-2572-99 Weizmann Preprint WIS-99/23/June-DPP hep-ph/9906321 Physics Letters B
7. CERN COMPASS proposal CERN/SPSLC 96-14, SPSC/P297
8. D. DeFlorian *et al. Phys. Rev.* **D57**, 5811 (1998),
9. C. Boros and A.W. Thomas hep-ph/9902372 (1999)
10. J. Ellis, M. Karliner, D.E. Kharzeev and M.G. Sapozhnikov *Phys. Lett* **B353**, 319 (1995).
11. J. Ellis, D. Kharzeev and A. Kotzinian, *Z. Phys.*, **C69**, 467 (1996).
12. Andrei D. Sakharov, Memoirs, Alfred A. Knopf, New York (1990) p. 261
13. Ya. B. Zeldovich and A.D. Sakharov, Yad. Fiz 4 (1966)395; Sov. J. Nucl. Phys. 4 (1967) 283
14. A. D. Sakharov, Pisma JETP 21 (1975) 554; JETP 78 (1980) 2113 and 79 (1980) 350
15. I. Cohen and H. J. Lipkin, Phys. Lett. 93B, (1980) 56
16. Harry J. Lipkin, Phys. Lett. B233 (1989) 446; Nuc. Phys. A507 (1990) 205c
17. A. De Rujula, H. Georgi and S.L. Glashow, Phys. Rev. D12 (1975) 147
18. Harry J. Lipkin, Nucl. Phys. A478, (1988) 307
19. Particle Data Group, European Physics Journal, C3 (1998) 1, p. 205
20. Z. Dziembowski and J. Franklin, J. Phys. G17 (1991) 213
21. EMC Collab., Phys. Lett. B206, (1988) 364; Nucl. Phys. B328 (1989) 1.
22. J. Ellis and M. Karliner, Erice Lectures, hep-ph/9601280.
23. M. Karliner, unpublished (1999).
24. SMC Collab., Phys. Lett. B302 (1993) 533.
25. E-142 Collab., Phys. Rev. Lett. 71 (1993) 959.
26. SMC Collab., Phys. Lett. B329 (1994) 399.
27. E143 Collab., Phys. Rev. Lett. 74 (1995) 346 and Phys. Rev. **D58** (1998)112003; Phys. Lett. **B412**, 414 (1997), Phys. Lett. **B442** (1998) 484;
28. CCFR Collab. A.O. Bazarko *et al.*, Z. Phys. **C65**, 189 (1995);
29. J. Lichtenstadt and H.J. Lipkin, Phys. Lett.

B353 (1995) 119
30. Harry J. Lipkin, Phys. Lett. B230 (1989) 135
31. Harry J. Lipkin, Phys. Lett. B214 (1988) 429
32. The CERN SMC collaboration, B. Adeva *et al. Phys. Rev.* **D58**, 112001 (1998).
33. The SLAC E143 collaboration, K. Abe *et al. Phys. Rev.* **D58**, 112003 (1998).
34. The HERMES collaboration, A. Airapetian *et al. Phys.Lett.* **B442**, 484 (1998).
35. The Fermilab E665 Collaboration, M.R. Adams, et al., to be published
36. A. Kotzinian *et al. Eur. Phys. J.*, **C2**, 329 (1998).
37. G. Gustafson and J. Hakkinen, *Phys. Lett.* **B303**, 350 (1993).
38. M. Burkardt and R.L. Jaffe *Phys. Rev. Lett.* **70**, 2537 (1993).
39. Stanley J. Brodsky, John Ellis and Marek Karliner, Phys. Lett. 206B, 309 (1988)
40. Harry J. Lipkin, Phys. Lett. B 337 (1994) 157.
41. J. Qiu *et. al.* Phys. Rev. D41, (1990) 65.
42. E665 Collab., D. Ashery, private communication
43. HERMES Collab. in [27].
44. Harry J. Lipkin, Physics Letters B335 (1994) 500

# Hyperon Static Properties

Peter S. Cooper [a*]

[a]Fermi National Accelerator Laboratory,
MS 122 P.O. Box 500 Batavia, IL 60510

I review the static properties of the hyperons including masses, lifetimes, magnetic moments and CPT test from the asymmetries of these quantities for hyperon and anti-hyperon.

## 1. INTRODUCTION

The static properties of the hyperons include masses, lifetimes, magnetic moments and CPT test from the asymmetries of these quantities for hyperon and anti-hyperon. I will review the present status of these measurements with an eye toward identifying places where new or improved measurements can have a significant physics impact. Most of these measurements are from the PDG [1] where there have been only two new measurements quoted since 1995. I also report two new measurements not yet published.

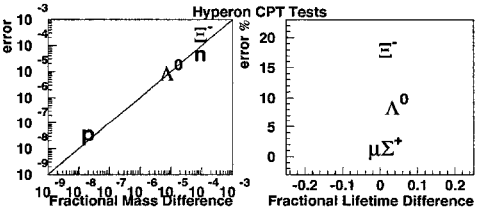


Figure 1. Hyperon mass, lifetime and magnetic moment CPT tests

## 2. CPT TESTS

All the hyperon static properties have invariant magnitudes under CPT, or hyperon, anti-hyperon transformations. The masses and lifetimes should be the same while the magnetic moments should change sign under CPT. If the mass of particle and anti-particle differ under CPT then the lifetimes will also differ just from the difference in available phase space. There are no real models for CPT violation. The $K^0$ system is probably the most sensitive place to look for such violations. Nonetheless, there are high precision measurements available in the baryon sector so we can, and therefore must, look. In Figure 1 I plot the asymmetries (absolute value of the difference over the average) for the measured hyperon masses, lifetimes and the $\Sigma^+$ magnetic moment. I also include the proton and neutron mass asymmetries since the proton mass asymmetry is by far the most precise test in this sector. All these measurements are consistent with zero to within their errors.

A new measurement of the lifetimes of the $\Sigma^+$ and $\overline{\Sigma}^-$ comes from E761, our old $\Sigma^+$ radiative decay experiment which took data in 1990. This experiment was originally mounted to make precise measurements of the branching ratio and asymmetry parameter in the hyperon weak radiative decays $\Sigma^+ \to p\gamma$ and $\Xi^- \to \Sigma^-\gamma$. In the course of this run a sample of data was taken with all the magnetic fields reversed yielding a matched set of positive and negative hyperon beam data in the same apparatus. A lifetime analysis of these data [2] yield $\tau[\Sigma^+] = 80.38 \pm 0.40 \pm 0.14$ psec and $\tau[\overline{\Sigma}^-] = 80.43 \pm 0.80 \pm 0.14$ psec based upon 640K and 132K events respectively. The $\Sigma^+$ lifetime asymmetry is $\Delta\tau/ < \tau > = -0.06 \pm 1.12\%$ making this measurement the best baryon lifetime CPT test.

## 3. MAGNETIC MOMENTS

The hyperon magnetic moments are major experimental success story. Since the advent the polarized hyperon beams in 1976 all the accessible magnetic moments in the baryon octet have been measured with high precision.

The traditional first level description of the hyperon magnetic moments is the simple $SU_6$ additive quark model which assumes fixed moments for each flavor of quark and no orbital angular

*email address: pcooper@fnal.fnal.gov

momentum. It predicts all the moments in terms of the measured moments of (p, n, $\Lambda^0$) which fix the (u, d, s) quark moments. The PDG [1] averages for the moments are shown in Table 1. The deviations from the $SU_6$ model are at the $5-10\%$ level as expected for an $SU_3$ based model. These deviations are very well measured. Many models have been advanced in the past 30 years to go beyond simple $SU_6$. However, no more advanced model seems to do substantially better than simple $SU_6$. This is an experimentally finished program until somebody can build a better baryon model which challenges the precisions of the present measurements.

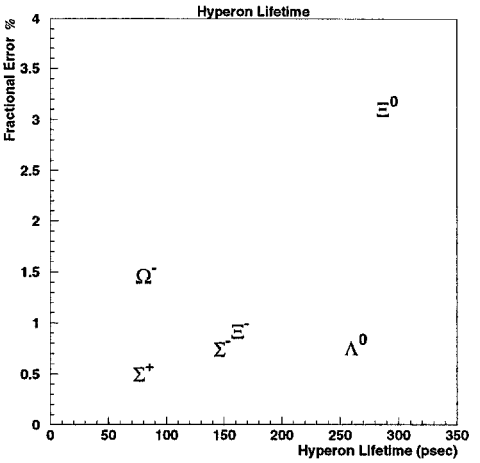


Figure 2. Present PDG values of the hyperon lifetimes and fractional precisions

## 4. LIFETIMES

The present status of the measurements of the lifetimes of the hyperons from the PDG [1] are shown in Figure 2. All are measured to better than 1% except $\tau_{\Xi^0}$ and $\tau_{\Omega^-}$. Both KTeV at Fermilab and NA48 at CERN are collecting large samples of $\Xi^0$. It is reasonable to project that this lifetime should be improved to the 1% level in the near future. Likewise HyperCP at Fermilab is collecting a large samples of $\Omega^-$ from which they should be able to improve this lifetime measurement to the 1% level.

Precision lifetime measurements require an apparatus with good resolution and excellent simulation of acceptance and resolution smearing effects. These are particular strengths of experiments like KTeV, NA48 and HyperCP. While it is difficult to foresee the systematic limitations of a given measurement in one of these experiments I have no doubt that each can make significant improvements to these measurements given the will to undertake the analysis.

A most important use of precision lifetimes is in the analysis of the hyperon semi-leptonic decays. The relationship between the directly measured semi-leptonic branching ratio [B] and the decay rate predicted by theory [$\Gamma$] is B=$\Gamma\tau$. The lifetime must be known more precisely, fractionally, than the branching ratio in order to fully exploit the semi-leptonic branching ratio measurements in testing the theory. This is particularly important in exploiting the recent $\Xi^0$ semi-leptonic decays observed by KTeV and NA48. This should provide the motivation for them to improve the lifetime measurement of this state.

## 5. MASSES

The mass spectrum of the baryons is an enduring subject. An early and seminal contribution is the Coleman-Glashow mass relation [3] which relates the the isopsin splittings of the three I spin multiplets of the baryon octet:

$$M_n - M_p + M_{\Xi^-} - M_{\Xi^0} + M_{\Sigma^+} - M_{\Sigma^-} = 0 \quad (1)$$

More recent work is this area includes papers by Jon Rosner [5] and Elizabeth Jenkins [4] and references therein. There are many sum rules of this type. All the others involve the masses of decuplet, charm or beauty baryons. Beyond 100 $KeV/c^2$ the precision of these sum rules should be limited by the theory.

The present status of the measurements of the masses of the hyperons from the PDG [1] are shown in Figure 3. All are known to the 100 $KeV/c^2$ level or better save the $\Xi^0$ and $\Omega^-$. NA48 has recently reported [6] a preliminary new measurement of the $\Xi^0$ mass with a precision of 200 $KeV/c^2$. The error given is dominated by systematics uncertainties which they may be able to improve further with a complete analysis of all their data. KTeV may also be able to improve this measurement. HyperCP at Fermilab has enormous samples of both $\Xi^-$ and $\Omega^-$ decays. In principle they ought to be able to significantly improve the mass measurements for both of these states.

Table 1
Hyperon Magnetic Moments (NM)

| Hyperon | Moment | Quark Model | Difference |
|---|---|---|---|
| p | +2.792847 | fixed | —— |
| n | −1.913043 | fixed | —— |
| $\Lambda^0$ | −0.613(04) | fixed | —— |
| $\Sigma^+$ | +2.458(10) | +2.67 | −0.210(10) |
| $\Sigma^0 \to \Lambda^0$ | −1.610(80) | −1.63 | +0.020(80) |
| $\Sigma^-$ | −1.160(25) | −1.09 | −0.070(25) |
| $\Xi^0$ | −1.250(14) | −1.43 | +0.177(14) |
| $\Xi^-$ | −0.6517(25) | −0.47 | −0.161(03) |
| $\Omega^-$ | −2.024(56) | −1.84 | −0.184(56) |

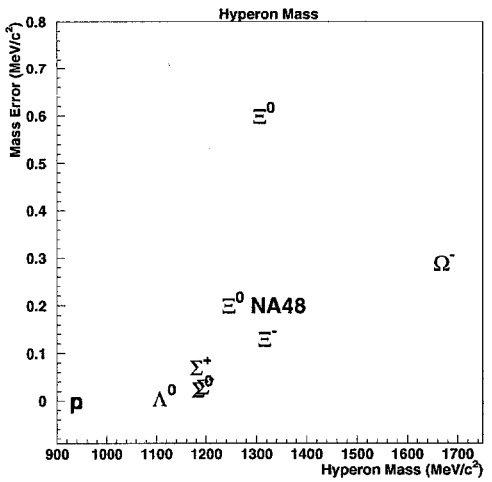


Figure 3. Present PDG values of the hyperon masses and precisions

The present experimental value for the Coleman-Glashow sum rule is $-0.37 \pm 0.62$ dominated by the uncertainty on $M_{\Xi^0}$. Using the preliminary NA48 value of $M_{\Xi^0}$ improves this the test of this sum rule to $-0.30 \pm 0.25$. The next biggest uncertainty is in $M_{\Xi^-}$ which HyperCP may be able to improve.

## 6. CONCLUSIONS

With the anticipated new results from NA48, KTev, HyperCP, and perhaps some older experiments like E761, typical precisions on the static properties of the hyperon will approach:

| | |
|---|---|
| mass | 100 $KeV/c^2$ |
| life time | 1% |
| magnetic moment | 0.025 NM |

In all three cases these precisions are higher than that expected from present theory and models. There does not appear to be a compelling reason to mount a new experiment to significantly improve any of these measurements at this time.

This body of work is an operational definition of precision particle physics. These measurements are all now sufficiently precise to present serious challenges to model builders. However in the tennis game between experiment and theory we experimentalists will have to wait for them to hit this ball back over the net before it is worth having another swing at it.

## REFERENCES


1. Particle Data Group, C. Caso et al. Eur Phys. J. C3,1, 1998.
2. R.F. Barbosa, et al. Submitted to PRD, October 1999.
3. S. Coleman and S.L. Glashow, Phys.Rev.Lett. 6, 423 (1961).
4. E. Jenkins, hep-ph/9803349.
5. J. Rosner, Phys. Rev. D57, 4310, (1998), hep-ph/9707473v4.
6. Lutz Kopke, Kaon99 Conference, Chicago, June 1999.

# Chapter 8

# Hyperon Production and Polarization


- J. Soffer
- L. G. Pondrom
- G. R. Goldstein
- U. Mueller

# Is the riddle of the hyperon polarizations solved?

J. Soffer [a]

[a]Centre de Physique Théorique, CNRS,
Luminy Case 907, F13288 Marseille Cedex 09, France

We review in this talk some aspects of the exciting field of hyperon polarization phenomena in high energy reactions, over the last twenty years or so. On the experimental side, a large amount of significant polarization data for hyperon and antihyperon inclusive production, has been accumulated in a rather broad energy range. Many theoretical attempts to explain that have been proposed and we will discuss some of them, showing their strong limitations in most cases.

## 1. INTRODUCTION

Naively it seems reasonable to expect no polarization effect in a one-particle inclusive reaction

$$a + b \to c + X \ , \tag{1}$$

since one is summing over many different inelastic channels $X$, which should have polarizations of random magnitudes and signs, such that the sum will average to zero. In reality the experimental situation is not so simple and single spin asymmetries have been observed in many specific reactions and we will first give a rapid tour of these data, mainly for hyperon production. Next we will present some current theoretical ideas, which have been proposed to explain the main features of the data. Finally, we will say a few words on future expectations and will make our closing remarks.

## 2. A RAPID TOUR OF THE HYPERON POLARIZATIONS DATA

There is a large amount of very significant data for hyperon and antihyperon inclusive production [1–4], some of them exhibiting a simple pattern, which may help to uncover the underlying particle production mechanism. This polarization effect was first discovered in 1976 at FNAL by studying hyperons produced by a 300 $GeV/c$ proton beam on a Beryllium target [5] and it was found that the $\Lambda's$ produced in the beam fragmentation region have a large polarization perpendicular to the production plane. Since then, many different experiments have collected high statistics data on $\Lambda$ inclusive production, which makes it the best known hyperon inclusive reaction.

Let us briefly recall the main characteristics of these proton induced data, which exhibit some interesting regularities [1]:

i) the invariant cross section $Ed^3\sigma/dp^3$ depends, to a good approximation, only on $x_F^\Lambda$, the fraction of incident proton momentum carried by the $\Lambda$ in the beam direction (in the center of mass ($c.m.$) system), and $p_T^\Lambda$, the $\Lambda$ transverse momentum, and does *not* depend on the $c.m.$ energy $\sqrt{s}$.
ii) the transverse polarization $P_\Lambda$ is *negative* with respect to the direction $\vec{n} = \vec{p}_{inc} \times \vec{p}_\Lambda$.
iii) $P_\Lambda$ is almost energy and target independent for an incident energy ranging from 12 $GeV/c$ on a Tungsen target [6] up to 2000 $GeV/c$ at ISR [7].
iv) for $p_T^\Lambda$ below 1 $GeV/c$ or so, the magnitude of $P_\Lambda$ is approximately linear in $p_T^\Lambda$, with a slope increasing with $x_F^\Lambda$.
v) for $p_T^\Lambda$ above 1 $GeV/c$, the magnitude of $P_\Lambda$ is independent of $p_T^\Lambda$, up to $p_T^\Lambda \sim 3.5$ $GeV/c$ and approximately linear with $x_F^\Lambda$ [8].

We also have data on other hyperon polarizations at FNAL energy, where one observes, with respect to the $\Lambda$ polarization, an effect of opposite sign for $\Sigma^\pm$ and same sign for $\Xi^-$ and $\Xi^0$ [9]. However it seems that $P_{\Xi^-}$ does *not* increase with energy, whereas $P_{\Sigma^+}$ decreases with energy [2].

Finally, the situation of the antihyperon polarizations is very puzzling since, on the one hand, $P_\Lambda \sim P_{\Xi^0} \neq 0$ and $P_{\bar{\Lambda}} \sim P_{\bar{\Xi}^0} = 0$, but on the other hand, $P_{\bar{\Sigma}^-} \sim P_{\Sigma^+}$ and $P_{\bar{\Xi}^+} \sim P_{\Xi^-}$ [2],[10]. Needless to say that all these peculiarities of the data constitute a real challenge for the theory, some aspects of which we start discussing now.

## 3. SOME THEORETICAL IDEAS FOR SINGLE TRANSVERSE SPIN ASYMMETRIES

Let us consider the reaction (1), where one observes the transverse polarization state of one

of the hadrons (initial or final). The simplest measurable quantity is the single transverse spin asymmetry (or up-down asymmetry), defined as, for example if $c$ is polarized

$$P_c = \frac{d\sigma_c^{\uparrow} - d\sigma_c^{\downarrow}}{d\sigma_c^{\uparrow} + d\sigma_c^{\downarrow}} , \qquad (2)$$

also usually called the $c$ polarization. The transverse spin asymmetry related to the initial particle ( $a$ or $b$) is called the analyzing power and is denoted by $A_N$. By using the generalized optical theorem, one can write

$$P_c d\sigma = Im[f_+^* f_-] , \qquad (3)$$

where $d\sigma = d\sigma_c^{\uparrow} + d\sigma_c^{\downarrow}$ is the corresponding unpolarized inclusive cross section. It is described by means of $f_+$, the forward *non-flip* $3 \to 3$ helicity amplitude $ab\bar{c}_\lambda \to ab\bar{c}_\lambda$, where $\lambda = \pm$ is the same on both sides. Moreover $f_-$ is the forward *flip* amplitude $ab\bar{c}_\lambda \to ab\bar{c}_{-\lambda}$. In order to get a non-vanishing $P_c$ (or $A_N$), one needs, a non-zero $f_-$ and furthermore it should have a phase difference with $f_+$. This point is important and should be taken seriously, if we want to have a real understanding of the available experimental data. It is another way to say that a non-zero $P_c$ corresponds to a non-trivial situation, which reflects a high coherence effect among many different inelastic channels. In principle, in addition to the *c.m.* energy $\sqrt{s}$, all these observables are expected to depend on two kinematic variables defined as $x_F^c = 2p_L^c/\sqrt{s}$ and $x_T^c = 2p_T^c/\sqrt{s}$, where $p_L^c$ and $p_T^c$ are the *c.m.* longitudinal and transverse momentum of $c$ with respect to the incident beam direction. Clearly one has the kinematic limits $-1 \leq x_F^c \leq +1$ and $0 \leq x_T^c \leq +1$ and one should distinguish two different kinematic regions:

i) The beam fragmentation region
It corresponds to a region where $c$ carries a sizeable $x_F^c$ say, $0.3 \leq x_F^c \leq 0.8$, with a small value of $x_T^c$ say, $0 \leq x_T^c \leq 0.1 - 0.15$. Similarly, one can consider the target fragmentation region, corresponding to $x_F^c$ of opposite sign.

ii) The hard scattering region
It corresponds to a region where $c$ carries a sizeable $x_T^c$ say, $x_T^c \geq 0.15$, with $x_F^c \sim 0$.

Rather different dynamical mechanisms are expected to be at work in these different kinematic regions and since most of the hyperon polarization data are in the fragmentation region, we will first consider it.

### 3.1. The fragmentation region

Actually, in this region the polarization mechanism is essentially based on a soft process, where perturbative QCD does not apply. There are *two* classes of dynamical models available in the literature which will be now discussed below.

*a) Semiclassical models*
These models provide simple arguments for a qualitative description of the hyperon polarizations, but since they fully ignore the relevance of the phase difference, which is crucial, as mentioned above, they are unable to make solid quantitative predictions.

a1) - The Lund model
We recall that in terms of the constituent quarks, the proton beam fragmentation into a $\Lambda$ with a $p_T^{\Lambda} \neq 0$, corresponds to the replacement of a valence $u$ quark, in the projectile, by a strange quark $s$ coming from the sea, which must be accelerated along the beam direction, and acquiring also a non-zero $p_T$. Moreover we will be assuming a $SU(6)$ wave function, where the $(ud)$ system of the $\Lambda$ is in a singlet state, so the $\Lambda$ polarization is that of the $s$ quark. In the Lund model [11], an incoming $(ud)$ diquark with spin $S = 0$ and isospin $I = 0$, stretches the confined color field in the collision region and a $s\bar{s}$-pair is produced. The $s$ quark is needed to make the final $\Lambda$ and since $p_T^{\Lambda} \neq 0$, one assumes that part of this transverse momentum is provided by the $s$ quark, which has to be compensated by that of the $\bar{s}$ quark. As a result, the $s\bar{s}$-pair has an orbital angular momentum which is assumed to be balanced by the spin of the $s\bar{s}$-pair. From this mechanism, one expects in proton induced reactions, a *negative* $\Lambda$ polarization increasing with $p_T^{\Lambda}$, in agreement with the sign of the data but whose magnitude is difficult to predict. The $\Sigma$ polarization follows from the knowledge of the $SU(6)$ wave functions and since for the $\Sigma$, the $(ud)$ diquark has a spin $S = 1$, it is natural to expect an opposite polarization, in accordance with the data. However this simple picture cannot be correct and we are now indicating, several drawbacks of the model:
- The case of the $\Xi$ requires the production of two strange quarks and involves additional assumptions in the model, which does not explain why $\Lambda$ and $\Xi$ have nearly equal polarizations. In addi-

tion, nothing is said about the description of the unpolarized cross sections, observables of crucial importance to pin down the dynamics and which are very different for $\Lambda$ and $\Xi$ production.
- The model does not suggest any $x_F$ dependence of the polarization.
- In this approach, $P_\Lambda$ increases linearly with $p_T^\Lambda$, but one does not know why it stops growing, which is needed since $|P_\Lambda| \leq 1$ and moreover, as recalled above, because the data saturates for $p_T^\Lambda$ above $1 GeV/c$.
- As we have seen, the $s$ quark and the $\bar{s}$ quark move into opposite directions. So for $\Lambda$ production, by looking at the final state $K^+\Lambda$, since $\vec{K}^+$, the direction of the $K^+$, gives the direction of the $\bar{s}$, one should observe that $P_\Lambda \neq 0$, only when $K^+$ and $\Lambda$ are in opposite hemispheres. The E766 experiment at BNL, with a proton beam of 27.5 $GeV/c$ [12], has made extensive studies of an *exclusive* channel $pp \to p\Lambda K^+\pi^+\pi^-$ and also other channels with more than one $(\pi^+\pi^-)$ pair produced [13]. They found that $P_\Lambda$ can be parametrized, in a limited kinematic region, according to

$$P_\Lambda(x_F^\Lambda, p_T^\Lambda) = (-0.443 \pm 0.037) x_F^\Lambda \cdot p_T^\Lambda \ , \quad (4)$$

in agreement with the inclusive data. However they found no correlation between $\vec{K}^+$ and the value of $P_\Lambda$.

At this point, it is worth to emphasize the importance of exclusive channels, in particular the simple diffractive reaction $pp \to p(\Lambda K^+)$, for which a large negative $P_\Lambda$ ($\sim -60\%$) has been observed at the ISR [14], consistent with a very recent result from the experiment E690 [15]. There is no indication for such a correlation between $\vec{K}^+$ and $P_\Lambda$ and it is conceivable to try to relate this large value of $P_\Lambda$ to a diffractive mechanism with Pomeron exchange, since one observes no energy dependence between $\sqrt{s} = 40\ GeV$ and $62\ GeV$.

a2) - The recombination model

This is another approach [16] based on semiclassical arguments, which are applied to a recombination mechanism. As we have already pointed out, to make a $\Lambda$ from the fragmentation of an incident proton, one needs to recombine a fast $(ud)$ diquark from the proton with a slow $s$ quark from the sea. If $\vec{F}$ denotes the unspecified color force which gives this acceleration, the $s$ quark of velocity $\vec{v}$ feels the effect of the Thomas precession given by $\vec{\omega}_T \sim \vec{F} \times \vec{v}$, which has the direction of the normal to the hadronic scattering plane $\vec{n} = \vec{p}_{inc} \times \vec{p}_\Lambda$. In order to minimize the energy $\vec{S} \cdot \vec{\omega}_T$ associated to this effect, the spin $\vec{S}$ of the $s$ quark must be opposite to $\vec{\omega}_T$, so this leads to expect a negative $\Lambda$ polarization in $pp \to \Lambda X$. Although this approach is different from the Lund model, it seems to lead to similar observable effects. However, one direct consequence of the recombination model is that, in the inclusive reaction $K^-p \to \Lambda X$, if the $\Lambda$ is produced in the $K^-$ beam fragmentation, the $s$ quark needed to make the $\Lambda$, is now coming from the $K^-$. It is fast and has to be decelerated when joining a $(ud)$ diquark from the sea, so the sign of $P_\Lambda$ is reversed. This is in agreement with the data [17], but the magnitude of $P_\Lambda$ in a $K^-p$ collision is approximately twice as large as in a $pp$ collision, so clearly the simplest version of the model does not explain this big difference. Let us recall that this large $P_\Lambda$ in $K^-p$ collision is also energy independent between $p_{inc} = 12\ GeV/c$ [18] and $176\ GeV/c$ [17], an interesting scaling property. Another strong prediction of this model is that the polarization of the antihyperons must be zero. This is in agreement with the data for $\bar{\Lambda}$, but at variance with some other cases, as we recalled above. Moreover the Thomas precession does not act exclusively on the strange quark, but also on the diquark and depends on its possible spin states $j = 0$ and $j = 1$. Consequently, one has to introduce more parameters to make relative predictions for a fair number of inclusive reactions, a situation not very satisfactory.

In addition to the polarization $P$, we have seen that one can consider the analyzing power $A_N$ and also another spin-observable, the spin transfer parameter denoted by $D_{NN}$, which measures the fraction of the transverse component of the beam polarization transferred to the hyperon. Another bad failure of the model is that, it predicts $A_N = D_{NN} = 0$, in strong contradiction with the results of the E704 experiment at FNAL. They found in $pp$ inclusive $\Lambda$ production at 200 $GeV/c$, a substantial negative $A_N$, at relatively large $x_F^\Lambda (\geq 0.5)$ [19], and a positive $D_{NN}$ up to about 30%, also at high $x_F^\Lambda$ [20].

a3) - The Berlin model

In this model [21,22], one is claiming that the existence of striking analyzing power $A_N$ observed in $\pi^\pm$ inclusive production at FNAL [23], is a strong indication for orbiting valence quarks in a polarized proton. So the orbital motion should be taken into account with the following semiclas-

sical picture:
A hadron is polarized, *if and only if*, its valence quarks are polarized and due to a significant *surface effect*, only valence quarks retain the information about polarization.

This leads to conclude that, for example, a meson which is formed by *direct fusion* of an upward valence quark with an antiquark from the sea, gets a transverse momentum from the orbital motion of the valence quark, to the left, looking downstream. So in $pp \to \pi^+ X$, since $\pi^+ = (u_v \bar{d}_s)$ one should have $A_N > 0$, whereas in $pp \to \pi^- X$, one should have $A_N < 0$, which are both in agreement with the data [23]. In order to make more quantitative statements, they must assume that the $x_F$ of the produced hadron ($\pi^+$ or $\pi^-$) is that of the initial polarized valence quark $x$, and use the information one has on the polarized quark distributions $\Delta u_v(x)$ and $\Delta d_v(x)$, obtained from polarized deep inelastic scattering. Of course the model makes no statement about the $p_T$ dependence. From the quark structure of the $K$ mesons, one predicts the same $A_N$ for $K^+$ and $\pi^+$ inclusive production and also the same for $K_s^0$ and $\pi^-$. The first prediction remains to be checked but there is a good indication that the second one is correct from the AGS data [24]. Another consequence is that $A_N$ is zero for $K^+$ and $\bar{K}_s^0$ inclusive production and this last prediction also, has not yet been verified.
Let us now return to hyperon inclusive production and more specifically to the $\Lambda$ case. There are three possibilities for the direct formation: the incident proton can release either a $(u_v d_v)$ diquark, or a $u_v$ quark or a $d_v$ quark, which must be combined with the appropriate missing piece from the sea, to make a $\Lambda$. The calculations lead to a reasonable agreement with the data for $P_\Lambda$, $A_N$ as shown in refs.[21,22], and $D_{NN}$ is predicted to be positive in accordance with [20]. To summarize, this model has some predictive power, but contains several key assumptions, which make it not fully convincing. Moreover, nothing is said about the other hyperons and neither about the puzzling situation of the antihyperons.

At this stage we will make a short digression on some positivity conditions, which are not necessarily well known. One can show that for any inclusive reaction of the type eq.(1), where $a$ and $c$ are any polarized spin-1/2 particles and $b$ is an unpolarized particle, of any spin, one has [25] the following very general constraints among $P_c$, $A_N$ and $D_{NN}$

$$1 \pm D_{NN} \geq |P_c \pm A_N| \; . \tag{5}$$

These inequalities, which are model independent rigorous conditions, must be satisfied for any kinematic values of the variables $x_F^c$, $p_T^c$ and $\sqrt{s}$. As an example, we have tested the results of the E704 experiment at $p_{inc} = 200\ GeV/c$:
for $p_T^\Lambda \sim 1\ GeV/c$ and $x_F^\Lambda \sim 0.8$, one has $D_{NN} \sim 30\%$, $A_N \sim -10\%$ and $P_\Lambda \sim -30\%$, showing that the above constraints are indeed well satisfied.

*b) Regge type models*
It is important to try to generate or to justify the origin of the phase difference between $f_+$ and $f_-$ occuring in eq.(3) and this is what one does, in the two phenomenological models, we are presenting now [1].

b1) - The Milano model
In the fragmentation region, this phase might be resulting from final state interactions and more precisely one can invoke a dynamical model [27] based on the production of various baryon resonances, in general out of phase, which then decay to give the observed $\Lambda$. Unlike the theoretical frameworks discussed so far, here one is trying, first, to provide a good representation of the inclusive unpolarized cross section. It is known that hadron fragmentation is well described by the triple-Regge model and for example for $\Lambda$ production, they consider three production mechanisms: (a) direct production, (b) intermediate baryon dissociation $(\Sigma, \Sigma^*)$, (c) $\Sigma^0$ electromagnetic decay. The calculation, which involves the relevant Regge residues, leads to a reasonable unpolarized $\Lambda$ spectrum. We note that the direct production contribution produces only unpolarized $\Lambda$ and dominates at large $p_T^\Lambda$. As a result, the predicted $P_\Lambda$, which has the right negative sign and the correct magnitude at low $p_T^\Lambda$, tends to decrease at high $p_T^\Lambda$, in contradiction with experiment. This has been extended to the $\Sigma$ case and although they get a positive sign, they fail to predict the right magnitude of $P_\Sigma$. It seems hard to use this approach for $\Xi$ production, since it would requiere a rather elaborate extension of the Regge model.

[1] There is also an attempt to produce the phase using one-loop diagrams in perturbative QCD and the recombination of polarized quarks to form polarized hadrons. This hybrid model is described in ref. [26].

b2) - The one-pion exchange model

Here one assumes that $\Lambda$ production in the fragmentation region is dominated by a reggeized one-pion exchange, a model proposed several years ago and which gives a successful description of various exclusive and inclusive reactions. As is well known, if quantum numbers allow, pion exchange generally dominates hadronic amplitudes, especially at small momentum transfers. Therefore the leading contribution involves the diagram such that, the multiperipheral chain reduces only to the binary reaction $\pi p \to K\Lambda$ and the total $\pi p$ cross section, connected by the exchange of an off-shell reggeized pion [28]. The $\Lambda$ spectrum is obtained from the $pp \to K\Lambda X$ cross section, after integration over the kaon phase space. Note that the binary reaction has a subenergy in the resonance region up to 10 $GeV/c$ or so. One predicts all the basic features of the $\Lambda$ spectrum, including the scaling property, with no free parameter. A crucial test of the model is the calculation of $P_\Lambda$, which is obviously directly related to the $\Lambda$ polarization of the binary reaction $\pi p \to K\Lambda$ at fairly low energy. It is essentially negative and therefore leads to a negative $P_\Lambda$, with a magnitude consistent with the data. It would be also interesting to know what this model predicts for $A_N$ and $D_{NN}$. Although the calculation was not done for $P_\Sigma$, one can anticipate a positive sign, due to the fact that in the binary reaction $\pi^+ p \to K^+\Sigma^+$, the polarization is positive. However it seems not possible to extend this approach to the $K$ induced reaction $K^- p \to \Lambda X$, which is unfortunate.

### 3.2. The hard scattering region

This kinematic region involves short distance interactions, where perturbative QCD is expected to apply. Naively, a transverse spin asymmetry in a parton subprocess is anticipated to be of the form

$$\hat{A}_N \sim \alpha_s \frac{m_q}{p_T} \ , \tag{6}$$

because the spin-flip amplitude is proportional to the quark mass and the imaginary part (see eq.(3)) must be produced by a one-loop diagram, which generates the strong coupling constant $\alpha_s$. Clearly this result, which is valid only at the twist-2 level in QCD, is extremely small and will lead also to a small hadronic asymmetry. On the experimental side, this kinematic region is hardly accessible, for statistical reasons. On the one hand, there is an indication for a large effect in $\pi^0$ production in $\pi$ induced reactions at 40 $GeV/c$ [29] and, on the other hand, from E704 in $pp \to \pi^0 X$ at 200 $GeV/c$ [30], $A_N$ is consistent with zero. However more then ten years ago, a self consistent approach to single spin asymmetries at the twist-3 level in QCD was developed [31]. In order to avoid the extra complication coming from the distributions and fragmentation functions, let us consider the simplest, perhaps, academic reaction $\gamma p^\uparrow \to \gamma X$. According to this theoretical approach the spin transverse proton asymmetry has the form

$$A_N \sim \frac{M_p b(x_1, x_2)}{p_T} \ , \tag{7}$$

where the quark mass $m_q$ has been replaced by the proton mass $M_p$ and the other killing factor $\alpha_s$ is now replaced by the quark-gluon correlator $b(x_1, x_2)$, a new two-arguments ($x_1$ and $x_2$) structure function, which must be extracted from the data, just like any ordinary parton distribution. Of course the remaining $p_T$ in the denominator reflects the fact that we are dealing with a twist-3 effect, which is expected to decrease for very large $p_T$ values. In the cases of $pp \to \Lambda^\uparrow X$ or $pp^\uparrow \to \pi X$, discussed before in the fragmentation region, the above result has to be convoluted by the quark distributions and the final hadron fragmentation functions, but the key question which remains to be answered is: how large are these quark-gluon correlators? It is an interesting experimental problem which, hopefully, will be solved in the near future, in particular, with the polarized $pp$ collider at RHIC-BNL, due to start operating very soon. This new unique facility will also allow to get some relevant information on the $\Lambda$ polarized fragmentation functions [32].

## 4. CONCLUDING REMARKS

We have shown that in hadronic spin physics at high energy, the field of transverse spin asymmetries is extremely rich, in particular, by looking of the available data. We are facing a considerable number of polarization effects in hyperon and antihyperon inclusive (and exclusive) production, which remain widely unexplained. Therefore we believe it is fair to conclude that, despite several theoretical efforts over the last twenty years or so, theory is left behind and has to make urgent progress, to catch up with the puzzling experimental situation. If there exists a universal physical picture to shade light on this important area

of high energy physics, it has not been discovered yet.

*Acknowledgements*

It is my pleasure to thank E. Monnier and all the organizers for their invitation and for setting up this excellent workshop in such a pleasant and stimulating atmosphere.

## REFERENCES

1. L. Pondrom, Physics Reports 122 (1985) 57.
2. K. Heller, Proceedings of Spin 96, Amsterdam 10-14/10/96, World Scientific (1997) p.23.
3. L.Pondrom, these Proceedings.
4. V.J. Smith, these Proceedings.
5. G. Bunce et al., Phys. Rev. Lett. 36 (1976) 1113.
6. F. Abe et al., Phys. Rev. Lett. 50 (1983) 1102.
7. A.M. Smith et al., Phys. Lett. B185 (1987) 209.
8. B. Lundberg et al., Phys. Rev. D40 (1989) 3557.
9. C. Wilkinson et al., Phys. Rev. Lett. 58 (1987) 855 and references therein.
10. A. Erwin, these Proceedings.
11. B. Andersson et al., Physics Reports 97 (1983) 31 and references therein.
12. J. Félix et al., Phys. Rev. Lett. 76 (1996) 22.
13. J. Félix et al., Phys. Rev. Lett. 82 (1999) 5213.
14. T. Henkes et al., Phys. Lett. B283 (1992) 155.
15. D. Christian , these Proceedings.
16. T. De Grand et al., Phys. Rev. D32 (1986) 2445 and references therein.
17. S.A. Gourley et al., Phys.Rev. Lett. 55 (1986) 2244.
18. T.A. Armstrong et al., Nucl. Phys. B262 (1985) 356.
19. A. Bravar et al., Phys. Rev. Lett. 75 (1995) 3073.
20. A. Bravar et al., Phys. Rev. Lett. 78 (1997) 4003.
21. C. Boros and Liang Zuo-tang, Phys. Rev. D53 (1996) R2279.
22. Liang Zuo-tang and C. Boros, Phys. Rev. Lett. 79 (1997) 3608.
23. D.L. Adams et al., Phys. Lett. B264 (1991) 462.
24. B.E. Bonner et al., Phys. Rev. D41 (1990) 13.
25. M.R. Doncel and A. Méndez, Phys. Lett. B41 (1972) 83.
26. G. Goldstein, these Proceedings.
27. R. Barni, G. Preparata and P.G. Ratcliffe, Phys. Lett. B296 (1992) 251.
28. J. Soffer and N.E. Törnqvist, Phys. Rev. Lett. 68 (1992) 907.
29. V.A. Apokin et al., Phys.Lett. B243 (1990) 461.
30. D.L. Adams et al., Phys. Rev. D53 (1996) 4747.
31. A.V. Efremov and O.V. Teryaev, Phys. Lett. B150 (1985) 383.
32. D. De Florian et al., Phys. Lett. B439 (1998) 176.

# HYPERON POLARIZATION NEWS

LEE G. PONDROM [a]

[a]University of Wisconsin
Madison, Wisconsin 53706

## 1. Introduction

Nature has no difficulty producing polarized hyperons. The phenomenon seems to be almost everywhere. While some experiments have been designed explicitly to study polarization, in many cases such studies have been ancillary to the main mission of the experiment. In this way information has been obtained on polarization in a wide variety of circumstances, involving proton, meson, and hyperon beams producing both hyperons and anti-hyperons.

The original discovery [1] of polarized $\Lambda$'s in $p \rightarrow \Lambda$ with $\vec{P}_\Lambda$ opposite to the normal to the production plane defined along $\vec{k}_{in} \times \vec{k}_{out}$ motivated early speculation that polarized s quarks with spin down plus SU(6) baryon wave functions could account for hyperon polarization. This led to $\vec{P}_\Lambda = \vec{P}_s$, and gave the correct signs for $\vec{P}_{\Sigma^+}, \vec{P}_{\Sigma^-}, \vec{P}_{\Xi^0}$, and $\vec{P}_{\Xi^-}$. However, experimentally the magnitude of $\vec{P}_{\Sigma^+} \sim -\vec{P}_\Lambda$ was too large for the model, which predicted $\vec{P}_{\Sigma^+} = -1/3\vec{P}_\Lambda$. In their model DeGrand and Miettinen (DG and M) [2] polarized the diquarks too to account for the large value for $\vec{P}_{\Sigma^+}$.

DG and M parametrized the single quark polarization with $\epsilon$, and the diquark polarization with $\delta$, and observed that to 20% accuracy experiment supported $\delta \sim \epsilon$. They summarized the experimental situation in a later paper [3] as shown in Table 1.

As seen from the Table, the DG and M model was quite comprehensive, and explained the pattern of known polarizations at that time rather well. Details such as the dependence of the polarization on kinematic variables were more difficult to explain quantitatively, but little was known in general except in the case of $p \rightarrow \Lambda$ [4].

Several experimental developments have occurred since that time. Some of the very recent measurements have been reported at this workshop [5]. Exclusive as well as inclusive channels have been studied; hyperon beams have been used as projectiles; spin exchange has been observed with polarized incident beams; anti-hyperon polarization has been observed; $\Lambda$ asymmetry has been observed from polarized protons; and last but not least, $\Lambda$ polarization has been studied at LEP from the decay $Z \rightarrow s\bar{s}$. Since many of these results are discussed elsewhere in these proceedings, this report will only touch on a selected subset.

## 2. Exclusive channels

Two new measurements have recently been reported. Results for $\Lambda$ polarization in $p + p \rightarrow \Lambda K^+ p$ at 800 GeV were given at this workshop by Christian [5]. A study at 27.5 GeV of $p + p \rightarrow \Lambda K^+ p + n(\pi^+\pi^-)$, where n=1 (5421 events), 2 (51195 events), 3 (48195 events), or 4 (14582 events), has recently been published [6]. These authors state that within statistical errors the $\Lambda$ polarizations in each exclusive channel can be adequately described by a single function $P_\Lambda = (-0.443 \pm 0.037) x_F \cdot p_t$, for $-1 \leq x_F \leq 1$, and $0 \leq p_t \leq 1.8$ GeV. Figure 1 shows this function scaled to the 400 GeV inclusive data of Heller, et al. [7]. The exclusive low energy polarization agrees well with the 400 GeV data for $x_F \leq 0.3$, but becomes larger at large x.

## 3. Hyperon beams as projectiles

Unpolarized hyperon beams have been used to search for polarization of produced hyperons. In some cases [8] [9] the main purpose of hitting a target with a hyperon beam was the production of charmed hadrons, and the hyperon studies were ancillary. One notable exception [10] was the use of a neutral hyperon beam to produce polarized $\Omega^-$. Here the ultimate goal was the successful measurement of the $\Omega^-$ magnetic moment, but interesting polarization data were obtained along the way. Their results are summarized in Table 2, which is taken from the Indiana Spin Conference

Table 1
Comparison of the asymmetries predicted by the model of DG and M with data from unpolarized beams as of 1985 with $\delta = \epsilon$

| Transition | Predicted | Observed | Energy(GeV) |
|---|---|---|---|
| $p \to \Lambda$ | $-\epsilon$ | 0.1 to 0.2 | 24-2000 |
| $p \to \Lambda$ | 0 | 0 | 24-2000 |
| $p \to \Sigma^+$ | $\epsilon$ | 0.1 to 0.2 | 400 |
| $p \to \Sigma^-$ | $\epsilon/2$ | 0.15 to 0.3 | 400 |
| $p \to \Xi^0$ | $-\epsilon$ | -0.1 to -0.2 | 400 |
| $p \to \Xi^-$ | $-\epsilon$ | -0.1 to -0.2 | 400 |
| $K^+ \to \Lambda$ | $\epsilon$ | $> 0.4, x > 0.3$ | 32,70 |
| $K^- \to \Lambda$ | $\epsilon$ | $> 0.4, x > 0.3$ | 32,70 |
| $\pi^- \to \Lambda$ | $-\epsilon/2$ | -0.05 | 18 |
| $\Sigma^- \to \Lambda$ | $-\epsilon/2$ | no data in 1985 | |
| Polarized $p \to \Lambda$ | no $\Lambda$ asymmetry | no data in 1985 | |

[11]. There are two angles listed in the Table: $\theta_1$ was the angle between the 800 GeV primary proton beam and the neutral beam, and $\theta_2$ was the angle between the neutral beam and the negative hyperon beam. The neutral beam was not polarized for $\theta_1 = 0$, but the $\Lambda$'s and $\Xi$'s were negatively polarized for $\theta_1 = 1.8$ mr. The polarization of the neutrons in the neutral beam was not measured, but was probably zero. So the first row represents the polarization of negative hyperons produced by unpolarized neutrals, while the second row represents spin transfer from polarized $\Lambda$ and $\Xi^0$ to $\Xi^-$ and $\Omega^-$.

The last row in the Table refers to direct production of the negative beam by 800 GeV/c protons. The value for $\vec{P}_{\Omega^-}$ in the lower right corner comes from Luk et al. [12]. The transfer of negative polarization from the neutral to the charged beam is sensible in the DG and M model. The positive polarization of the $\Omega^-$ in the first row of the Table cannot be explained by negatively polarized strange quarks, and therefore lies outside the model. The vanishing of the $\Xi^-$ polarization is also unexpected, but can be understood if the dominant component of the neutral beam for $\Xi^-$ production was $\Xi^0$.

New results for hyperon polarization by unpolarized $\Sigma^-$ have been reported at this workshop. Reference [9] used a 610 GeV $\Sigma^-$ beam to measure $\vec{P}_\Lambda$, while new data with a 340 GeV unpolarized $\Sigma^-$ beam have extended the earlier published results of WA89 [8]. Figure 2 shows the $\Lambda$ polarization results from two experiments combined. The results are consistent, and show an unambiguous positive polarization, in contradiction with the DG and M model.

## 4. Anti-hyperon polarization

Any sensible model would predict that protons produce unpolarized anti-hyperons. Nature cooperates in some instances, but not in others. New data were presented at the workshop from KTeV on the absence of polarization of $\Xi^0$'s [13]. The present experimental situation is summarized in Figure 3. The $\Omega^-$ result from Table 2 is also plotted, because it is another three quark exchange. The other references are: $\bar{\Sigma}$ [14]; $\bar{\Xi}$ [15]; and $\bar{\Lambda}$ [16]. Given that the two non-zero mirror image points on the plot are sensational, the new result of $\vec{P}_{\bar{\Xi}^0} = 0$ is equally mysterious.

## 5. $\Lambda$ asymmetry

The polarized proton should not transmit any of its spin information to the $\Lambda$, since the (u,d) quarks are in a singlet spin state. Figure 4 taken from Bravar et al [17] shows that this is not the case. Indeed, at large x the $\Lambda$ asymmetry resembles the polarization from unpolarized protons, an identity from elastic scattering!

## 6. $Z \to s + \bar{s}$

The decay of the Z is a wonderfully simple laboratory for the study of how quarks dress themselves to form colorless hadrons. The helicity of the s quarks is predicted by the Standard Model to be -91%. This very strong quark polarization has been studied by measuring the polarization of the $\Lambda$'s which result from the fragmentation of the quark. Both OPAL [18] and ALEPH [19] have published analyses based on a fragmentation model which calculates the fraction of hyperons

Table 2
Comparison of the asymmetries predicted by the model of DG and M with data from unpolarized beams as of 1985 with $\delta = \epsilon$

| $\theta_1$ | $\theta_2$ | $\vec{P}_{\Xi^-}$ | $\vec{P}_{\Omega^-}$ |
|---|---|---|---|
| 0. | 1.8 mr | $0.0062 \pm 0.0042$ | $0.053 \pm 0.012$ |
| 1.8 mr | 0. | $-0.1172 \pm 0.0062$ | $-0.076 \pm 0.021$ |
| no target | 1.8 mr | $-0.120 \pm 0.005$ | $-0.01 \pm 0.01$ |

containing the leading s quark as a function of $x_E$, the fraction of the $\Lambda$ momentum along the thrust axis of the event. Figure 5 shows the results from OPAL, and demonstrates that, within experimental errors, the s quark carries all of the spin of the $\Lambda$, and that the depolarization can be understood in terms of various contributions to the hyperon signal, rather than a depolarization of the leading quark itself during the fragmentation process. We may thus conclude that fragmentation does not depolarize the quarks.

It is possible that the fragmentation process creates a transverse component of the $\Lambda$ polarization, where the plane is defined by $\vec{p}_{jet} \times \vec{p}_\Lambda$. One can imagine that this plane is formed when the diquark attaches to the primary quark, thus deflecting the final hyperon. Studies of $Z \rightarrow$jet + jet have shown that when a baryon-antibaryon pair is produced, they tend to both be in the same hemisphere [20], so the picture of the diquark-antidiquark pair is reasonable. The hadronic reaction which might resemble the s quark fragmetation in Z decay is $K^- + p \rightarrow \Lambda$ in the beam fragmentation region, where large positive transverse $\Lambda$ polarization (consistent with the DG and M model) has been observed [21] in the range $x_F \sim 0.4$.

Unfortunately, no transverse polarization is observed [18]. Using our sign convention, their results are $P_T^\Lambda = (-0.9 \pm 0.9 \pm 0.3)\%$ for $p_t > .3 GeV/c$, where $p_t$ is defined as the $\Lambda$ momentum component normal to the jet thrust direction. The conclusion from this result is that the fragmentation process is not responsible for the observed polarization in $K^- \rightarrow \Lambda$.

## 7. Discussion

It is clear that high energy polarization phenomena are very diverse and quite common. The statement that several different mechanisms may be at work in different reactions may be true, but does not help synthesize the information. The DG and M model is successful at synthesis in many cases, but fails in others. An assumption of DG and M is that 'leading partons decelarate and acquire positive polarization, while trainling partons accelerate and acquire negative polarization'. Surely the s quark in the decay of the Z is a leading parton which decelarates to form the $\Lambda$, yet no transverse polarization was observed.

## REFERENCES


[1] G. Bunce, et al, Phys Rev Lett **36**, 1113(1976).
[2] T. DeGrand and H. Miettinen, Phys Rev D **23**, 1227 (1981), and Phys Rev D **31**, 661 (E),(1985).
[3] T. DeGrand, J. Markkanen, and H. Miettinen, Phys Rev D **32**, 2445(1985).
[4] For a review of the kinematic dependence of the $\Lambda$ polarization at about the same time see Lee Pondrom, Phys Rep **122**, 57(1985).
[5] See the reports in the New Results section of this workshop.
[6] J. Felix, et al, Phys Rev Lett **82**, 5213 (1999).
[7] K. Heller, et al, Phys Rev Lett **41**, 607 (1978).
[8] M Adamovich, et al (WA89 collaboration), Z Phys A **350**, 379 (1995). See also V.J. Smith, these proceedings, and David Newbold, PhD thesis, University of Bristol (1998).
[9] K.Nelson, et al (SELEX collaboration), these proceedings.
[10] D.M. Woods, et al, Phys Rev D **54**, 6610 (1996).
[11] L. Pondrom in AIP Conference Proceedings 343, High Energy Spin Physics Ed K Heller and S. Smith, New York (1995). p365.
[12] K. B. Luk et al., Phys Rev Lett **70**, 900 (1993).
[13] A. Erwin, these proceedings.
[14] A. Morelos, et al., Phys Rev Lett **71**, 2172 (1993).
[15] P.M. Ho et al., Phys Rev D **44** 3402 (1991).
[16] E.J.Ramberg et al., Phys Lett B **338**, 403 (1994).
[17] A. Bravar, et al., Phys Rev Lett **75**, 3073 (1995).

[18] K. Ackerstaff et al. (OPAL collaboration), Eur Phys J C2, 49 (1998).
[19] D. Buskulic et al. (ALEPH collaboration), Phys Lett B **374**, 319 (1996).
[20] P. Acton et al. (OPAL collaboration), Phys Lett B **305**, 415 (1993).
[21] S. Gourlay et al., Phys Rev Lett **56**, 2244 (1986). These authors use the opposite sign convention for the polarization.

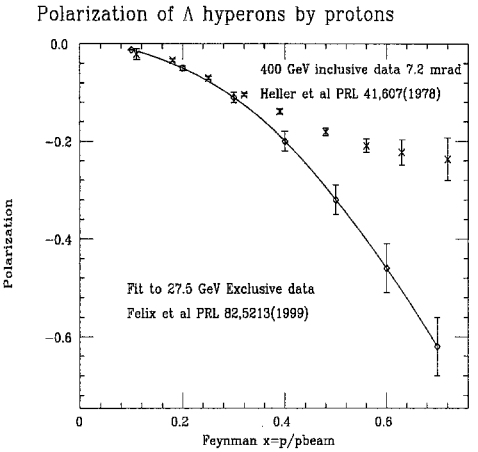


Figure 1. Comparison of the functional fit to the exclusive data of Felix et al [6] with the early inclusive data of Heller [7]

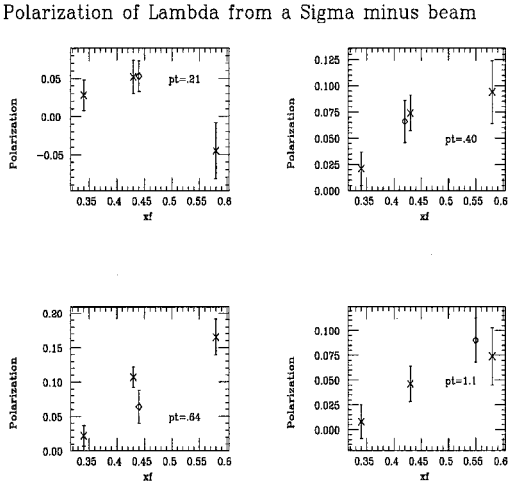


Figure 2. $\vec{P}_\Lambda$ from a $\Sigma^-$ beam. Selex (x's) and WA89 (open squares) data plotted.

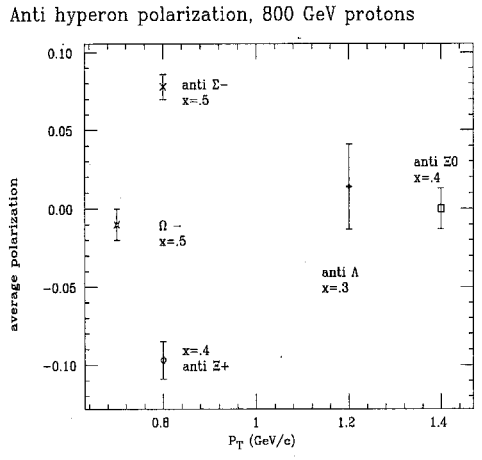


Figure 3. Plot of the average polarizations of anti hyperons produced by 800 GeV protons

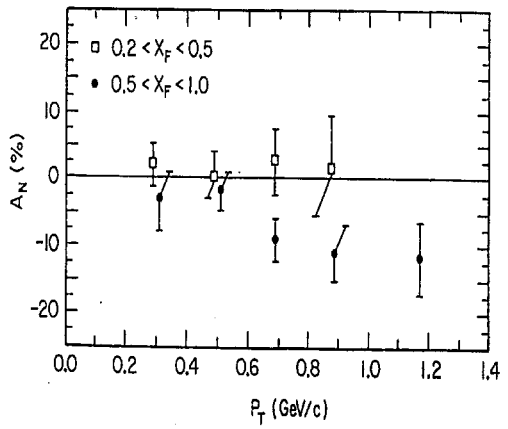


FIG. 4. $A_N$ data for $p\uparrow + p \rightarrow \Lambda^0 + X$ as a function of $p_T$.

Figure 4. Plot of the $\Lambda$ asymmetry from polarized protons

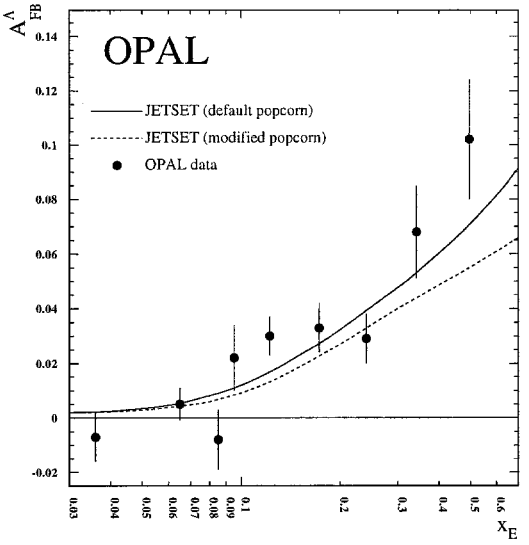


Figure 5. Lambda helicity as a function of $x_E$ as a measure of s quark helicity in $Z \rightarrow \bar{s}s$

# Polarization of Inclusive $\Lambda_c$'s in a Hybrid Model

Gary R. Goldstein [a*]

[a]Department of Physics, Tufts University
Medford, MA 02155

A hybrid model is presented for hyperon polarization that is based on perturbative QCD subprocesses and the recombination of polarized quarks with scalar diquarks. The updated hybrid model is applied to $p+p \to \Lambda + X$ and successfully reproduces the detailed kinematic dependence shown by the data. The hybrid model is extended to include pion beams and polarized $\Lambda_c$'s. The resulting polarization is found to be in fair agreement with recent experiments. Predictions for the polarization dependence on $x_F$ and $p_T$ is given.

## 1. INTRODUCTION

Inclusively produced strange hyperons can have sizeable polarization [1] over a wide range of energies. Evidence now indicates that charmed hyperons also have sizeable polarization [2,3]. Many theoretical models have been proposed to explain various aspects of hyperon polarization data with varying success [4–6]. All try to explain the large negative $\Lambda$ polarization. Because the hyperon data is in the region of high CM energy but relatively small transverse momentum ($p_T \sim 1$ GeV/c), soft QCD effects should play a major role in any theoretical explanation. Several years ago Dharmaratna and Goldstein developed a hybrid model for $\Lambda$ polarization in inclusive reactions [7]. The model involves hard scattering at the parton level, gluon fusion and light quark pair annihilation, to produce a polarized heavy quark which then undergoes a soft recombination that, in turn, enhances the polarization of the hyperon. This scheme provided an explanation for the characteristic kinematic dependences of the polarization in $p+p \to \Lambda + X$. The use of perturbative QCD to produce the initial polarization for strange quarks, with their low current or constituent quark mass (compared to $\Lambda_{QCD}$) made the application of perturbation theory marginal, however.

In the heavy quark realm the perturbative contribution is more reliable. Given these circumstances, I have modified the original hybrid model to apply to heavy flavor baryons produced inclusively from either proton or pion beams. The results are encouraging, as the following will show (see ref. [8] for a more complete treatment).

*This work is supported in part by funds provided by the U.S. Department of Energy (D.O.E.) #DE-FG02-92ER40702.

## 2. HYBRID MODEL

All of the models for $\Lambda$ polarization begin with the observation that $Q$-flavor hyperons of the type $\Lambda_Q \sim [ud]Q$ have their polarization carried primarily by the $Q$; the [ud] must be a color antitriplet isospin 0 spin scalar diquark (to the extent that *gluons* + **L** + *sea* contributions can be ignored). How does the $Q$ itself get polarized in a production process? Consider $parton + parton \to Q_\uparrow + \bar{Q}$. At tree level in QCD, there can be no single quark polarization for these two-body subprocesses, all diagrams being relatively real. This can be seen when the polarization is written in terms of helicity amplitudes $f_{a,b,c,d}$ for particles $A + B \to C + D$ as

$$\begin{aligned} \mathcal{P}_Q &\propto \sum_{a,b,d} f^*_{a,b;c,d} f_{a,b;c',d} (\sigma \cdot \hat{\mathbf{n}})_{c,c'} \\ &\propto Im \sum f_{a,b;+,d} f^*_{a,b;-,d}, \end{aligned} \tag{1}$$

where $\hat{\mathbf{n}}$ is the normal to the scattering plane. Hence there has to be a phase difference and a flip–non-flip interference. In QCD with zero quark masses there are only non-flip vertices; helicity flip requires non-zero quark masses. And a relative imaginary part only arises beyond tree level [9]. So the hybrid model incorporates the order $\alpha_s^2$ QCD perturbative calculation of interference between tree level and the large number of one loop diagrams to produce massive heavy quark polarization. (Only the imaginary parts of the one loop diagrams were needed, so the Cutkosky rules were used to simplifiy the calculation. For the lengthy results see ref. [10,11] as well as an independent calculation in ref. [12].) This gives rise to significant polarization [11], proportional to $\alpha_s(Q^2)$ and to complicated functions of the constituent quark mass. The scale here is

$Q^2 \sim m_Q^2 \gg \lambda_{QCD}^2$. The results are illustrated in fig. 1 for the $g+g \to Q_\uparrow + \bar{Q}$ case, with CM energy 26 GeV and outgoing quark flavors $Q = d, s, c, b$. The symmetry requires $\mathcal{P}(\pi - \theta) = -\mathcal{P}(\theta)$, so backward $Q$ has $\mathcal{P} < 0$. The magnitude of $\mathcal{P}$ reaches $\sim 6\%$ for the b-quark. It is clear that the polarization increases roughly as the quark mass. Similar results are obtained for $q + \bar{q} \to Q_\uparrow + \bar{Q}$.

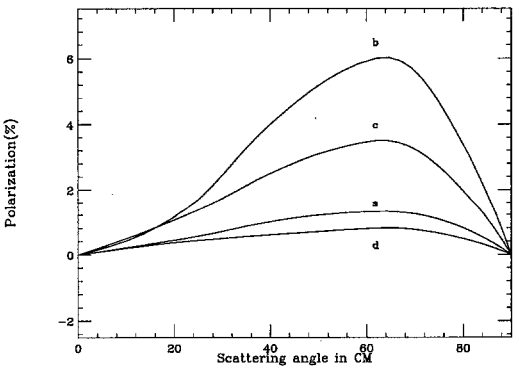


Figure 1. Polarization for the QCD subprocess of gluon fusion to quark pairs. The curves are for d, s, c, b quarks.

The cross sections for polarized $Q$-quarks (polarized normal to the production plane) must then be convoluted with the relevent structure functions for the hadronic beam and target. The inclusive cross section for *hadron + hadron* $\to Q(\uparrow \text{ or } \downarrow) + X$ is obtained thereby. For protons on protons gluon fusion is the more significant subprocess.

The hadronization process, by which the polarized $Q$ recombines with a [ud] diquark system to form a $\Lambda_Q$, is crucial for understanding the subsequent hadron polarization. The backward moving, negatively polarized heavy quark must be accelerated to recombine with a fast moving diquark (resulting from remnants of the $pp$ or $\pi p$ collision) to form the hadron with particular $x_F$ while preserving the quark's $p_T$ value. Letting $x_Q$ be the Feynman $x$ for the heavy quark, the simple form, a linear mapping of the $Q$ kinematic region,

$$x_F = a + b x_Q \tag{2}$$

is used for the recombination. Naively, if the Q has 1/3 of the final hyperon momentum (in its infinite momentum frame) and the diquark carries 2/3 of that momentum, then $a = 2/3$ and $b = 1$. The values actually used, $a = 0.86$ and $b = 0.70$, were chosen to fit the $pp \to \Lambda + X$ data (that existed in 1990) at one $x_F$ value. These parameters in eqn. 2 are not far from the naive expectation.

This recombination prescription is similar to the semi-classical dynamical mechanism used in the "Thomas precession" model of hyperon polarization [5], which posits that the s-quark needs to be accelerated by a confining potential or via a "flux tube" [6] at an angle to its initial momentum in order to join with the diquark to form the hyperon. The skewed acceleration gives rise to a spin precession for the s-quark. With the precession rate, $\omega_\mathbf{T} = (\gamma - 1)\mathbf{v} \times \mathbf{a}/v^2 \propto \mathbf{p_Q} \times \mathbf{\Delta p_L} \sim -\hat{\mathbf{n}}$, an energy shift $-\mathbf{S} \cdot \omega_\mathbf{T} \propto +\mathbf{S} \cdot \hat{\mathbf{n}}$ occurs. Hence negative values of $\langle \mathbf{S} \cdot \hat{\mathbf{n}} \rangle$ are energetically favored. In the Hybrid Model the $Q$ has acquired negative polarization already from the hard subprocess before it is accelerated in the hadronic recombination process. That "seed" polarization gets enhanced by a multiplicative factor $A \simeq 2\pi$ which simulates the Thomas precession. The Hybrid Model combines hard perturbative QCD with this simple model for non-perturbative recombination.

In summary, the hyperon polarization is given as

$$\mathcal{P}_{\Lambda_Q}(x_F, p_T) = A \cdot \mathcal{P}_Q(x_Q(x_F), p_T) \tag{3}$$

for each reaction $g(x_1) + g(x_2)$ or $q(x_1) + \bar{q}(x_2) \to Q\bar{Q}$, with the mapping function $x_Q(x_F)$ obtained by inverting eqn. 2. From eqn. 3 the subprocess polarized cross sections,

$$\frac{d^2\sigma(\uparrow \text{ and } \downarrow)_{i,j}}{dx_Q dp_T} \tag{4}$$

for partons $(i, j)$ at $(x_1, x_2)$ can be obtained. These cross sections are convoluted with the gluon, quark and antiquark structure functions for the proton and pion [13], $g^{p,\pi}(x), q^{p,\pi}(x), \bar{q}^{p,\pi}(x)$, or generically $f_i^{p,\pi}(x)$ leading to

$$\frac{d^2\sigma(\uparrow \text{ and } \downarrow)}{dx_Q dp_T} = \sum_{i,j} \int_0^1 dx_1 \int_0^1 dx_2 f_i^{p,\pi}(x_1) \cdot f_j^p(x_2) \frac{d^2\sigma(\uparrow \text{ and } \downarrow)_{i,j}}{dx_Q dp_T}. \tag{5}$$

Next the recombination formula, eqn. 2, is applied to obtain the corresponding $\Lambda_Q$ polarized

cross section at $x_F(= a + bx_Q)$ and $p_T$. The polarization is obtained via

$$\mathcal{P}_{\Lambda_Q}(x_F, p_T) = A\frac{d^2\sigma(\uparrow) - d^2\sigma(\downarrow)}{d^2\sigma(\uparrow) + d^2\sigma(\downarrow)}, \quad (6)$$

in an obvious notation.

Note that the linear form of eqn. 2 maps the $Q$-quark Feynman x region $[-1, (1-a)/b]$ into the $x_F$ region $[(a-b), +1]$ for the $\Lambda_Q$. The $p+p \to Q$ differential cross section, $d^2\sigma/dx_Q dp_T$ is mapped correspondingly into the $p+p \to \Lambda_Q$ cross section $d^2\sigma/dx_F dp_T$. The measured cross sections for the latter are known to fall with positive $x_F$ and to fall precipitously with $p_T$, roughly as

$$(1 - x_F)^\alpha e^{-\beta p_T^2} \quad (7)$$

overall [2], where $\alpha$ and $\beta$ are greater than 1.0 (for $\pi + p \to \Lambda + X$ $\alpha, \beta \approx 3.0$). However, the directly computed lowest order p+p→s-quark cross section grows with $x_Q$ in the region (-1,0) and it falls more gradually with $p_T$ than the exponential in eqn. 7. Hence the more complete recombination scheme would have to temper the $x_F$ dependence and narrow the $p_T$ distribution. This will not affect the polarization calculation, though, since the individual up or down polarized cross sections will be alterred in the same way. For a more thorough calculation this should be done, and work is underway on this point. The polarization results are the focus of this work.

## 3. COMPARISON WITH DATA AND PREDICTIONS

Applied to strange $\Lambda$ production, the hybrid model reproduces the detailed $(x_F, p_T)$ dependence of the data, with very slow energy dependence [14], as fig. 2 shows.

Note that an estimated 20 to 30% of the $\Lambda$'s come from $\Sigma^0 \to \gamma\Lambda$ [15], so the parameter $A$ in eqn. 6 is increased to 7.9. The agreement of the hybrid model with the wide range of data is excellent.

It is worth remarking that recently extensive data have been collected on $\Lambda$ polarization in many *exclusive* reactions [17], for which a simple form, $P = (-0.443 \pm 0.037)x_F p_T$, approximates all the polarization data at $p_{lab} = 27.5$ GeV/c. That form provides lower bracketing values for the inclusive polarization, as fig. 2 indicates. In the hybrid model all the final states other than the $\Lambda$ arise from the hadronization of the $\bar{s}$-quark and the remains of the incoming baryons. Therefore, in the hybrid model it would be anticipated

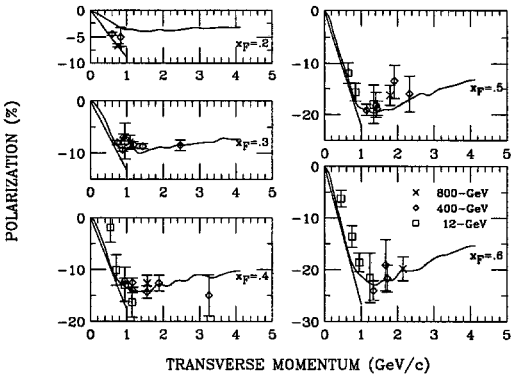


Figure 2. Hybrid model $\Lambda$ polarization in $p + p \to \Lambda + X$ as a function of $p_T$ for various values of $x_F$. The data at 12 GeV [14], 400 GeV [15], 800 GeV [16] are shown. Exclusive data at 27.5 GeV/c [17] is approximated by the straight line from the origin to $p_T \approx 1$ GeV/c.

that as the beam energy increases and/or more final states are included in the determination of the $\Lambda$ polarization, more complicated final states will be accompanied by much lower polarization as $p_T$ increases beyond 1 GeV/c.

In turning to $\Lambda_c$ production, there is a straightforward scaling up that occurs in the $\mathcal{P}$ equations for $g + g$ and $q + \bar{q} \to c\uparrow + \bar{c}$. The seed polarization increases by $\sim 3$. The recombination with a fixed force/mass should have the same Thomas factor, but the overall recombination could scale as $M_{hadron}$, so a factor of $M_{\Lambda_c}/M_\Lambda \sim 2$ could apply. The scaled polarization in the reaction $\pi + p \to \Lambda_c \uparrow + X$ is obtained from the convolution of eqn. 5 with the $\pi$ structure functions for the beam [13]. The predicted kinematic dependences for $\mathcal{P}(x_F, p_T)$ are shown in fig. 3 (without the hadron mass enhancement). Integrating over $x_F$ from -0.2 to +0.6 allows the comparison with the data of E791 [3,18], as fig. 4 shows. The lower curve has taken the additional factor of 2 that could apply to the scaling of the recombination. The higher curve does not have that factor and gives a poorer fit, albeit not far from the large uncertainties in the data points.

## 4. CONCLUSION

In conclusion, these results are encouraging for the hybrid model. The Thomas enhanced gluon fusion model has been modified to include quark-

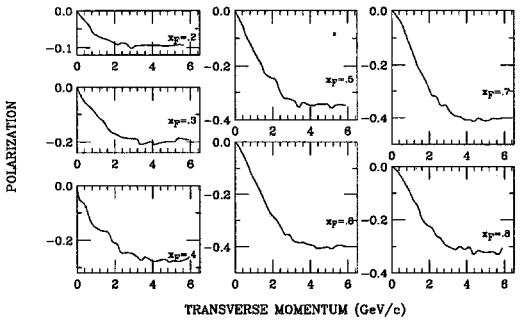


Figure 3. $\Lambda_c$ polarization in $\pi^- + p \to \Lambda_c + X$ as a function of $p_T$ for various values of $x_F$. Multipying these polarizations by $m(\Lambda_c)/m(\Lambda)$ will incorporate the hadron mass enhancements as in fig. 4.

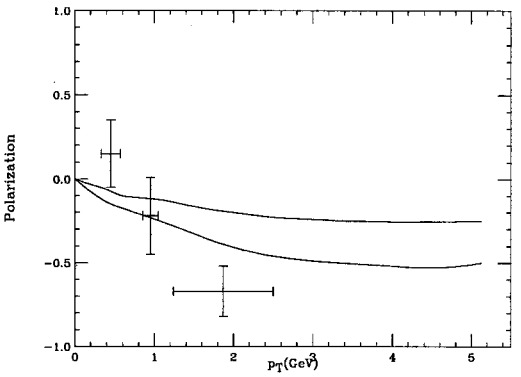


Figure 4. Estimate of $\Lambda_c$ polarization from $\pi^- p \to \Lambda_c + X$. The larger polarization includes heavy mass enhancements. The preliminary data [3] is from E791.

anti-quark annihilation, which should be more prominent for heavy baryon polarization in pion induced reactions, like the above $\pi^- + p \to \Lambda_c + X$. Experimental data can be analyzed into $x_F$ as well as $p_T$ bins, so the predictions from the hybrid model can be checked in detail. It is important to realize that the results for the $\Lambda_c$ were obtained without changing the parameters of the model that had been applied to the strange hyperons. Aside from the possible enhancement in $A$, everything else was simply scaled up by quark mass. This gives further credence to the results herein.

The somewhat *ad hoc* prescription for the recombination is being studied further in order to accommodate both the polarization and the cross section behavior of eqn. 7, with the kinematic variables $x_F$ and $p_T$. The overall factor $A$ may have some dependence on those variables as well, given that the semi-classical Thomas precession may have such dependence. Furthermore, an investigation of other hyperon production reactions, involving $\Sigma, \Sigma_c$, and $\Xi$, for example, is underway. Will $\bar{p} + p \to \Lambda + X$ carry significant, near energy independent polarization at collider energies? Can photoproduction of $\Lambda$ produce large polarizations also? These can be answered within the hybrid model.

The related strange meson asymmetries in $p \uparrow + p \to K$ or $\pi$ or $\Lambda$ will be investigated in future work as well.

## 5. ACKNOWLEDGMENTS

The author thanks Austin Napier and appreciates correspondence with members of E791, particularly M.V. Purohit, G.F. Fox and J.A. Appel. He is grateful to the organizers of Hyperon99 for inviting him and for producing a lively conference.

## REFERENCES

1. K. Heller, *"Inclusive hyperon polarization: a review" in* Proceedings of the 6th International Symposium on High Energy Spin Physics, Marseille, edited by J. Soffer, Les Editions de Physique (1985), p.C2-121.
2. S. Barlag, *et al.* (ACCMOR Collaboration), Phys.Lett. **B325**, 531 (1994).
3. E.M. Aitala, *et al.* (E791 Collaboration) *"Multidimensional Resonance Analysis of* $\Lambda_c^+ \to pK^-\pi^+$*"*, preprint, Fermilab 1999; M.V. Purohit, contribution to this symposium.
4. J. Szwed, Phys. Lett. **105B**, 403 (1981); S.M. Troshin and N.E. Tyurin, Sov. J. Nucl. Phys. **38**, 693 (1983); *ibid*, Phys. Rev. **D55**, 1265 (1997); J. Soffer and N.E. Törnqvist, Phys. Rev. Lett. **68**, 907 (1992).
5. T.A. De Grand and H.I. Miettinen, Phys. Rev. **D24** 2419 (1981).
6. B. Andersson, G. Gustafson, and G. Ingelman, Phys. Lett. **B85** 417 (1979).
7. W.G.D.Dharmaratna and Gary R. Goldstein,

Phys. Rev. **D41** 1731 (1990).
8. Gary R. Goldstein, preprint hep-ph/9907573 (1999).
9. G.L. Kane, J. Pumplin and W. Repko, Phys. Rev. Lett. **41** 1989 (1978).
10. W.G.D. Dharmaratna, *"Massive Quark Polarization in Quantum Chromodynamics Subprocesses"*, Ph.D. dissertation, Tufts University (1990).
11. W.G.D.Dharmaratna and Gary R. Goldstein, Phys.Rev. **D53** 1073 (1996).
12. W. Bernreuther, A. Brandenburg and P. Uwer, Phys. Lett. **B368**, 153 (1996).
13. D.W. Duke and J.F. Owens, Phys. Rev. **D30**, 49 (1984).
14. K. Heller, *et al.*, Phys. Rev. Lett. **41** 607 (1978).
15. B. Lundberg, *et al.*, Phys.Rev. **D40** 3557 (1989).
16. E.J. Ramberg, *et al.*, Phys. Lett. **B338** 404 (1994).
17. J. Félix, *et al.*, Phys. Rev. Lett. **82** 5213 (1999).
18. G.F. Fox, private communication.

# Strange particle production by $\Sigma^-$, $\pi^-$ and neutrons in WA89

The WA89 Collaboration*, presented by Ulrich Müller [a]

[a] Institut für Kernphysik, Universität Mainz, 55099 Mainz, Germany

We report on results on strange particle production obtained by the WA89 CERN hyperon beam experiment. The inclusive production cross sections for $\Sigma^{\pm}$, $\Sigma^{\pm}(1385)$ and $\Sigma^{\pm}(1670)$ hyperons have been measured; a strong leading effect was observed for all negative $\Sigma$ hyperons. Differential and total cross sections of $\Xi^*$ resonances have been measured. The first observation of the $\Xi(1690) \rightarrow \Xi^-\pi^+$ decay mode confirms the existence of this resonance. For simultaneously produced $\Lambda\Lambda$ pairs, correlations in $x_F$ were studied: clear deviations from the assumption of independent production are seen. The differential cross sections of $\Lambda$ and $K$ particles show strong non-gaussian and non-thermal enhancements at large transverse momenta $p_T$. In a search for the $U(3100)$ particle, no signal was observed.

## 1. Introduction

The main physics goals of WA89 can be summarized as follows:

- Production and properties of charmed baryons: $\Lambda_c$, $\Sigma_c$, $\Xi_c$, $\Omega_c$;
- Search for exotic states: $U(3100)$, Hexaquark $H$;
- Production of hyperons and hyperon resonances: $\Lambda$, $\Sigma$, $\Xi$;
- Hyperon polarization.

The experiment was performed at the CERN Omega spectrometer facility between 1990 and 1994. In this report we will concentrate on results obtained for strangeness production.

An overview of the WA89 charm and polarization results and results from previous hyperon beam experiments at CERN have already been presented by V. J. Smith [1].

### 1.1. Hyperon beam and apparatus

The hyperon beam was derived from an external proton beam of the CERN-SPS, hitting a hyperon production target placed 16 m upstream of the experimental target. Negative secondaries with a mean momentum of 345 GeV/c and a momentum spread $\sigma(p)/p \approx 9\%$ were selected in a magnetic channel. The production angles relative to the proton beam were smaller than 0.5 mrad. At the experimental target, the beam consisted of $\pi^-$, $K^-$, $\Sigma^-$ and $\Xi^-$ in the ratio 2.3 : 0.025 : 1 : 0.008. A transition radiation detector (TRD) made up of 10 MWPCs interleaved with foam radiators allowed to suppress $\pi^-$ at the trigger level. Typically, about $1.8 \cdot 10^5$ $\Sigma^-$ and $4.5 \cdot 10^5$ $\pi^-$ were delivered to the target during one SPS-spill, which had an effective length of about 1.5 s.

$\Sigma^-$ decays upstream of the target were a source of neutrons used in our measurement as a neutron beam. The momenta of these neutrons were defined as the difference between the average $\Sigma^-$ momentum and the momentum of the associated $\pi^-$ measured in the spectrometer. The neutron spectrum has an average momentum of 260 GeV/c and a width of $\sigma(p)/p = 15\%$. More details can be found in [2].

The setup of the experiment is shown in Fig. 1. The experimental target consisted of one copper and three carbon blocks arranged in a row along the beam, with thicknesses corresponding to $0.026\,\lambda_I$ and three times $0.0083\,\lambda_I$, respectively. At the target, the beam had a width of 3 cm and a height of 1.7 cm (FWHM). Microstrip detectors upstream and downstream of the target allowed to measure the tracks of the incoming beam particle and of the charged particles produced in the target blocks. The target was positioned 14 m upstream of the centre of the Omega spectrometer magnet [3] so that a field-free decay region of 10 m length was provided for hyperon and $K_S$ decays. Tracks of charged particles were measured inside the magnet and in the field-free regions upstream and downstream by MWPCs and drift chambers, with a total of 130 detector planes. The Omega magnet provided a field integral of 7.5 Tm, and the momentum resolution achieved was $\sigma(p)/p^2 \approx 10^{-4}\,(\mathrm{GeV/c})^{-1}$.

*Supported by the Bundesministerium für Bildung, Wissenschaft, Forschung und Technologie, Germany, under contract numbers 05 5HD15I, 06 HD524I and 06 MZ5265.

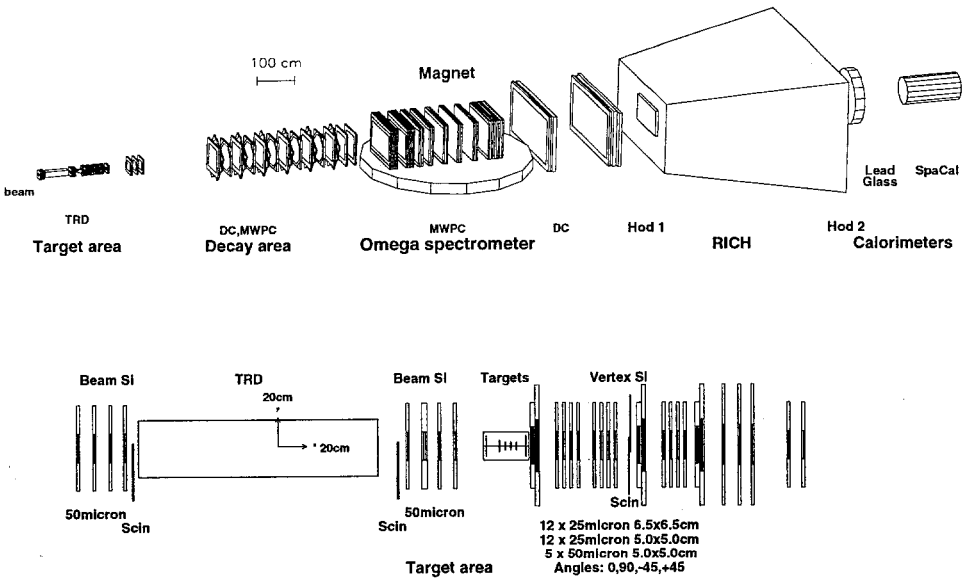


Figure 1. Setup of the WA89 experiment in the 1993 beam time. The lower part shows an expanded view of the target area.

Downstream of the spectrometer, a ring-imaging Cherenkov detector [4], an electromagnetic calorimeter and a hadron calorimeter (SPACAL) [5] were placed. The hadron calorimeter was used for the identification of neutrons coming from $\Sigma^{\pm} \to n\pi^{\pm}$ decays.

The main trigger selected about 25% of all interactions, using multiplicities measured in microstrip counters upstream and downstream of the target and in scintillator hodoscopes and MWPCs behind the Omega magnet. Correlations between hits in different detectors were used in the trigger to increase the fraction of events with high-momentum particles, thus reducing background from low-momentum pions in the beam. Part of statistics was obtained with a pion trigger. In addition, a reduced sample of beam triggers was recorded for trigger calibration purposes.

The results presented here are based on 100 million events recorded in 1993.

A summary on the measurements of total inclusive production cross sections for hyperons and kaons produced by $\Sigma^-$, neutrons and $\pi^-$ beam particles is given in Tab. 1.

## 2. First observation of the $\Xi^0(1690) \to \Xi^-\pi^+$ decay mode

More than three decades after the first observations of excited states of hyperons, the excited states of $\Xi^-$ and $\Omega^-$ are still largely unexplored. Of the $\Xi^*$ states, only the $\Xi(1530)$ rates four stars in the PDG ranking. Four other states, including the $\Xi(1690)$, rate three stars [6].

First evidence for the $\Xi(1690)$ came from threshold enhancements in $\Sigma\overline{K}$ and $\Lambda\overline{K}$ mass spectra, observed in a bubble chamber experiment using a $K^-$ beam [7]. The first direct observation as a resonance in the $\Lambda K^-$ spectrum resulted from a previous hyperon beam experiment at CERN [9,8].

In the framework of the non relativistic quark potential model, a $\Xi(1/2^+)$ state was predicted with a mass around 1690 MeV/c$^2$, with dominating $\Xi\pi$ decay [10]. A relativistic version of this model, however, pushed the first excited $\Xi(1/2^+)$ to about 1800 MeV/c$^2$ [11], and left no state to be identified with the observed $\Xi(1690)$. Also within a more recently developed chiral boson exchange interaction model the $\Xi(1/2^+)$ state is expected at an energy far above 1690 MeV/c$^2$ and close to 1800 MeV/c$^2$ [12].

In our measurement [13], events were selected as follows: The $\Xi^-$ candidates were selected by

| Particle | Copper $\sigma$/mb | Carbon $\sigma$/mb |
|---|---|---|
| $\Xi^-$ | $16.72 \pm 0.21$ | $5.4 \pm 0.07$ |
| | $10.3 \pm 0.4$ | $2.3 \pm 0.1$ |
| | $4.1 \pm 0.2$ | $0.9 \pm 0.05$ |
| $\Xi^0(1530)$ | $4.3 \pm 0.9$ | $1.3 \pm 0.26$ |
| $\overline{\Xi}^+$ | $0.64 \pm 0.01$ | $0.18 \pm 0.01$ |
| | $1.4 \pm 0.3$ | $0.3 \pm 0.1$ |
| | $1.4 \pm 0.2$ | $0.5 \pm 0.2$ |
| $\Omega^-$ | $0.80 \pm 0.01$ | $0.21 \pm 0.01$ |
| $\Sigma^-$ | $123.8 \pm 3.22$ | $46.16 \pm 1.12$ |
| $\Sigma^+$ | $39.78 \pm 1.9$ | $12.25 \pm 0.68$ |
| $\Sigma^-(1385)$ | $27.01 \pm 0.43$ | $10.20 \pm 0.15$ |
| | $25.1 \pm 1.8$ | $8.3 \pm 0.5$ |
| | $5.3 \pm 0.5$ | $1.8 \pm 0.1$ |
| $\Sigma^+(1385)$ | $14.45 \pm 0.26$ | $5.29 \pm 0.09$ |
| | $9.2 \pm 1.1$ | $2.69 \pm 0.3$ |
| | $3.9 \pm 0.4$ | $1.0 \pm 0.1$ |
| $\overline{\Sigma}^-(1385)$ | $1.49 \pm 0.12$ | $0.42 \pm 0.03$ |
| $\Sigma^-(1660)$ | $23.02 \pm 0.35$ | $8.89 \pm 0.13$ |
| $\Sigma^+(1660)$ | $11.32 \pm 0.2$ | $4.04 \pm 0.07$ |
| $\Lambda$ | $109.97 \pm 4.12$ | $41.26 \pm 1.51$ |
| | $55.56 \pm 2.49$ | $18.14 \pm 0.78$ |
| | $25.52 \pm 0.89$ | $8.29 \pm 0.29$ |
| $K^0$ | $66.52 \pm 3.70$ | $22.25 \pm 1.2$ |
| | $52.14 \pm 3.24$ | $16.61 \pm 1.01$ |
| | $58.99 \pm 1.6$ | $19.09 \pm 0.55$ |
| $\overline{\Lambda}$ | $6.99 \pm 0.47$ | $2.21 \pm 0.15$ |
| | $7.65 \pm 0.58$ | $2.39 \pm 0.19$ |
| | $12.55 \pm 0.7$ | $3.89 \pm 0.20$ |
| $K^-(890)$ | $34.7 \pm 0.8$ | $12.0 \pm 0.3$ |
| | $13.15 \pm 2.$ | $5.7 \pm 1.$ |
| | $24.9 \pm 1.4$ | $8.4 \pm 0.5$ |
| $K^+(890)$ | $11.7 \pm 0.6$ | $4.4 \pm 0.2$ |
| | $15.5 \pm 2.2$ | $4. \pm 0.5$ |
| | $12.2 \pm 0.9$ | $4.8 \pm 0.4$ |

Table 1
Preliminary production cross sections for different particles. The cross sections for production by $\Sigma^-$, neutron, and $\pi^-$ beam particles are given, respectively, if three rows are listed. Otherwise, only the cross section for the $\Sigma^-$ beam is listed in a single row. Only statistical uncertainties are given.

their decay cascade $\Xi^- \to \Lambda\pi^-$, $\Lambda \to p\pi^-$, where a $3\sigma$ cut on the reconstructed $\Lambda$ and $\Xi^-$ masses was applied. Furthermore, the measured track of the $\Xi^-$ candidate in the vertex detector had to agree within errors with the $\Xi^-$ momentum direction and decay vertex position reconstructed from its $\Lambda\pi^-$ daughter particles.

The invariant $\Xi^-\pi^+$ mass distribution for all combinations of $\Xi^-$ candidates with positively charged particles from the interaction vertex is shown in Fig. 2 a. The mass spectrum is dominated by the $\Xi^0(1530)$ peak. In the mass region between 1600 and 1800 MeV/c$^2$ (Fig. 2 b and c), a resonance signal with a number of $1400 \pm 300$ observed events is visible above a large background.

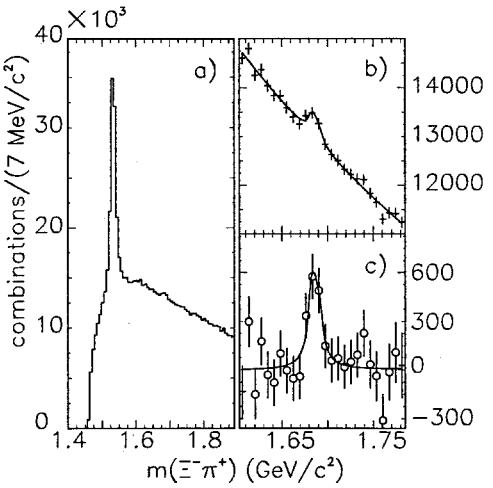


Figure 2. Invariant $\Xi^-\pi^+$ mass distribution: a) the $\Xi^0(1530)$ and $\Xi^0(1690)$ mass region; b) the $\Xi^0(1690)$ mass region only; c) the $\Xi^0(1690)$ mass region after background subtraction.

We measure a mass and intrinsic width of the resonance of $M = 1686 \pm 4\,\mathrm{MeV/c^2}$, $\Gamma = 10 \pm 6\,\mathrm{MeV/c^2}$. For the product of cross section and branching ratio, we obtain

$$\frac{\sigma \cdot BR(\Xi^0(1690))}{\sigma \cdot BR(\Xi^0(1530))} = 0.022 \pm 0.005$$

in the region of our acceptance $x_F > 0.1$, corresponding to $\sigma \cdot BR = 6.8 \pm 0.2\,\mu$b/nucleon.

A check for possible reflections from a $\Xi^- K^+$ state was performed by selecting $K^+$ with the RICH detector, and taking them as $\pi^+$ candidates. The $\Xi^-\pi^+$ mass spectrum obtained in this

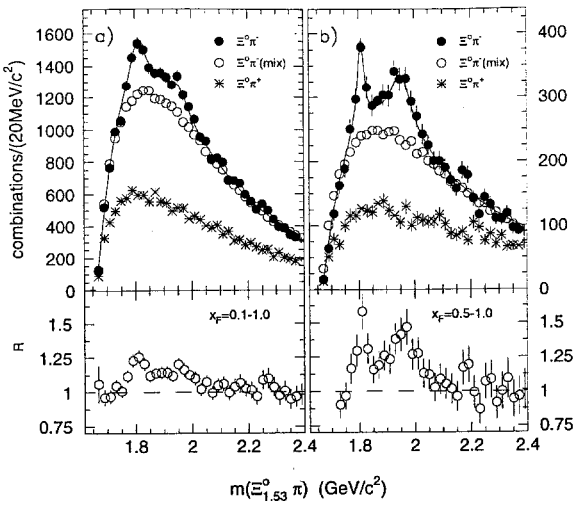


Figure 3. The $\Xi^-\pi^+\pi^-$ invariant mass distribution in different $x_F$ regions. Open circles: fake events generated by 'event mixing'; stars: background shape from 'wrong sign' ($\Xi^-\pi^+\pi^+$) combinations. Bottom part: ratio of observed spectra and background from event mixing.

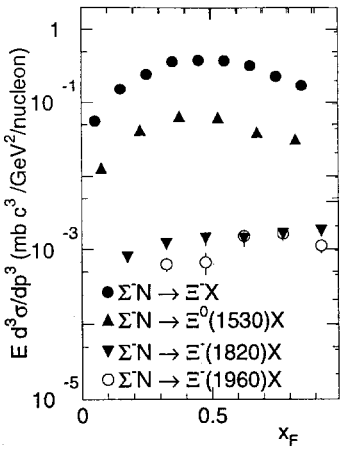


Figure 4. Invariant cross sections per nucleon of inclusive $\Xi^-$ and $\Xi^*$ production by $\Sigma^-$.

way contains about 4% of the total sample and shows no resonant structure.

## 3. Production of Ξ resonances

Only few data on the production of $\Xi^*$ resonances in hyperon beams exist so far [9,14,15]. In the present experiment, the differential and total cross sections of inclusive production of the $\Xi^0(1530)$, $\Xi^0(1690)$, $\Xi^-(1820)$, $\Xi^-(1950)$ resonances have been measured.

For this analysis [16], $\Xi^-$ candidates were selected in a similar way as described in Section 2. For the study of $\Xi^{-*} \to \Xi^0(1530)\pi^-$ decays, $\Xi^0(1530)$ candidates were selected from combinations of a $\Xi^-$ candidate with a positive particle emerging from the interaction vertex.

In Fig. 3, the $\Xi^-\pi^+\pi^-$ invariant mass distribution for combinations of a $\Xi^0(1530)$ candidate with a negative particle is shown for $x_F > 0.1$ (a) and $x_F > 0.5$ (b). A clear signal at 1820 MeV/c$^2$ and a second wider peak at about 1960 MeV/c$^2$ are visible. Masses and width are in good agreement with earlier experiments.

Figure 4 shows the differential cross sections per nucleon for the $\Xi^-$ hyperon and for the $\Xi^0(1530)$, $\Xi^-(1820)$ and $\Xi^-(1950)$ resonances.

The cross section for inclusive $\Xi^0(1530)$ production is about a factor of 5 below that of $\Xi^-$ hyperons. The products of cross section and branching ratio for the observed channels $\Xi^0(1690) \to \Xi^-\pi^+$, $\Xi^-(1820) \to \Xi^0(1530)\pi^-$ and $\Xi^-(1950) \to \Xi^0(1530)\pi^-$ are lower by yet another order of magnitude. The $\Xi^-(1820)$ and $\Xi^-(1950)$ resonances show significantly harder $x_F$ and $p_T$ distributions than $\Xi^-$ and $\Xi^0(1530)$ hyperons. A detailed report on the cross section measurements is given in Ref. [16].

## 4. Production of Σ hyperons

The $\Sigma^-$ beam gives the exceptional opportunity to study hadroproduction of $\Sigma$ hyperons both in the ground and in excited states. There are only few publications about $\Sigma$ production cross section measurements up to date. As for high excited $\Sigma$ states, the only source of information was a partial wave analysis from bubble chamber experiments with a low momentum $K^-$ beam.

We will discuss in more detail the observed signal of excited $\Sigma$ states. An effective mass distribution for $\Lambda\pi^\pm$ combinations is shown in Fig. 5. The slices at high $x_F$ (Fig. 5 b,d) show that two peaks are present in the distribution for both charge combinations. The $\overline{\Lambda}\pi^-$ combinations is shown in Fig. 6. The bin width corresponds to our mass resolution at this mass region.

While the first peak in Fig. 5 definitely corresponds to the well established state $\Sigma^\pm(1385)$, the second one needs some comments: Several

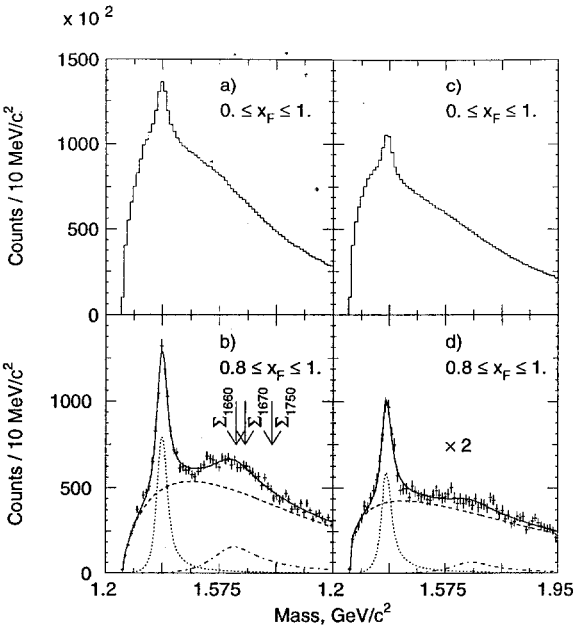


Figure 5. The $\Lambda\pi^{\pm}$ effective mass distribution in different $x_F$ regions. Separately shown are the contributions from resonances (dotted and dash-dotted curves) and the background (dashed curve) as estimated from event mixing. The solid curve represents the overall fit.

candidates for excited $\Sigma$ states were observed in the region of 1.6–1.8 GeV/c$^2$ as a result of differential partial wave analysis (DPWA) of data obtained in bubble chamber experiments with low momentum $K^-$ beam in the region 0.5–2 GeV/c. The usual number of solutions found was about 6–7. In [17] there is also a weak evidence for two peaks in the effective mass distribution. These peaks were attributed by the authors to $\Sigma(1620)$ and $\Sigma(1690)$. The masses and the widths of the candidates are the only parameters cited in that publication.

Thus, there are certain indications for the presence of three $\Sigma$ resonances in the mass range indicated in Fig. 5 b. Some of these resonances are considered as well established according to the PDG rating [6]. We cannot exclude that the observed signal is due to contributions from different (wide and overlapping) resonances. Unfortunately, we are unable to separately determine their quantum numbers, and so treat them as a single $\Sigma$ like state, hereafter denoted as $\Sigma(1660)$, with its mass and width given by the overall fit.

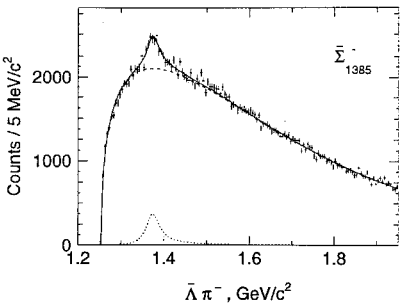


Figure 6. The $\overline{\Lambda}\pi^-$ effective mass distribution for the region $0 < x_F < 1$.

### 4.1. The $\Sigma$ production cross sections

The differential production cross section of $\Sigma$ hyperons was measured as a function of the Feynman variable $x_F$ and the squared transverse momentum $p_t^2$. In Fig. 7 (left) we show the invariant production cross sections for the observed $\Sigma$ signal in a $\Sigma^-$ beam and additional data for $pA \to pX$ [18] and $\Xi^- A \to \Xi^- X$ [19]. In the right part of Fig. 7 b the $\Sigma^{\pm}(1385)$ invariant production cross sections are shown for $\pi^-$ and neutron beam.

The production of $\Sigma^-$ hyperons by a $\Sigma^-$ beam is clearly dominated by the elastic contribution, which is responsible for the steeply rising cross section at $x_F \to 1$. At low $x_F$ the cross section depends of number of strange quarks in the product with the suppression factor about 10.

The leading effect depends on the number of common quarks in the projectile and produced particle, as it is clearly seen in the $\Sigma^{\pm}(1385)$ data. The data seem to be consistent with the assumption that the $x_F$ spectra are universal, according to the identical quark content of all excited states.

The data show clearly different behaviour for the $\Sigma^+(1385)$ spectra obtained with $\Sigma^-$ and neutron beams. This may be naturally attributed to the role of the strange quark, passing directly from the initial to final state particles in the case of a hyperon beam. The data show essentially no difference in the production of $\Sigma^-(1385)$ by neutrons and hyperons, possibly indicating the important role of the common $d$-quark pair.

Finally, the absence of common quarks in the initial hyperon and the final anti-$\Sigma$ hyperon manifests in the rapidly falling $\overline{\Sigma}^-(1385)$ spectrum in the $\Sigma^-$ beam.

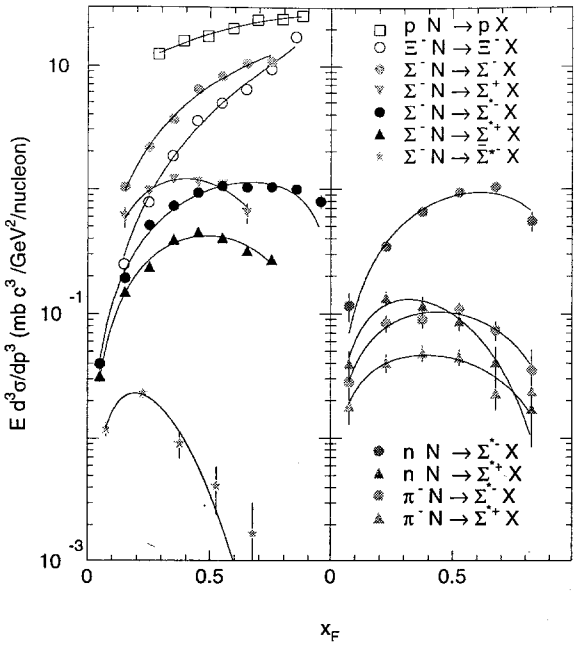


Figure 7. The $\Sigma$ invariant production cross section in $\Sigma^-$, $\pi^-$ and neutron beams. Also shown are the $pA \rightarrow pX$ and $\Xi^- A \rightarrow \Xi^- X$ invariant production cross sections for comparison (see text).

## 5. $\Lambda\Lambda$ correlations

The strong 'leading effects' showing up in the $x_F$-distributions suggest two distinct production mechanisms for baryons: A soft hadronisation process described e. g. by several break-ups of a colour string which is stretched between the partons, may dominate at low $x_F$. In addition, at high $x_F$ a recombination processes of produced quarks with projectile spectator valence quarks may be involved. It is the latter process which is generally believed to be responsible for the leading effect. Clearly, the existence of two distinct production mechanisms present even within a single event would be problematic for any 'equilibrium motivated' interpretation of hadron yields [20]. However the superposition of 'equilibrated' particle sources with different kinematic distributions and production ratios for baryons and anti-baryons may also result in an apparent leading effect in inclusive studies. Particularly in hadron-nucleus collisions – as it is the case in the present study – such a mixture of various particle sources can not be excluded a priori. In such a scenario two coincident produced baryons will be characterized by two identical kinematical distribution functions.

In order to distinguish between these two scenarios we have investigated $x_F$ correlations between two coincident $\Lambda$ particles or two $\overline{\Lambda}$ particles. Observing two coincident strange baryons, apparently only one of them can contain the strange quark from the incident $\Sigma^-$. Fig. 8 shows the $x_F$ distribution of the two $\Lambda$ particles after sorting with respect to their $x_F$ value. As expected due to the sorting procedure, the faster $\Lambda$ shows a harder $x_F$ distribution than the slow one. Indeed if both $\Lambda$ particles are produced according to the same probability distribution $P(x_F) = N(1 - x_F)^{n_0}$, the apparent $x_F$ distribution of the slow particle 1 will be given by

$$P_1(x_F) = 2N\left[(1 - x_F)^{n_0} - (1 - x_F)^{2n_0+1}\right] \quad (1)$$

while the fast particle 2 will be distributed as

$$P_2(x_F) = 2N(1 - x_F)^{2n_0+1}. \quad (2)$$

Within this ansatz, the slopes of the two distributions at large $x_F$ should be related as $n_0 : (2n_0 + 1) \approx 1 : 2$. Calculations according to Eqs. 1 and 2 are shown by the dashed and dash-dotted lines in Fig. 8. In these calculations the parameter $n_0$ has been adjusted to describe the $x_F$ distribution of the faster $\Lambda$. The expected limits for the $x_F$ distribution of the slower $\Lambda$ are indicated by the two lower curves. It is obvious from this figure that the distribution of the slower $\Lambda$ is not described by Eq. 1.

The corresponding analysis for two $\overline{\Lambda}$ particles produced in $\Sigma^-$ induced interactions is displayed in Fig. 9. Here the distribution of the slow as well as the fast $\overline{\Lambda}$ can be described by the same initial exponent $n_0 \approx 6$–9. Of course this does not exclude additional short [21] or long range [22] correlations between the two $\overline{\Lambda}$ particles. However such correlations will effect both baryons equally and will require a more quantitative analysis of the $x_F$ correlations.

Finally, Fig. 10 shows the $x_F$ distributions for two $\Lambda$ particles produced in neutron induced interactions. As a consequence of the common $d$ quarks in the neutron and the $\Lambda$ we again observe a clear deviation from an independent production mechanism of the two coincident $\Lambda$ particles.

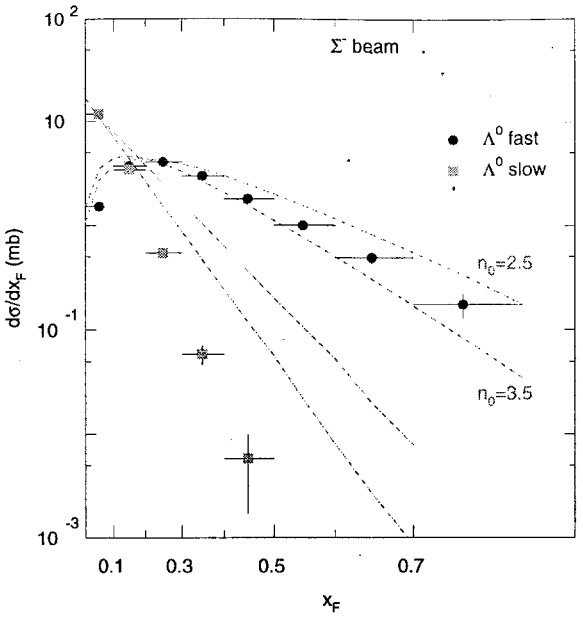


Figure 8. $x_F$ distribution of the fast (points) and slow (squares) $\Lambda$ produced in $\Sigma^- + \mathrm{Cu}$ reactions. The dash-dotted lines show the result of a calculation assuming identical emission probability distributions for the two $\Lambda$ particles.

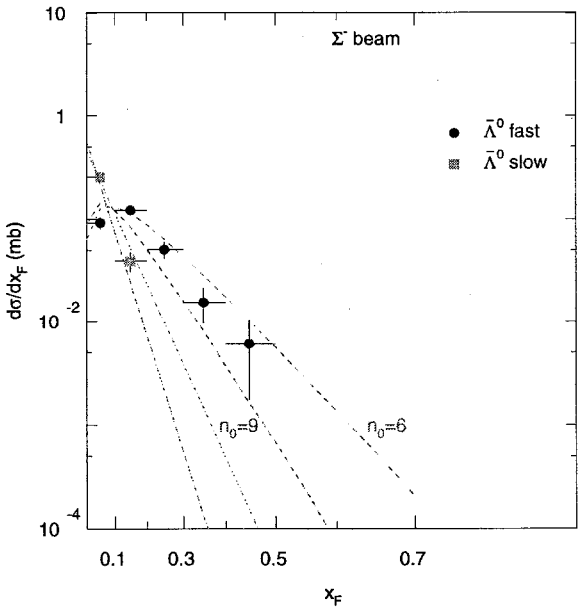


Figure 9. $x_F$ distribution of the fast (points) and slow (squares) $\overline{\Lambda}$ produced in $\Sigma^- + \mathrm{Cu}$ reactions.

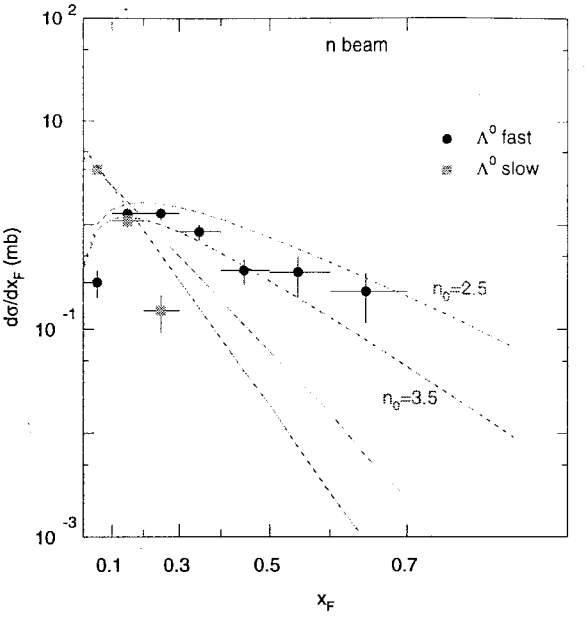


Figure 10. Same as in Fig. 8 but for neutron induced interactions.

## 6. $p_T^2$ distributions for inclusive hyperon and kaon production by $\Sigma^-$

Figure 11 shows the measured differential cross sections for $\Lambda$, $\overline{\Lambda}$ and $K_S^0$ plotted versus the transverse momentum squared, $p_T^2$. In general three different functions are used to parametrize the $p_T$ distributions of produced partices:

- $\mathrm{d}\sigma/\mathrm{d}p_T^2 \propto \exp(-Bp_T^2)$: Gaussian behaviour.
- $\mathrm{d}\sigma/\mathrm{d}p_T^2 \propto m_T^{3/2}\exp(-m_T/kT)$: 'thermal distribution'.
- $\mathrm{d}\sigma/\mathrm{d}p_T^2 \propto \exp(-bp_T)$: non-Gaussian tails at high $p_T$.

Fig. 11 shows that neither a pure Gaussian nor a single thermal distribution are able to describe the observed $p_T$ spectra. Using on the other hand an exponential ansatz, a reasonable fit to the spectrum over the full observed range can be achieved.

## 7. Non-observation of the $U(3100)$

A search for the possibly existing exotic state $U(3100)$ decaying into $\Lambda\overline{p}$ and pions was performed. The previous CERN hyperon beam ex-

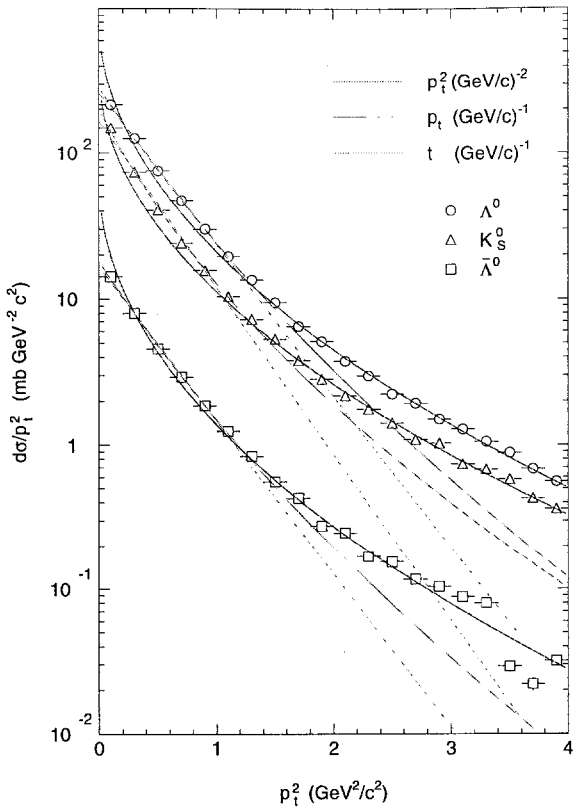


Figure 11. Differential cross sections $d\sigma/dp_T^2$ for $\Lambda$ (circles) and $\overline{\Lambda}$ (squares) hyperons and for $K_S^0$ mesons (triangles). Dashed lines: Gaussian fit $\exp(-Bp_T^2)$; lower solid lines: thermal distribution $m_T^{3/2}\exp(-m_T/t)$; upper solid lines: $p_T$ fit $\exp(-bp_T)$.

periment WA62 had obtained an $U^+ \to \Lambda\bar{p}\pi^+\pi^+$ signal [23] by suppressing $\pi^-$ in their $\bar{p}$ sample using threshold Cherenkov counters. The same technique had been applied by the neutron beam experiment BIS-2 at Serpuchov, who obtained impressive evidence for the decay $U^0 \to \Lambda\bar{p}\pi^+$ [24].

In WA89, using a RICH detector [4] with its excellent antiproton identification should have greatly improved the signal to background ratio of such signals. However, no signal in the decay channels quoted above was observed. In the $\Lambda\bar{p}\pi^+\pi^+$ channel, the upper limit on $\sigma \cdot BR$ was lower by at least a factor of 3 than the value reported from experiment WA62.

## REFERENCES


1. V. J. Smith, Overview talk at Hyperon 99.
2. Yu. A. Alexandrov et al., CERN-SL-97-60 EA and *Nucl. Instr. and Meth. A 408* (1998) 359.
3. W. Beusch, CERN/SPSC/77-70.
4. U. Müller et al., *Nucl. Instr. and Meth. A 433* (1999) 71 and references therein.
5. D. Acosta et al., *Nucl. Instr. and Meth. A 302* (1991) 36; *305* (1991) 55; *308* (1991) 481.
6. Particle Data Group, C. Caso et al., *Eur. Phys. J. C 3* (1998) 1.
7. C. Dionisi et al., *Phys. Lett. B 80* (1978) 145.
8. S. F. Biagi et al., *Z. Phys. C 34* (1987) 15.
9. S. F. Biagi et al., *Z. Phys. C 9* (1981) 305.
10. K. T. Chao, N. Isgur and G. Karl, *Phys. Rev. D 23* (1981) 155.
11. S. Capstick and N. Isgur, *Phys. Rev. D 34* (1986) 2809.
12. L. Ya. Glozman and D. O. Riska, *Phys. Rep. 268* (1996) 263.
13. M. I. Adamovich et al., *Eur. Phys. J. C 5* (1998) 621.
14. S. F. Biagi et al., *Z. Phys. C 31* (1986) 33.
15. O. Schneider et al., *Z. Phys. C 46* (1990) 341.
16. M. I. Adamovich et al., *Eur. Phys. J. C 8* (1999) 593.
17. H. C. Fenker et al., *Phys. Rev. D 30* (1984) 872.
18. W. F. Baker et al., *Phys. Lett. 51B* (1974) 303.
19. S. F. Biagi et al., *Z. Phys. C 34* (1987) 187.
20. R. Stock, *Phys. Lett. B 456* (1999) 277 and references therein.
21. J. K. Ahn et al., *Nucl. Phys. A 639* (1998) 379c.
22. P. Abreu et al., *Phys. Lett. B 416* (1998) 247.
23. S. F. Biagi et al., *Phys. Lett. 172B* (1986) 113.
24. A. N. Aleev et al., *Z. Phys. C 47* (1990) 533.

# Chapter 9

# Excited Hyperon Properties and Extension to Heavy Flavors


- J. S. Russ

# Excited Hyperons - Charmed and Strange

J. S. Russ [a]

[a]Carnegie Mellon University

## 1. Introduction

The charge for this talk was to explore the connection between the strange and charmed hyperon excited states. At first blush, this is an odd combination. The general picture of the hyperon family, based on broken flavor-SU(3) and broken spin-SU(6), is organized around the symmetries of the $\mathbf{3} \otimes \mathbf{3} \otimes \mathbf{3}$ decomposition of flavor-SU(3). Within the SU(3) structure, the hyperon and nucleon excitations should be parallel. This relationship has been built into a number of models for baryon excitations, most notably the color string model of Capstick and Isgur [1]. We shall say more about this model calculation later.

For the charmed baryons, Heavy Quark Effective Theory links the charm baryon structure to charm meson structure, rather than to hyperon states. Within the HQET framework [2] the charm quark spin decouples from the light quark pair. This fixes the color of the qq system and puts it into either a $\overline{\mathbf{3}}$ or a $\mathbf{6}$ of flavor SU(3). This greatly reduces the possible complexities of the system. The spin-flavor correlation separates the $\Lambda_c^+$ excitations and the $\Sigma_c$ excitations via isospin for the (ud) pair. For (us) or (ds) systems in the $\Xi_c$ family, both $\overline{\mathbf{3}}$ and $\mathbf{6}$ configurations are allowed. It is therefore of interest to see whether the two configurations are well-separated in excitation or perhaps mixed in the $\Xi_c$ system.

## 2. Hyperon History

Experimentally, the rich resonance structure of the hyperon systems was uncovered in the early years of accelerator experiments with separated $K^-$ beams. These studies, begun concurrently with the evolution of bubble chamber and spark chamber detector systems, occupied a significant fraction of the total experimental effort in high energy physics for more than two decades. It was soon found that the density of states required phase shift analysis to untangle overlapping states. Even so, there were ambiguities in the solutions. Extensive studies using production data, scattering data and polarized target data attempted to make $J^P$ assignments to the many narrow and broad states. The mass spectrum is densely populated from the lowest excitation $\Sigma(1385)$ to a point where analysis tools were incapable of making further state separations, in the vicinity of 2300 MeV.

The present experimental state of affairs is summarized by the Particle Data Group at the beginning of the section on $\Lambda$ and $\Sigma$ Resonances:

> There are no new results at all on $\Lambda$ and $\Sigma$ resonances. The field remains at a standstill ....

Theoretically, the striking regularities between the nucleon resonances and the hyperon resonances provided the final information needed to move toward our modern picture of hadron structure: unitary symmetry and the quark model. This led to the Nobel Prize award to Gell-Mann and Zweig after the discovery of the $\Omega^-$ baryon confirmed their picture of baryon structure.

Because SU(3) is a broken symmetry, the basic multiplet structure is complicated by mass effects. Several empirical formulae, based on SU(3) operators, gave excellent descriptions of the mass splittings **within** a given multiplet [ **8** or **10** ] but had no ability to correlate these splittings between different multiplets. While it was clear that successful mass relationships could be found using matrix elements of the broken symmetry operators of SU(3), there was no predictive power about which relationships would be successful for the excited states.

The necessity of having color antisymmetry in the quark wave functions which determine allowed quark internal degrees of freedom was understood but presented a formidable computational challenge. Octet-singlet mixing was another complication in developing a theoretical description of the observed mass spectra; the observed masses of the singlet and central octet candidate states are not necessarily the masses that

a proper baryon spectrum prediction would give.

Because the hyperon resonances involve only light quarks, theoretical calculations have to handle the full complexity of nonperturbative QCD. Not even lattice calculations have begun to attempt spectral predictions. However, several QCD-informed model calculations have done an impressive job of predicting the mass spectra. Width calculations for the states, however, are not included in the models.

The most successful approach, in my opinion, is the Capstick-Isgur relativized color-string model mentioned above. Their approach applies to all hadrons, and they made a simultaneous fit to the meson and baryon spectra, using the same parameters for each. I refer the reader to their Physical Review paper for details and other references. Here, we will concentrate on the general features of their results.

### 2.1. Capstick and Isgur - the Good News

The achievement of having a single model with fixed parameters fit the entire meson and baryon spectrum cannot be overlooked. The hyperfine interaction parameters give correct predictions for $\rho/\pi$, $\Delta/\mathrm{p}$, and $\Sigma/\Lambda$ mass splittings, among many others. The predicted masses agreed well with the empirical octet and decuplet mass formulae but gave no further clue about the origin of these relations.

The authors also used this parameter set plus the mass of the charm constituent quark determined from the D meson mass to predict the excitation spectra of charm baryons. We shall return to that story later.

### 2.2. Capstick and Isgur - the Bad News

On the other hand, the Capstick and Isgur model calculation, like all model calculations of this sort, predicts far more states than are found. For the nucleon sector, they found an empirical test that isolated which states are actually populated: the states that couple to the $\pi$N production channel. There is no understanding of the origin of this selection rule. Its existence suggests there is some additional unrecognized symmetry in the data that is not yet incorporated in the model.

The Capstick and Isgur model is not fully antisymmetrized in the 3-quark wave functions. They found this too daunting a task and settled for a partial antisymmetrization. It is not clear to what extent this shortcoming affects the predictions of the model.

There is also a problem with the $\Lambda(1405)$. In the PDG listings, this state is given an entire section to discuss the interpretation conflict between a 3-quark picture and the meson-baryon bound-state picture. The Capstick-Isgur model gives far too high a mass for the state. This subject, too, will be revisited.

## 3. Hyperon Spectroscopy Summary

Despite a wealth of hard-won experimental information about the SU(3) multiplets in the light-quark family, both nucleons and hyperons, there is no clear theoretical picture that describes the situation. There are many degrees of freedom in the problem, and the mass spectra show that very high internal levels of excitation are reached.

How can one make progress in understanding hyperons?

## 4. Charmed Hyperon Spectroscopy

As mentioned briefly in the introduction, the new news in baryon spectroscopy comes from the study of charmed baryons. These states can be analyzed within the framework of HQET plus correction terms going as $1/\mathrm{m_Q}$. The fundamental hypothesis of HQET is that the heavy quark degrees of freedom are unchanged by transitions. For excited states, then, one can characterize the excitation spectrum by the angular momentum and $\mathrm{SU(3)_f}$ quantum numbers of the light quarks. Because the baryons can have their (qq) pair in the same $\overline{\mathbf{3}}$ state as the meson antiquark, one should see identical excitation spectra for such states. There is no HQET prediction for the relationship between the $\overline{\mathbf{3}}$ configurations and the $\mathbf{6}$ configurations. For example, the $\Sigma_c/\Lambda_c$ mass separation is introduced from experiment.

HQET predictions are most useful in describing the widths and decay modes of the excited states, rather than their excitation spectrum. The excitations, though, within HQET should be very similar for charm mesons and charm baryons AND should be almost independent of the spin projection of the heavy quark. Indeed, both for charm mesons and baryons, there are closely-spaced doublets as HQET suggests. [4]

Because the light-quark states only change angular-momentum quantum numbers in the de-excitation process, HQET predicts that the predominant decays will be a chain of pion emissions. This is seen in the data. Phenomenologically the Q value of the decay is related to the width of the state by the orbital angular momentum L given

to the decay pion. The angular momentum barrier effect goes like $|p_\pi|^{2L+1}$. Therefore, states with high L and small Q will be strongly inhibited compared to S-wave states.

HQET analysis of this sort has been useful in categorizing the excitations of the charm baryons. Figure **??** shows the charm meson and baryon excitation energies, along with quantum number labels from HQET. The assignment of the light quark pair to a flavor $\overline{\mathbf{3}}$ or **6** state reflects the HQET spin-flavor symmetry. NO quantum number measurements for any of these states have as yet been made. This is a great outstanding problem in the field - how can one measure $J^P$ for the charm baryon states?

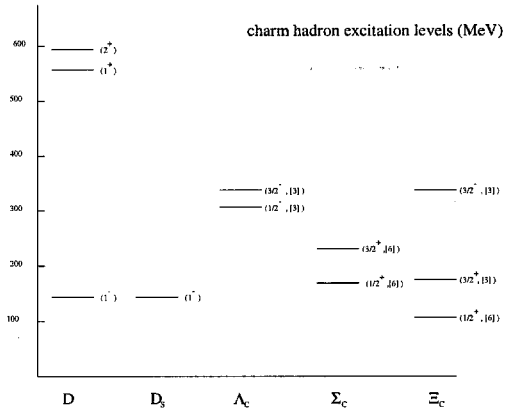


Figure 1. charm meson and baryon excitation spectra.

What can this analysis of charm baryons tell us about the hyperons? There are still a number of experimental questions to be addressed about HQET descriptions of the charmed baryons besides the fundamental issue of determining quantum numbers:

- Where are the missing states in the charm meson spectra?
- What is the role of $1/m_Q$ mixing in the charm spectra?
- Where are the orbitally-excited **6** baryons?

## 5. $N_C$ Theorems and Light-quark Spin-Flavor Symmetry

One of the major simplifying features of HQET analyses is the spin-flavor symmetry that results from decoupling the heavy quark from the other two quarks, resulting in a large reduction in the degrees of freedom in the description of the baryon system. In recent years a number of authors have used the $1/N_C$ expansion of baryon operators within a SU($2N_f$) framework to look again at the regularities within the hyperon and, more generally, light baryon spectra. A good review with a list of references to previous work may be found in [3].

The $1/N_C$ analysis of baryons, introduced by Witten in 1979 [5], investigates QCD operators in the limit of a large number of available color states $N_C$. For a given baryon, allowing $N_C$ to become large makes valence quarks dominate over glue, thus putting the dominant baryon characteristics into operator expressions for n-body interactions of the quarks. Jenkins and co-workers look at the implications of the physically-relevant case $N_C$=3 for $N_f$=3. The calculational procedure groups baryon operators that involve the same order of the parameter $1/N_C$. Because of $SU(3)_f$- breaking, there must be a simultaneous expansion in $1/N_C$ and the SU(3)-breaking operators. This has been done for the light-quark baryons, for example, in [6]. This procedure recovers the octet and decuplet mass formulae as a unified whole, rather than two empirically-matched SU(3)-breaking operator selections. As the authors point out, this QCD-based analysis points out that corrections due EITHER to higher-order $1/N_C$ corrections OR to $SU(3)_f$-breaking are of the same order, so both effects must be considered together to have a consistent picture of the processes. Furthermore, the theoretical treatment combining $1/N_C$ ordering and $SU(2N_f)$-ordering identifies mass relationships that do not appear in non-relativistic SU(6) models.

The $1/N_C$-generated spin-flavor correlation between light quarks has been combined with HQET spin-flavor correlations for heavy baryon system in [7]. Corrections to the leading order properties are ordered by $1/[N_C \cdot m_Q]$. The combined theory has more predictive power than HQET by itself. Some predictions agree well with data. Others are somewhat off. In particular, the split between the higher-lying $\Xi_c'$ in the

light-quark **6** and the ground state $\Xi_c$ in the $\overline{\mathbf{3}}$ is too large. It will be good to get more data on the charm system and begin to identify beauty baryons, to look more deeply into the behaviour of this combined symmetry.

## 6. Summary and Prognosis

### 6.1. Dealing with the Present

Despite the long lull in experimental study of hyperon excitations, the task of understanding the wealth of data in hyperon spectroscopy remains formidable. Recent advances in theory have generated an understanding of the empirical SU(3)-based mass formulae from the early days of unitary symmetry. Predictions of mass spectra within the $1/N_C$ model give reasonable agreement with data without suffering from the excess of states that plagued color-string models like Capstick and Isgur.

However, one should note that the color-string model had impressive range. In addition to predicting the light meson AND baryon spectra with a limited set of parameters common to both, Capstick and Isgur turned their attention to charmed baryons as well. They used the D meson to set the constituent mass $m_c$. With that additional parameter, they calculated correctly the mass of the $\Lambda_c^+$, the $\Sigma_c/\Lambda_c$ mass splitting, and predicted the p-wave $\Lambda_c^*$ doublet within 20 MeV of the center of gravity a decade before it was measured, albeit with too small a splitting. It presents a challenge to modern theory to do as well.

### 6.2. The next experiments

The status of the $\Lambda(1405)$ state remains a prickly issue in hyperon spectroscopy. Quark-model calculations tend to put it much closer in mass to the $\Lambda(1520)$, its spin-3/2 partner. The role of the meson-nucleon bound state effects in shifting the observed mass of the state are hard to assess. If hyperon structure and charm baryon structure are related, what can be learned from the small splitting of the $\Lambda_c^+(2594)$ and the $\Lambda_c^+(2626)$?

One way to study the state is to look at a different mechanism for producing it. Up till now, hyperon spectroscopy has been done in scattering experiments, in which there are many other quarks and gluons to hadronize. One might do well to study the properties of the $\Lambda(1405)$ as seen in semileptonic decays of the $\Lambda_c^+$. In these decays an orbital excitation of the light quarks can happen only in the $1/m_c$ correction, so high statistics are required. Perhaps this will be a useful exploration in the off-resonance data from the B-factories in the next several years.

In Fermilab Run II one should have significant samples of b-baryons from CDF and D0. D* signals are routinely used in CDF Run I analyses, showing that one can attach a slow pion from the primary interaction to a charm secondary vertex - the essence of doing Heavy Flavor spectroscopy. One might try to do b-baryon spectroscopy with the large sample sizes expected in the coming few years. This would rigorously test the $1/N_C$ ideas about Heavy Flavor baryons.

The final experimental challenge is to figure out ways to measure the spin and parity of the heavy-quark baryons. This was a long-term experimental task for hyperon spectroscopy. Now, assignments to the observed charm or beauty baryons are made either on quark-model or HQET treatments. This is not a satisfactory state of affairs. We should do better.

The new theoretical treatments and the increased level of activity in lattice gauge calculations of the excitation properties of hyperons indicates that the field is not moribund, just difficult. We look forward to new data and further useful comparisons between the spectroscopy of the light and heavy baryons.

## REFERENCES


1. S. Capstick and N. Isgur, Phys. Rev. **D34**(1986)2809
2. N. Isgur and M. Wise, Phys. Rev. Lett. **66**(1991)1130
3. E. Jenkins, *Ann. Rev. of Nucl. and Particle Science 48* 81 (1998)
4. Particle Data Group,C. Caso, et al., Eur. Phys. Jour. C3 (1998)1
5. E. Witten, Nucl. Phys. **B160**(1979)57
6. E. Jenkins and R.F.Lebed, Phys. Rev. **D52**(1995)282
7. E. Jenkins, Phys. Rev. **D54**(1996)4515

# Chapter 10

# Beyond the Typical Hyperon Field


- R. Bellwied

# The Role of Hyperons in Relativistic Heavy Ion Collisions

R. Bellwied [a]

[a]Wayne State University,
Department of Physics and Astronomy,
Detroit, MI 48202, U.S.A., E-mail: bellwied@physics.wayne.edu

In the last two decades nuclear physicists were trying to discover a new phase of nuclear matter called the Quark Gluon Plasma (QGP). This plasma state was predicted as one of the transient phases during the de-excitation of the cosmological big bang. It is assumed that a reenactment of these initial conditions is possible through the collision of two highly relativistic heavy ions. The generated plasma phase will correspond to a short lived and highly excited state of matter, which will convert back into a conventional hadron gas after less than $10^{-21}$ sec, but the composition of the particle emission spectrum from the produced fireball is expected to have ramifications for cosmology and the standard model. Measurements that were proposed as signatures for this phase transition were obtained in heavy ion collisions at the Bevalac (LBL), AGS (BNL), and SPS (CERN) accelerators. No unambiguous evidence for the QGP formation has yet been found, though. With the advent of the Relativistic Heavy Ion Collider (RHIC) at Brookhaven National Laboratory (BNL), heavy ion physics will enter a new energy regime and the question is whether the originally proposed signatures are still sensible and detectable at these higher incident energies. In particular measurements related to hyperon formation were advocated as potential signatures and were tested in numerous fixed target experiments at the AGS and the SPS. In this article I will first review the existing set of hyperon measurements and then extend the scope of hyperon physics to the RHIC energy regime.

## 1. Introduction

Since the beginning of Relativistic Heavy Ion Collisions at the BEVALAC, the quest for evidence of a phase transition between hadronic matter and a chirally symmetric and deconfined phase, called the Quark Gluon Plasma, has led to numerous proposed hadronic and leptonic signatures. In the hadronic sector the properties of hyperon production are of particular interest. Suggested measurements relating to hyperon properties are numerous and span from simple hyperon yields (as evidence for strangeness enhancement), over hyperon-antihyperon ratios (as evidence for strangeness equilibration) to strange quark matter formation.

The main condition for a successful measurement of hyperons in heavy ion collisions is the proper reconstruction of a secondary vertex in an environment that is dominated by pion, kaon, and proton emission. In a standard central Au-Au collision at RHIC around 10,000 charged particles are produced of which around 2,500 are within the acceptance of a standard collider detector with $2\pi$ azimuthal and full radial coverage. Only about 2% of those particles originate from hyperon decays. By adopting high resolution position detector concepts (e.g. the RHIC-STAR detector is relying on a Silicon Vertex Tracker and Time Projection Chamber combination) and track reconstruction techniques that were successfully applied in high energy physics to measure charm, bottom and ultimately top quark physics, the Relativistic Heavy Ion community was successful in measuring hyperon production with good efficiency and excellent resolution. Kinematic properties allow further to distinguish between a variety of neutral strange particles. Fig.1 shows a so-called Armenteros plot based on the statistics obtained in around 1000 simulated central Au-Au collisions at RHIC energies.

By plotting the fractional difference of the daughter momenta ($\alpha$) on the x-axis and the momentum component of the positive decay product transverse to the parent trajectory ($p_T$) on the y-axis a clear separation of the neutral strange mesons ($K^0_s$ have a symmetric decay and form a large arc around $\alpha$=0) from the hyperons ($\Lambda$,$\overline{\Lambda}$ have asymmetric decays and form small arcs away from $\alpha$=0) is apparent. The techniques also aid in measuring an almost background free sample of multiply strange baryons. Besides the measurements of $\Lambda$, $\Xi^-$, $\Omega^-$ and their respective anti-particles, we also attempted the discovery of more exotic hyperon related objects, like the H-dibaryon and strangelets, which should form

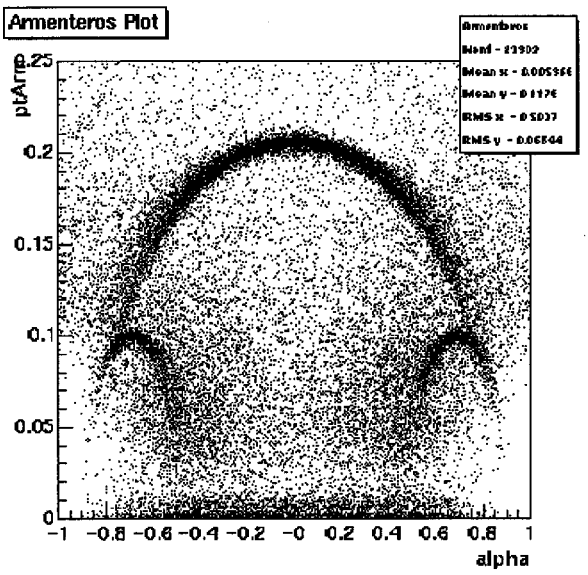


Figure 1. Typical Armenteros plot for strange particles ($K^0_s$, $\Lambda$, and $\overline{\Lambda}$) for 1000 central Au-Au events at RHIC energies.

when the hyperon density in a part of phase space exceeds a critical value. Heavy ion reactions are considered an ideal environment for hyperon clustering, simply because the high density, low temperature environment favors a coalescence type interaction. In this sense the lower energy fixed target experiments, which typically generate very high particle density in the central fireball region are more suitable for strangelet formation than the very high energy collider collisions in which the beam nuclei are considered to be transparent. Here the central particle density is small but the temperature is high, which will lead to high escape velocities for produced hyperons. Thus, the coalescence probability is low.

In the following I will give a detailed review of the present status of measurements in those key sectors after two decades of fixed target experiments and then relate this information to future measurements made possible by the new Relativistic Heavy Ion Collider (RHIC) at BNL.

## 2. Past Hyperon Measurements in AGS and SPS fixed target experiments

The main motivation for hyperon measurements in relativistic heavy ion collisions goes back to the prediction that strange quark production will be strongly enhanced and chemically equilibrated in the case of a QGP formation [1]. Fig.2, taken from [1], summarizes the predictions for the simple measurement of anti-hyperon over hyperon ratios in the case of a hadron gas model (HG) and a Quark Gluon Plasma model (QGP).

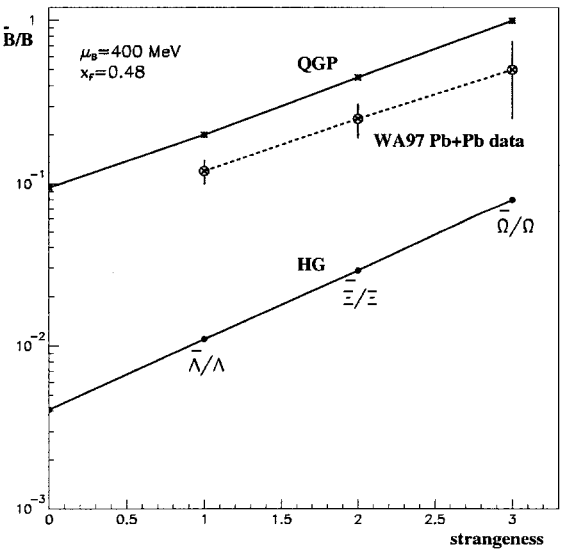


Figure 2. Theoretical Predictions for the Anti-Baryon over Baryon ratios in the case of a Hadron Gas (HG) and a Quark-Gluon Plasma (QGP) under Certain assumptions (fixed $\mu_B$ and $x_F$). Predictions are based on [1], data are taken from [3].

Certain assumptions, in particular the magnitude of the baryochemical potential ($\mu_B$) will modify these calculations slightly, but the signature is preserved as long as thermal equilibration can be assumed. The main argument in this theory is that in a QGP the $s\bar{s}$-pair formation is dominated by the early partonic interaction, specifically gluon-gluon processes, which strongly enhance strangeness production [2] compared to simple rescattering processes that are required in a hadron gas to generate hyperons and anti-hyperons. In addition, the hard processes as described by QCD generate as many s-quarks as $\bar{s}$-quarks. Thus strangeness will equilibrate as predicted for the $\Omega/\overline{\Omega}$-ratio in a QGP

(see Fig.2). In a hadron gas the processes generating the hyperon are always favored over the anti-hyperon production, simply because the remnant light quark multiplicity leads to matter rather than anti-matter production.

High statistics measurements, in particular at the CERN SPS accelerator, where the incident energy is sufficiently large to produce measurable quantities of multiply strange hyperons, have led to strong indications that hyperon production is indeed enhanced and maybe even equilibrated. Fig.3 shows the latest strangeness enhancement factors, as measured by CERN experiment WA97 [3], by comparing the actual measured abundances in nucleus-nucleus collisions at 160 GeV per nucleon to scaled-up abundances from proton-nucleus collisions at the same incident energy. The scaling assumes that a nucleus-nucleus collision is simply a superposition of single proton-proton collisions. Agreement with the superposition model would indicate that a nucleus in a collision at relativistic energies behaves like a collection of independent nucleons, whereas any deviation from this model indicates collective behavior of the nucleus, which is widely considered a pre-requisite for a thermally equilibrated system. A phase transition will require thermalization of a finite size volume of hadrons. Fig.3 seems to indicate evidence for such a collective behavior of the fireball generated in a nucleus-nucleus collision. Obviously the enhancement is statistically significant and seems to rise as a function of strangeness content.

The most recent ratios, measured with the same experimental setup than the abundances in Fig.3, are shown as dots in Fig.2. This interpretation of the strangeness data led to considerable discussions about whether the QGP had been found at the SPS or not [5]. It is interesting to note that models that assume a very hot thermally equilibrated hadron gas [6] seem to describe most of the features just as well as a QGP model [7]. Only for the heaviest hyperons the thermal hadron gas picture seems to fail. The QGP models can explain every ratio, but their assumptions regarding the plasma hadronization are very drastic and do not seem to be in agreement with a series of additional measurements for non-strange particle production. In particular, the QGP models require sudden hadronization, which means that the strange baryon abundances have to stay constant after hadronization. The kinematics of the hyperons can change through

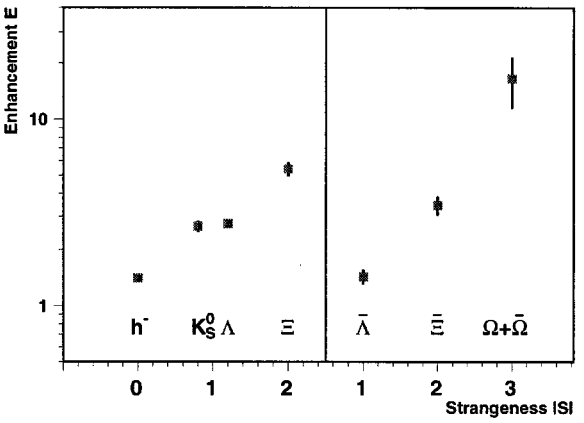


Figure 3. Strangeness Enhancement factors as measured by WA97 (from [4])

elastic rescattering with co-moving hadrons before thermal freezeout is reached, but the abundances and ratios which would be changed by inelastic scattering processes, are frozen. This is a drastic assumption in light of the fact that the system is very dense and that the cross sections for hadronic final state interactions are large. In a recent paper [8] we actually show that the probability of producing Λ's well after hadronization is quite large and should lead to a strong modification of any particle ratio that involved the Λ yield (see Fig.4).

Besides measuring the particle abundances and particle ratios additional information can be obtained from the kinematic spectra (transverse momentum and rapidity spectra). In particular, the inverse slope of the invariant cross section ($\sigma_{inv} \propto 1/p_T\ dN/dp_T$) as a function of transverse momentum, should, in the case of particle emission from a thermally equilibrated source, be related to the temperature of the source, based on Boltzmann statistics. Fig.5 shows the particle specific emission temperatures extracted from the measured transverse momentum spectra as a function of the particle mass [9]. The line indicates a simple scaling law that assumes that the emitting source is not at rest by taking into account the expansion velocity to calculate the 'real' emission temperature. Several thermal calculations (e.g. [10]) show that with a single expansion velocity for all particle species the transverse momentum spectra yield a common thermal freezeout tem-

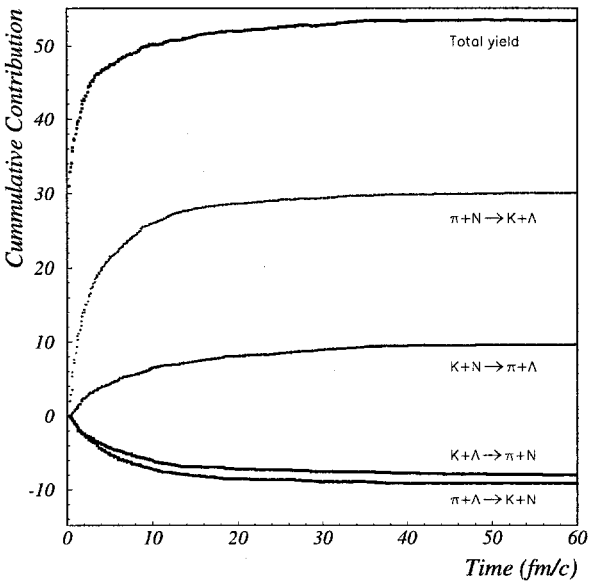


Figure 4. Contributions to the Λ yield after hadronization and before thermal and chemical freeze-out

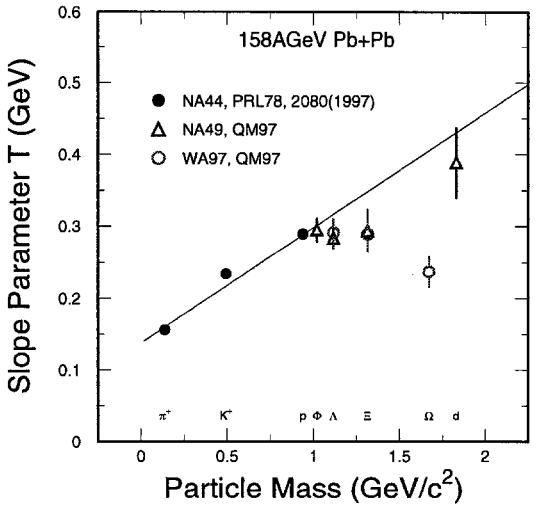


Figure 5. Inverse slope parameters (temperature) of particle identified transverse momentum spectra measured in CERN Pb+Pb collisions plotted against the particle mass (from [9])

perature for all particle species, see Fig.6.

Only the Ω particle strongly deviates from this collective behavior as shown in Fig.5. One possible explanation is that the Ω's decouple early from the fireball and thus do not 'flow' with the other emitted particles [9]. Still, the vast majority of the particle spectra indicate a common kinetic freezeout temperature T.

Taking this information together with chemical spectra (abundances, ratios) the situation is less clear,though. A typical ratio analysis is shown in Fig.7 on the basis of NA36 data [11]. This analysis is comparable to the determination of the temperature and expansion velocity through the kinetic spectra. Thermodynamically, the particle ratios carry additional information, though. They define the temperature and baryochemical potential phase space. The deduced temperature is higher than the thermal freezeout temperatures obtained from the particle ratios.

This discrepancy in calculated freeze-out temperature led to an interpretation that suggests that chemical freezeout is decoupled from kinetic freezeout and happens at an earlier stage.In essence this means that inelastic rescattering ceases before elastic rescattering. The phase transition picture in Fig.8 depicts our present understanding under the assumption that this simple thermal theory is correct [12].

Based on Fig.5 it seems that only the heaviest hyperons do not follow the general trend and decouple even kinetically early from the fireball (no boost in temperature due to the expansion velocity leads to lower temperature [9]) and thus are less susceptible to any kind of re-scattering which could potentially dilute any QGP signature. They also show the largest enhancements factors, which can be interpreted as a QGP signature. Still, the Ω measurements are not unambiguous in particular because of our understanding that the phase transition is a collective effect and should manifest itself in a variety of transition signatures. If one forms an event class of events that exhibit Ω enhancement, the other potential signatures do not seem to follow the hyperon trend. In summary, the present state of heavy ion measurements does not allow a definite conclusion regarding the formation of a plasma phase.

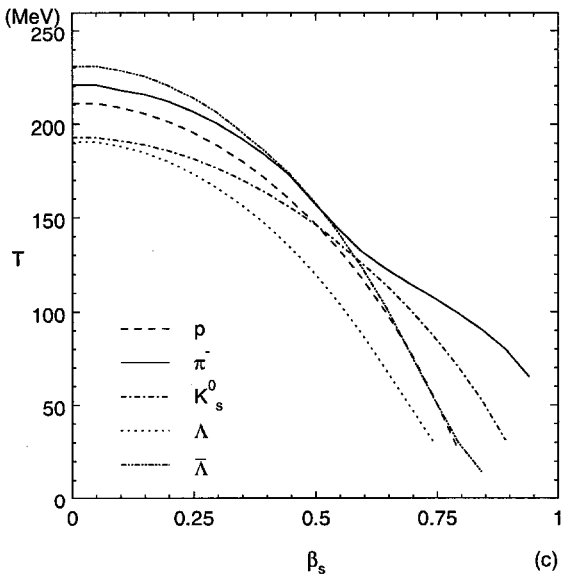


Figure 6. Calculation based on a thermal model [10] showing that all particle spectra can be described with a common emission temperature if a certain expansion velocity for the source is taken into account.

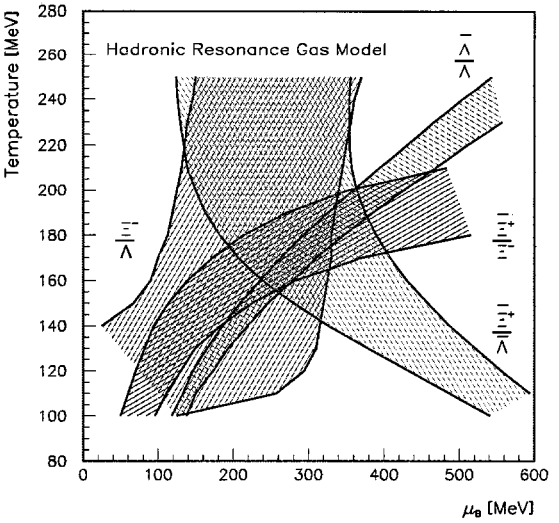


Figure 7. Thermal model analysis on the basis of strange particle ratios as measured by NA36

## 3. Λ Polarization

The study of hyperon polarization in relativistic heavy ion collisions is relevant not only as a comparison to the measurements in p-p and p-A reactions, but also as a potential, if indirect, QGP signature. Jacob and Rafelski [13] have suggested that the longitudinal polarization of the Λ in heavy ion collisions could be interpreted as a signature for an enhanced multi-strange hyperon production.

In addition the measurement of the transverse polarization in heavy-ion collisions might shed further light on the polarization production mechanism which seems to be independent of energy and system size [14].

The presently available Λ polarization measurements based on heavy-ion collisions are shown in Fig.9 in comparison to p-Be data. Both heavy ion measurements, taken in the late 80's by E810 [15] at the AGS and NA35 [16] at the SPS, respectively, lack the necessary statistical significance to determine the polarization level in the produced Λ's. In addition the momentum range covered might be too low to expect polarization based on the p-Be data. Thus, neither data set was ever published except in conference proceedings.

Experiment E896 at the AGS is presently analyzing Λ polarization in two different detectors [17]. More conclusive results should be available in the near future.

## 4. Λ Interferometry

A common analysis in heavy-ion collisions is the correlation of two or more identical particles emitted from a single source. This method is often referred to as HBT analysis [18]. Hanbury-Brown and Twiss used a similar analysis to measure the size of stars from the correlation function of the emitted photons. In the analysis the width of the correlation is inverse proportional to the size of the source. The method was quite successfully applied to the emission of pions, protons, and kaons from the fireball after a heavy-ion collision at AGS and SPS energies. Although the results leave room from many different interpretations, the data can be connected to the spatial extension of the thermally emitting source at kinetic freezeout. Due to the lack of statistics of events with two or more Λ's at the available incident energies it was never possible to measure

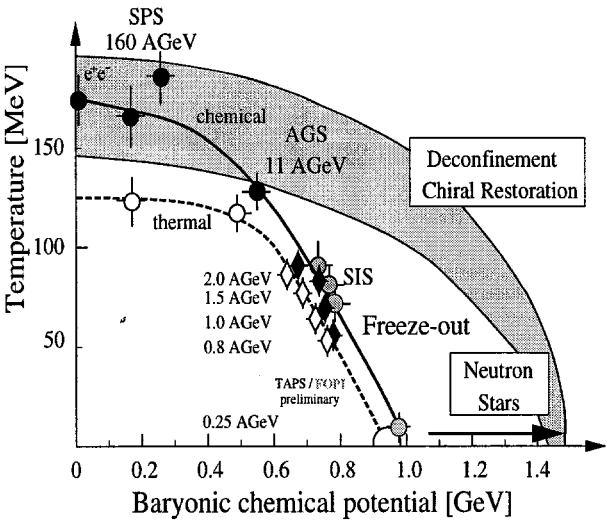


Figure 8. Phase transition plot on the basis of all available data from SPS, AGS, and SIS analyzed with a simple thermal model [12]

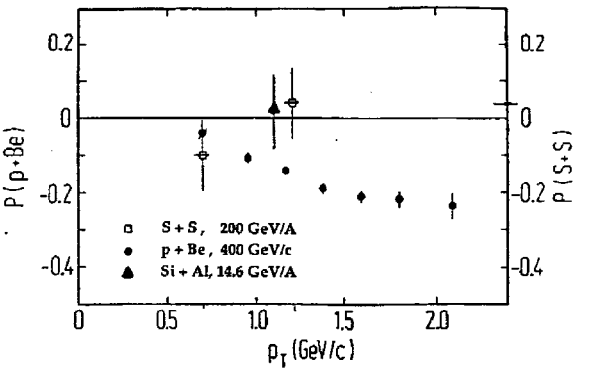


Figure 9. Preliminary low statistics heavy ion measurements of Λ polarization, in comparison to p+Be data. All presently available heavy-ion data are consistent with zero Λ polarization, but the statistics are low.

Λ correlations. Based on realistic event generators, though, the measurement should be possible at RHIC energies. Greiner and Mueller [19] have proposed several scenarios in which a difference in the Λ correlation function compared to e.g. the pion correlation function could be interpreted as a QGP signature or evidence for an enhanced strange quark matter generation probability. Very little is known about the Λ-Λ interaction and it seems that the resonant state that can be excited might affect the width and shape of the correlation function. But even in this case, a measurement of the resonance would shed new light on our understanding of the Λ interaction potential.

## 5. Search for Strange Quark Matter

Another even more speculative signature of a phase transition is the formation of strange quark matter [20]. Strange Quark Matter was postulated as a potential solution to the cosmological 'missing mass' problem [21].

Pure strange quark matter is comparable to hyperon clusters held together by an attractive binding energy. As a consequence of the bag model, Jaffe has postulated that the smallest hyperon cluster, namely the H-Dibaryon (udsuds) should be stable due to a color-magnetic attractive force. That means six-quark bags are possible within the standard model [22]. To be detectable as a particle the H mass has to be below the ΛΛ-mass, otherwise it might still exist as a resonance. It is not the ground state of conventional matter, thus it has to have a mass higher than the two neutron mass. Within this range of masses more than twenty accelerator based experiments have been performed. A nice summary can be found in [23]. Heavy ion data that suggest a set of H-Dibaryon candidates are described in [24]. Ongoing dedicated H experiments that employ higher resolution tracking devices focus on the H-mass region just below the Di-Λ mass, mainly because of recent discoveries of double strange hypernuclei, which exclude lower masses for the H [25]. In the remaining mass range the most likely decays are weak decays with a lifetime comparable to the Λ lifetime itself. The most prominent channel will be $H \rightarrow \Sigma^- p$ with a subsequent $\Sigma^- \rightarrow n\pi^-$ decay. A dedicated experiment (E896) has been built to search for short lived H-Dibaryons [17]. It features a Silicon Vertex Tracker as well as a Distributed Drift Chamber to cover different regions of phase space. The experiment took data in 1998 and is presently analyzing its data set, which should contain on the order of 200 reconstructible H-Dibaryons based on predictions by Dover et al. [27].

In recent years it was predicted by Greiner et al. [26] and Dover et al. [27] that in addition

to possibly generating hyperon dibaryons, heavy ion reactions are particularly suitable to form so-called strangelets, clusters of many strange and light quarks that are held together in a single bag according to the bag model [20]. The main argument can be described as 'strange nucleosynthesis'. Greiner argues that a fireball with high particle density but relatively little energy density can generate a large number of hyperons in a small volume. In this case the hyperons can coalesce, simply by sufficient wavefunction overlap. The system is relatively cold, so there is little rapid expansion. In addition the existing baryon density caused by the stopping of the projectile in the target will cause the generated anti-strange quarks to combine with the existing light quarks to kaons which will be radiated off the fireball, whereas the strange quarks will stay in the fireball. This net strangeness will lead to enhanced hyperon production in a small volume. The penalty factors for hyperon coalescence were assumed to be comparable to simple baryon coalescence [27]. Recent measurements by the E864 Collaboration at the AGS, though, seem to indicate that there is an extra penalty factor for including a hyperon instead of a proton or neutron [28]. The group has measured the ${}^{3}_{\Lambda}$H hyper nucleus and compared its production rate to the production of ${}^{3}$He. Based on these measurements it seems that the inclusion of a single hyperon leads to an additional penalty factor of about five. Thus, the original strangelet production rate predictions might be overly optimistic. Still, a variety of conclusive heavy-ion experiments have been performed or are still ongoing. E864 has set convincing upper limits to positive, neutral, and negative strangelet production. Their measurements are based on detecting a color-singlet configuration that has a mass of A = 10-15 amu and a small charge to baryon ratio. The detection method of choice is calorimetry in combination with a 'late energy trigger' to subtract background. Details can be found in [29]. Their strangelet limits (90% confidence level) vary between $10^{-9}$ and $10^{-7}$ depending on the charge state. No evidence for a strangelet has yet been found, but E864 is still analyzing data.

## 6. Future Measurements at RHIC

The main difference in stepping from fixed target experiments at AGS and SPS to the RHIC collider is the expected large increase in energy density in the collision [30]. Contrary to the fixed target experiments the probability of stopping will be drastically reduced, which means the two beams will be almost transparent to each other. That leads to a large energy density in the central collision region, but only a small baryon density. The initial temperatures will be higher, but the likelihood of forming a cold, particle dense plasma will be reduced. This has some implications on the various aspects of the RHIC hyperon program. The probability of forming strange quark matter might be reduced due to the high energy density and low particle density. In return the probability of enhancing and equilibrating strangeness might be increased. An interaction at RHIC is expected to undergo several distinct stages, beginning with a parton-parton interaction, followed by a parton cascade and finally a hadron cascade. It is unclear whether either cascade will lead to chemical equilibration, but the time before hadronization as well as the time for thermal equilibration after hadronization is enhanced. Geiger has shown that on the basis of the initial parton interaction, which will be dominated by gluonic processes, and the subsequent parton cascade, strangeness should be enhanced by an order of magnitude in the case of a QGP compared to a simple hadron gas scenario [2]. Strangeness equilibration will be more likely, simply due to the longer time the QGP will have to equilibrate. Estimates based on hydrodynamical models show that the hadronization time is expected to double (from about 8 fm/c to about 16 fm/c).

Based on these predictions, the RHIC hyperon program will initially be very similar to the just completed AGS and SPS programs. The main goal of the early measurements will be to establish the hyperon abundances, the hyperon-antihyperon ratios and the hyperon kinematic spectra. Although the particle production is much higher at RHIC than in the fixed target experiments we do not expect to generate hyperons at a rate that will allow us to measure their production on an event by event basis. Pions will be reconstructed by the thousands in each event, but the hyperon rate is still sufficiently small to require a many event sample for the spectra and the ratio measurements. The main detector for strangeness reconstruction is the STAR detector [32]. STAR is a typical cylindrical collider detector, featuring a large Time Projection Chamber (TPC) as its main tracking volume. The TPC is radially preceeded by a Sil-

icon Vertex Tracker (SVT). This device with its superior position resolution and particle identification capabilities allows the reconstruction of all short lived hyperons up to the $\Omega$. The SVT/TPC tracking combination resides in a 0.5 T solenoidal magnetic field and is backed up by an electromagnetic calorimeter (EMC) and a time-of-flight patch (TOFp) as well as a small ring imaging Cherenkov counter (RICH) for high momentum particle identification. The central tracker covers a pseudo-rapidity range $\eta$=$\pm$1. In forward direction STAR is equipped with two radial time projection chambers (FTPC) that extend coverage and possibly $\Lambda$ reconstruction capabilities out to about $\eta$=4.

By combining the capabilities of the SVT and the TPC, hyperon reconstruction is sufficiently efficient to produce spectra within a short period of time during a RHIC running year (36 weeks/year). Figs.10 and 11 show the anticipated mass resolutions and accumulated statistics for $\Lambda$'s and $\Xi$'s, that can be obtained in 5 minutes and about a day of running, respectively.

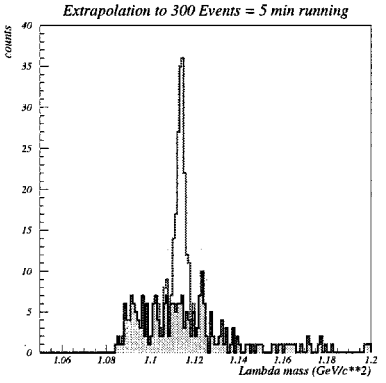


Figure 10. $\Lambda$ mass reconstruction. Simulation result based on statistics comparable to a few minutes of RHIC running

The efficiency in the $\Lambda$ reconstruction is sufficiently high to yield a good sample of events with more than one reconstructed $\Lambda$ which will allow a correlation analysis based solely on $\Lambda$'s. Even though there will be no event-by-event hyperon signature, the hyperon reconstruction will aid in specifying event classes with enhanced hyperon production. These classes will then be analyzed

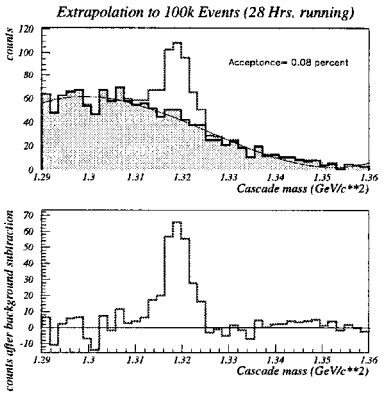


Figure 11. $\Xi$ mass reconstruction. Simulation result based on statistics comparable to one day of RHIC running

for other potential QGP signatures, rather than having to analyze all recorded events.

Even though the probability for strange quark matter production based on coalescence type models might be reduced, the search for exotic forms of matter, like the strangelets or the H-Dibaryon will certainly be attempted. The tools are in place and the efficiency estimates show that it should be feasible to determine the probability of strange quark matter formation. A more detailed summary of the present state of strangeness related simulations for RHIC can be found in [31].

The results at RHIC will be groundbreaking. They will lead the field of relativistic heavy ion physics into an energy regime, where the transition into a new phase of matter is almost guaranteed as long as this phase really exists. Therefore even a negative result will be conclusive and lead to important ramifications for high energy, nuclear, and cosmological physics. We can all look forward to exciting results from the four experiments at RHIC: STAR [32], PHENIX [33], BRAHMS [34], and PHOBOS [35].

## 7. Acknowledgments

I would like to thank Matt Lamont for preparing the Armenteros plot. I also kindly acknowledge fruitful discussions with Helen Caines, Tom Humanic, Carsten Greiner, and Jan Rafelski on the issues of hyperon and strangelet production.

## REFERENCES


1. P. Koch, Z.Phys. C38 (1988) 269
2. K. Geiger, Phys.Rev. D48 (1993) 4129
3. R. Lietava, J.Phys. G25 (1999) 181
4. J. Rafelski, J.Phys. G25 (1999) 451
5. R. Stock, Prog.Part.Nucl.Phys. 42 (1999) 295
6. P. Braun-Munzinger et al., Phys.Lett. B365 (1996) 1
7. J.Letessier and J. Rafelski, J.Phys. G25 (1999) 295
8. R. Bellwied, H. Caines, T. Humanic, Phys.Rev. C, to be published
9. H. van Hecke et al., Phys.Rev.Lett. 81 (1998) 5764
10. E. Schnedermann and U. Heinz, Phys.Rev. C50 (1994) 1675
11. E. Andersen et al. (NA36 Collab.), Phys.Lett. B327 (1994) 433
12. U. Heinz, J.Phys. G25 (1999) 263
13. M. Jacob and J. Rafelski, Phys.Lett. 190 (1987)
14. A.D. Panagiotou, Phys.Rev. C33 (1986) 1999
15. T. Hallman for E810 Collab., HIPAGS 90 Conference, BNL print 44911 (1990)
16. S. Kabana for NA35 Collab., Strange Quark Matter 94 conference, World Scientific (1994)
17. H. Caines for the E896 Collab., QM99, Nucl.Phys.A, to be published (1999)
18. D. Boal et al., Rev.Mod.Phys. 62 (1990) 553
19. C. Greiner and B. Mueller, Phys.Lett. B 219 (1989) 199
20. E. Farhi and R.L. Jaffe, Phys.Rev. D32 (1985) 2452
21. E. Witten, Phys.Rev. D30 (1984) 272
22. R. Jaffe, Phys.Rev.Lett. 38 (1977) 195
23. D. Ashery, AIP Conf.Proc. 432 (1998) 293
24. R. Longacre for the E810 Collab., QM95, Nucl.Phys. A590 (1995) 477c
25. K. Imai, Nucl.Phys. A547 (1992) 199c
26. C. Greiner et al., Phys.Rev.Lett. 58 (1987) 1825
27. A.J. Baltz and C. Dover, Phys.Lett. B325 (1994) 7
28. C. Pruneau for the E864 Collab., QM99, Nucl.Phys. A, to be published
29. T.A. Armstrong et al. (E864 Collab.), Phys.Rev.Lett. 79 (1997) 3612
30. A. Dumitru and D.H. Rischke, Phys.Rev. C59 (1999) 354
31. R. Bellwied, J.Phys. G25 (1999) 437
32. J. Harris et al., (STAR Collaboration), Nucl.Phys. A566 (1994) 277c
33. S. Nagamija et al., (PHENIX collaboration), Nucl.Phys. A566 (1994) 287c
34. F. Videbaek et al. (BRAHMS Collaboration), Nucl.Phys. A566 (1994) 299c
35. B. Wyslouch et al. (PHOBOS Collaboration), Nucl.Phys. A566 (1994) 305c

# Chapter 11

# Panel Discussion

The goal of this panel discussion was to address questions and comments on where we are going or might go in hyperon physics in a near and far future.

The chairman of the Panel was Mike Albrow and the Panel Members where N. Cabibbo, P. Cooper. W. Foster, D. Kaplan, L. Landsberg, P. Zenczykowski. The discussion lead by Mike Albrow started by several short theoretical and experimental introductions given by the panel members on their thought on hyperon physics in the future in terms of theory, experiment and machine. Some of these introductions are reported here.

# Should $\bar{p}p \to \bar{\Lambda}\Lambda$ be revived?

Daniel M. Kaplan [a*]

[a]Physics Division, Illinois Institute of Technology,
Chicago, IL 60616, USA

The continued interest of *CP* violation in hyperon decay (as well as many other physics topics that could be addressed by such a facility) suggests that a dedicated $\bar{p}$ storage ring at Fermilab ought to be reconsidered. With recent and anticipated technical progress, sensitivity many orders of magnitude beyond that achieved in LEAR may be possible, including $10^{-5}$ sensitivity for the $\Lambda/\bar{\Lambda}$ *CP*-asymmetry parameter $A_\Lambda$.

From 1984 until LEAR was shut down in 1996, the reaction $\bar{p}p \to \bar{\Lambda}\Lambda$ was extensively studied by the PS185 experiment [1]. This technique was proposed by Donoghue, Holstein, and Valencia [2] in 1986 (and during 1990–1992 further elaborated by the CERN CP-Hyperon Study Group [3]) as a possible avenue to detection of *CP* violation in hyperon decay. The PS185 group has since published [4] the world's most sensitive limit to date on the $\Lambda/\bar{\Lambda}$ *CP* asymmetry [5] $A_\Lambda \equiv (\alpha + \bar{\alpha})/(\alpha - \bar{\alpha}) = 0.013 \pm 0.022$, based on $\approx 10^5$ events, and analysis of the large PS185 data sample continues.[1]

The CERN hyperon-*CP*-violation study also stimulated the 1992 Fermilab Proposal 859 by Hsueh and Rapidis [6]. By this time PS185 had demonstrated $\mathcal{O}(10^{-2})$ sensitivity, and the goal of P859 was sensitivity of $1 \times 10^{-4}$, where model calculations [7] predicted a possibly-detectable effect. They proposed a modification of the PS185 approach, with a new dedicated $\bar{p}$ storage ring to be built at Fermilab for the purpose. The proposal was turned down, with the comment that it would take $10^{-5}$ sensitivity to justify building a new storage ring [8]. A 1993 proposal for a fixed-target experiment at $1\times10^{-4}$ sensitivity was eventually approved, leading to the HyperCP experiment now running in the Meson Center beamline [9].

While the large value of $\epsilon'/\epsilon = (21.2 \pm 4.6) \times 10^{-4}$ [10,11] suggests the possibility that $A_\Lambda$ might be similarly large [10], whether HyperCP observes a few $\times\, 10^{-4}$ to $10^{-3}$ effect or not, it is of interest whether sensitivity at the $10^{-5}$ level is feasible.[2] This would require $\sim 10^{11}$ events, 100 times as many as in HyperCP — probably not feasible in the fixed-target approach. Thus we should explore whether $\bar{p}p \to \bar{\Lambda}\Lambda$ could be pushed to $10^{-5}$.

The P859 sensitivity estimate was based on 3 months of running at an average luminosity of $1.6 \times 10^{32}\,\mathrm{cm}^{-2}\mathrm{s}^{-1}$, to be achieved with 260 mA of 1.64 GeV/$c$ antiprotons, in a ring about 1/3 the size of the Accumulator, incident on a hydrogen-gas-jet target of $1 \times 10^{14}\,\mathrm{atoms/cm}^2$. This luminosity requires antiproton production at a minimum rate of $6 \times 10^{10}$/hour.

While these numbers were ambitious for 1992, they have since been surpassed by the $\bar{p}$ source and the E835 gas-jet target. A factor 100 in event sample is nevertheless a tall order. It might be achievable with (for example) luminosity $1 \times 10^{33}\,\mathrm{cm}^{-2}\mathrm{s}^{-1}$ over four years of running, with 500 mA of antiprotons and target density of $3 \times 10^{14}\,\mathrm{atoms/cm}^2$. While this target density has been achieved by the E835 collaboration [12], the required antiproton production rate of $3.6 \times 10^{11}$/hour is a factor $\approx$2 extrapolation beyond current plans for Tevatron Run II [13]. This is not unreasonable, especially given plans for a substantial proton-source upgrade at Fermilab [14].

Of course, the establishment or refutation of feasibility at $10^{-5}$ sensitivity will require a great deal more work — for example, on storage-ring optics and cooling, triggering and data acquisition, and especially a detailed study of systematic uncertainties. The importance of this physics suggests that such an effort is worthwhile. More generally, the availability of a $\bar{p}$ source orders of magnitude beyond LEAR in intensity should

*E-mail: kaplan@fnal.gov

[1]Here $\alpha$ is the up-down asymmetry parameter for $\Lambda \to p\pi^-$ decay and $\bar{\alpha}$ is that for the charge-conjugate decay.

[2]Since HyperCP measures the sum of the $\Xi$ and $\Lambda$ asymmetries, a direct measurement of $A_\Lambda$ will be important even if HyperCP observes a large value for the sum $A_\Xi + A_\Lambda$.

make possible a wide range of interesting physics. Given the relatively modest cost of such a project, it should be seriously considered as an add-on to the Fermilab program in the coming decade.

## REFERENCES


1. http://hpfr02.physik.uni-freiburg.de/ps185/ps185.html.
2. J. F. Donoghue, B. R. Holstein, and G. Valencia, Phys. Lett. **178B**, 319 (1986) and *Int. J. Mod. Phys.* A, **2**, 319 (1987).
3. N. Hamann *et al.* (CP-Hyperon Study Group), "*CP* Violation in Hyperon Decays: The Case $\bar{p}p \to \bar{\Lambda}\Lambda \to \bar{p}\pi^+ p\pi^-$," CERN/SPSLC 92-19 (1992).
4. P. D. Barnes *et al.*, Phys. Rev. C **54**, 1877 (1996).
5. J. F. Donoghue and S. Pakvasa, Phys. Rev. Lett. **55**, 162 (1985).
6. S. Hsueh and P. Rapidis, Fermilab Proposal 859 (1992).
7. J. F. Donoghue, X. G. He, and S. Pakvasa, Phys. Rev. D **34**, 833 (1986).
8. J. Peoples, letter to P. Rapidis and S. Hsueh, July 16, 1992.
9. K. S. Nelson, this conference; see also
   S. Antos *et al.*, Fermilab Proposal 871 (Revised Version), Mar. 1994;
   see also E. C. Dukes, "A New Fermilab Experiment to Search for Direct *CP* Violation in Hyperon Decays," in **High Energy Spin Physics**, K. J. Heller and S. L. Smith, eds., AIP Conference Proceedings **343** (1994);
   K. B. Luk, "Experimental Prospects for Observing *CP* Violation in Hyperon Decay," in **Heavy Quarks at Fixed Target,** *Proc. HQ94 Workshop*, B. Cox, ed., Frascati Physics Series **3** (1994), p. 81;
   D. M. Kaplan, "Fixed Target *CP* Violation Experiments at Fermilab," IIT-HEP-96-2, presented at *5th Hellenic School and Workshops on Elementary Particle Physics*, Corfu, Greece, 3–24 Sept. 1995, hep-ex/9509009.
10. X.-G. He *et al.*, "CP Violation in Hyperon Decays from Supersymmetry," ISU-HEP-99-7, hep-ph/9909562 (1999).
11. A. Alavi-Harati *et al.*, Phys. Rev. Lett. **83**, 22 (1999);
    V. Fanti *et al.*, "A New Measurement of Direct CP Violation in Two Pion Decays of the Neutral Kaon," CERN-EP-99-114, hep-ex/9909022 (1999).
12. S. Pordes, private communication.
13. E. Harms, private communication.
14. W. Chou, *Proc. 1999 Particle Accelerator Conference*, A. Luccio and W. MacKay, eds., IEEE, New York (1999), p. 3285.

# An outlook for the hyperon physics at the beginning of the next millennium

L.G.Landsberg
Institute for High Energy Physics, Protvino, Moscow region, 142284, Russia

Future possibilities for hyperon physics in the experiments on VLHC 3 TeV booster are outlined.

We had a very interesting conference in the last 2 days. A lot of new results in hyperon physics were presented. It was also clear that many future works in studying of hyperon properties would be very important for the further advance in this field. We need a new generation of precision study for weak hyperon decays. We only begin the study of electromagnetic properties of hyperons and hyperon resonances. There are many open questions in the spectroscopy of hyperon resonances and strange-charmed baryon states, in the search for exotic strange, hidden-strange and charmed-strange hadrons.

But our possibilities to make such experiments are greatly reduced now. In the next decade we lose the 600 GeV hyperon beam of the Tevatron Fermilab, the best one in the world. I do not know well the situation with a hyperon beam in CERN, but it seems to me that this situation is not very optimistic. I do not believe in hyperon beams in the Main Injector — it is a very good machine as a kaon factory, but its energy is too low for a good hyperon beam. Certainly, it is possible to study hyperons not only on hyperon beams, but to my mind the experiments with hyperon beams are the most straightforward and effective.

Thus, it seems to me that the real prospects for hyperon physics at the beginning of the next millennium are connected with VLHC project in Fermilab with its 3 GeV proton booster. The fixed target experiments on this booster would provide us with a possibility to perform a qualitatively new step in properties of hyperon beams and in studying of the hyperon physics. The transition from energy of 1 TeV to 3 TeV may be not so important in other fields, but for the hyperon physics a high primary energy allows one to produce pure intense hyperon beams, whose characteristics are close to those of usual hadron beams. At these energies the decay length for charged hyperons is about $50 \div 100$ m and it becomes possible to form a focused hyperon beam in the channel with magnetic optics, as well as to construct a very reliable shielding, designed for the operation with the ultimate intensity of the proton beam (up to $\sim 10^{13}$ p/s). The shielding includes an active guard system of magnetized iron slabs, which greatly reduces the muon background in the setup area. All these measures taken together make it possible to realize the operational modes in the range of $x_F > 0.9$, where $I(\Sigma^-) \gg I(\pi^-)$. Almost pure $\Sigma^-$ beam with momentum of $P_\Sigma = 2.7$ TeV/c and intensity $> 10^7 s^{-1}$ can be obtained at 3 TeV machine. These properties of an expected hyperon beam are unique.

To present more detailed quantitative results I will use the data from our proposal [1,2] for the experiments with the hyperon beam of UNK proton accelerator with energy 3 TeV which was being constructed in IHEP a decade ago. At that time we expected the UNK project to be completed in the middle of nineties and developed the fixed target program for this facility with great enthusiasm. Unfortunately, the UNK project was stopped, as is well known. But existing proposals can illustrate the possibilities of fixed target experiments on VLHC 3 TeV booster machine.

The scheme of the UNK hyperon beam, which includes a system of particle quadrupole focusing and active muon shielding, was presented in [1,2]. The main parameters of the hyperon beam are: beam line $L = 100$ m; total deflection angle 9.6 mrad; beam dimensions in the focus $\sigma_x \approx \sigma_y \approx (2 \div 3)$ mm; momentum bite $\sigma_p \approx 5\%$; momentum resolution in the beam spectrometer $\sigma_p < 1\%$. Almost pure $\Sigma^-$ beam (with pion admixture $< 15\%$) with momentum $P_\Sigma = 2.7$ TeV/c and intensity $1.5 \cdot 10^7$ $\Sigma^- s^{-1}$ can be produced per $10^{12}$ $p \cdot s^{-1}$. The integral fluxes of hyperons $N(\Sigma^-) \simeq 3 \cdot 10^{13} \Sigma^-$; $N(\overline{\Sigma^+}) \simeq 3 \cdot 10^7$ $\overline{\Sigma^+}$; $N(\Xi^-) \simeq 3 \cdot 10^{11}$ $\Xi^-$; $N(\Omega^-) \simeq 4 \cdot 10^8$ $\Omega^-$ may be obtained per 100 days of the UNK machine operation ($3 \cdot 10^6$ s with an account of the 30% duty factor). The decay of $\pi$, $K$ mesons from hadronic cascades produced in the target and beam channel elements is the main muon source in the hyperon beam channel. An effi-

cient shielding against muons may be provided if muons are deflected vertically with the help of an optimized system of two magnetic spoilers with oppositely directed currents. The system reduces the muonic flux onto experimental area $\simeq 10^2$ times and thus lowering muon background $N_\mu(halo/m^2)/N_\Sigma$ (beam) down to $< 3\%$.

For comparison let us present the characteristics of Fermilab Tevatron hyperon beam with momentum 600 GeV/c which was used in the experiments of the SELEX Collaboration: $I(\Sigma^-) \simeq 2.5 \cdot 10^5\ \Sigma^-/s/(1 \div 1.5) \cdot 10^{11} p/s$; $N_\mu(halo/m^2)/N_\Sigma(beam) \sim 5$; $N_{\Sigma^-}/N_{beam} \simeq 50\%$. Certainly, for some experiments it was possible to increase intensity 2–3 times, but this increase is limited by heavy background conditions.

Let us outline the main possible trends of the research program on a future unique $\sim$ 3 TeV pure hyperon beam (see [1,2] for more details).

1. Search for exotic strange-charmed and strange-beauty quasistable hadrons of Lipkin's type [3,4]. Pure strange beam has advantages in these searches [1,2,5,6].

2. Search for exotic strange baryons in the diffractive-like processes with the hyperon beam (see [1,2,5]).

3. Study of strange-charm and strange-beauty baryons (the prolongation of the SELEX type experiments).

4. The elastic and inelastic hyperon scattering on the atomic electron target and the study of the $\Sigma^-$, $\Xi^-$, $\Omega^-$ hyperon formfactors and transition $\Sigma - \Sigma^*$ formfactors. For example, it was demonstrated that in $10^2$ hours of measurements it is possible to determine $F_{\Sigma^-}(q^2)$ formfactor up to the momentum transfer $q^2 = 1.5$ (GeV/c)$^2$ and $SU(3)$ suppressed transition formfactor $F_{\Sigma^-\Sigma^{*-}}(q^2)$ up to $q^2 \simeq 0.8$ (GeV/c)$^2$ [1].

5. The Coulomb production of the excited hyperon states $\Sigma(1385)^{*-}$, $\overline{\Sigma(1385)^{*+}}$, $\Xi(1530)^*$, $\Lambda(1520)^*$, etc. and the measurements of their radiative decay widths. Some of these radiative processes are $SU(3)$ and $SU(6)$ suppressed. A very high primary energy is a great advantage of the Coulomb production experiments (because of the extinction of background of coherent strong production processes with energy).

6. Measurements of the hyperon polarizabilities in the Coulomb production reactions $\Sigma^- + Z \to \Sigma^- + \gamma + Z$), etc.

7. The measurement of the $\Sigma^-$ hyperon structure function and its comparison with the proton structure function in the reaction $\Sigma^- N \to (\mu^+\mu^-) + X$ and $pN \to (\mu^+\mu^-) + X$ at 3 TeV.

8. Weak decays of $\Sigma^-$, $\Lambda^o$, $\Xi^-$, $\Omega^-$ hyperons (high precision studies of weak hyperon decays and search for rare processes of this type). The sensitivity of the relevant experiments may be $10^{-13}$ for $\Sigma^-$ decays, $10^{-11}$ for the $\Xi^-$ and $\Lambda^o$ decays, and $10^{-8}$ for $\Omega$ decays (the decay $\Xi^- \to \Lambda^o\pi^-$ is the source of the tagged polarized $\Lambda^o$ hyperons). For example, it was estimated, that it would be possible to obtain $10^7$ events of rare decay $\Sigma^- \to \Lambda e^-\bar{\nu}_e$ (BR $= 5.7 \cdot 10^{-5}$) for 1 day of measurements [1] and $\gtrsim 10^4$ events/day of the decay of $\Sigma^+ \to \Lambda e^+\nu_e$ in exposition on positive beam. The problem of precise determination of the ratio $\Gamma(\Sigma^- \to \Lambda e^-\nu_e)/\Gamma(\Sigma^+ \to \Lambda e^+\nu_e) = R \cdot$ (phase space factor) $= R(1.228 \pm 0.009)$ was discussed in several talks at this conference. From existing experimental data (the world statistics of $\Sigma^+ \to \Lambda e^+\nu_e$ is $\sim 20$ events, and for $\Sigma^- \to \Lambda e^-\bar{\nu}$ is $\sim 1850$ events) $R = 1.25 \pm 0.25$. In the new measurements it would be possible to measure $R \simeq 1$ with precision $\sim 10^{-2}$ which is very important for the search for $\Sigma^o - \Lambda$ mixing and for weak currents of second kind.

9. A conventional program for study of the hyperon strong interactions in a new energy region (total cross section, elastic scattering, polarization experiments, etc.).

In conclusion, let me stress, that in my opinion it was a great mistake not to continue the experiments on the Tevatron 600 GeV/c $\Sigma^-$ beam in the last fixed target run. Let me also hope that the possibility to continue the hyperon physics studies at a new qualitative level on the future 3 TeV VLHC booster would be realized.

## REFERENCES


1. V.I.Garkusha et al., Preprint IHEP 90-81, Protvino (1990).
2. L.G.Landsberg, Nucl. Phys. (Proc. Suppl.) **B21** (1991) 306.
3. H.J.Lipkin, Phys. Lett. **B70** (1977) 113.
4. H.J.Lipkin, Phys. Lett. **B195** (1987) 484.
5. L.G.Landsberg et al., Preprint IHEP 94-19, Protvino (1994).
6. M.A.Moinester et al., Z. Phys. **A356** (1996) 207.

# Weak radiative hyperon decays: suggestions

P. Żenczykowski [a]

[a]Institute of Nuclear Physics,
Radzikowskiego 152, 31-342 Kraków, Poland

A short discussion is given as to which data are expected to provide additional clues on the puzzle of weak radiative hyperon decays. It is stressed that the much-awaited experimental result for the asymmetry of the $\Xi^0 \to \Lambda\gamma$ decay may be corroborated independently by measuring the $\Lambda \to n\gamma$ asymmetry. Theoretical predictions for those weak radiative decays which are due solely to the $s \to d\gamma$ single-quark transition are briefly presented. It is argued that the most interesting parameters to measure would be the asymmetries of the $\Xi^-$ and $\Omega^-$ weak radiative decays.

## 1. INTRODUCTION

There are two types of quark-level weak radiative processes. The first one is the two-quark transition $su \to ud\gamma$, and the other - single-quark decay $s \to d\gamma$. Properties of the two-quark transition are intimately related to the issue of possible violation of Hara's theorem. I believe that when all relevant experimental results on decays dominated by two-quark transitions become finally available, this issue will be phenomenologically settled. The data on single-quark decays should then help make our understanding of weak radiative hyperon decays (WRHD's) complete.

## 2. TWO-QUARK TRANSITIONS

Experimental and theoretical figures that are most important to the issue of a possible violation of Hara's theorem are given in Table 1.

The data in Table 1 favor the Hara's-theorem-violating VMD description. I think that the VMD prediction of the $\Xi^0 \to \Sigma^0\gamma$ asymmetry is very good, particularly when taking into account the fact that it was obtained at the time when the (erroneous) experimental figure for that asymmetry was $+0.20 \pm 0.32$, which pulled the prediction of the one-parameter VMD fit towards zero. The VMD prediction depends on a parameter describing the size of the parity-violating amplitude for single-quark radiative transition. The complete $\Xi^0 \to \Sigma^0\gamma$ parity-violating amplitude is given as a sum of this single-quark amplitude and a contribution from two-quark transitions. Small size of the previous experimental number for the $\Xi^0 \to \Sigma^0\gamma$ asymmetry required substantial cancellation between the two contributions, forcing a larger value for the single-quark amplitude, and a value for the $\Xi^- \to \Sigma^-\gamma$ branching ratio greater than that measured experimentally.

As discussed in my review talk [1], crucial information concerning the violation of Hara's theorem will be known when a more precise experimental data for the $\Xi^0 \to \Lambda\gamma$ asymmetry becomes finally available from KTeV. The positive (negative) sign would signify that Hara's theorem is violated (satisfied). This sign depends on whether symmetry-related contributions from diagrams (2) (Fig. 1 of ref.[1]) should be added to (or subtracted from) symmetry-related contributions from diagrams (1) (cf. last two columns in Table 1). The addition (subtraction) procedures pick the symmetric $g_{1,kl}$ (antisymmetric $g_{2,kl}$) terms in the axial current [1]. Whatever the outcome of KTeV, the obtained result may be independently corroborated by measuring the asymmetry of the $\Lambda \to n\gamma$ decay, which behaves in a way similar to that for $\Xi^0 \to \Lambda\gamma$. I believe therefore that it is quite important to measure the asymmetry of the $\Lambda \to n\gamma$ decay as well.

Given the asymmetry and branching ratio for a given decay, one may extract the size of the amplitudes up to two-fold ambiguity (parity violating $\leftrightarrow$ parity conserving). Thus, even though a model that predicts the related asymmetries and branching ratios with almost no parameters is apparently correct, it would still be nice to see experimental data concerning the amplitudes themselves.

## 3. SINGLE-QUARK TRANSITIONS

Although single-quark transition is not relevant as far as the issue of the violation of Hara's theorem is concerned, it is nonetheless important to understand this transition as well. At present we

Table 1
WRHD asymmetries: comparison of theoretical predictions with experiment

| Decay | Asymmetries | | | Weights for Fig.1, ref.[1] | |
|---|---|---|---|---|---|
| | Experiment | VMD [4] | GLOPR [5] | (1) | (2) |
| $\Lambda \to n\gamma$ | | $+0.8$ | $-0.49$ | $\frac{1}{6\sqrt{3}}$ | $\frac{1}{2\sqrt{3}}$ |
| $\Xi^0 \to \Lambda\gamma$ | $+0.43 \pm 0.44$ [1] | $+0.8$ | $-0.78$ | 0 | $-\frac{1}{3\sqrt{3}}$ |
| $\Xi^0 \to \Sigma^0\gamma$ | $-0.65 \pm 0.13$ [2] | $-0.45$ | $-0.96$ | $\frac{1}{3}$ | 0 |

[1] ref.[2]
[2] ref.[3]

have only one fairly precise experimental figure concerning the size of this transition: the branching ratio of the $\Xi^- \to \Sigma^-\gamma$ decay was measured to be $(0.128 \pm 0.023) \cdot 10^{-3}$ [6]. There is a weak indication that the corresponding asymmetry is positive. In addition, there is an upper experimental bound of $0.46 \cdot 10^{-3}$ on the branching ratio of the $\Omega^- \to \Xi^-\gamma$ decay.

The simple quark model predicts that the asymetries in the $\Xi^-$ and $\Omega^-$ decays are equal to the $s \to d\gamma$ asymmetry which should be [7]

$$\alpha(s \to d\gamma) = \frac{m_s^2 - m_d^2}{m_s^2 + m_d^2} \qquad (1)$$

Its value is positive ($+0.4$ for constituent quark masses and $+1$ for current quark masses). The VMD fit [4] gave $\alpha(\Xi^- \to \Sigma^-\gamma) \approx +0.6$. The question is whether these predictions are confirmed when more elaborated theoretical calculations are performed. Calculations of various short-distance contributions lead to the $\Xi^- \to \Sigma^-\gamma$ branching ratios which are at least an order of magnitude below the present experimental value [8]. Short-distance contributions to the branching ratio of the $\Omega^-$ radiative decay are also small.

Extensive analyses of long-distance contributions to single-quark transitions were carried out by Singer [8,9], who considered the amplitudes generated by the VMD dynamics as well as the unitarity contributions generated by rescattering.

In the $\Xi^-$ decay, the unitarity-generated contribution from the process $\Xi^- \to \Lambda\pi \to \Sigma^-\gamma$ gives a branching ratio of $0.18 \cdot 10^{-3}$, i.e. approximately of the size experimentally observed. The predicted asymmetry is $-0.13 \pm 0.07$. In the $\Omega^-$ decay, the contribution to the branching ratio from the process $\Omega^- \to \Xi^0\pi^- \to \Xi^-\gamma$ (considered to be dominant) was calculated to be very small: $0.015 \cdot 10^{-3}$.

The VMD prescription gives similar predictions for both $\Xi^-$ and $\Omega^-$ branching ratios: $0.1 \cdot 10^{-3}$ for $\Xi^-$, and $0.4 \cdot 10^{-3}$ for $\Omega^-$. Furthermore, VMD gives the same prediction of $+0.4$ for both the $\Xi^-$ and the $\Omega^-$ asymmetries. After adding the contributions from both long distance mechanisms, Singer estimates that the asymmetry in the $\Xi^-$ decay should be fairly small, between $-0.2$ and $+0.3$, while for the $\Omega^-$ he expects a value of $+0.4$, similar to that in the consitutent quark model.

There are two questions that may be asked here. The first one concerns reliability of unitarity calculations in which only one intermediate state is taken into account (even though believed to be dominant). Furthermore, the VMD prescription may be applied to the rescattering process $\Xi^- \to \Lambda\pi \to \Sigma^- V$ with $V = \rho, \ldots$ (and similarly for $\Omega^-$). Thus, the question of double counting appears when the VMD and rescatterring contributions are added. In other words, VMD might include all rescatterring corrections. One would expect then that both the $\Xi^-$ and $\Omega^-$ decays are characterized by the same asymmetry, presumably $+0.4$ or greater. Clearly, it would be very interesting to have these asymmetries measured.

## REFERENCES


1. P. Żenczykowski, this conference.
2. C. James et al, Phys. Rev. Lett. 64, 843 (1990).
3. U. Koch, this conference.
4. J. Lach, P. Żenczykowski, Int. J. Mod. Phys. A10, 3817 (1995).
5. M. B. Gavela et al., Phys. Lett. B101, 417 (1981).
6. T. Dubbs et al., Phys. Rev. Lett. 72, 808 (1994).
7. N. Vasanti, Phys. Rev. D13, 1889 (1976).
8. P. Singer, Phys. Rev. D42, 3255 (1990)
9. G. Eilam, A. Ioannissyan, P. Singer, Mod. Phys. Lett. A11, 2091 (1996).

# Chapter 12

# Summary Talks

- P. Ratcliffe
- E. Ramberg

# Theory Summary

Philip G. Ratcliffe [a*]

[a] Dip. di Scienze, Univ. degli Studi dell'Insubria—sede di Como, via Lucini 3, 22100 Como, Italy
and Istituto Nazionale di Fisica Nucleare—sezione di Milano, via Celoria 16, 20133 Milano, Italy

A summary is presented of the more theoretical aspects of the presentations made at Hyperon 99. In addition, some material is covered which was not presented at the symposium but which I feel is pertinent to the main theme of hyperons and/or, more in particular, to discussions conducted during the symposium.

## 1. INTRODUCTION

In this summary talk I shall attempt not only to highlight some of the issues touched upon by the speakers at this symposium but also to cover some of those topics which, for one reason or another, were left uncovered. All or most of the topics mentioned by Holstein in his opening overview talk were indeed dealt with during the last few days. However, some deserving issues, notably hypernuclei, were left untouched as too were other aspects of hyperon physics not considered by Holstein [1]. One of these is the large-$N_c$ expansion, which has been promoted in this context by the San Diego group and which should have been aired by Liz Jenkins who unfortunately was unable to attend, another is the possibility of using perturbative QCD to describe large-$p_T$ semi-inclusive hyperon production and the associated surprisingly large measured transverse hyperon polarisations. Last but not least, is the case of hypernuclei, which was only very briefly mentioned by Holstein.

While I hope to do justice to the speakers and, in particular, to the missing subjects, time and space clearly do not permit as complete a job as I might have liked. Thus, I shall only attempt to give a flavour of what was discussed here at Fermilab and its relevance to the future of hyperon physics programmes but leave the details to the speakers contributions; and also to fill in what I feel were important gaps, with at least a hint of what might have been said. Of course, for the full details the reader is referred to the original talks.

Before turning to the more serious part of the talk, the use of the expression "perturbative QCD" reminds of something that struck me on the flight from Italy to Chicago. Along with the pre-packed lunch, came a salad and a small container of what purported to be "Creamy Italian Dressing". Now, it might even be that the long list of exotic ingredients adds to its appeal in the eyes of some, and, certainly, hidden in there were the three prime ingredients I have been taught to use in Italy: namely, oil (though it should be of the olive variety and not soybean), vinegar and salt. However, I strongly doubt that any Italian in the audience will ever have put such a concoction onto his or her salad at home. That is to say: we have on occasions (albeit only a very few) at this symposium heard the words QCD mentioned, but it would be very hard indeed, given the usual trimmings or non-perturbative model input, to extract anything about the presumed fundamental theory of hadronic interactions itself from the sort of phenomenology discussed. On the one hand, this is refreshing for those of us who are a little weary of hearing about the latest $n$-loop or next-to-next-to...-leading-order calculation. On the other, there should be a wariness that much of the model building that goes on in hadronic physics, with the ever-comforting benefit of hindsight, often risks being little more than a patching-up job on a rather cloudy situation.

Let me now turn to the task in hand, I have divided the summary talk into sections describing: the static properties of hyperons; semi-leptonic, radiative and non-leptonic hyperon decays; hyperon polarisation and hypernuclei; with a little space dedicated to some concluding remarks.

## 2. STATIC PROPERTIES

I shall consider here the description of masses and magnetic moments (in particular, those of the baryon octet). Lipkin [2] reminded us of a remarkable series of predictions of the naïve quark model: *e.g.*, the relation between the baryon and

*E-mail: pgr@fis.unico.it

pseudoscalar and spin-one meson octet masses,

$$m_\Lambda - m_N \simeq \frac{3(m_{K^*} - m_K) + (m_K - m_\pi)}{4}; \quad (1)$$

experimentally, the left-hand side is 177 MeV and the right-hand side, 180 MeV. A similarly successful relation between the baryon octet and decuplet and pseudoscalar and spin-one meson masses is provided by

$$\frac{m_\Delta - m_N}{m_{\Sigma^*} - m_\Sigma} \simeq \frac{m_\rho - m_\pi}{m_{K^*} - m_K}; \quad (2)$$

where experimentally the two sides are 1.53 and 1.61 respectively. The simple but nevertheless important conclusion to be drawn is that quarks bound inside mesons behave just like quarks inside baryons.

With regard to the magnetic moments, there exist further simple relations:

$$\mu_p + \mu_n \simeq \frac{2m_p}{m_N + m_\Delta}, \quad (3)$$

where the experimental values are 0.880 and 0.865 respectively, and

$$\mu_\Lambda \simeq -\frac{1}{3}\mu_p \frac{m_{\Sigma^*} - m_\Sigma}{m_\Delta - m_N}, \quad (4)$$

here the experimental values are both -0.61!

Since Liz Jenkins was unable to be present at the symposium and despite Lipkin's bold attempt at an impersonation, we did not learn anything about the $1/N_c$-expansion approach [3] and the work of the San Diego group. It is impossible here to do justice to this field and the interested reader is referred to the comprehensive review article by Jenkins [4]. Let me simply try to give a flavour of what is involved and the results achieved.

A spin-flavour symmetry is found to emerge for baryons in the large-$N_c$ limit; large-$N_c$ baryons form irreducible representations of the spin-flavour algebra, and their static properties may be computed in a systematic expansion in $1/N_c$. Symmetry relations for static baryon matrix elements may then be obtained at various orders in the $1/N_c$ expansion by neglecting subleading $1/N_c$ corrections. These symmetry relations (such as those already mentioned) may then be arranged according to a $1/N_c$ hierarchy, *i.e.*, the higher the order in $1/N_c$ is the sub-leading correction, the better one expects the relation to be satisfied. For QCD baryons with $N_c = 3$ one then naturally expects such a hierarchy to be based on steps of roughly 1/3.

Thus, for example, the celebrated Coleman-Glashow mass relation,

$$(p - n) - (\Sigma^+ - \Sigma^-) + (\Xi^0 - \Xi^-) = 0, \quad (5)$$

is $\mathcal{O}(1/N_c)$ in the $1/N_c$ expansion, so that the mass relation should be more accurate than would be predicted by mere flavour-symmetry breaking arguments alone. In fig. 1 the diagram, taken from Jenkins and Lebed [5], shows a hierarchy of baryon-mass relations in both $1/N_c$ and an $SU(3)$ flavour-symmetry breaking parameter, $\epsilon \sim 0.3$, as predicted by the theoretical analysis. The accuracy with which the magnitude of the deviations follows the expected pattern is striking.

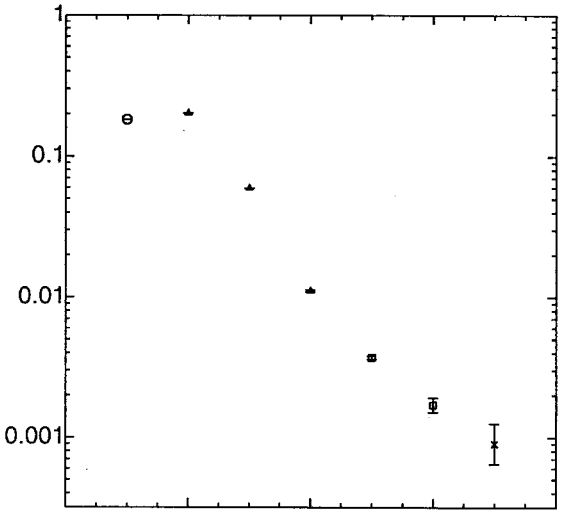


Figure 1. Isospin-averaged baryon-mass (normalised) combinations from [5]. The error bars are experimental and the horizontal scale is merely a label for the given combinations. The open circle is an $\mathcal{O}(1/N_c^2)$ mass combination; the three solid triangles are $\mathcal{O}(\epsilon/N_c)$, $\mathcal{O}(\epsilon/N_c^2)$, and $\mathcal{O}(\epsilon/N_c^3)$ mass relations; the open squares are $\mathcal{O}(\epsilon^2/N_c^2)$, and $\mathcal{O}(\epsilon^2/N_c^3)$ relations; and the cross is an $\mathcal{O}(\epsilon^3/N_c^3)$ relation.

Analogously, the baryon magnetic moments may also be studied. Results show that in the large-$N_c$ limit the isovector baryon magnetic moments are determined up to a correction of relative order $1/N_c^2$, so that the ratios of the isovector magnetic moments are determined for $N_f = 2$ flavours up to a correction of relative order $1/N_c^2$.

And again one finds that the general $1/N_c$ hierarchy is respected.

## 3. SEMI-LEPTONIC DECAYS

Another problem to which the $1/N_c$ expansion has been applied is that of hyperon semi-leptonic decay (HSD). Moreover at this symposium members of the KTeV collaboration have presented their results for the hitherto completely unexplored $\Xi^0$ $\beta$-decay, $\Xi^0 \to \Sigma^+ e\bar{\nu}$. Let us first examine the experimental situation: in fig. 2 the measured decay modes and nature of the data available are indicated, and in table 1 the values obtained for the decay widths and angular asymmetries are displayed.

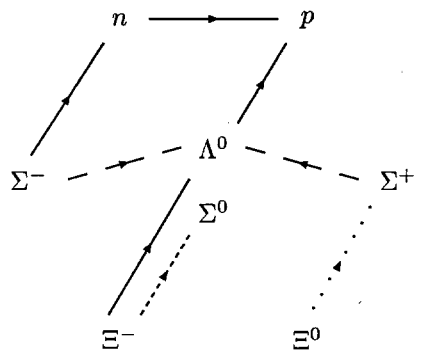


Figure 2. The SU(3) scheme of the measured baryon-octet $\beta$-decays: the solid lines represent decays for which both rates and asymmetry measurements are available; the long dash, only rates; the short dash, $f_1 = 0$ decays; and the dotted line, the recent KTeV data.

Noticeably missing from the data table is the recently published preliminary KTeV measurement of the decay $\Xi^0 \to \Sigma^+ e\bar{\nu}$, the interested reader is referred to the talks presented here by Alavi-Harati [7] and Bright [8]. The interesting point here is that the various approaches to dealing with SU(3) breaking in this sector provide well-defined and strongly bound predictions for both the decay rate and axial form factor; the data are now tantalisingly close to differentiating between the various predictions. It must be said (to the authors chagrin), however, that the present world data actually still marginally favour the original SU(3)-based prediction of Cabibbo theory [9] (more than a third of a century old).

A discussion of the theoretical problems involved was presented by García [10]. While pointing out that the only severe discrepancy (*i.e.*, larger than three standard deviations) with respect to Cabibbo theory lies with the rate for $\Sigma^- \to \Lambda^0 e\nu$, García also stressed that the to exploit the experimental information to the full, one should fit to the asymmetry parameters ($\alpha_{e\nu}$, $\alpha_e$, $\alpha_\nu$ and $\alpha_{B_f}$) and not merely to the extracted value of $g_1$ alone.

### 3.1. $F$ and $D$ or $g_A$'s (a rose by any other name ...)

Besides the obvious possibility as a measurement of the Cabibbo-Kobayashi-Maskawa (CKM) matrix element $V_{us}$, the solidity of which has been cast into doubt (see, *e.g.*, [6]), the study of HSD provides unique access to the $F$ and $D$ parameters necessary for a complete analysis of polarised deep inelastic scattering (DIS). Let me recall briefly the proton-spin story. Longitudinally polarised DIS is governed by the structure function $g_1(x, Q^2)$, whose integral in $x$ (the Bjorken scaling variable or partonic momentum fraction) is given in terms of quark spin contributions to the nucleon:

$$\begin{aligned} \Gamma_1^p &= \int_0^1 \mathrm{d}\, g_1(x, Q^2) \\ &= \tfrac{1}{2}\left[\tfrac{4}{9}\Delta u + \tfrac{1}{9}\Delta d + \tfrac{1}{9}\Delta s\right] \\ &\qquad \times \left[1 + \delta_{\mathrm{PQCD}} + \ldots\right] \end{aligned} \tag{6}$$

(note that here and in what follows the representation of the radiative corrections *etc.* is only intended to be schematic). The SMC experiment, for example, measures [11]

$$\Gamma_1^p = 0.120 \pm 0.005 \pm 0.006, \tag{7}$$

which, combined with the prediction that

$$\Gamma_1^p = \tfrac{1}{2}\left[F - \tfrac{1}{9}D + \tfrac{2}{3}\Delta s\right]\left[1 + \delta_{\mathrm{PQCD}} + \ldots\right], \tag{8}$$

leads to an extracted value for the strange-quark spin $\Delta s \simeq -0.1$ (using $g_A^n = 1.267$ and $F/D = 0.58$), which is a surprisingly large value for a sea contribution and constitutes the variously denominated spin "crisis", "problem" or "puzzle". The point is that if $F/D$ were to shift to 0.5 say, then the extracted value would become $\Delta s \simeq 0$, neatly resolving all conflict.

Given the obviously important rôle that HSD plays in this analysis, it is clearly vital to understand to what extent the values of $F$ and $D$

Table 1
The present world HSD rate and angular-correlation data [6]. The numerical values marked $g_1/f_1$ are those extracted from angular correlations.

| Decay | Rate ($10^6\,s^{-1}$) | | $g_1/f_1$ | $g_1/f_1$ |
|---|---|---|---|---|
| $A \to B\ell\nu$ | $\ell = e^{\pm}$ | $\ell = \mu^-$ | $\ell = e^-$ | SU(3) |
| $n \to p$ | $1.1274 \pm 0.0025$ [a] | | $1.2601 \pm 0.0025$ | $F + D$ |
| $\Lambda^0 \to p$ | $3.161 \pm 0.058$ | $0.60 \pm 0.13$ | $0.718 \pm 0.015$ | $F + D/3$ |
| $\Sigma^- \to n$ | $6.88 \pm 0.23$ | $3.04 \pm 0.27$ | $-0.340 \pm 0.017$ | $F - D$ |
| $\Sigma^- \to \Lambda^0$ | $0.387 \pm 0.018$ | | | $-\sqrt{2/3}\,D$ [b] |
| $\Sigma^+ \to \Lambda^0$ | $0.250 \pm 0.063$ | | | $-\sqrt{2/3}\,D$ [b] |
| $\Xi^- \to \Lambda^0$ | $3.35 \pm 0.37$ [c] | $2.1 \pm 2.1$ [d] | $0.25 \pm 0.05$ | $F - D/3$ |
| $\Xi^- \to \Sigma^0$ | $0.53 \pm 0.10$ | | | $F + D$ |

[a] Rate given in units of $10^{-3}\,s^{-1}$. [b] Absolute expression for $g_1$ given ($f_1 = 0$). [c] Scale factor 2 included in error (PDG practice for discrepant data). [d] Data not used in these fits.

extracted from HSD are to be considered reliable and, perhaps more to the point, just what they are. Thus, I would respond to Lipkin's earlier comments by saying that "playing" with parametrisations (of SU(3) breaking) *is* legitimate in the context of attempting to understand what may be happening, in order to place (reliable) bounds on other predictions. And certainly, it is only a cosmetic question whether to parametrise using $F$ and $D$ or $g_A$ or any other description that may have physical meaning in a given analysis.

### 3.2. $V_{us}$ or $\sin\theta_C$

In the context of this symposium probably the more interesting aspect of HSD is the possibility of measuring $V_{us}$. It was noted during one of the talks that the Particle Data Group no longer considers HSD as a reliable source of this Standard Model parameter, preferring the so-called $K_{e3}$-decay data [6]. Let me note in passing that the proton-spin analysis does not yet require the same level of precision.

There are several difficulties that render the extraction of $V_{us}$ from HSD data a delicate process. First, but not foremost in the discussion of hadronic physics, is the continuing saga of neutron $\beta$-decay; the discrepancies present in this sector cloud the issue of CKM unitarity and therefore need to be resolved before real progress can be made with regard to $V_{us}$. An oft neglected question is that of the rôle of so-called second-class currents. These have not yet been investigated experimentally to any real extent, except to show that their presence could have a profound effect on the extracted value of $g_A$, possibly even shifting the ratio $F/D$ back to its original SU(6) value.

The area where most theoretical effort has been made, and using a number of approaches, is that of SU(3) breaking. The problem here is that most of the analyses presented in the literature to date are highly model dependent (indeed, often the main aim is to *test* the model and not necessarily provide a reliable analysis of parameters at all). Moreover, a severe failing of many published analyses is that they are highly selective of the data used. While it may make sense to examine the effect of neglecting this or that data set, if data are discarded on the basis of apparent discrepancy with SU(3) symmetry predictions, then the resulting bias is as obvious as it is unacceptable.

It is evident then that to resolve these difficulties, an improved experimental database is required: the presently available data do not sufficiently over-constrain the system, which needs different combinations both of the $F$ and $D$ parameters and of $\Delta S = 0$ and $|\Delta S| = 1$ decays, and also of both rates and angular correlations for the *same* decay modes. The KTeV data will go some way to meeting this request, providing as it does an evaluation of $F + D$, the same combination as found in neutron $\beta$-decay. However, there are several modes that have been measured but not yet with sufficient precision to be of real use; attempts should be made to improve these, not forgetting an eye towards the possibility of second-class current contributions.

In conclusion, a few comments are in order regarding the decay mode $\Xi^0 \to \Sigma^+ e\bar{\nu}$. The two predictions that have been compared at this symposium to the KTeV results are those of Flores-Mendieta, Jenkins and Manohar [12], using the

above-mentioned $1/N_c$ expansion, and mine [13], using the centre-of-mass corrections as proposed in [14]. I should remark that the difference between the results of these last two papers is due in part to the publication of new data between the two, but mainly to the large strange-quark wave-function mismatch correction applied in the latter and not in the former (owing to its incompatibility with the later data). Thus, for this type of approach one finds relatively small deviations (at most a few percent) and an overall good description of the data. As for the $1/N_c$ approach, it should be noted that there a much larger fit was performed, including data on the weak nonleptonic decuplet decays, which apparently have a very strong influence and lead to very large corrections in *both* sectors.

### 3.3. Isospin Violation

However, before moving on to the next section, I should like to recall Karl's talk on isospin violation in semi-leptonic decays [15], indeed his comments could have a wider impact than just on these decays. The question regards the possible mixing between $\Lambda^0$ and $\Sigma^0$. If isospin is conserved, then these two particles should simply correspond to the standard SU(3) states. If, on the other hand, the isospin SU(2) is broken (as evidently it is, slightly), then the physically observed particles will be mixture of the naïve SU(3) states. The related mixing angle is typically taken to be $\sin\phi \simeq -0.015$.

Clearly the decays in which the effects should be most felt are those involving both $\Lambda^0$ and $\Sigma$ hyperons. Thus, for example, the ratio of decay widths:

$$R(\phi) = \frac{\Gamma(\Sigma^+ - \Lambda^0 e^+ \nu)}{\Gamma(\Sigma^+ - \Lambda^0 e^- \bar{\nu})} \quad (9)$$

$$= (1 - 4\phi)\, R(0), \quad (10)$$

should be shifted by about 6% owing to the mixing [16]. Unfortunately, present experimental precision is too poor (for the $\Sigma^+$ decay) to detect such a shift. There would also be consequences for the vector coupling in these decays, which should vanish in pure Cabibbo theory but will be nonzero if there is $\Lambda^0$-$\Sigma^0$ mixing.

## 4. WEAK RADIATIVE DECAYS

The subject of weak radiative hyperon decays has been discussed in detail by Żenczykowski [17]. One of the central problems here is the apparent violation of Hara's theorem [18], again in existence for over a third of a century. The decays $B \to B'\gamma$ can be described in terms of the weak Hamiltonian matrix element:

$$\langle B'\gamma|\mathcal{H}_W|B\rangle \propto \bar{u}(p')\varepsilon_\mu \sigma^{\mu\nu} q_\nu \,(C + D\gamma_5)\, u(p), \quad (11)$$

where the term in $C$ is magnetic and $D$ is electric. Hara's theorem is based on U-spin and states that $D = 0$ for $B$ and $B'$ belonging to the same U-spin multiplet. From the observation that U-spin is not badly broken, one expects $D$ to be small (say, of order 10%). The experimental implication is a small asymmetry parameter:

$$\alpha = \frac{2\,\Re\mathrm{e}\, C^* D}{|C|^2 + |D|^2}, \quad (12)$$

for the decays $\Sigma^+ \to p\gamma$ and $\Xi^- \to \Sigma^-\gamma$. Experimentally the former is $-0.76 \pm 0.08$; *i.e.*, the theorem is almost maximally violated. Such a large value is indeed very difficult to explain consistently.

Successful approaches (salvaging Hara's theorem) may be found in the literature, due to Le Younac *et al.* [19] and Borasov and Holstein [20]. The central idea of these two groups is the insertion of additional intermediate states, from the $(70, 1^-)$ in the case of the former and $\frac{1}{2}^\pm$ in the latter, into the pole diagrams (see fig. 3) used in calculating the radiative decays. On the other hand, Żenczykowski has argued that there are strong indications that Hara's theorem may indeed be violated. Such a violation would, of course, imply a failure of one or more of the fundamental input assumptions to the theorem: gauge-invariance, CP conservation and a local (hadronic) field theory. The last (in the case of finite-size hadrons) is the weakest of these assumptions.

Figure 3. The pole diagrams contributing to hyperon radiative decays; the cross indicates the intermediate-state insertions.

The point then is that one cannot infer from this asymmetry alone the violation (or otherwise) of Hara's theorem. The key to unravelling the situation can only be found in further experimental data on the other weak radiative hyperon decays: for example, the experimental asymmetry for the decay $\Xi^0 \to \Lambda^0\gamma$ is $0.43\pm0.44$, which, if confirmed as large and positive, would contradict most of the models that allow Hara's theorem to be maintained. In any case more data are required to perform serious theoretical investigations.

## 5. NON-LEPTONIC DECAYS

### 5.1. CP Violation

The subject of CP violation in non-leptonic hyperon decays was addressed in the talk by Valencia [21]. In order to gain access to CP violation one has to measure asymmetries between hyperon and anti-hyperon decays. As pointed out by Holstein in his talk, Nature has constructed a perverse sort of hierarchy, whereby the processes that are easiest to measure are those least sensitive to CP violation (owing to small prefactors) and *vice versa*. One of the best candidates in the trade-off between experimental feasibility and sensitivity is the asymmetry parameter, $\alpha$ (governing the correlation between the parent polarisation and daughter momentum), in the non-leptonic hyperon decays: *e.g.*, $\Lambda^0 \to p\pi^-$ and $\Xi^- \to \Lambda^0\pi^-$. One thus constructs the following asymmetry:

$$\begin{aligned}\mathcal{A} &= \frac{\alpha+\bar{\alpha}}{\alpha-\bar{\alpha}} \\ &= -\tan(\delta_P-\delta_S)\,\sin(\phi_P-\phi_S), \qquad (13)\end{aligned}$$

where $\delta_{P,S}$ are the strong ($\Delta I = \frac{1}{2}$) phases and $\phi_{P,S}$ are the weak (CP-violating) phases. The estimated size of such an asymmetry, *e.g.*, for the mode $\Lambda^0 \to p\pi^-$ is $\mathcal{O}(10^{-5})$, which is doable experimentally but tough.

The ingredients that go into the calculation of such an asymmetry are clearly the two types of phases. The strong phases can be accessed theoretically via Watson's theorem, which relates $A \to B\pi$ to $B\pi$ scattering. This is, of course, of no practical use for any decay other than $\Lambda^0 \to p\pi^-$. Recent calculations using chiral perturbation theory suggest that the phases might be very small for all other modes. For the $S$ and $P$ waves in $\Lambda^0$ decay they are found to be

$$\delta_S^{\frac{1}{2}} \sim 6^\circ, \qquad (14)$$

$$\delta_P^{\frac{1}{2}} \sim -1.1^\circ, \qquad (15)$$

where the errors are estimated (assumed) to be of the order of $\pm1^\circ$.

The weak phases are calculable via an effective weak-interaction Hamiltonian:

$$\begin{aligned}\mathcal{H}_{\rm eff}^{|\Delta S|=1} &= \frac{G_{\rm F}}{\sqrt{2}}V_{ud}^*V_{us} \\ &\quad\times\sum_{i=1}^{12}c_i(\mu)\mathcal{O}_i(\mu)+\text{h.c.} \qquad (16)\end{aligned}$$

The short-distance coefficients, $c_i(\mu)$, are well-known while the matrix elements of the relevant operators are rather model dependent and are certainly not known with any precision. Using vacuum saturation, one can show that one of the operators, $\mathcal{O}_6$, dominates; its matrix element is calculated to be $y_6 \simeq -0.08$ and the uncertainty in the calculation outweighs the uncertainty from neglecting the other operators. At this point we have

$$\phi_P - \phi_S \sim -0.4y_6A^2\lambda^4\eta, \qquad (17)$$

where the last three factors are the CKM matrix parameters of the Wolfenstein parametrisation and provide $A^2\lambda^4\eta = 10^{-3}$; thus, one obtains $\mathcal{A}(\Lambda^0) \simeq -3\cdot10^{-5}$. The errors on such an estimate are probably best set at around 100%.

A particular interest in such numbers is stimulated by the effect of possible extensions to the Standard Model, the most popular being Supersymmetry. For example, if the recently confirmed large value for $\epsilon'/\epsilon$ is to be ascribed to new Supersymmetric couplings, then the same would produced an enhanced CP-violating asymmetry in non-leptonic decays, with $\mathcal{A}(\Lambda^0) \sim \mathcal{O}(10^{-3})$ being possible.

### 5.2. $\Delta I = \frac{3}{2}$ Amplitudes

A related subject, dealt with by Tandean [22], is the study of the little-known $\Delta I = \frac{3}{2}$ amplitudes in hyperon non-leptonic decays. In view of the situation with regard to the $\Delta I = \frac{1}{2}$ amplitudes and the problem of simultaneously fitting the S- and P-wave contributions, it is instructive to study the $\frac{3}{2}$ amplitudes. The analysis presented was based on calculations performed in chiral perturbation theory [23]. On the theoretical side the situation is rather favourable: at leading order, the amplitudes can be described in terms of just one weak parameter and this can be fixed from the S-wave amplitudes measured in $\Sigma$ decays. This then allows a full set of predictions for the P-waves. Unfortunately, as is often the case, the experimental situation is less favourable

and, despite the large corrections found in their one-loop calculations, the large errors on the measured values does not yet allow a meaningful comparison of data and theory.

## 6. HYPERON POLARISATION

Another long-standing puzzle in hadronic physics (although a relative youngster compared to other topics discussed above) is that of the large transverse hyperon polarisations observed in large-$p_T$ semi-inclusive hyperon production (for example, see [24] for recent data). A related phenomena is that of the left-right asymmetry in pion production of transversely polarised targets (see [25], for example). The general phenomenology was presented here by Pondrom [26] and the more theoretical aspects of the problem were discussed by Soffer in his talk [27]; I would like to enlarge on some of the points made and touch upon a few others. Let me first stress that, in the absence of parity violation, the only single-spin asymmetries allowed are those which correlate the polarisation vector to the normal of the scattering plane, just as in the examples mentioned above.

The archetypal process is $pp \to \Lambda^{0\uparrow} X$, where *neither* initial-state hadron is polarised while the final-state $\Lambda^0$ hyperon is found to emerge strongly polarised along the normal to the scattering plane. The principal characteristics of this phenomenon are as follows (see also Fig. 4): the polarisation

1. is large, reaching values of the order of tens of percent;
2. grows more-or-less linearly with $x_{\rm F}$;
3. grows more-or-less linearly with $p_T$ up to $p_T \sim 1\,{\rm GeV}$;
4. remains large and approximately constant for $p_T \gtrsim 1\,{\rm GeV}$, up to the largest measured values of $p_T \sim 4 - 5\,{\rm GeV}$;
5. follows the expected SU(6) pattern of signs and relative magnitudes.

To the extent that it has been studied, a similar description also applies to the pion and other asymmetries where the spin vector belongs to the initial state.

It is not difficult to see (by expressing the amplitudes in a suitable helicity basis) that such single-spin asymmetries must be proportional to the imaginary part of the interference between

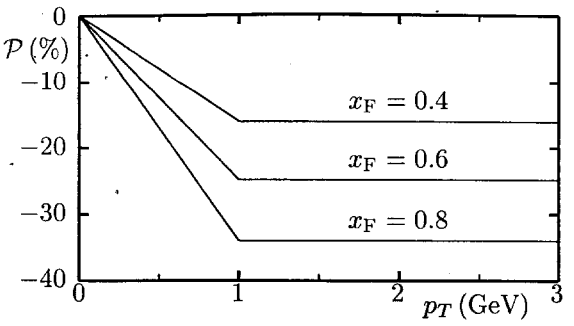


Figure 4. A schematic representation of the semi-inclusive $\Lambda^0$ polarisation data: the polarisation is given as a function of $p_T$ for various values of $x_{\rm F}$.

a spin-flip and a non-flip amplitude. This poses a two-fold difficulty in gauge theories with light fermions:

- tree-level or Born amplitudes are always real,
- spin-flip amplitudes are proportional to a current fermion mass.

The first requires loop diagrams, which lead to suppression by a power of $\alpha_S$ and which typically also lead to colour-factor and kinematical mismatch. The second, naïvely, implies suppression by, at best, a power of the strange-quark mass divided by $p_T$. Thus, Kane, Pumplin and Repko [28] (*prior* to the release of any experimental results) were led to the conclusion that such large effects would spell doom for perturbative QCD. As history now tells, the effects were far from zero but perturbative QCD is still very much alive and kicking!

As usual, there is a "get-out" clause: the typical $p_T$ of the data is not considered large enough yet for perturbative QCD to be reliable. Having said that, a great deal of progress has been made since the early perturbative calculations and it is now known that such effects are possible even within a framework of purely perturbative QCD. Before discussing these developments, I would like to briefly discuss two of the non-perturbative approaches.

Together with other semi-classical models, Soffer already mentioned the Lund string-model approach [29] and illustrated some of its shortcomings; I shall add to this by highlighting the inconsistency in the logic from which it derives such polarisation effects. The initial motivation is conser-

vation of angular momentum in the string break-up process, producing the strange anti-strange pair. Orbital angular momentum is generated by a finite length of string being consumed to produce the energy necessary to create the pair, which are then necessarily spatially separated. This separation, combined with a finite $p_T$, leads to non-zero orbital angular momentum of the pair, which can only be compensated by their spin (*i.e.*, by aligning or anti-aligning, as necessary). Trivial considerations show that the predicted sign is correct, assuming the strange quark polarisation is correlated to that of the final-state hyperon via SU(6) type wave-functions. However, while the spin of the $s\bar{s}$ pair is limited in magnitude to a total of one unit, the orbital contribution is essentially unbounded as $p_T$ increases (roughly speaking, $|\vec{L}| \propto p_T\sqrt{p_T^2+m^2}$). And thus the serpent bites its own tail.

Soffer also went into some detail with regard to the use of models based on Regge theory [30,31]. While to a certain degree such models may provide better insight (they do at least contain explicit reference to imaginary phases, which the Lund model does not), they cannot expect to apply to very large $p_T$ configurations. Moreover, all such models are at a complete loss in trying to explain the large polarisations observed in anti-hyperon production.

Let me now turn to the developments in perturbative QCD over the past years. A great deal of new understanding has developed since the days of Kane *et al.* and there are now good reasons for believing that explanations can be constructed within the framework of perturbative QCD. Nearly fifteen years ago Efremov and Teryaev pointed out that there exist so-called twist-three contributions that can come to the rescue [32]. First of all, they note that the mass scale, as required by gauge invariance, is not that of a current quark but a typical hadronic mass, *i.e.*, $\sim\mathcal{O}(1\,\mathrm{GeV})$.

The fact that twist-three contributions are invoked is *not* the unnecessary complication it might seem. Indeed, it was well-known beforehand that such would have to be the case owing to the spin-flip requirement: spin-flip always implies a mass proportionality and therefore higher twist (note that twist effectively counts the inverse power of $Q^2$, or in this case $p_T$, that appears in expressions for physical cross-sections). Thus, the type of diagrams one is led to contemplate are such as that shown in Fig. 5. The extra gluon leg is attached to the polarised hadron and is symptomatic of the twist-three nature. The deeper and crucial observation of Efremov and Teryaev is that when the momentum fraction, $x_g$, carried by the odd gluon goes to zero, the propagator marked with a cross in the figure encounters a pole. This is not say that it propagates freely; it is more a statement of how to perform a contour integral. Indeed, if we adopt the usual $\mathrm{i}\varepsilon$ prescription and split the propagator into its real (principal value) and imaginary parts:

$$\frac{1}{x_g s + \mathrm{i}\varepsilon} = \mathbb{P}\frac{1}{x_g s} + \mathrm{i}\pi\delta(x_g), \tag{18}$$

where $s$ is the usual (hadronic) Mandelstam variable, then one immediately sees how an imaginary part arises. Note that, although this may look like a loop diagram, once again for reasons of gauge invariance, one can show that the factor of $\alpha_s$ is absorbed into the definition of the hadronic blob itself and thus it is formally a Born-level contribution. Note also that such three-legged blobs are exactly what one encounters in the structure function $g_2$ governing transversely polarised DIS, presently under study in various high-energy experiments.

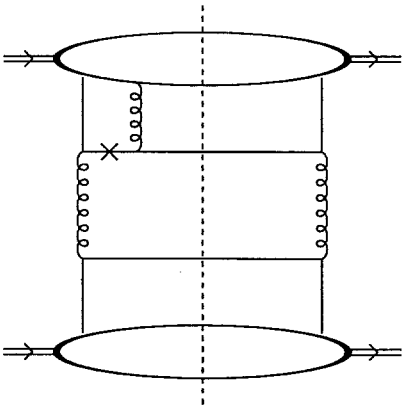

Figure 5. An example of the twist-three diagrams that may contribute to semi-inclusive $\pi$ asymmetry. The dashed line represents the cut through the final states, the upper, cut quark line should, in fact, fragments into the detected pion. The cross indicates the propagator that reaches the pole and that thus provides the imaginary contribution

Such diagrams have been exploited by Qiu and Sterman [33], who have shown that they can pro-

duce large asymmetries. Moreover, I have recently shown [34] that in the particular kinematic limit $x_g \to 0$ a novel form of factorisation occurs and it is then easy to see why these diagrams give a contribution of the same order of magnitude as the normal twist-two Born diagrams.

The advantage of such an approach is that one is clearly free of the usual model dependence (providing the necessary information on input structure and fragmentation functions is available). Moreover, through the common hard-scattering diagrams, such an approach automatically links the many different possible types of processes in which single-spin asymmetries may be observed. Note also that it will naturally be applicable to the case of $\Lambda_c$ polarisation, discussed here by Goldstein [35], which could then provide a key to the transition from the non-perturbative to perturbative regimes. On the down side, there are a large number of possible contributions (*e.g.*, twist-three *fragmentation* functions) and there may also be a shortage of information, although many phenomenological analyses are now being performed to identify the origins of the effects and experiments are continuing to gather information on polarised hadronic structure.

## 7. HYPERNUCLEI

Very little was said at this symposium about hypernuclei. As this is another long-standing, as-yet unsettled problem and there are experiments planned to examine it in detail, I decided it would be useful to redress the balance a little here. The main observation is that a $\Lambda^0$ (or even a $\Sigma^0$) can move freely within a nucleus (and indeed nuclear matter in general) without the usual hinderance of the Pauli exclusion principle, which applies to the standard nuclear contents: namely, neutrons and protons. Apart from its slightly larger mass it is very much like (but not *identical* to) a neutron and therefore is an ideal probe of the nuclear potential and the forces at work inside a nucleus.

An old question, still debated, is whether or not $\Sigma$-hypernuclei actually exist. Early reports have never been corroborated although it is hard to completely rule out the possibility and theoretically there is no solid argument against their existence.

A more recent and certainly pressing problem regards the observation of an apparent violation of the age-old $\Delta I = \frac{1}{2}$ rule in the decays of $\Lambda$-hypernuclei [36]. The situation is, on the face of it, rather simple. A $\Lambda^0$ bound inside a nucleus does not have access to the standard decay channels $\Lambda^0 \to N\pi$ for reasons of energy. However, it may decay via an exchange reaction with another nucleon inside the nucleus:

$$\Lambda^0 + p \;\to\; n + p, \tag{19}$$

$$\Lambda^0 + n \;\to\; n + n. \tag{20}$$

From the data on decays of ${}_{\Lambda}\mathrm{H}^4$ ${}_{\Lambda}\mathrm{He}^4$, it appears that one has the following ratio for the $\Delta I = \frac{1}{2}$ and $\frac{3}{2}$ amplitudes:

$$\frac{A(\frac{1}{2})}{A(\frac{3}{2})} \sim 1. \tag{21}$$

It is rather difficult to believe that a nuclear environment with its typical binding energies of a few MeV could have such a profound effect on hadronic interactions that have typically much higher energy scales. Indeed, an interesting approach pioneered by Preparata and co-workers [37], in which a coherent dynamic pion background field plays an important rôle, arrives at results compatible with the experimental data while avoiding explicit violation of the $\Delta I = \frac{1}{2}$ rule at the hadronic level.

These questions and the nature of the hypernuclei system will come under close scrutiny in the near future in the FINUDA experiment planned for DA$\Phi$NE the Frascati $\phi$ factory. This is an $e^+e^-$ facility designed to operate at a centre-of-mass energy corresponding to the $\phi$ mass (1020 MeV). The dominant $K$-$\overline{K}$ decay mode means that this machine will provide a copious source of $K$ and $\overline{K}$ mesons. In the CHLOE experiment this will be exploited to study, *e.g.*, CP violation and the $K^0$-$\overline{K}^0$ itself, and in FINUDA to produce large clean samples of hypernuclei.

## 8. CONCLUSIONS

There is little point in trying to summarise a summary. However, it is worth making the overall observation that, at least in those areas of hyperon physics discussed at this symposium, the main stumbling block to progress at the present is the lack of precision data. Or to put it another way, in many cases the precision of experiment and theory are roughly equivalent. Indeed, in some cases the precision of the theory is limited by the lack of precision input data. This means that it is often impossible to distinguish between the different models found in the literature and, with no hint as to the way forward, the theorist is

left floundering. During the symposium we have thus heard various pleas from the theorists for the production of data of better quality, greater quantity or wider variety, as the case may be, and we have also heard from the experimentalists that new experiments are planned or in progress and that new data will be forthcoming.

What is also clear is that many of the problems connected to hyperon physics are of a very general hadronic nature and thus the answers to the questions posed here could have far-reaching repercussions. Let us hope that at the next edition of this symposium some of the models will be swept away, allowing theorists and experimentalists alike to concentrate their efforts and resources on the more promising routes.

## REFERENCES


1. B.R. Holstein, these proceedings.
2. H.J. Lipkin, these proceedings.
3. G. 't Hooft, *Nucl. Phys.* **B72** (1974) 461.
4. E. Jenkins, e-print hep-ph/9803349.
5. E. Jenkins and R.F. Lebed, *Phys. Rev.* **D52** (1995) 282.
6. Particle Data Group, C. Caso *et al.*, *Eur. Phys. J.* **C3** (1998) 1.
7. A. Alavi-Harati, these proceedings.
8. S. Bright, these proceedings.
9. N. Cabibbo, *Phys. Rev. Lett.* **10** (1963) 531.
10. A. García, these proceedings.
11. D. Adams *et al.* (SM collab.), *Phys. Lett.* **B329** (1994) 399; *erratum ibid.* **B339** (1994) 332.
12. R. Flores-Mendieta, E. Jenkins and A.V. Manohar, e-print hep-ph/9805416.
13. P.G. Ratcliffe, *Phys. Rev.* **D59** (1999) 014038.
14. J.F. Donoghue, B.R. Holstein and S.W. Klimt, *Phys. Rev.* **D35** (1987) 934.
15. G. Karl, these proceedings.
16. G. Karl, *Phys. Lett.* **B328** (1994) 149; *erratum ibid.* **B341** (1995) 449.
17. P. Żenczykowski, these proceedings.
18. Y. Hara, *Phys. Rev. Lett.* **12** (1964) 378.
19. A. Le Younac *et al.*, *Nucl. Phys.* **B149** (1979) 321.
20. B. Borasov and B.R. Holstein, *Phys. Rev.* **D59** (1999) 054025.
21. G. Valencia, these proceedings.
22. J. Tandean, these proceedings.
23. A. Abd El-Hady, J. Tandean and G. Valencia, *Nucl. Phys.* **A651** (1999) 71.
24. A. Bravar *et al.* (FNAL E704 collab.), *Phys. Rev. Lett.* **75** (1995) 3073.
25. D.L. Adams *et al.* (FNAL E704 collab.), *Phys. Lett.* **B264** (1991) 462.
26. L. Pondrom, these proceedings.
27. J. Soffer, these proceedings.
28. G.L. Kane, J. Pumplin and W. Repko, *Phys. Rev. Lett.* **41** (1978) 1689.
29. B. Andersson, G. Gustafson, G. Ingelman and T. Sjöstrand, *Phys. Rep.* **97** (1983) 31.
30. R. Barni, G. Preparata and P.G. Ratcliffe, *Phys. Lett.* **B296** (1992) 251.
31. J. Soffer and N.A. Tornqvist, *Phys. Rev. Lett.* **68** (1992) 907.
32. A.V. Efremov and O.V. Teryaev, *Phys. Lett.* **B150** (1985) 383.
33. J.-W. Qiu and G. Sterman, *Nucl. Phys.* **B378** (1992) 52.
34. P.G. Ratcliffe, *Eur. Phys. J.* **C8** (1999) 403.
35. G.R. Goldstein, these proceedings.
36. J.P. Bocquet *et al.*, *Phys. Lett.* **B182** (1986) 146.
37. R. Alzetta, G. Liberti, M. Gibilisco and G. Preparata, *Mod. Phys. Lett.* **A8** (1993) 2335.

# Hyperon99 Experimental Summary: A 40 Year Perspective

Erik Ramberg [a]

[a]Fermi National Accelerator Laboratory,
P.O. Box 500 Batavia, IL 60510-500

Summaries of the experimental results for the Hyperon 99 Symposium at Fermilab are given in this article. An attempt is made to view these results in a larger framework so that an idea of future experimental priorities can be obtained.

## 1. INTRODUCTION

The Hyperon 99 Symposium was held in a very timely fashion and place. Fermilab is likely making the last 800 GeV fixed target run for a very long time. As has been true since Fermilab began, hyperon physics continues to play an important role in the fixed target program. Both of the active fixed target experiments, KTeV and HyperCP, have strong hyperon physics programs, and both have reported results at this symposium. In addition, it should be pointed out that both experiments have strong kaon physics programs. This linkage of kaons and hyperons is, of course, not coincidental, but mirrors the gradual discovery of strangeness through associated production of kaons and hyperons in the early 1950's.[1] As an overview of the long history of hyperon physics, Vince Smith gave a very thorough presentation of the CERN hyperon physics program and showed how it relates to the work done at Brookhaven and Fermilab.

I have arranged this summary in five sections. The first three correspond to the way in which hyperons are studied: they exist (with static properties such as mass and lifetime), they are produced (with production properties such as polarization) and they decay (with decay properties such as form factors). I then summarize some of the data presented at the symposium reflecting strangeness in other baryonic forms of matter than the standard hyperon. In the last section I try to summarize what I believe are the important future measurements we should make in the field of hyperon physics.

## 2. HYPERONS EXIST

The static properties of hyperons have historically been an incredible hotbed of experimental activity. Fortunately, this data is of great quality and is challenging theoretical models to this day. Unfortunately, it doesn't leave eager experimentalists much to do on this front. Nontheless, many significant new measurements were presented.

Peter Cooper gave an excellent overview of hyperon static properties, such as magnetic moments, mass and lifetimes. In magnetic moments, he pointed out that there are no new measurements, but this is to be expected since no theory can test the precision in the current set of measurements. He presented the CERN NA48 experiments' new result on the mass of the $\Xi^\circ$. This value is $m_{\Xi^\circ} = 1314.83 \pm 0.06 \pm 0.20$, bringing the error on this poorly measured mass in line with other hyperon mass measurements. The Coleman-Glashow relation[2] is now tested at a more significant level:

$$\begin{aligned} M_n - M_p + M_{\Xi^-} - M_{\Xi^\circ} + M_{\Sigma^+} - M_{\Sigma^-} \quad (1) \\ = 0 \ (Theory) \\ = -0.30 \pm 0.25 \ (Experiment) \end{aligned}$$

Peter also presented what he called "the new last results from E761", namely a new measurement of the lifetimes of the $\Sigma^+$ and its antiparticle. The result for the fractional difference in lifetimes is:

$$\frac{\Delta\tau}{<\tau>} = -0.06 \pm 1.12\% \quad (2)$$

making it the best baryon lifetime CPT test. The $\Xi^\circ$ lifetime is still poorly measured, but this should (MUST!) be measured by NA48 and KTeV in the near future.

Henning Krueger showed how the charm baryon experiment, SELEX, at Fermilab has

made significant new measurements with its hyperon beam. The total cross section for $\Sigma^- N$ interactions at $\sqrt{s} = 34$ GeV has been measured and matches very well a prediction of Harry Lipkin's from 1975.[3] A cross check has been made by also measuring the $\pi^-$ total cross section and this matches well the trend in previous lower energy data. As well, SELEX has measured the charge radius of the $\Sigma^-$, along with the proton and $\pi^-$. The latter two match previous measurements, while the former is the first such measurement. It shows that the $\Sigma^-$ has a slightly smaller charge radius than the proton.

## 3. HYPERONS ARE PRODUCED

There is one word in hyperon production that tends to overshadow the others: polarization. It is an unexpected phenomenon, hard to explain and there is always another measurement that can be made. This symposium saw a plethora of new results in hyperon polarization, as well as other production properties such as hyperon-antihyperon asymmetries. Even if there is no comprehensive theoretical model that adequately challenges the current data set, measuring new aspects of this phenomenon is like putting money in the bank - it most assuredly will be taken out and used when the time is right.

To begin with, Ulrich Miller showed the WA89 result for polarization of $\Lambda$'s produced by several different incident particles. The statistically significant result is for $\Sigma^-$ production of $\Lambda$, with a systematically increasing positive polarization as you increase $x_F$, and relatively flat in $p_T$. Vince Smith also showed WA89 results, this time for $\Sigma^-$ production of $\Sigma^\circ$, showing a rather large negative polarization of about -40%.

Ed McCliment showed two new polarization results from SELEX. The first was the production polarization of $\Sigma^+$ hyperons. Although lower in statistics than E761, SELEX extends the $p_T$ range to 2 GeV/c and the $x_F$ range to 0.67, with a substantial positive polarization still seen at these limits. The second result was the polarization of $\Lambda$ hyperons using an incident $\Sigma^-$ beam, similar to the WA89 data. The SELEX data and WA89 data both show that $\Lambda$'s produced in this way have the opposite polarization from proton production.

Al Erwin showed KTeV's new result on $\Xi^\circ$ polarization from 800 GeV proton production. These results agree very well with the 400 GeV data at twice the targeting angle, indicating that there is no energy dependence in this mode. KTeV saw no indication of polarization for the anti-$\Xi^\circ$.

In a very intriguing result, Dave Christian showed new exclusive $\Lambda$ polarization data from E690. For a $\Lambda - K^+$ final state, the data is rather irregular in $p_T$ and $x_F$ bins. However, if binned in terms of the effective mass, there is a simple monotonic behavior ranging from positive to negative 50%. This data confirms and extends a previous result.[6]

In his fine overview of polarization phenomena, Lee Pondrom discussed the issue of regularities in exclusive reactions, as reported in BNL E766 this year.[7] For four different exclusive $\Lambda - K^+$ final states, they can characterize the $\Lambda$ polarization as a simple linear combination:

$$P_\Lambda = -a x_F p_T \tag{3}$$

Pondrom showed how this functional form fits the 400 GeV inclusive data for the lower values of $p_T$, but overestimates the polarization at higher values. Clearly this kind of synthesis between exclusive and inclusive reactions needs further study, especially for exclusive production of hyperons other than the $\Lambda$.

As a final note on polarization, Milind Purohit showed an impressive first result on $\Lambda_c$ charm baryon polarization from E791, using a sample of almost 1000 decays. There seems to be an increasingly negative polarization with respect to $p_T$, much like the normal $\Lambda$ data. More statistics will tell.

Beyond polarization, Joao Anjos presented other E791 results on production distributions of many hyperons (2.5 million $\Lambda$'s, 1 million $\Xi^-$, etc). There are significant $\Lambda$ decay statistics beyond a production $p_T$ of 3 GeV/c, enough to show an enhancement above most theoretical models. He also showed large hyperon-antihyperon production asymmetries as a function of $x_F$ and $p_T^2$, whose magnitude and shape are clearly not predicted by the Pythia/Jetset models.

## 4. HYPERONS DECAY

Hyperons, due to their low mass, have a fairly simple set of final states into which they decay. For the most part there is the standard nonleptonic weak decay, the beta decay and the weak radiative decay. Each of these three had significant exposure at this symposium.

One of the most ambitious hyperon experiments has to be HyperCP at Fermilab, which is continuing to run this year. Ken Nelson reported on the status of the search for CP violation in the normal mode decay of the $\Xi^-$ hyperon and its antiparticle. They have an astounding 1997 sample of 245 million anti-$\Xi^-$ decays, with 4 times that number for the particle counterpart. They expect a statistical sensitivity on the CP violation parameter of

$$\delta A_{\Xi\Lambda} = 2 \times 10^-4 \quad (4)$$

with 4 times more events in 1999! Ken presented evidence that systematic effects such as residual targeting angles do not show up in the ultimate center of mass angular distributions. Although most models of hyperon CP violation predict effects smaller than HyperCP's ultimate sensitivity, the latest results on $\epsilon'$ in the kaon sector show that Standard Model predictions of CP violation in even the simplest systems may turn out wrong.

Uwe Koch reviewed the status of hyperon radiative decays. The weak radiative decays have been a theoretical puzzle for many years, with an unexpected large negative asymmetry showing up in the decay $\Sigma^+ \to p\gamma$. Unfortunately, that is about as far as the experimental situation goes, while the theory has developed somewhat more.[8] Uwe showed KTeV's new result on the asymmetry in the decay $\Xi^\circ \to \Sigma^\circ\gamma$, which also shows a large negative value. KTeV also has on the order of 1000 events of the $\Lambda\gamma$ decay mode of the $\Xi^\circ$, although with no measurement of the asymmetry yet. Lest KTeV rest on its laurels, Uwe showed NA48's plans for dedicated $K_S$ running in the spring of 2000. Because their $K_S$ production target is quite close to their detector, as compared to KTeV, their yield for hyperons is significantly greater. They may reach 50,000 events of both types in 30 days of running. Uwe also showed preliminary observations at KTeV of the decay $\Sigma^\circ \to \Lambda e^+e^-$, tagged from the rare decay $\Xi^\circ \to \Sigma^\circ\gamma$. Although this decay has been seen in bubble chambers, this has the potential to be the first measurement of its branching ratio and angular distribution properties.

Steve Bright continued the KTeV presentation by showing their new result on the first observation of $\Xi^\circ$ beta decay, with measurement of its branching ratio and form factors. With almost 500 candidate events, the branching ratio matches exactly the straight Cabibbo Theory prediction, with no SU(3) correction. Steve also showed that the form factor results, obtained from center of mass angular correlations, coincide quite precisely with the straight Cabibbo Theory. Since with two strange quarks you would expect significant SU(3) effects, this result is somewhat surprising.

Ashkan Alavi-Harati gave an overview of the experimental side of hyperon beta decays, where the KTeV result was put in perspective with the other hyperon beta decays. All of the experimentally accessible hyperon beta decays have now been observed. The $\Sigma^\circ$ and $\Xi^-$ decays suffer from very small branching ratios. Ashkan discussed how global fits to the beta decay data set have been affected by large shifts in the neutron data. The search for SU(3) symmetry breaking is rather elusive and Ashkan showed how a case can be made that any such symmetry breaking is minimal in hyperon beta decays.

## 5. BEYOND HYPERONS

The hyperon is a well known beast which has been tamed over the course of decades. This symposium saw a hint of perhaps new exotic animals, related to the hyperon, but excitingly different.

Rene Bellwied gave a comprehensive overview of strange quarks in nuclear matter. One of the key signatures for the elusive quark-gluon plasma is an enhancement in anti-hyperon to hyperon production ratio. He showed evidence from NA35 and NA49 of net strangeness enhancement in nuclear collisions-perhaps another signature. Rene then discussed the plans for such measurements at the new RHIC nuclear collider at Brookhaven. With 10,000 charged particles per collision, they have their work cut out for them. Rene also showed preliminary results from several searches for the H dibaryon, containing 2 each of u,d and s quarks. This 6 quark semi-stable state will decay into a $\Lambda$, proton and $\pi$ if its mass is below the di-$\Lambda$ threshold. Several experiments from Brookhaven see an enhanced production in this mass region. Not shown at this conference is the new KTeV result on a search for the H dibaryon, which found no effect.[9]

Another hypothetical particle is 'diquarkonium', which contains 2 quarks and 2 anti-quarks. Ulrich Muller discussed how WA62 saw a mass peak in several final states containing a $\Lambda$, an anti-proton and two or three $\pi$'s. There is also some confirming evidence from the BIS-2 experiment at Serpukhov. Ulrich showed WA89's new

result on a search for this final state, with no observation at a sensitivity level where they should have seen it. As scientisits are always fond of saying: "we need more data".

Finally, Leónid Landsberg perked everyone up by showing an intriguing observation of a new resonance obtained from diffractive proton production at SPHINX in Serpukhov. In both the coherent region and at higher $p_T^2$ a significant resonance structure is apparent in the $\Sigma^\circ K^+$ mass region around 2 GeV/$c^2$. The interesting aspect of this state is its narrow width (less than 100 MeV/$c^2$) and the fact that its decay into the strange final state is greater than its decay into the normal nucleon isobar final state. Both of these facts make it a serious candidate for the pentaquark exotic baryon ($uuds\bar{s}$). Leonid also showed how Primakoff production from the $\Sigma^-$ beam in SELEX gives a slight enhancement at this same mass value for the $\Sigma^- K^+$ final state. This work will be extended with a new SPHINX run and we are all looking forward to the results.

## 6. THE FUTURE

Besides showcasing the latest results in hyperon physics, which I have tried to summarize above, the symposium has given experimentalists, theorists and accelerator physicists a chance to meet and discuss the potential future of this field. The key questions are 1) what remains to be done and 2) how can we accomplish it?

Both KTeV and NA48 have plans to finish out their round of neutral hyperon measurements. HyperCP is also running again and will obtain incredible amounts of data on many decays of the charged hyperons. We are all looking forward to the results from that experiment. If a signal of CP violation is seen in their hyperon data sample then this may give a great impetus to further studies. Unfortunately, the calorimeter in that experiment is insufficient to reconstruct photons and electrons in the final state, so beta and radiative decays will not be analyzed.

Looking further afield, a panel met to discuss the possibilities of future experiments. It seems that a major criteria for a new hyperon experiment, or any new high energy phyics experiment for that matter, is that it should have a measurable and interesting goal in mind. A few relevant issues in hyperon physics that stand out in my mind as meeting this criteria are:

- $\Sigma^+ \rightarrow \Lambda e^+ \nu$ decay: As many speakers pointed out, this decay has been very poorly measured, with only 21 events ever seen.[4] Besides measuring the branching ratio to test the Cabibbo theory prediction, this decay is interesting in that it can resolve the issue of whether there is isospin mixing between the $\Sigma$ and the $\Lambda$, as discussed in this symposium by Gabriel Karl.[5] After all this time, do we really know what a $\Lambda$ is?

- Weak Radiative Decays: Now that new high statistics samples of the $\Xi^\circ$ weak radiative decays have been obtained, it is time to close the door on the experimental side of weak radiative hyperon decays. The decays $\Xi^- \rightarrow \Sigma^- \gamma$ and $\Lambda \rightarrow n\gamma$ are eminently measurable, especially considering that the latter can be measured in an experiment for the former by tagging the plentiful $\Xi^- \rightarrow \Lambda \pi^-$ decay.

- Polarization in anti-hyperons: To my mind, the observation of polarization in anti-hyperons (the $\bar{\Xi}^+$ and $\bar{\Sigma}^-$) is an amazing fact and the most telling of all polarization results. If it is possible to polarize sea quarks, then all of the current models are wrong and we MUST reconsider this interesting phenomenon. The anti-hyperon results must be repeated and studied in more detail.

Please note that these three examples are really all aspects of a single well-designed hyperon experiment - a multipurpose high intensity charged hyperon experiment with good tracking and calorimetry. The main sticking point is how and where to make the beam? If we think about such an experiment at Fermilab, it is clear that an 800 GeV fixed target beam will have to wait for completion of the collider Run II in 2006 or so. Even then it would have to justify competing against a collider run. The 120 GeV Main Injector beam is available for fixed target experiments, but several members of the panel were concerned at the prospect of losing the advantage that higher energy gives for hyperon physics. And Bill Foster urged us to consider a new Fermilab 3 TeV machine as the obvious candidate. To my mind, the Main Injector option should be considered as the default candidate until it can be shown as unworkable. Although I've always been a Fermilab regular, I would urge that this kind of dedicated charged hyperon experiment also be considered for other laboratories.

## 7. CONCLUSION

I call this summary a 40 year perspective partly because the oldest reference to experimental hyperon data in the Particle Data Book is from 1959 - a measurement of the branching ratio of $\Lambda \to p\pi^-$.[4] But another reason is that I turned 40 years old myself during this symposium. My hope is that I have matured in high energy physics as gracefully as the field of hyperon studies. And my sincerest wish and belief is that the future is promising for us both.

## REFERENCES


1. See the cosmic ray V particle paper of Anderson's: Phys. Rev. 78; 290; (1950)
2. Coleman,Glashow; Phys.Rev.Lett.6:423,(1961)
3. Phys. Rev. D 11; 1827; (1975)
4. Review of Particle Physics; Eur. Phys. Jour. C 3;(1998)
5. G. Karl, Phys. Lett. B 328; 149; (1994)
6. Henkes, et.al.; Phys. Lett. B 283; 155; (1992)
7. Felix, et.al.; Phys. Rev. Lett. 82; 5213; (1999)
8. See Piotr Zenczykowski's talk at this symposium.
9. Alavi-Harati, et.al.; submitted to Phys. Rev. Lett.; hep-ex/9910030

# Chapter 13

# Finale !

- N. Cabibbo

# Hyperons and Quark Mixing

N. Cabibbo [a]

[a]Università di Roma — La Sapienza,
Piazzale A. Moro 5, 00181 Roma, Italy

This is a very personal summary of the conference. After noting some of the exciting new results presented here, I briefly discuss the CKM matrix and its central importance as a pointer to physics beyond the Standard Model. I close with a short wish list for future hyperon research.

## 1. What is new in hyperons

The study of hyperons and their weak decays has led in the early sixties to discoveries which are central to the Standard Model of particle physics, among which the octet $SU(3)$ symmetry, quarks, quark mixing. This is the first time that I take part in a conference expressily devoted to hyperon physics, but I have a certain affection for this field, since the core of my 1963 paper [1] on what we now call quark mixing was a detailed prediction of the pattern of rates and form factors for hyperon beta decays. It has been a refreshing experience to verify in this meeting that Hyperon physics is today, after many decades from the first discoverieries, a very active subject, and for this I am grateful to the organizers of Hyperon99.

Many of the results presented here point to the need of further work. A new generation of experiments is needed, and one can identify the necessity of further theoretical work to match the level of precision that these new experiments will make available, a need which is already evident in some of the recent results.

In my talk I will concentrate on results related to the study of weak hyperon decay, and I will not discuss the many results related to the the hadronic interactions of hyperons and their static properties, among which new measurements of the $\Sigma^-$ cross section at very high energy, a determination of the $\Sigma^-$ charge radius, and the new measurements of hyperon polarization in hyperon beams. The latter remains, in spite of the various theoretical efforts, a surprising and somewhat mysterious effect. All of these subjects have been the object of excellent reviews in the course of this meeting.

### 1.1. The last hyperon beta decay.

I have been particularly impressed by the new results on the beta decay of the neutral cascade,

$$\Xi^0 \to \Sigma^+ + e^- + \bar{\nu}_e$$

presented here by Steve Bright for the KTeV collaboration. The new results include both a determination of the branching fraction for this mode and a determination of the axial/vector coupling ratio,

$$g_1/f_1 = 1.24 \pm^{0.20}_{0.17} (stat) \pm 0.07(syst)$$
$$B.R. = (2.54 \pm 0.11 \pm 0.16) \times 10^{-4}$$

these numbers are in excellent agreement with the predictions of the 1963 quark mixing paper [1], according to which cascade beta decay should behave exactly as the ordinary beta decay of the neutron, and have the same $g_1/f_1$. In the quark language, as the $\Xi^0$ decay is a $ssu \to suu$ transition, and the neutron decay is $ddu \to duu$, these two processes are simply related by exchanging $d \leftrightarrow s$ which has no effect on the weak interactions, other than an exchange of a factor of $\sin\theta$ with one of $\cos\theta$.

In the limit of exact $SU(3)$ symmetry the predictions on the beta decay of $\Xi^0$ involve only the value of the $\theta$ angle. Apart from phase space, the ratio of the rates for $\Xi^0$ and neutron beta decay is $\tan^2\theta$, and does not depend on the value of the $F$ and $D$ parameters which appear in the case of other semileptonic decays of hyperons. The interpretation of cascade beta decay is thus more straightforward than is the case with other hyperon beta decays.

It is interesting to note that the results on cascade beta decay are in better agreement with the exact $SU(3)$ predictions than with the fits [2] to hyperon beta decays which include effects of $SU(3)$ violation. Including the new results would then lead to a change in the fitted parameters.

The time is ripe for a reevaluation of $SU(3)$ breaking effects. The existing fits to hyperon beta decays are based on models which were adequate for a first exploration of quark physics, but are now somewhat dated.

The bag model, for instance, constrains the wave functions of the three quarks in a baryon to the same volume, while one would expect the wave functions of light quarks to be more widely spread than those of heavier quarks.

The technology of lattice QCD simulation, which is already yelding important results on the physics of heavy flavours, should be able in the coming years to offer an evaluation of the effects of symmetry breaking which is really derived from first principles. Waiting for new results from QCD simulations it might be interesting to revisit the models for the breaking of $SU(3)$ taking into account the new experimental results. More accurate values of the charge radius of hyperons should be very relevant here, as one would expect that the main source of symmetry breaking originates from the less than perfect overlap of the initial and final baryon wave function.

### 1.2. Sigma-Lambda beta decays

Gabriel Karl presented an interesting theoretical contribution [3] on the strangeness conserving $\Sigma \to \Lambda$ beta decays. It has been known for some time that the main contribution to what used to be known as "electromagnetic mass differences", e.g. the proton-neutron mass difference, are really [4] due to a difference in mass of the up and down quarks. This mass difference also causes a mixing between $\Lambda$ and $\Sigma^0$,

$$\begin{aligned} \Lambda &= \Lambda_8 \cos\phi + \Sigma_8 \sin\phi \\ \Sigma &= -\Lambda_8 \sin\phi + \Sigma_8 \cos\phi \end{aligned}$$

¿From the currently accepted values for the quark masses, Karl obtains a prediction for the mixing, $\phi = 0.015$. The effect of the mixing is enhanced if we consider the ratio of the rates of $\sigma^{\pm}$ beta decays,

$$R(\phi) = \frac{\Gamma(\Sigma^+ \to \Lambda e^+ \nu)}{\Gamma(\Sigma^- \to \Lambda e^- \bar{\nu})} = R(0)(1 - 3.95\phi)$$

a 6% deviation from the unmixed prediction $R(0)$, which is essentially determined by the difference in phase-space of the two channels.

V.J. Smith analysed the experimental possibilities for exploring the mixing effect, which appear promising. The present situation for these decays is in a sorry state. This is true in particular for the $\Sigma^+ \to \Lambda e^+ \nu$ decay, which, being the only beta decay of a positive hyperon has been neglected in modern post bubble-chamber experiments. As a consequence, only 21 events of this type have been detected, and even its branching ratio is poorly known.

A concerted effort on both the $\Sigma \to \Lambda$ beta decays would also offer an elegant test of the CVC, which leads to the prediction [5] that in these transitions the main vector form factor $f_1$ should vanish, apart from the small contribution originating from $\Sigma - \Lambda$ mixing. The main vector contribution in these decays comes from the "weak magnetism" $f_2$ form factor, related to the well measured $\Sigma^0 \to \Lambda\gamma$ transition. The effect of $f_2$ is a correction to the electron spectrum, linear in energy, and of opposite sign in the two decays. We have here, transposed to the world of hyperons, a copy of the classical test of CVC based on the $B_{12} - C_{12} - N_{12}$ isospin triplet.

A different test of CVC in these decays, discussed in [6], is based on a measurement of the polarization of the final state $\Lambda$, which arises from Vector-Axial interference.

### 1.3. Radiative transitions

Both NA48 and KTeV presented new results on $\Xi^0 \to \Lambda\gamma$ and $\Xi^0 \to \Sigma\gamma$. More accurate results are expected by both groups, either in data to be analyzed or in future runs.

An interesting aspect of these experiments is the possibility of producing a sample of well identified $\Sigma^0$ decays. This allows the study of so far undetected decay modes such as $\Sigma^0 \to \Lambda e^+ e^-$, $\Sigma^0 \to \Lambda\gamma\gamma$.

While the experimental situation in hyperon radiative decays seems due for a rapid improvement, there is a problem on the theoretical front. We have very reasonable models of these decays, but I do not see any immediate prospect of theoretical predictions which are really derived from first principles, i.e. from the Standard Model itself. The reason for this is that these decays require both a weak interaction and an electromagnetic one, for a total of three currents, which can act on different quarks within the hyperons, leading to a very complex situation, one that is difficult to analyse.

The fact that these decays cannot be *at the moment* analysed in a model—independent way should not deter experimentalists from doing their best in improving the measurements, ex-

pecially since the necessary data are available in high intensity runs with hyperon beams.

## 2. Quark mixing and the CKM matrix

Quark mixing is essentially a phenomenon related to the superposition principle of quantum mechanics. The fact that[1] the amplitude for the $d \to u$ transition is $\cos\theta$ and that for $s \to u$ is $\sin\theta$ implies that there exists a mixed state $d' = d\cos\theta + s\sin\theta$ and $s' = s\cos\theta - d\sin\theta$, whose transition amplitudes into a $u$ quark are respectively equal to 1 and 0. In a world where $m_s = m_d$, one could choose $s', d'$ as the basic quark states, with $s'$ being stable.

This elementary facts leads in the limit of exact $SU(3)$ symmetry to simple predictions for the complex of baryon beta decays in terms of $\theta$ and two further parameters, $D, F$, needed to describe the axial vector form factors $g_1$ in the different decays. The vector $f_1$ form factor is directly predicted in terms of $\theta$, and the weak magnetism $f_2$ form factor, which gives small but interesting contributions, is predicted in terms of $\theta$ and the value of baryon magnetic moments, which are now known with adequate precision.

If we extend this idea to include the three heavy quarks, we arrive at the present formulation where a $3 \times 3$ unitary matrix $V$, the CKM matrix first introduced in [7], represents the network of transition amplitudes between the charge $-1/3$ quarks, $d, s, b$, and the charge $2/3$ quarks, $u, c, t$. This can the be seen as a mixing between the $d, s, b$ quarks,

$$\begin{pmatrix} d' \\ s' \\ b' \end{pmatrix} = \begin{pmatrix} V_{ud} & V_{us} & V_{ub} \\ V_{cd} & V_{cs} & V_{cb} \\ V_{td} & V_{ts} & V_{tb} \end{pmatrix} \begin{pmatrix} d \\ s \\ b \end{pmatrix}$$

Kobayashi and Maskava noted that while the corresponding matrix in the case of four quarks can always be reduced to a form with real elements, and thus preserves $CP$, in the six quark case there is an uneliminable phase factor which is currently assumed to be *the* explanation for the violation of $CP$ and $T$. The existence of a fifth and a sixth quark would thus offer a natural explanation for the observed violation of $CP$ symmetry. This happened one year before the discovery at Fermilab of the $Y$ $(b\bar{b})$ states.

In the simplified form introduced by L. Wolfenstein [8],

$$V = \begin{pmatrix} 1-\lambda^2/2 & \lambda & A\lambda^3(\rho - i\eta) \\ -\lambda & 1-\lambda^2/2 & A\lambda^2 \\ A\lambda^3(1-\rho-i\eta) & -A\lambda^2 & 1 \end{pmatrix}$$

we see that $V$ depends on four parameters, $\lambda, A, \rho, \eta$, the last of which is $CP$ violating. The first parameter, $\lambda$, coincides with $\sin\theta$ within the precision of the Wolfenstein form.

The unitarity of $V$ implies that different columns are orthogonal, for example,

$$V_{ud}V_{ub}^* + V_{cd}V_{cb}^* + V_{td}V_{tb}^* = 0$$

The three terms of the r.h.s form a triangle in the complex plane, the *unitarity triangle*. The area of the triangle gives a measure of how much the triangle extends into the imaginary axis, and is thus a measure of the amount of $CP$ violation. The Wolfenstein form approximately satisfies the unitarity conditions up to some high power of $\lambda$.

During this conference G. Valencia and K. Nelson discussed the possibility of investigating $CP$ violations in hyperon decays. The possibilities seem marginal, but these experiments can become very valuable if the observed effects result much larger than those expected, thus offering arguments *against* the validity of the Standard Model.

The study of hyperon beta decays can give an essential contribution to the verification of this scheme, both by establishing the validity of the predicted pattern of branching ratios and form factors, and by contributing to the determination of the parameter $\lambda$. The first task is substantially achieved at the present level of accuracy, and has been completed with the results on the beta decay of the neutral cascade presented here. In the second task hyperon physics still lags behind $K$ meson physics, to the point that the Particle data Group has not included hyperon results in the listed value of $\sin\theta$. This situation can be improved by future hyperon beam experiments, with the important prerequisite of a more accurate theoretical treatment of $SU(3)$ breaking effects.

## 3. Quark mixing beyond the Standard Model

If the quark masses where all vanishing, as is the case in the absence of breaking of the $SU(2) \times U(1)$ electroweak gauge symmetry, the mixing matrix could be simply eliminated by choosing $d', s', b'$ as the base states for charge $-1/3$ quarks.

[1] We are now putting the clock back to before the discovery of the three heavy quarks

It is the Higgs phenomenon which produces quark masses and selects which combination of $d', s', b'$ are particles with a definite mass. In terms of $d', s', b'$, mass is a matrix $M_d$ whose elements are directly related to the couplings of the Higgs field. The same happens for charge 2/3 quarks, with a mass matrix $M_u$. The diagonalization of $M_d$, $M_u$ leads to the mixing $V$ and to the "observed" quark masses.

C. Jarslog has demonstrated [9] a remarkable relation between $CP$ violation in $V$ and the commutator of the mass matrices,

$$\det[M_u, M_d] \approx$$
$$i(m_t - m_c)(m_t - m_u)(m_c - m_u)$$
$$\times(m_b - m_s)(m_b - m_d)(m_s - m_d)$$
$$\times(Area\ of\ unitarity\ triangle)$$

This means that $CP$ violation in the mixing matrix $V$ is already inscribed in the pattern of couplings of the Higgs boson, and this must happen at an energy scale which is higher than that involved in the breaking of $SU(2) \times U(1)$, perhaps close to the Planck mass, or some intermediate mass at which interesting new physics is happening.

This is why the CKM matrix, and the companion matrix which enters in neutrino oscillation phenomena, are so interesting: they are among the few relics of physics which lies beyond the Standard Model.

## 4. Hyperons Physics—a wish list

¿From what precedes it should be clear that very high on my list is the ensemble of hyperon beta decays. I would like to see an improvement across the board of all these data.

I would certainly like to see a new precision experiment on the strangeness conserving $\Sigma \to \Lambda$ beta decays, where a lot remains to be done. These decays offer a multiplicity of interesting themes:

- A direct determination of the $D$ parameter.
- A new test of CVC
- Detection of isospin breaking through $\Sigma^0\Lambda$ mixing

The study of $CP$ violation in Hyperon decays merits all of our attention, and it would complement the large efforts lavished on the measurement of $\epsilon'/\epsilon$ and of $CP$ violation in the $B$ meson system.

On the theoretical side I would like to see renewed efforts for the determination of $SU(3)$ breaking effects in hyperon beta decays. While it is quite possible to improve the present situation on the quark-model front, my best hopes lie in the use of the technology of lattice $QCD$ simulations.

I would like to conclude by noting a wish which is outside the realm of hyperon physics. The hope is that some of the very bright experimentalists in the audience could come up with a clever scheme for obtaining a high precision measurement of pion beta decay, $\pi^+ \to \pi^0 e^+ \nu$. This is equivalent to a Fermi nuclear beta decay, and gives a direct measurement of $V_{ud} \approx \cos\theta$. In contrast to Fermi transitions in nuclei, it is not affected by Coulomb corrections and the radiative corrections can be computed with confidence. It is perhaps the only case of a beta decay where radiative corrections are finite [10] at the level of the Fermi lagrangian. Theoretical uncertainties are thus minimal, and we could use an experimental result with a $10^{-3}$ error bar. We are very far from this level of precision.

## REFERENCES


1. Nicola Cabibbo, Phys. Rev. Lett. 10 (1963) 531.
2. For a review, and a list of references, see C. Caso et al. (Particle Data Group), Eur. Phys. Journal C3 (1998) 1.
3. G. Karl, Phys. Lett. B328 (1994) 149-152.
4. N. Isgur, Phys. Rev D21 (1980), 779.
   An analysis of non-electromagnetic isospin breaking was given by N. Cabibbo and L. Maiani, Phys. Rev. 1 (1970) 707 in the framework of the chiral model.
5. N. Cabibbo and R. Gatto,
   Nuovo Cimento XV (1960) 160.
6. N. Cabibbo and P. Franzini,
   Phys. Lett. 3 (1963) 217.
7. M. Kobayashi and T. Maskawa,
   Progr. Theor. Phys. 49 (1973) 652.
8. L. Wolfenstein,
   Phys. Rev. Lett. 51 (1983) 1945.
9. C. Jarlskog,Phys. Rev. Lett. 55 (1985) 1039.
10. N. Cabibbo, L, Maiani and G. Preparata,
    Phys. Lett., 25B (1967) 31.